Innovative Applications of Naturalistic Driving Data for In-Depth Analysis of Freeway Interchange Deceleration Lane Design and Work Zone Mobility

by

Dan Xu

A dissertation submitted to the Graduate Faculty of
Auburn University
in partial fulfillment of the
requirements for the Degree of
Doctor of Philosophy

Auburn, Alabama
December 11, 2021

Keywords: Naturalistic Driving Study; Deceleration Lane Design; Work Zone Mobility; Driver Behavior; Freeway

Approved by

Huaguo H. Zhou, Chair, Professor of Civil and Environmental Engineering
Rod E. Turochy, Professor of Civil and Environmental Engineering
Jeffrey J. LaMondia, Associate Professor of Civil and Environmental Engineering
Ana M. Franco-Watkins, Professor of Psychological Sciences
Xinyu Zhang, Professor of Chemical Engineering

Abstract

This dissertation investigates two innovative applications of the Second Strategic Highway Research Program Naturalistic Driving Study (SHRP 2 NDS) data: (1) freeway interchange deceleration lane design and (2) work zone mobility analysis.

For freeway interchange deceleration lane design, the objective is to determine the minimum lengths of freeway deceleration lanes based on naturalistic driving speeds and deceleration rates from the SHRP 2 NDS database. SHRP 2 NDS has the distinct advantage of providing insight into driver behavior based on a wide-ranging collection of data regarding the driver, the vehicle, and the environment, whereas previous studies of this subject relied primarily on crash data, radar data, computer simulations, and driving simulators. Ten study locations that are located on I-75 in Florida with varying deceleration lane lengths and off-ramp lengths were used. The analysis included (1) speed distribution on different lengths of freeway deceleration lanes and off-ramps based on polynomial regression models; (2) drivers' behavior, including brake pedal usage, critical speed change point detection, and the distribution of deceleration rates compared with the American Association of State Highway and Transportation Officials (AASHTO) *Green Book* assumptions; and (3) a new method to determine the minimum deceleration lane lengths based on naturalistic driving speeds and deceleration rates. The results revealed that (1) typically, vehicle speeds reduced by 10% to 25% on deceleration lanes while 75% to 90% on off-ramps; (2) deceleration rates on deceleration lanes and off-ramps before critical speed change points are lower than assumptions from the *Green Book*; and (3) deceleration lanes can be shorter when off-ramps are long at diamond interchanges (e.g., greater than 1,550 ft). The research results provided guidance to improve freeway deceleration lane design.

For freeway work zone mobility analysis, the objective is to study work zone mobility by utilizing the SHRP 2 NDS data. The NDS data provides a unique opportunity to study car-following behaviors for different driver types in various work zone configurations, which cannot be achieved through traditional field data collection. The complete NDS work zone trip data of 200 traversals by 103 individuals, including time-series data, forward-view videos, radar data, and driver characteristics, was collected at four work zone configurations (two-to-one and three-to-two lane closure, and two-to-two and three-to-three shoulder closure), which encompasses nearly 1,100 vehicle miles traveled (VMT), 19 vehicle hours traveled (VHT), and over 675,000 data points at 0.1-s intervals. First, the gap and headway were analyzed for different drivers (gender, age group, and risk perceptions) to develop the gap and headway selection tables. Then, the speed profiles for different work zone configurations were established to explore the speed change through the entire work zones. The generalized additive model (GAM) was used to develop the best-fitted curves of time headway and speed distributions. The change point detection method was used to identify where significant changes in mean and variance of speeds occur. The research results provided additional information on the potential impact of human factors on car-following models at work zones that have been implemented in current work zone planning and simulation tools. Additionally, it can also be helpful to improve the Adaptive Cruise Control (ACC) gap spacing setting at the work zone for the automotive industry.

Acknowledgments

This dissertation was funded by Auburn University Intramural Grants Program (AU IGP), Alabama Department of Transportation (ALDOT), and Region 4 University Transportation Centers (UTC). Many people provided their expert assistance and cordial cooperation in the successful completion of this study.

I would like to acknowledge the advice, guidance, continued support, and encouragement received from my advisor, Dr. Huaguo Zhou. Without him, this dissertation would have not been possible. I wish to express my gratitude to Dr. Turochy, Dr. LaMondia, Dr. Franco-Watkins, and Dr. Zhang for their service as advisory committee members. My sincere appreciations go to all professors who taught me during my time at Auburn University.

Finally, I would like to thank my husband Dr. Chennan Xue, our parents, and our families for their priceless love and support.

Table of Contents

List of Tables

List of Figures

List of Abbreviations

AASHTO	American Association of State Highway and Transportation Officials
ACC	Adaptive Cruise Control
AIC	Akaike Information Criterion
CMS	Changeable Message Sign
CV	Connected Vehicle
DAS	Data Acquisition System
DOT	Department of Transportation
DUL	Data Use License
ERB	Ethical Review Board
FHWA	Federal Highway Administration
GAM	Generalized Additive Model
GPS	Geographic Positioning System
HCM	Highway Capacity Manual
IEC	Independent Ethics Committee
IRB	Institutional Review Board
LC	Lane Closure
MUTCD	Manual on Uniform Traffic Control Devices
MVMT	Million Vehicle Miles Traveled
NCHRP	National Cooperative Highway Research Program
NDS	Naturalistic Driving Study
NHS	National Highway System
NIMH	National Institute of Mental Health

PBC	Pre-Breakdown Capacity
PCE	Passenger Car Equivalents
PII	Personally Identifying Information
QDR	Queue Discharge Rate
REB	Research Ethics Board
RTOR	Right-Turn-On-Red
SC	Shoulder Closure
SDE	Secure Data Enclave
SHRP 2	The Second Strategic Highway Research Program
TCD	Traffic Control Device
TTC	Temporary Traffic Control
UTC	University Transportation Centers
VHT	Vehicle Hours Traveled
VMT	Vehicle Miles Traveled
VTTI	Virginia Tech Transportation Institute

Chapter 1. Introduction

1.1 Background

Freeways are essential components in the highway system that are designed under the highest highway design standards. In the United States, the interstate highway system constitutes only 2% of the nation's total rural lane miles, yet it conveys 25% of the annual rural vehicle miles traveled (VMT) (Pisarski and Reno 2015). Similarly, the urban interstate with under 4% of the nation's total urban lane miles carries 24% of urban VMT (Pisarski and Reno 2015). Freeways are controlled access multilane divided facilities for safer high-speed operation of automobiles through the exclusion of at-grade junctions. Two sections of freeways deserve more attention: diverge areas and work zones because (1) approximately half of crashes at freeway interchanges occurred at ramp diverging areas (McCartt, Northrup, & Retting, 2004); (2) approximately 24% of the nonrecurring freeway delay is caused by work zones (FHWA Work Zone Facts and Statistics, 2019).

1.2 Problem Statement

1.2.1 Safety Issues in Freeway Diverge Areas

Freeway diverge areas, including deceleration lanes and off-ramps, are critical elements that provide exits for traffic from freeway mainline segments via off-ramps to adjacent crossroads. The design intent of freeway diverge areas is to provide drivers with an effective, safe, and smooth transition from high-speed mainline to low-speed off-ramps and crossroads. This area is supposed to improve traffic safety and operation, reduce vehicle interference between through and exiting

traffic, and increase freeway capacity. However, it has been found to have high crash rates on deceleration lanes and off-ramps for nearly half a century.

As early as the 1960s, the operation and safety performance in freeway diverge areas had raised the attention of the public and the transportation agencies. The California Department of Public Works conducted a three-year study of 722 freeway ramps with 1,643 crashes occurred to investigate the geometric features in ramp safety and to classify these geometric features by ramp type and relative safety measures. It was found that the crash rates on exit ramps were consistently higher than those on entrance ramps and the highest percentages of exit ramp crashes occurred on the deceleration lane (Lundy 1965). In the 1970s, the Highway Users Federation for Safety and Mobility investigated the relationship between interchange design features and traffic safety. It was claimed that crashes are more frequent and severe at interchanges than at freeway mainlines (Oppenlander and Dawson 1970). During the decades, researchers aimed to reduce crash rates and improve safety and operational perspectives of freeway diverge areas. It was suggested to upgrade and rehabilitate freeway interchanges and ramps to guarantee the capacity, efficiency, and safety (Harwood & Graham, 1983). Researchers in Northern Virginia examined a sample of 1,150 crashes that occurred on heavily traveled urban interstate ramps and found that about half of all crashes occurred when drivers were exiting interstates in the diverge areas, 36% occurred when drivers were entering, and 16% occurred at the ramp terminal areas. They recommended to increase ramp design speed, use surveillance systems to alert drivers, and extend the length of speed-change lanes (McCartt, Northrup and Retting 2004). In Alabama, among all crashes involved on interstate ramps from 2012 to 2016, 73.5% of all crashes occurred at diverge areas when drivers were existing interstates (Critical Analysis Reporting Environment (CARE) (Computer Software), 2018).

Although studies, countermeasures, and efforts have been taken in the past decades to alleviate the safety problems in freeway diverge areas, the safety issues have not been solved and have been tending to be intensified. More recently, according to a National Cooperative Highway Research Program (NCHRP) report in 2012 (Torbic, et al. 2012), the average crash rate at freeway deceleration lanes was 0.68 crashes per million vehicle miles traveled (MVMT), which is three times higher than crashes on acceleration lanes (0.16MVMT) and 15.3% higher than crashes at freeway mainline sections near exit ramps (0.59MVMT). Furthermore, 42.4% of the crashes that occurred at freeway deceleration lanes were rear-end crashes resulting from speed differential. In Alabama, similarly, 201 crashes that occurred on freeway deceleration lanes were rear-end crashes, accounting for 71.28% of total freeway deceleration lane crashes from 2012 to 2016 (Critical Analysis Reporting Environment (CARE) (Computer Software), 2018). Therefore, there is an urgent need to reduce crash rates on freeway deceleration lanes.

Previous studies revealed that crash rates can be related to the deceleration lane length (Cirillo 1970, Chen, et al. 2009, Bauer and Harwood 1998, Bared, Giering and Warren 1999, Lord and Bonneson 2005). In other words, crash rates would be reduced with an optimal length of the deceleration lane. Referring to the deceleration lane design, three aspects that determine the deceleration lane length are recommended by the American Association of State Highway and Transportation Officials (AASHTO) *Green Book* (AASHTO 2018). The first is drivers' speeds while they initially diverge onto the auxiliary lane. The second is drivers' speeds at the end of the deceleration lane. The third is their manners of deceleration. Additionally, it requires the consideration of the speed differential between vehicles on the mainline and the ramp. However, the *Green Book* only provides the minimum lengths of deceleration lanes according to the design speed differential from the freeway mainline and off-ramp. Moreover, similarities of

recommended design lengths were found in the 2018 *Green Book* and 1965 *Blue Book*. The method to determine the minimum length remained the same between the two versions. Data that was used in both editions were collected in the 1930s. Thus, new data and research are required to update the design guide.

However, the majority of past studies on safety issues in freeway diverge areas focused on the analysis of crash data on deceleration lanes, which have not resulted in new guidelines for planners and designers with clear and updated criteria for appropriately designing deceleration lanes. Naturalistic driving data recorded diverging and deceleration behaviors of drivers and the vehicle braking mechanisms that can provide in-depth analysis of freeway deceleration lane design and develop new design guides.

1.2.2 Mobility Issues in Freeway Work Zones

As the National Highway System (NHS) is aging, an increasing number of work zones has occurred to address the growing needs of maintenance and construction. However, reduced operating speeds, narrowed lane widths and shoulder clearances, along with other construction activities, not only result in crashes but also cause excessive delays (FHWA Work Zone Facts and Statistics 2019). It has been well stated that the capacity per lane in the work zone is lower than that in the nonwork zone due to the reduced operating speed, lane width, and shoulder clearance (Yeom, Rouphail and Rasdorf 2015). Different passing behaviors along the work zone area can contribute to the loss of work zone capacity as well (Yeom, Rouphail and Rasdorf 2015). According to the Federal Highway Administration (FHWA), work zones led to approximately 24% of the nonrecurring freeway delay, which was equivalent to about 888 million vehicle hours in 2014 (FHWA Work Zone Facts and Statistics 2019). Moreover, work zone activities occurred

on roads that were often already congested, which brought more mobility issues on the busy arterials.

Thus, in order to arrange for construction work on the freeway and mitigate delay issues, the State Departments of Transportation (DOTs) and transportation agencies have applied various simulation models and planning tools to estimate or predict work zone capacity (Yeom, Rouphail and Rasdorf 2015, Weng and Meng 2015, Weng and Meng 2011, Transportation Research Board 2016, Weng and Meng 2012, Heaslip, et al. 2009, Kan, Ramezani and Benekohal 2014). In the sixth edition of the Highway Capacity Manual (HCM), the new freeway work zone capacity model estimates work zone capacity as a function of the lane closure severity index, barrier type, area type, lateral clearances, and day- or nighttime work conditions (Transportation Research Board 2016). Meanwhile, microscopic traffic simulation models, such as CORSIM (University of Florida, USA) and VISSIM (PTV Group, Germany), have been applied to estimate and calibrate the operational capacity of work zones with different lane closure configurations for decades (Heaslip, et al. 2009, Chatterjee, et al. 2009, Heaslip, Jain and Elefteriadou 2011). The calibration of these models requires quite an amount of field data to ensure the accuracy of the estimated results. Meanwhile, the planning-level work zone simulation tools such as QUEWZ (University of Florida, USA) and QuickZone (FHWA, USA) are also popular among DOTs, although it was reported that the QUEWZ and QuickZone were inaccurate due to outdated field data and parameters (Benekohal, Kaja-Mohideen and Chitturi 2003, Ramezani and Benekohal 2012, Ishimaru and Hallenbeck 2019, Trask, et al. 2015).

Although the freeway work zone capacity methodology proposed in the latest edition of the HCM has been substantially improved over previous editions, it is still limited by the macroscopic model, which cannot account for various work zone configurations (Weng and Meng

2011). In order to represent the increasingly complex freeway systems and freeway work zones, it was suggested that further calibrations are needed to address other issues with specific work zone configurations (Yeom, Rouphail and Rasdorf 2015).

1.3 Research Objectives

The Second Strategic Highway Research Program Naturalistic Driving Study (SHRP 2 NDS) has been used in many safety studies of driver behaviors. However, few studies focused on its application in studying highway geometric design and freeway operations. This dissertation investigates two innovative applications of NDS data: (1) freeway interchange deceleration lane design and (2) work zone mobility analysis.

Considering the safety issues of deceleration lane and outdated design guides, the first part of this dissertation is to analyze the impact of freeway deceleration lane design features on the drivers' diverging behavior and vehicle braking mechanisms. Past studies heavily relied on field data collection (e.g., radar gun) to collect vehicle speeds and trajectories. They have been either time-consuming or labor-intensive tasks, which may also result in erroneous conclusions due to intrinsic biases, such as false reading that resulted from incorrect calibration. To fill this gap, using the SHRP 2 NDS data is a new approach to investigate the driver behavior during daily trips through unobtrusive data gathering equipment and without experimental control (Van-Schagen, et al. 2011). Data including speed, acceleration–deceleration rate, brake status, traffic condition, pavement markings, etc., can provide insight into the interrelationship among drivers, vehicles, and deceleration lane designs.

The detailed objectives of the first part are to:

1. explore speed distributions along deceleration lanes and off-ramps;

2. investigate drivers' braking behaviors on deceleration lanes and off-ramps; and
3. develop a method for estimating minimum lengths of deceleration lane for naturalistic driving speed.

The second part of this dissertation is for an in-depth analysis of the impact of driver behavior on freeway work zone mobility. Compared with traditional field data collection techniques, the NDS data offers a unique opportunity to observe actual work zone layouts, traffic conditions, and driver behaviors while negotiating freeway work zones (Dingus, et al. 2015). Past data collection methods cannot collect driver characteristics, such as gender, age, risk index, etc. This part of the study was funded by the Region 4 UTC project. In the first phase of this project, researchers utilized the NDS data to evaluate capacity, car-following characteristics, and driver types in three freeway work zone configurations [two-to-one lane closure (LC 2-1), two-to-two shoulder closure (SC 2-2), and SC 3-3)] (Zhou, Turochy and Xu 2019). It was the first attempt to apply NDS data to study the headway distribution at work zones based on driver characteristics. In the second phase of this study, researchers collected more complete trips that traverse the entire work zone for further study.

The detailed objectives were set to:

1. develop gap and headway selection tables based on different driver characteristics (i.e., gender, age group, and risk perception) at four work zone configurations; and
2. perform a speed analysis to develop speed distribution models and identify key speed change points at work zones.

1.4 Dissertation Organization

This dissertation contains six chapters. Chapter 1 discusses the background, research objectives, and organization of the dissertation. A comprehensive review of previous research on SHRP 2 NDS data, freeway diverge areas, and freeway work zones is provided in Chapter 2. The methodology is documented in Chapter 3, which includes detailed discussions on data collection and reduction, site description, and data analysis methods. Chapter 4 discusses the results of freeway diverge area design and work zone mobility analysis. Chapter 5 concludes the findings from this study. Chapter 6 points out the limitations of this study and the needs of future studies.

Chapter 2. Literature Review

The literature review is divided into four sections for this dissertation to better summarize the existing literature regarding SHRP 2 NDS data, freeway diverge areas, and freeway work zones. First, an overview of SHRP 2 NDS data is provided. This is followed by a review of previous studies that related to freeway diverge area designs and their impacts. Next, a summary of research focused on work zone mobility is presented. Lastly, the final section summarizes the gaps in previous research and proposed work.

2.1 SHRP 2 NDS Data Overview

The purpose of SHRP 2 was to identify strategic solutions to three national transportation challenges: improving highway safety, reducing congestion, and improving methods for reviewing roads and bridges (The National Academies of Sciences, Engineering, and Medicine, 2020). Extensive data collection was conducted to achieve the goal of SHRP2, which offers a unique opportunity to address different research questions that were not able to be studied before. To fulfill the critical gap in data about driver behavior, the SHRP 2 Safety Program conducted the most comprehensive NDS that collected large-scale data from six states, including Florida, Indiana, New York, North Carolina, Pennsylvania, and Washington (Strategic Highway Research Program 2014). This section summarizes details of the NDS background, how the dataset can be accessed, and the NDS data applications on transportation studies.

2.1.1 Background

SHRP 2 NDS aims at improving safety and reliability for motorists and providing answers to key traffic- and safety-related questions (Dingus, et al. 2015). It involves understanding how

the driver interacts with and adapts to the vehicle, environmental condition, roadway geometric characteristics, and traffic control devices (TCDs) (Campbell 2012). The NDS database contains comprehensive video and vehicle sensor data collected from drivers and their vehicles over a three-year period in six locations across the United States. More than 3,500 volunteer drivers from the six study sites participated in this study with their everyday or "natural" driving behavior recorded. During three years of data collection from 2010 to 2013, over five million trips with nearly 50 million miles of driving were monitored with more than 4 petabytes (4 million gigabytes) of naturalistic information. The volunteer drivers were balanced distributed with approximately equal numbers of male and female in all age groups as presented in **Figure 1**. Six data collection areas were selected to represent a mix of road types and weather conditions. The participants were recruited through call centers and traditional methods (Campbell 2012). The call centers screened for eligible drivers and vehicles from household phone number lists at each NDS site. Traditional recruitment applied advertisements in various media such as the web-based Craigslist, flyers, presentations, mass mailing, and e-mails.

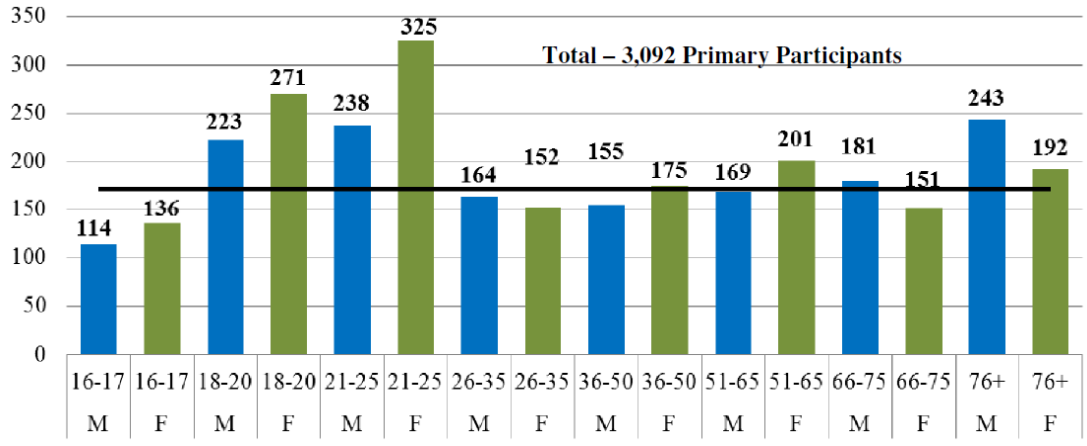

Figure 1 Primary participants enrolled in NDS by age and gender (Dingus, et al. 2015).

(Blue = male; green = female).

The Virginia Tech Transportation Institute (VTTI) developed the Data Acquisition System (DAS) to collect and maintain data of all trips made during the study period (Campbell 2012). The DAS was manufactured by American Computer Development, Inc., which includes forward radar, four video cameras, accelerometers, vehicle network information, Geographic Positioning System (GPS), on-board computer vision lane tracking plus other computer vision algorithms, and data storage capability (Dingus, et al. 2015). **Figure 2** shows the schematic view and key components of the DAS used in the data collection process. As demonstrated in **Figure 3**, the participant's vehicle was equipped with forward view (upper left), driver and left side view (upper right), instrument panel view (lower left), and rear and right view (lower right) cameras to record both the in-vehicle and out-of-vehicle environment. Data were continuously recorded while the participant's vehicle is operating. The study resulted in the successful collection of 4 petabytes of real-world driving video and sensor data (Strategic Highway Research Program 2014).

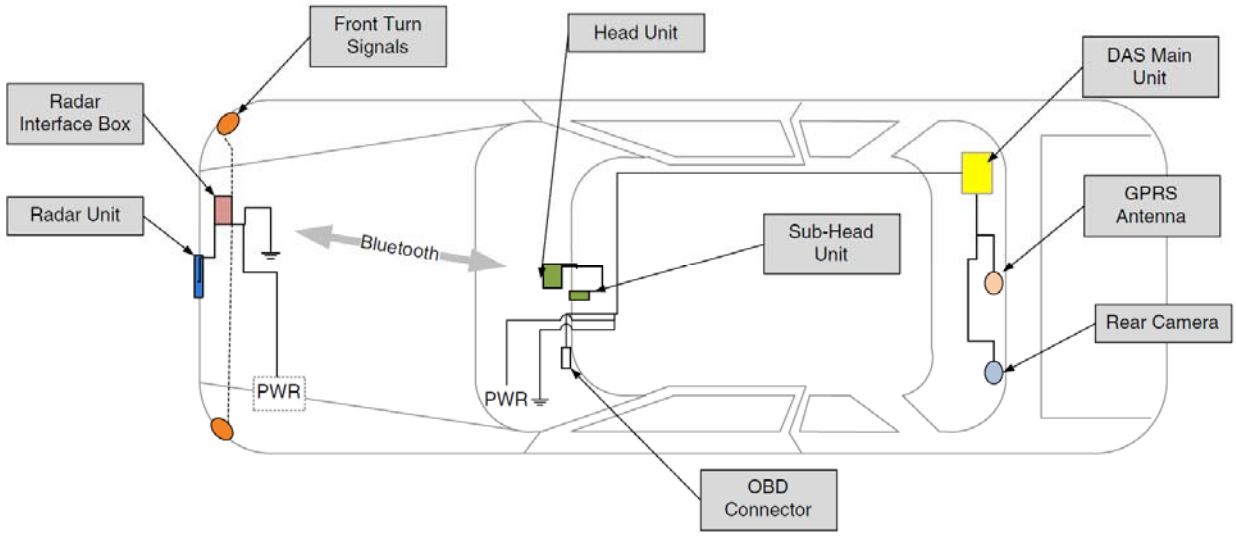

(a)

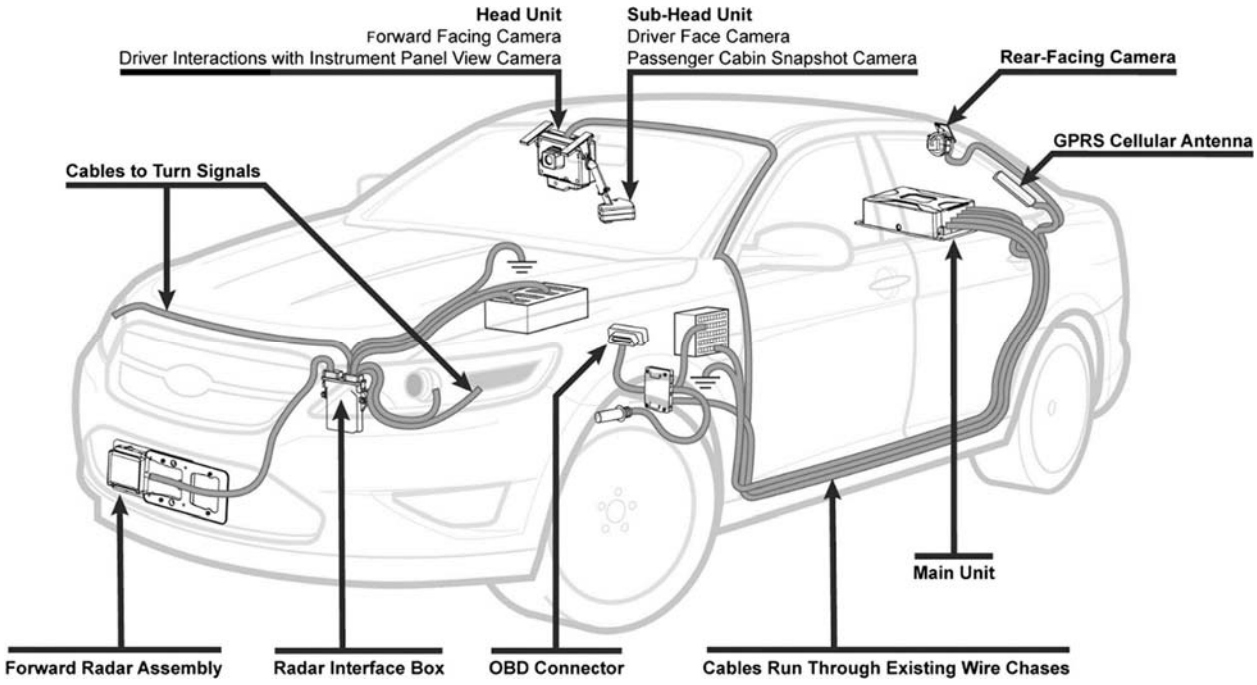

(*b*)

Figure 2 Installed DAS schematic: (*a*) top view diagram of DAS components (Dingus, et al. 2015); (*b*) side view diagram of DAS components (Antin, Lee and Perez, et al. 2019).

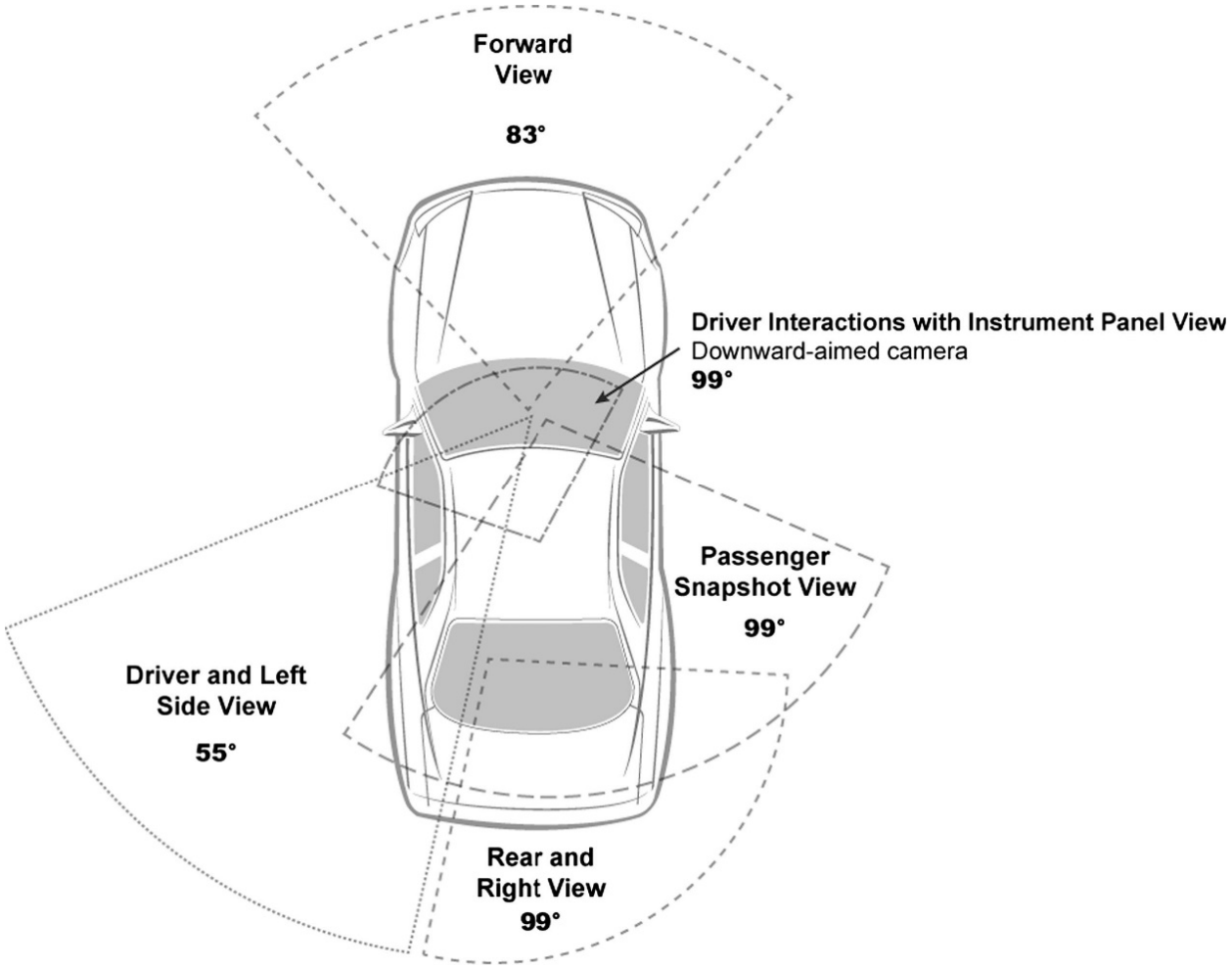
Forward
View
83°
Driver Interactions with Instrument Panel View
Downward-aimed camera
99°
Passenger
Snapshot View
99°
Driver and Left
Side View
55°
Rear and
Right View
99°

(*a*)

(*b*)

Figure 3 Video camera views: (*a*) fields of view for the DAS (Antin, Lee and Perez, et al. 2019); (*b*) quad image of four video camera views (Dingus, et al. 2015).

The NDS adheres to appropriate informed consent and privacy requirements as it deals with human subjects (Campbell 2012), which has been approved by the institutional review board (IRB) for the National Academies of Science (Dingus, et al. 2015). The IRB, also known as Independent Ethics Committee (IEC), Ethical Review Board (ERB), Research Ethics Board (REB), etc., is an administrative body established to protect the rights and welfare of human research subjects recruited to participate in research activities conducted under the auspices of the institution with which it is affiliated (U.S. Food & Drug Administration 2019). The data were protected from the moment they were collected through migration from vehicle to the final research repository (Dingus, et al. 2015). Human subjects protection in the NDS required the

secure usage of Personally Identifying Information (PII), which is any data that could potentially be used to identify a particular person. As NDS data collected driver face video, GPS traces that might contain the participant's home, work location, or school, etc., a Certificate of Confidentiality was secured from the National Institute of Mental Health (NIMH) to protect PII data collected during the data collection period, so that the researchers and study sponsors cannot be forced to disclose information that may identify any participants (Dingus, et al. 2015). Nonidentifying and deidentified data are allowed to be widely shared and the data was encrypted from the moment it was collected. Only qualified researchers can access the PII through a secure data enclave (SDE), which is a physically isolated environment that restricts data access and protects the PII (Dingus, et al. 2015). Thus, the NDS data were divided into two portions (InSight and InDepth) with regard to their nature.

2.1.2 InSight and InDepth

The InSight Website (https://insight.shrp2nds.us/) contains a subset of NDS data that excludes PII but is publicly available. Any registered researchers who had successfully taken the IRB training and passed the exam can access this type of data through the InSight Website online. The InSight data are divided into four categories: vehicle, drivers, trips, and events. The information provided under each category is summarized in **Table 1**. The data was either directly captured by the DAS during the data collection period or through questionnaire surveys. A query builder is provided on the website to select variables and conditions, submit a query, assess results, build cross-tabulations, view graphs of output, and view the table of individual records for researchers' needs. This allows for preliminary analysis of aggregated data or getting some preview and background on the data for further request and analysis. The data on the InSight Website has been extracted and coded through manual review of the videos by VTTI in the SDE

that can only be viewed, without any sort of extraction or export of data. Unique identifiers were developed for each event, trip, driver, and vehicle to allow for efficient PII protection and easy linkages among them to perform analysis. A driver may have multiple trips and events associated, and a trip may consist of several events.

Table 1 Summary of InSight data categories.

Vehicles	Vehicle types (car, truck, van, etc.)
	Vehicle ages and condition
	Amount of data collected per vehicle
	Quantities of vehicles installed (the number of vehicles that had a system installed and were actively collecting data for at least one day during the calendar month)
	Vehicle technologies and equipment
Drivers	Numbers of participating drivers
	Amount of data collected per driver
	Driver demographics and driving history (the demographic characteristics and driving knowledge of participating drivers)
	Driver physical and psychological state (physical strength tests including left- and right-hand grip strength and a rapid pace walk test; psychological tests including Barkley's ADHD

	screening, risk perception, sensation seeking scale survey, etc.)
	Driver participation experience
Trips	Summary measures describing trips
	Trip length, duration, start time, stop time
	Min, max, mean for speed, acceleration
	Trip summary record table
	Trip density maps
Events	Crashes, near-crash, and baseline event records
	Events by type and severity
	Event viewer

The second portion of NDS data is known as InDepth, which data includes information that may potentially result in identifying the participants. These data contain time-series data and video data, which are not available online (InSight). To access the data at InDepth, further investigation as to the eligibility of the involved researchers and research questions must be performed. An IRB application should be submitted regarding research questions, the details of data variables requested, how will the data be used, how the data will be maintained and secured, etc. Finally, authorized researchers who obtained a data use license (DUL) will be provided with the requested NDS data from InDepth under certain agreements and fees.

2.1.3 NDS Data Applications in Transportation

NDS data applications in transportation paid more attention to safety aspects, as the intent of NDS is to address traffic- and safety-related questions (Dingus, et al. 2015). The data fill in the

gap about driver behavior, including how drivers really drive, how they interact with vehicular, roadway, and environmental features, what they are doing just before they crash, and why some risky situations do not result in crashes. Thus, existing NDS data applications on transportation mainly concentrate on refining existing countermeasures and developing new ones to reduce crashes, injuries, and fatalities. A recent study investigated the changes in driving behavior, before, during, and after near-crash events on freeways by applying NDS data to identify the driving patterns (Ali, Ahmed and Yang 2020). Victor *et al*. performed a study to determine the relationship between driver inattention and crash risk in lead-vehicle pre-crash scenarios by utilizing NDS data (Victor, et al. 2015). The results of this study were reported to support distraction policy, regulation, and guidelines; improve intelligent vehicle safety systems; and teach safe glance behaviors. Wu and Lin explore driver perception time prior to the occurrence of the safety-related event by using NDS data (Wu and Lin 2019). They analyzed a total of 1,417 rear-end crashes and near-crashes, and reported that critical driving situations, driving environment, and driver behavior are influential factors in explaining the variation of driver perception times in safety-related events. Hao *et al*. performed an in-depth investigation of crashes involving roadway objects and animals based on NDS data including 2,689 events (Hao, et al. 2020). The results indicated that driver errors, involvement of secondary tasks, roadway characteristics, lighting condition, and pavement surface condition are significant factors that contributed to the occurrence and increased severity outcomes of crashes.

NDS data can be used to evaluate geometric design features. A study conducted by Hallmark *et al*. evaluated driving behavior on rural two-lane curves using the SHRP 2 NDS data to propose appropriate countermeasures for mitigating crash rates on rural horizontal curves (Hallmark, et al. 2015). The results suggested that better curve delineation with delineation

countermeasures would allow drivers to better gauge upcoming changes in roadway geometry with better speed selection and decreased risk of an encroachment. Wu and Xu analyzed right-turn driver behavior at signalized intersections with NDS data (Wu and Xu 2017). This research revealed that drivers have high acceleration and low observation frequency under Right-Turn-On-Red (RTOR) controlled intersections. It suggested that the implementation of traffic safety countermeasures at signalized intersections is necessary to reduce right-turn crashes.

There have been some studies focused on the impacts of adverse weather conditions on driver behaviors. A group of researchers from the University of Wyoming investigated the effect of adverse weather on driver speed selection behavior by using SHRP 2 NDS data (Khan, Das and Ahmed 2020). They suggested that a weather-specific distribution should be used to model driver behavior more representatively in microsimulation platforms. By employing NDS data, another study showed how drivers compensated differently according to weather conditions to avoid the crash event and provided a discrimination threshold in vehicle kinematics (e.g., speed, acceleration rates, yaw rates, etc.) between normal and risky driving patterns in both rainy and clear weather conditions (Ali, Ahmed and Yang 2020). The same group of researchers also explored the impacts of heavy rain on speed and headway behaviors. They compared driver behavior in clear and heavy rain conditions using the trips with the same driver, same vehicle, and same traversed routes. The study concluded that drivers were more likely to reduce their speed by more than 5 kilometers per hour on average below the speed limits in heavy rain than in light rain (Ahmed and Ghasemzadeh 2018).

NDS data can help with connected vehicle (CV) application development as well. A study utilized trajectory analysis and unsupervised machine learning techniques to identify normal and risky driving patterns based on vehicle kinematics data from NDS (Ali, Ahmed and Yang 2020).

It stated that the identification of these patterns can distinguish between different driving patterns in a CV environment using basic safety messages.

2.2 Research on Freeway Diverge Areas

This section covers a review of design guides and relevant research in freeway diverge areas. Firstly, a review of current design guidance in the AASHTO *Green Book* was provided. This was followed by safety and operational effects of freeway diverge areas, specifically freeway deceleration lanes. Next, driver diverge maneuvers regarding deceleration rates and diverge speeds when exiting the freeway were discussed. Finally, the related research that utilized NDS data was summarized.

2.2.1 AASHTO Design Policy

According to the *Green Book* definition, a deceleration lane is a speed-change lane that intends to minimize conflicts between vehicles on the mainline and diverging area (AASHTO 2018, Bared, Giering and Warren 1999). There are two general forms of declaration lane (as shown in **Figure 4**): the parallel-design which has an added lane for changing speed and the tapered design which provides a direct exit at a flat angle (AASHTO 2018). The length of a deceleration lane is measured from the point of a 12-ft right-tapered wedge, or a 12-ft added parallel lane to the point of the exit ramp curvature beginning (AASHTO 2018). In practice, it is hard to control and measure the beginning of the exit ramp alignment because exit ramp curvature beginning is difficult to determine. Thus, this study measured the deceleration lane length from the same starting point defined by AASHTO to the point of the physical gore (after the painted nose).

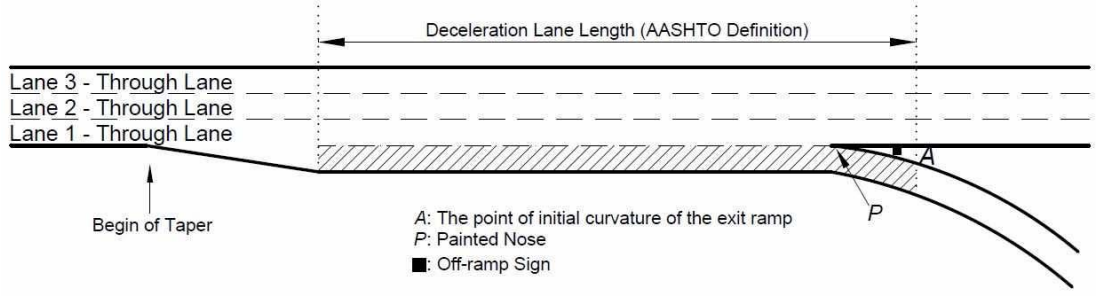

(*a*)

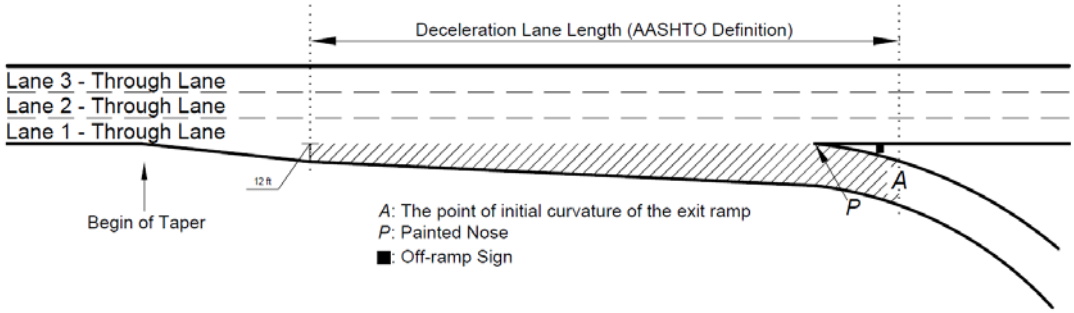

(*b*)

Figure 4 Definition of deceleration lane length: (*a*) parallel-design deceleration lane and (*b*) tapered-design deceleration lane.

Equations 1 and **2** present the procedure of calculating the minimum deceleration lane length in the 1965 *Blue Book* (AASHTO 1965). AASHTO policies used a basic two-step process for establishing design criteria (Torbic, et al. 2012). Deceleration is accomplished as follows: the driver removes his or her foot from the gas pedal, the vehicle slows in gear for a period of time (assumed to be 3 seconds) without braking, and then the driver applies the brake pedal and decelerates at a comfortable rate. The length is primarily determined by the speed differential between the average speed on the mainline and the off-ramp.

$$L_{Decel} = 1.47V_h t_n - 0.5d_n(t_n)^2 + \frac{(1.47V_r)^2 - (1.47V_a)^2}{2d_{wb}} \quad (1)$$

$$V_a = \frac{1.47V_h + d_n t_n}{1.47} \quad (2)$$

Where, L_{Decel} = Deceleration lane length, ft

V_h = Highway speed, mi/h

V_a = Speed after t_n seconds of deceleration without brakes, mi/h

V_r = Entering speed for controlling exit ramp curve, mi/h

t_n = Deceleration time without brakes (assumed to be 3 s), s

d_n = Deceleration rate without brakes, ft/s^2

d_{wb} = Deceleration rate with brakes, ft/s^2

Two assumptions were made during calculation (Fitzpatrick, Chrysler and Brewer 2012) that (1) most vehicles travel at the average speed instead of the design speed when traffic volumes are low (e.g., on a freeway with a 70 mi/h design speed, the assumption is that a driver will enter the auxiliary lane at 58 mi/h as presented in **Table 2**.); and (2) a 3s deceleration before braking is applied on the taper section, which results in two deceleration rates (d_n and d_{wb}).

Table 2 Minimum deceleration lane lengths for exit terminals with flat grades of less than 3%, adopted from AASHTO *Green Book* (2018).

Deceleration Lane Length, L_a (ft) for Design Speed of Controlling Feature on Ramp, V' (mph)										
Highway Design Speed, V (mph)	Diverge Speed, V_a (mph)	Stop Condition	15	20	25	30	35	40	45	50
		Average Running Speed at Controlling Feature on Ramp, V'_a (mph)								
		0	14	18	22	26	30	36	40	44
30	28	235	200	170	140	–	–	–	–	–
35	32	280	250	210	185	150	–	–	–	–
40	36	320	295	265	235	185	155	–	–	–

45	40	385	350	325	295	250	220	–	–	–
50	44	435	405	385	355	315	285	225	175	–
55	48	480	455	440	410	380	350	285	235	–
60	52	530	500	480	460	430	405	350	300	240
65	55	570	540	520	500	470	440	390	340	280
70	58	615	590	570	550	520	490	440	390	340
75	61	660	635	620	600	575	535	490	440	390
80	64	705	680	665	645	620	580	535	490	440

V = design speed of highway (mph)

V_a = average running speed on highway (i.e., diverge speed) (mph)

V' = design speed of controlling feature on ramp (mph)

V'_a = average running speed at controlling feature on ramp (mph)

L_a = deceleration lane length (ft)

The *Green Book* provides minimum requirements for the design of deceleration lengths for exit terminals. **Table 2** adopted the table available in the *Green Book* 2018 edition. The AASHTO's deceleration lane lengths from **Table 2** were calculated from old studies in which data was collected in the 1930s (Fitzpatrick, Chrysler and Brewer 2012). The only difference between the 2004 *Green Book* and the 1965 *Blue Book*, regarding minimum lengths of freeway deceleration lanes, is that the taper length is included in the deceleration lane length in the 1965 *Blue Book* while being listed separately in the 2004 *Green Book*. Comparing three recent versions of the *Green Book*, parameters in **Equations 1** and **2** turn out to be the same in 2018, 2011, and 2004 editions (AASHTO 1965, AASHTO 2004, AASHTO 2011, AASHTO 2018). This revealed that the minimum deceleration lane lengths provided in **Table 2** from the *Green Book* 2018 edition

were calculated from the data collected in the 1930s. Given that vehicle technology has been improved and driver behaviors and driving patterns have been changed, these values need to be updated based on the current drivers' diverging behavior and vehicle braking mechanisms.

2.2.2 Safety and Operational Impacts of Freeway Deceleration Lane

If the deceleration distance was judged to be short, a harder deceleration would be applied by the diverging driver which would also start on the mainline before the deceleration lane starts. When the following vehicles, which could be either on the freeway mainline or deceleration lane, do not take action accordingly, a conflict or a crash would happen. Similarly, if the deceleration lane was too long, the diverging driver would be accelerating on the deceleration lane. When the leading vehicles on the deceleration lane are at a lower speed, and the diverging driver does not accommodate accordingly, a conflict or a collision may occur. These examples relate operational performance to safety. There have been a lot of studies that explored safety and operational impacts on the freeway deceleration lane.

FHWA conducted a study to model crash frequency on deceleration lanes, but they found it was difficult to develop models because of the low crash frequencies at most locations (Bauer and Harwood 1998). They finally applied the negative binomial regression in modeling crash frequency and the geometric design and traffic volume characteristics of ramps. This method has been widely used among researchers who focused on the safety performance of freeway diverge areas. There have been several studies utilized regression models to optimize the deceleration lane length and the configuration of off-ramps (Cirillo 1970, Chen, et al. 2009, Bauer and Harwood 1998, Bared, Giering and Warren 1999, Lord and Bonneson 2005). However, the results from past studies were inconsistent or even contradictory.

Some studies suggested that increasing the deceleration lane length would reduce crash rates. A study conducted in 1970 identified the relationship of crashes to lengths of deceleration lanes (Cirillo 1970). Data from 20 states were collected between 1950 to 1965 and 700 weaving areas were analyzed. The lengths of deceleration lane were categorized in less than 200 ft, between 200 ft and 299 ft, between 300 ft and 399 ft, …, and more than 700 ft. It was found that longer deceleration lane has few crashes with the percentage of diverging traffic being less than 6% of the mainline volume. The results also compared the benefits from additional lengths of deceleration lane and acceleration lane. It was concluded that the deceleration lane has less reduction in crashes compared to acceleration lane with the length increasing. This study used the crash rates in the analysis, which could be misleading as locations with lower traffic volumes would have high rates and vice versa. Similar to this study, Bared, Giering, and Warren evaluated the safety performance of acceleration and deceleration lane lengths (Bared, Giering and Warren 1999). They developed a crash model for ramps from a sample of Interstate highways in Washington State, which contained 276 exit ramps equally located in rural and urban areas. The results of this study illustrated the importance of providing longer deceleration lane since deceleration lane has higher number of crashes than acceleration lane related to their lengths due to the higher complexity of the driver's tasks on deceleration lanes compared to acceleration lanes. Similar findings were achieved by Twomey *et al*., who identified that deceleration lane of 900 ft or more can reduce traffic friction on through lanes, therefore, reducing crash rates (Twomey, et al. 1993). Wang *et al*. also evaluated the impacts of various factors on injury severity at freeway diverge areas (Wang, Chen and Lu 2009). They collected crash data and roadway information from 231 freeway exit segments in Florida and applied partial proportional odds regression to predict injury severity at freeway diverge areas. They found that the length of deceleration lanes is a

significant factor affecting injury severity and addressed that a longer deceleration lane is more likely to reduce injury severity.

On the contrary, some studies implied that increasing the deceleration lane length would increase crash occurrence. Garcia and Romero found that a long deceleration lane would encourage accelerating maneuver before drivers exit the deceleration lane (Garcia and Romero 2006). As a result, they noted that vehicles do not initially decelerate, instead, an acceleration maneuver often appears before drivers start braking on the deceleration lane. They also found that overtaking scenarios occur on the excessively long deceleration lane in order to precede the vehicle on the mainline, thus increasing crash risks at freeway diverge areas. These results are also consistent with other studies on this topic (Chen, et al. 2009, Chen, et al. 2011, Chen, Zhou and Lin 2014). Chen *et al*. conducted a traffic conflict study to evaluate the safety performance of left-side off-ramps (Chen, et al. 2011). They collected crash data from 11 left-side and 63 similar right-side freeway diverge areas in Florida and the left-side off-ramp were found to have higher average crash counts, crash rate, and percentage of severe crashes. They also developed a crash predictive model to identify the factors that contribute to the crashes. The model revealed that the crash frequency increases with the lengthening of the deceleration lane for both left-side and right-side diverge areas. Another study conducted by Chen, Zhou and Lin evaluated the safety and operational performance of different deceleration lane lengths at freeway diverge areas (Chen, Zhou and Lin 2014). They collected crash data from 218 sites and categorized them into nine groups based on their lengths for crash analysis. 360 simulation models were developed to examine the operational effects of deceleration lane lengths for one-lane exits with parallel/tapered designs and two-lane exits with parallel design. Different scenarios considered the number of exit lanes, through movement lanes, exiting volume, design speed on the freeways and exits, and the

deceleration lane lengths. For both one and two-lane exits, crash counts and crash rates were compared to deceleration lengths. Their results indicated that the optimal deceleration lane length between 500 ft and 700 ft significantly reduces the crash severity and delay for through traffic. They also noted that when the deceleration lane is long, crash frequencies and crash rates start increasing. However, drivers may accelerate which caused the extra deceleration distance to have no positive safety effect at a long deceleration lane. When considering different types of off-ramps, Lu *et al*. concluded that parallel-designed sites with a one-lane exit had the lowest crash frequency and crash rate (Lu, et al. 2010).

2.2.3 Diverge Maneuver

When the assigned driving tasks increase complexity, drivers' maneuver becomes more complex. A series of decisions should be made when drivers proceed to exit a freeway. First, a satisfactory gap and a diverge point with appropriate diverge speeds would be selected where drivers change lanes from the freeway mainline to the deceleration lane. After accomplished the first step, if the deceleration lane was judged to be long, the driver might not decelerate immediately; instead, either slight acceleration or deceleration could be applied. Then, drivers would select a point to start decelerating with an initial deceleration rate. Their deceleration rate would increase when they are approaching the gore area. Finally, a final speed based on the controlling features (e.g., stopped controlled intersection, signalized intersection, sharp curvature, etc.) of off-ramps would be selected.

Deceleration rates of deceleration lanes vary depending on the length, which is initially calculated based on the speed differential between the average speed on the mainline and the off-ramp. The AASHTO *Green Book* provides a table of minimum lengths of freeway deceleration lane but does not offer a table of deceleration rates they used to determine deceleration lane length

(Torbic, et al. 2012). However, based on the NCHRP 730 report, two methodologies to back-calculate deceleration rates used in the *Green Book* 2004 edition were provided with one using **Equations 1** and **2**, and the other using a constant deceleration approach (Torbic, et al. 2012). **Table 3** andTable 4 summarized corresponding deceleration rates used in the *Green Book* 2004 edition. As mentioned in Section 2.2.1, the minimum deceleration lane lengths values presented in **Table 2** remained the same in the *Green Book* 2004, 2011, and 2018 editions. Thus, although **Table 3** and**Table** 4 were adapted from the *Green Book* 2004 edition, they actually provide corresponding deceleration rates for the latest version of *Green Book* (2018 edition). In this NCHRP report, the authors compared the back-calculated deceleration rates to the rates measured from the field. They found that field-measured deceleration rates were lower than the derived AASHTO values, which indicated that the *Green Book* assumed higher deceleration rates than what drivers really applied. This research also found that drivers applied various deceleration rates while driving on the deceleration lane instead of constant deceleration rates.

Table 3 Corresponding deceleration rates for minimum deceleration lane lengths, adopted from AASHTO *Green Book* (2004).

Deceleration Rate (ft/s^2) for Design Speed of Controlling Feature on Ramp (mph)										
Highway Design Speed (mph)	Diverge Speed (mph)	Stop Condition	15	20	25	30	35	40	45	50
		Average Running Speed at Controlling Feature on Ramp (mph)								
		0	14	18	22	26	30	36	40	44
1st Deceleration Rates (ft/s^2) While Coasting in Gear used to Reproduce Deceleration Lane Lengths										
30	28	-1.04	-1.04	-1.04	-1.04	–	–	–	–	–
35	32	-1.53	-1.53	-1.53	-1.53	-1.53	–	–	–	–

40	36	-1.52	-1.52	-1.52	-1.52	-1.52	-1.52	–	–	–
45	40	-2.01	-2.01	-2.01	-2.01	-2.01	-2.01	–	–	–
50	44	-2.51	-2.51	-2.51	-2.51	-2.51	-2.51	-2.51	-2.51	–
55	48	-2.01	-2.01	-2.01	-2.01	-2.01	-2.01	-2.01	-2.01	–
60	52	-2.98	-2.98	-2.98	-2.98	-2.98	-2.98	-2.98	-2.98	-2.98
65	55	-2.50	-2.50	-2.50	-2.50	-2.50	-2.50	-2.50	-2.50	-2.50
70	58	-2.50	-2.50	-2.50	-2.50	-2.50	-2.50	-2.50	-2.50	-2.50
75	61	-2.99	-2.99	-2.99	-2.99	-2.99	-2.99	-2.99	-2.99	-2.99
2^{nd} Deceleration Rates (ft/s^2) While Braking used to Reproduce Deceleration Lane Lengths										
30	28	-5.75	-6.42	-5.49	-8.97	–	–	–	–	–
35	32	-5.83	-5.75	-5.38	-6.68	-10.29	–	–	–	–
40	36	-5.66	-5.22	-5.11	-5.66	-5.95	-4.42	–	–	–
45	40	-6.38	-6.05	-5.68	-6.91	-6.83	-6.18	–	–	–
50	44	-6.74	-6.57	-6.28	-7.20	-7.86	-6.55	-6.23	N/A	–
55	48	-7.10	-7.08	-6.86	-7.55	-7.86	-7.46	-7.49	-7.86	–
60	52	-7.07	-7.19	-6.99	-7.45	-7.70	-7.34	-6.98	-7.43	-16.84
65	55	-7.55	-7.43	-7.27	-8.03	-7.76	-7.49	-7.51	-7.66	-9.60
70	58	-7.40	-7.41	-7.27	-7.77	-7.53	-7.60	-7.45	-7.54	-8.17
75	61	-7.76	-8.02	-7.90	-8.06	-7.85	-7.65	-7.70	-7.62	-8.49

Table 4 Corresponding deceleration rates for minimum deceleration lane lengths assuming a constant deceleration, adopted from AASHTO *Green Book* (2004).

Deceleration Rate (ft/s^2) for Design Speed of Controlling Feature on Ramp (mph)

Highway Design Speed (mph)	Diverge Speed (mph)	Stop Condition	15	20	25	30	35	40	45	50
		Average Running Speed at Controlling Feature on Ramp (mph)								
		0	14	18	22	26	30	36	40	44
30	28	-3.59	-3.16	-2.91	-2.30	–	–	–	–	–
35	32	-3.93	-3.56	-3.59	-3.14	-2.50	–	–	–	–
40	36	-4.36	-4.01	-3.95	-3.72	-3.60	-2.75	–	–	–
45	40	-4.47	-4.31	-4.22	-4.07	-3.98	-3.42	–	–	–
50	44	-4.79	-4.62	-4.50	-4.40	-4.30	-3.91	-3.06	-2.07	–
55	48	-5.16	-4.98	-4.84	-4.77	-4.61	-4.31	-3.80	-3.22	–
60	52	-5.49	-5.39	-5.33	-5.19	-5.07	-4.79	-4.33	-3.96	-3.44
65	55	-5.71	-5.63	-5.59	-5.47	-5.38	-5.19	-4.77	-4.51	-4.18
70	58	-5.88	-5.78	-5.74	-5.63	-5.56	-5.41	-5.06	-4.86	-4.52
75	61	-6.06	-5.97	-5.89	-5.80	-5.70	-5.67	-5.32	-5.18	-4.92

Generally, conventional studies employed field observation to monitor driving behaviors of diverging drivers on deceleration lanes and off-ramps. Garcia and Romero concluded that the drivers start to decelerate before exiting the mainline with a speed reduction of 10.5 mph even on a long deceleration lane (Garcia and Romero 2006). Based on the NCHRP project, vehicles that diverge early on the deceleration lane are likely to diverge at speeds that are close to freeway speeds while late diverging vehicles have lower diverging speeds (Torbic, et al. 2012). A recent study conducted by Ma *et al*. used an advisory speed limit sign located on the freeway deceleration lane to accommodate the speed changes ahead of the gore area in China (Ma, et al. 2019). They

collected 12 hours of data that contains 480 vehicles speed profiles from seven sections at 3 similar freeway diverge areas. They observed an average10 kmph (6.21 mph) speed reduction on the mainline before entering the deceleration lane at tapered-designed locations based on the speed profiles without advisory speed limit signs. The authors also observed a slight acceleration around the gore areas, which they explained might be due to sufficient deceleration on the deceleration lane.

Driving simulators were also used for this topic. Three groups of researchers led by Calvi did three studies on diverging performance on deceleration lanes with a driving simulator (Calvi, Benedetto and De Blasiis 2012, Calvi, Bella and D'Amico 2015, Calvi, et al. 2020). The first study simulated three different traffic scenarios to analyze driving performance while approaching a diverge area and decelerating during the exiting maneuver (Calvi, Benedetto and De Blasiis 2012). Thirty drivers were recruited to collect their lateral position, speed, and deceleration. This study revealed that lower traffic volumes result in higher existing speeds, higher average and maximum deceleration rates, and earlier braking on the mainline. The second study was conducted to analyze the effects of traffic flow and deceleration lane geometry on the driving performance of diverging drivers (Calvi, Bella and D'Amico 2015). This study took thirty-one volunteers in the experiments with parallel and tapered designed deceleration lanes under low and high traffic flow conditions. Findings from the second study indicated that the taper type of deceleration lane contributes to the significantly higher speed difference. Furthermore, lower traffic volumes lead to higher deceleration rates. The most recent study by Calvi *et al*. validated the driving simulator for use by designers in adopting the best solution for freeway acceleration and deceleration lanes (Calvi, et al. 2020). This time ninety participants took part in the experiment. They were recorded in real and simulated scenarios using an instrumented vehicle and a driving simulator for driving performance

of merging and diverging maneuvers. The authors compared the field and simulation data in terms of driving speeds and trajectories and validated the simulator usage. This study suggested that drivers significantly reduced their speeds before diverging from the mainline and entering the deceleration lane based on both field and simulator results.

2.2.4 Related Research that Utilizing NDS Data

Few studies that utilizing NDS data focused on freeway diverge areas. Brewer and Stibbe used SHRP 2 NDS data to identify relationships between ramp design speed characteristics and drivers' choices of operating speeds on those ramps (Brewer and Stibbe 2019). The results of this study suggested that the type of traffic control at crossroad terminal has a larger effect on off-ramps speed selection. Recent research explored the lane-change behaviors in freeway off-ramp areas by utilizing Shanghai NDS data (Zhang, et al. 2018). The authors identified 433 lane-change events with trajectory data and applied the speed variance of the following vehicle on the deceleration lane as a safety surrogate index. However, this study was more on the modeling that did not provide practical insights into freeway diverge area design.

2.3 Research on Freeway Work Zone Mobility

This section synthesizes relevant literature on the topic of freeway work zone mobility. Firstly, a review of work zone capacity estimation was provided in terms of parametric, nonparametric, and simulation-based methods. This follows by headway and gap distribution of freeway work zones. Next, speed studies regarding speed distribution and speed change in work zones were discussed. Finally, the related research that utilized NDS data was summarized.

2.3.1 Capacity Estimation

Numerous studies have focused on work zone capacity issues, including several methods that have been proposed to estimate and predict work zone capacity. These methods can be divided into three categories, i.e., parametric, nonparametric, and simulation-based (Weng and Meng 2015). The following sections summarize these methods.

2.3.1.1 Parametric Method

Many studies have used the parametric method to estimate work zone capacity. This method uses a predetermined form to predict work zone capacity based on the field data so that the coefficients of predictors can be determined (Lu, et al. 2018).

In 1994, Krammes and Lopez developed a multi-regression model to estimate the short-term work zone capacity based on the data collected in 33 work zones in Texas (Krammes and Lopez 1994). It only included parameters such as work intensity, presence of ramps, and heavy vehicle adjustment factor. Therefore, Kim *et al*. proposed another multi-regression model that considered more capacity-influencing factors for short-term work zones, including the number of closed lanes, lane closure locations, heavy vehicle percentage, lateral distance to the lane closure, work zone length, work intensity, and the work zone grade (Kim, et al. 2000). As for long-term work zones, a generic multiplicative model was proposed to investigate capacity with lane closure conditions in Ontario, Canada (Al-Kaisy, Zhou and Hall 2000, Al-Kaisy and Hall 2003). The variables included in the model are temporal variations, grade, day of week, and weather conditions, which were found to have significant impacts on the long-term work zone capacity.

In addition, the sixth edition of the HCM offered detailed guidance on determining work zone capacity. It defined the capacity as “the maximum sustainable hourly flow rate at which

persons or vehicles reasonably can be expected to traverse a point or a uniform section of a lane or roadway during a given time period under the prevailing roadway, environmental, traffic, and control conditions" (Transportation Research Board 2016). Upon the work zone capacity, Yoem, Rouphail, and Rasdorf performed an extensive literature search, established a relationship between the queue discharge rate (QDR) and pre-breakdown capacity (PBC), and provided a regression model for estimating work zone capacity under different conditions (Yeom, Rouphail and Rasdorf 2015). This work, currently included in the sixth edition of the HCM, was based on 90 archival literature sources and 12 data sets collected from the field. It stated that freeway work capacity corresponds to the maximum sustainable flow rate immediately preceding a breakdown, which is the PBC (Transportation Research Board 2016). However, it is not feasible to measure the pre-breakdown value in the work zone. Thus, the HCM proposed a method to calculate the QDR first, which can be easily measured via video cameras or other data collection tools, and then converted the QDR to the corresponding PBC by using a conversion ratio. The QDR is calculated as follows in **Equation 3**:

$$QDR_{WZ} = 2{,}093 - 154 \times LCSI - 194 \times f_{Br} - 179 \times f_{AT} + 9 \times f_{LAT} - 59 \times f_{DN} \quad (3)$$

Where, QDR_{WZ} = The average 15-min queue discharge rate at the work zone bottle neck

$LCSI$ = Lane closure severity index

f_{Br} = Indicator variable for barrier type (0 for concrete; 1 for cone or drum)

f_{AT} = Indicator factor for area type (0 for urban; 1 for rural)

f_{LAT} = Lateral distance from the edge of travel lane adjacent to the work zone to the barrier, barricades, or cones (0-12 ft)

f_{DN} = Indicator variable for daylight or night (0 for daylight; 1 for night)

The lane closure severity index is illustrated In Exhibit 10-15 in the HCM. It also applies to shoulder closures without lane closures. This index is calculated as follows in **Equation 4**:

$$LCSI = \frac{1}{OR \times N_O} \quad (4)$$

Where, $LCSI$ = Lane closure severity index

OR = Open ratio, the ratio of the number of open lanes during road work to the total (or normal) number of lanes (decimal)

N_O = Number of open lanes in the work zone

After obtaining the QDR, the PBC can be calculated as follows in **Equation 5**:

$$C_{WZ} = \frac{QDR_{WZ}}{100 - a_{WZ}} \times 100 \quad (5)$$

Where, C_{WZ} = Pre-breakdown flow rate

a_{WZ} = Percentage drop in pre-breakdown capacity at the work zone due to queuing conditions (%), an average value of 13.4% in freeway work zones

Another way to estimate the work zone capacity is to derive the capacity from speed-flow curves. Over the years, some researchers adopted this method to derive information from the prediction model (Weng and Meng 2015, Sarasua, et al. 2006, Racha, et al. 2008, Avrenli, Benekohal and Ramezani 2011, Bharadwaj, Edara, et al., Traffic Flow Modeling of Diverse Work Zone Activities 2018). For example, Benekohal *et al*. presented a step-by-step methodology to estimate the operating speed and capacity on lane closure two-to-one work zones in Illinois (Benekohal, Kaja-Mohideen and Chitturi 2004). The authors recorded 30 hours of video data from 11 work zones on the Interstate and compared the field data with predictions for validation. In this study, the operating speed was modeled as a function of work intensity, lane width, lateral clearance, and other factors to examine the influences of external factors on traffic speed. Sarasua *et al*. conducted a study to develop the speed-flow curves for lane closure in two-to-one, three-to-two, and three-to-one work zones (Sarasua, et al. 2006). The authors revealed that passenger car equivalents (PCEs) differed for various speed ranges, and PCEs for various speed groups are recommended in calculating capacity. Racha *et al*. collected field data from 22 work zones in South Carolina and modeled the work zone capacity from the relationships among speed, flow, and density (Racha, et al. 2008). The authors also demonstrated that a non-linear hyperbolic model was developed to depict the speed–density relationship for two-to-one lane closure configurations of Interstate highway work zones. Avrenli *et al*. examined the speed-flow relationship of work zones with no lane closure (Avrenli, Benekohal and Ramezani 2011). The authors developed two nonlinear models for work zones with no lane closure under uncongested and congested conditions. It was found that the flow rate of the free-flow regime was much lower than the capacity that the HCM 2000 model predicted.

2.3.1.2 Nonparametric Method

When estimating the work zone capacity, sometimes it is not feasible to describe the capacity by mathematical functions due to nonlinear relationships and complex interactions between a large number of variables and capacity (Adeli and Jiang 2003). Therefore, several non-parametric methods, such as neural-fuzzy logic, decision tree, and ensemble tree models, have been applied to provide work zone capacity estimations (Weng and Meng 2015). The nonparametric method is a technique that does not assume that the structure of a model is fixed (Corder and Foreman 2014). Because of fewer assumptions being made by nonparametric methods, these models are more flexible, robust, and applicable to nonquantitative data (Yau 2013). However, it was also pointed out that nonparametric approaches typically require generous historical traffic data to provide accurate and reliable predictions (Karim and Adeli 2003).

The neural-fuzzy logic method was the first nonparametric method applied to estimate the work zone capacity (Adeli and Jiang 2003). The study introduced a novel adaptive neural-fuzzy logic model, including 17 different factors that have an impact on the work zone capacity. The authors concluded that this model could provide a more accurate estimate, compared with two empirical equations. However, due to its complexity, the model was hardly applicable to the users. In another study, Karim and Adeli proposed a radial-basis function neural network model, which considered 11 parameters to learn the mapping from quantifiable and nonquantifiable factors in the estimation of work zone capacity (Karim and Adeli 2003). In 2011, a decision-tree-based model was developed to provide higher estimation accuracy of the work zone capacity (Weng and Meng 2011). This model considered 16 influencing factors; in addition, the data in this study were collected from 14 states. The results demonstrated that this model outperformed the neural-fuzzy approach, as it predicted more accurately; further, it was applicable to all users. The weakness of

this method is that the tree structure is highly dependent on the training and testing data. In other words, a slight change in the training and testing data set will dramatically alter the results. In order to address this weakness, an ensemble tree method was applied in another research (Weng and Meng 2012). Weng and Meng built an ensemble tree consisted of 105 individual decision trees by using a bootstrap aggregation method. It proved that the ensemble tree was more accurate and stable than the decision tree method. However, due to the absence of graphical-display results, it was complicated to understand the detailed relationship between the capacity and factors. In addition, the decision tree and ensemble tree both discretize the continuous factors based on the *F*-test to make them categorical when building the tree structure. This process may lower the accuracy of the entire work (Weng and Meng 2013).

2.3.1.3 Simulation-Based Method

According to the use of traffic analysis tools and simulation models in the FHWA Traffic Analysis Toolbox, simulation tools have been widely applied in much traffic analysis research (Dowling, Skabardonis and Alexiadis 2004). Focused on different aspects, simulation tools can be grouped into four categories: sketch-planning tools; macroscopic simulation models; mesoscopic simulation models; and microscopic simulation models.

Sketch-planning methodologies and tools produce general order-of-magnitude estimates of travel demands and traffic operations in response to transportation changes (Zhang, Morallos, et al. 2012). The planning level work zone simulation tools include software such as QUEWZ (University of Florida, USA), QuickZone (FHWA, USA), FREEVAL-WZ (North Carolina, USA), etc. (Alexiadis, Jeannotte and Chandra 2004). As high-level planning applications, these deterministic tools aid in simpler approaches in that data requirements, calibration, and interpretation of the results are highly aggregated. Thus, they cost the least time or money in which

to facilitate rapid analysis. These advantages, however, are coupled with the weakness in that the network complexity, potential network impacts, vehicle interactions, and high-level analysis are limited. It was found that the QUEWZ and QuickZone were not accurate in past studies (Benekohal, Kaja-Mohideen and Chitturi 2003, Ramezani and Benekohal 2012). Research conducted by Benekohal Kaja-Mohideen, and Chitturi stated that QUEWZ overestimated the capacity and average speed; further, the queue length from QuickZone did not match the field data (Benekohal, Kaja-Mohideen and Chitturi 2003). Ramezani and Benekohal also reported that the maximum queue length was overestimated by these tools (Ramezani and Benekohal 2012). The inaccurate results were caused because QUEWZ and QuickZone applied outdated HCM methodology to estimate performance measures in work zones. For example, the QUEWZ models were developed based on the 1965 HCM general speed-flow relationship and regression based on field data (Ishimaru and Hallenbeck 2019). Although the FREEVAL-WZ applied the latest methodology of 2016 HCM and can model different work zone scenarios as well as quantify effects of congested periods over time and space (Trask, et al. 2015), its effectiveness has not been fully explored.

Macroscopic simulation models are based on the deterministic relationships of the flow, speed, and density of the traffic stream that treat traffic flows as an aggregate quantity without analyzing individual vehicle movement (Zhang, Morallos, et al. 2012). These simulation models include software such as the TRANSYT-7F (University of Florida, USA) package within the *Highway Capacity Software* from McTrans (Alexiadis, Jeannotte and Chandra 2004). While these models have the ability to model a large geographic area and provide slightly more details than the sketch-planning tools, they are still limited to their simple representation of traffic movement and are unaccounted for the stochasticity of work zone environments.

Mesoscopic simulation models are a combination of both microscopic and macroscopic simulation models (Zhang, Morallos, et al. 2012). While they still model at an aggregate level and the focus is on the movement of a platoon of vehicles, their unit of traffic flow is the individual vehicle; further, different platoons' interactions are considered. One example of mesoscopic simulation software is DYNASMART-P (University of Florida, USA), developed by the University of Maryland and distributed by FHWA in 2004 (Alexiadis, Jeannotte and Chandra 2004). It provides the capability to model the evolution of traffic flows in a traffic network when individual travelers can make decisions on selecting the best path (Mahmassani, Sbayti and Zhou 2004). These models are able to model both large geographic areas and corridors, but their primary limitation is their inability to model detailed operational strategies. Thus, these tools may not be helpful for individual work zones.

Microscopic models simulate the movement of every vehicle in the network based on car-following, lane-changing, and gap-acceptance theories (Zhang, Morallos, et al. 2012). These tools are based on a stochastic process, and every vehicle in the network can be tracked over short time intervals so that the result of each run is unique. Popular microscopic simulation software includes CORSIM and VISSIM, which are developed by FHWA and the PTV Group, respectively (Alexiadis, Jeannotte and Chandra 2004). These models aim to represent transportation systems accurately at the individual vehicle level and are effective in modeling plenty of scenarios such as heavily congested conditions, complex geometric configurations, and system-level improvement impacts. CORSIM and VISSIM have been used in several studies to estimate the capacity of work zones with different lane closure configurations (Heaslip, et al. 2009, Chatterjee, et al. 2009, Heaslip, Jain and Elefteriadou 2011). However, the detailed and comprehensive analysis requires a substantial amount of roadway geometry, traffic control, and traffic pattern data. In addition, to

represent real-world traffic conditions, it was suggested that further calibration work is needed to address other issues with specific work zone configurations (Yeom, Rouphail and Rasdorf 2015). This calibration process is usually tedious and expensive.

2.3.2 Headway and Gap Distribution

2.3.2.1 Headway

Vehicle time headway is a critical traffic flow characteristic that affects the level of service and capacity (May 1990). Thus, in work zones, this factor is of utmost importance to analyze so that accurate vehicle dynamics in work zones can be generated. Headway distribution modeling has been studied for decades (Ye and Zhang 2009). Many vehicle headway distribution models have been proposed to model the vehicle headway at various traffic flow levels, including exponential distribution, Weibull distribution, gamma distribution, lognormal distribution, Erlang distribution, and inverse Gaussian distribution (Cowan 1975, Sun and Benekohal 2006, Greenberg 1966). These studies only fit the models in the mixed vehicular traffic without consideration of vehicle headways for different types of vehicle following patterns. Thus, researchers began to disaggregate vehicle headways into various types as the leader and follower vehicle pairs, such as the car-truck pair, truck-car pair, truck-truck pair, and car-car pair (Ye and Zhang 2009, Hoogendoorn and Bovy 1998, Weng, Meng and Fwa 2014). However, as work zone traffic has unique characteristics, few studies explored vehicle headway distribution in work zones (Sun and Benekohal 2006, Weng, Meng and Fwa 2014). Moreover, none of the existing studies takes into account the effects of driver characteristics on headway in work zones, despite the fact that different drivers exhibit various influences due to their unique driving behaviors. Therefore, there is a need to develop headway selection tables based on driver characteristics in work zones.

2.3.2.2 Gap

Gap spacing is the distance between two consecutive vehicles during vehicle following, which is the core of adaptive cruise control (ACC) systems (Swaroop and Rajagopal 2001). There are two major gap spacing categories in the previous research, including constant spacing policy and variable spacing policy (Swaroop and Huandra 1998). The constant spacing policy always keeps a constant spacing between two consecutive vehicles which is independent of driving environment (Gerdes and Hedrick 1996, McMahon, Hedrick and Shladover 1990, Chehardoli and Homaeinezhad 2018). If a small spacing is chosen, a high traffic capacity will be provided (Darbha, Rajagopal and Tyagi 2008). However, no ACC systems have adopted the constant spacing policy on the market in practice due to the failure of string stability (Xiao, Gao and Wang 2009, Sheikholeslam and Desoer 1990, Seiler, Pant and Hedrick 2004, Farnam and Sarlette 2019, Căilean and Dimian 2017).

The variable spacing policy treats the desired spacing between consecutive vehicles as a function of the ACC vehicle's speed, which includes the time headway-based, traffic flow stability, constant safety factor, and human driving behavior spacing policies. The most common spacing policy in both academia and the automotive industry is the time headway-based spacing (Wang and Rajamani 2004). In the previous studies, the term "time gap" was used instead of "time headway" (van der Heijden, Lukaseder and Kargl 2017, Căilean and Dimian 2017, Lin, et al. 2008, Moon, Kang and Yi 2010, Bageshwar, Garrard and Rajamani 2004). As aforementioned, "time gap" refers to the time between the rear bumper of the leading vehicle and the front bumper of the following vehicle when passing a fixed position, while "time headway" refers to the time between the front bumper of the leading vehicle and the front bumper of the following vehicle when passing a fixed position. "time gap" and "time headway" are different in quantity, but they lead to the same

vehicle behavior based on the qualitative perspective (Stüdli, Seron and Middleton 2017). In the automotive industry, ACC systems normally select the range of time gap between 1 to 2 seconds (Naranjo, et al. 2006). However, the time headway-based spacing is not suitable for high-density traffic conditions due to the failure of traffic flow stability (Marsden, McDonald, & Brackstone, 2001; Darbha & Rajagopal, 1999; Wang & Rajamani, 2004).

Thus, the traffic flow stability spacing is introduced to solve this problem. One of the traffic flow stability spacing policies was designed based on the Greenshield's model, which was proven to maintain traffic flow stability and ensure safety (Wang and Rajamani 2004, Swaroop and Huandra 1998, Zou and Levinson 2002). The other one was developed based on the traffic volume flow rate curve with the desired spacing being a nonlinear function of the following vehicle's speed (Santhanakrishnan and Rajamani 2003).

Constant safety factor spacing was proposed to improve safety as safety is one of the major concerns in ACC systems (Xiao and Gao 2010, Shladover, et al. 2015). This policy can be obtained by analyzing the emergency braking process (Mackinnon 1975). However, the safety factor spacing emphasizes more on the safety perspective and it is more conservative safety-wise (Tomizuka and KARL HEDRICK 1995).

The fourth gap spacing is human driving behavior spacing, which is to enhance driver comfort and take human driving behaviors into consideration for ACC systems (Fancher, Bareket and Ervin 2001). It was stated that the ACC spacing should be similar to human driver's spacing behavior (Zhou and Peng 2005) and real human driving data was employed to develop ACC systems (Moon and Yi 2008, Kesting and Treiber 2008, Fancher, Bareket and Peng, et al. 2003). In a previous study, Peng *et al*. recorded 107 drivers' driving behaviors to develop a human driving behavior spacing policy. It was proved that this spacing policy can improve customer acceptance

and system utilization by introducing driver characteristics (Gao, et al. 2015). However, more research is needed to further expand and develop the human driving behavior spacing policy that is similar to human drivers to reflect their physical and mental capabilities. From this perspective, the SHRP 2 NDS data offers the potential for developing the human driving behavior spacing policy for ACC systems in the automotive industry.

2.3.3 Speed Studies

Various factors affect the speed of vehicles passing through a work zone, including roadway geometrics, such as the number of lanes, lane width, horizontal and vertical curvature, lateral clearance; traffic warning signs (variable speed limit signs, speed monitoring and display, flaggers), and law enforcement (Noel, et al. 1988). Previous work zone speed studies mainly addressed factors affecting speed limits, driver compliance with speed limits, enforcement, and safety issues (J. Migletz, J. Graham, et al. 1998, Bham and Mohammadi 2011, Benekohal, Kaja-Mohideen and Chitturi 2004, J. Migletz, J. L. Graham, et al. 1999, Pesti and McCoy 2001, Li and Bai 2008).

It was found that narrowed lane widths contributed to greater speed reduction (Chitturi and Benekohal 2005). Another study evaluated the effectiveness of signs usage to reduce speed of traffic through work zones. As recommended by the NCHRP, the normal posted speed is typically reduced by 10 mph for work zones (J. Migletz, J. Graham, et al. 1998). It was stated that Changeable Message Sign (CMS), speed display trailers or CMS with radar, innovative signs, flagging treatments, lane narrowing, late merge, transverse striping, and rumble strips are the commonly used speed reduction methods and strategies (Bham and Mohammadi 2011, Benekohal, Kaja-Mohideen and Chitturi 2004). For driver compliance, it was found that compliance was the greatest where the speed limit was not reduced, and compliance decreased where the speed limit

was reduced by 10 mph or more (J. Migletz, J. L. Graham, et al. 1999). In a recent study, Adeli evaluated driver speed variations according to speed limits and road work signs based on driving simulator data (A. Adeli 2014). The results found that drivers' age, road familiarity, and experience had a noteworthy impact on speed limit compliance. However, research has shown that once the enforcement tool (police vehicle patrolling or a speed feedback trailer) is out of sight, vehicle speeds will return to their previous levels (Pesti and McCoy 2001). As for safety issues, it was revealed that the greatest number of fatal crashes occurred on highways with speed limits between 61 and 70 mph, which confirmed that high speeds increase the severity of work zone crashes (Li and Bai 2008). Furthermore, the previous speed studies in work zones did not provide a full picture of speed profiles when utilizing spot-measured data. Thus, it would be useful to perform a speed analysis that explores the speed distribution and speed change in the form of time series at work zones.

2.3.4 Related Research that Utilizing NDS Data

There have been a few work zone studies utilizing NDS data, but none of them aims to explore work zone mobility issues; instead, the main focus of these work zone studies was on the safety aspect. Goswamy used NDS data to investigate work zone safety, especially the role of speed and distraction in work zone crashes and near-crashes (Goswamy 2019). Another work zone study used statistical descriptions of normal driving behavior to identify abnormal behavior as the basis for countermeasures by utilizing NDS data (Flannagan, et al. 2019). Bharadwaj *et al*. investigated risk factors and developed a binary logistic regression model to estimate the crash risk in work zones (Bharadwaj, Edara and Sun 2019). The authors also quantified the risk of different contributing factors. For instance, it was found that the odds ratio of driver inattention is 29, which is the most critical behavioral factor contributing to crashes. Chang and Edara applied four

machine-learning algorithms to work zone events with NDS data to predict the occurrence of a safety-critical event by using pre-event variables (Chang and Edara 2017). These algorithms included the random forest, deep neural network, multilayer feed forward neural network, and *t*-distributed stochastic neighbor embedding. It was concluded that the random forest algorithm performed the best in classifying different safety-critical events with a prediction accuracy of 97.7%.

2.4 Gaps in Previous Research and Proposed Work

For freeway diverge areas, according to the literature review, conventional studies heavily relied on field data collection (e.g., radar gun). They have been either time-consuming or labor-intensive tasks, which may also result in erroneous conclusions due to intrinsic biases. Furthermore, the *Green Book* only provides the minimum lengths of deceleration lanes according to the design speed differential from the freeway mainline and off-ramp. Moreover, similarities of recommended design lengths were found in the 2018 *Green Book* and 1965 edition. Data that was used in both editions were collected in the 1930s. Thus, new data and research are required to update the design guide. The literature review also illustrated that none of the previous studies that used SHRP 2 NDS data explored speed and deceleration rates on freeway deceleration lane and off-ramp. To fill this gap, using the SHRP 2 NDS data is a new approach to investigate the driver behavior during daily trips through unobtrusive data gathering equipment and without experimental control (Van-Schagen, et al. 2011). As SHRP 2 NDS data consists of various information such as the driver's interaction with the vehicle, the traffic environment, and roadway characteristics, it provides an opportunity to conduct a first-ever study on determining deceleration lane lengths based on distributions of naturalistic driving speeds and deceleration rates on freeway diverge areas.

For freeway work zone mobility, in summary, the review of the available literature indicated that very few work zone studies in the past considered driver characteristics and their car-following behaviors. The NDS data can provide this unique information that could not be obtained from field data collection or traffic simulation models, which have been used to evaluate the freeway work zone mobility in the past. The driver types and their gap and headway distributions in work zones would be helpful to identify how driver behaviors affect work zone capacity. Moreover, the NDS data can be used to develop gap spacing policies for ACC systems based on human driving behavior in work zones. The literature review also revealed that none of the previous studies that applied SHRP 2 NDS data investigated the work zone mobility. The impact of driver characteristics on gap and headway selection and speed distribution during the entire work zone areas has never been studied. Furthermore, the results can be used to enhance work zone planning and simulation models by considering different headway distributions based on driver characteristics and their speed profiles traversing the entire work zone.

Chapter 3. Methodology

3.1 Data Collection and Reduction

This section provides the extensive data collection and reduction process for freeway diverge areas and work zones.

Data collection was mainly controlled by the availability of NDS data. For freeway diverge areas, the diverge area of diamond interchanges with relatively straight off-ramps was targeted because diamond interchanges are the most widely used service interchange, which consists of 79% of all interchanges in the United States (Missouri DOT 2017). The number of trips and drivers available at each potential site was checked from "Traversal Density Data" on the Insight Website (https://insight.shrp2nds.us/) to ensure a relatively large sample size on the off-ramp and the freeway mainline. The sites were checked to collect their geometric design features such as taper length, deceleration lane length, off-ramp length, divergence angle, off-ramp controlling feature (e.g., sharp curvature, stop-controlled intersection, signalized intersection, etc.), and deceleration lane type. It should be noted that sites within the same state were preferred to minimize the design differences. Subsequently, 10 study locations were selected from Florida. Later, the data request was sent to VTTI, which is responsible for the compilation and dissemination of NDS data, for extracting NDS data from locations of interest. After the IRB approval from the Office of Human Research in Auburn University (https://cws.auburn.edu/OVPR/pm/compliance/irb/home) obtained, VTTI would approve the DUL and deliver NDS data afterward.

For freeway work zone locations, work zones are dynamics and cannot be identified from "Traversal Density Data" on the Insight Website (https://insight.shrp2nds.us/). However, the "Events" dataset on the InSight could be utilized to find baselines, crashes, and near-crash events

in work zones. Then, a list of event IDs of interest along with IRB approval from Auburn University was sent to VTTI staff so that they can use the roadway link IDs and dates of these events to find trips that pass through the same area around the same timeframe. To make this process more smooth, a conference call was scheduled with VTTI staff for requesting proper work zone NDS data. They delivered data in two steps. First, over 58-hour sample video clips were delivered. Work zone start and end mileposts were identified so that the trips traversed the same locations during the same time periods can be exported. Then, the final dataset was delivered with exported time interval which covers at most 20 weeks (10 weeks before and 10 weeks after the identified sample events occurred). However, as work zone activity proceeded, the configuration changed very quickly. For example, although work zone start and end milepost were identified from the first sample data, work zone configuration might have changed within 2 weeks (1 week before and 1 week after the identified sample events). Thus, all received NDS videos were reviewed to ensure that they were categorized into the proper work zone configuration.

The data delivered for freeway diverge areas and work zones are two subsets of the SHRP 2 NDS dataset, both including video clips of the forward-view and rear-view videos, corresponding time-series reports for each trip, driver risk perception, driver demographics, and vehicle information. The time-series report contains speeds (km/h), acceleration–deceleration rates (*g*), the brake pedal status (0 or 1), etc. **Table 5** provides the data dictionary in time-series reports. The time-series report of each traversal provides all data at 0.1-s intervals. By reviewing the forward-view videos, which were taken from cameras mounted inside the vehicles to provide drivers' views, the traffic condition (free-flow or non-free-flow), environmental condition (lighting and weather), roadway geometric features (freeway diverge area or work zone layout), and the presence of traffic control devices (traffic sign and pavement marking) can be identified to assist

with understanding driver behavior. Driver risk perception and driver demographics were also requested. The driver risk perception was collected from the questionnaire designed to gauge the participant's perception of dangerous or unsafe driving behaviors or scenarios (Transportation Research Board 2013). This questionnaire includes 32 driving-behavior-related questions and driver risk perceptions were calculated based on self-reported measures, which indicated their perceptions of risk associated with different driving behaviors. For example, how would the participant evaluate the risk when not yielding the right of way, the participant's associated risk with passing other cars on the right side or the shoulder of the road, the participant's associated risk with turning without signaling, etc. Each question was assigned a score from 1 (No Greater Risk) to 7 (Much Greater Risk); thus, it is assumed that a higher score indicates that the driver self-reported to be cautious and obedient to traffic rules with greater risk perceptions. The total risk perception score of drivers is the sum of all the scores from questions in the questionnaire which ranges from 32 to 224.

Table 5 NDS time-series data dictionary.

Variable Name	Description
vtti_timestamp	Time since beginning of trip, in milliseconds
vtti_speed_network	Vehicle speed indicated on speedometer collected from network, in km/h
vtti_accel_x	Vehicle acceleration in the longitudinal direction versus time, in *g*
vtti_pedal_brake_state	On or off press of brake pedal, 0 = off; 1 = on

LEADVEHICLE_HEADWAY	Time gap between the participant vehicle front bumper and the lead vehicle rear bumper, in seconds

For freeway diverge areas, the video of each trip was reviewed to ensure that it is a complete traversal beginning before the deceleration lane and ending after the off-ramp terminal. At the bottom left corner of the forward-view video, the continuous timestamp is offered to refer to the corresponding time-series report as presented in **Figure 5**, where details of the vehicle maneuver were provided at 0.1-s intervals. These details include the vehicle speed from the speedometer, the longitudinal acceleration rate, and the brake pedal status. The original dataset contained 971 trips from 10 locations, but some time-series reports were incomplete. Further, some trips began after the off-ramp or ended before the terminal were filtered. Finally, 709 complete trips driven by 272 unique drivers were used for analysis in this study as presented in **Table 6**.

System.Time_Stamp	vtti.timestamp	vtti.file_id	vtti.speed_network	vtti.speed_gps	vtti.accel_x	vtti.accel_y	vtti.pedal_brake_state	vtti.gyro_z	vtti.video_frame
22	1301200	8003352	102.93		-0.0493	0.0145	0	0	19468
23	1301300	8003352	102.71		-0.0174	0.0174		0	19469
24	1301400	8003352	102.48	115.3326	-0.0348	-0.0116	0	0	19471
25	1301500	8003352	102.31		-0.0493	0.0058	0	0	19472
26	1301600	8003352	102.15		-0.0377	0.0522	0		19474
27	1301700	8003352	101.81		-0.0145	0.0638	0	0.975586	19475
28	1301800	8003352	101.75		-0.0464	0.0957	1	1.625977	19477
29	1301900	8003352	101.41		-0.0435	0.116	1	1.951172	19478
30	1302000	8003352	101.3		-0.0435	0.1015	1	2.276367	19480
31	1302100	8003352	100.8		-0.0174	0.1189	1	2.276367	19481
32	1302200	8003352	100.57		-0.0551	0.1189	1	1.951172	19483
33	1302300	8003352	99.95		-0.0812	0.0957	1	1.625977	19484
34	1302400	8003352	99.73	110.666	-0.0957	0.0609	1	0.650391	19486
35	1302500	8003352	99.11		-0.0841	0.0406	1	0.325195	19487
36	1302600	8003352	98.94		-0.087	0.029	1		19489

(a)

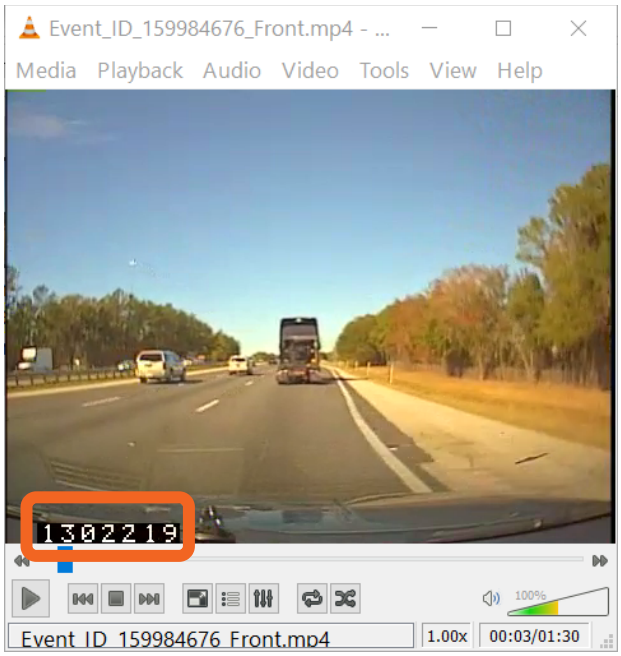

(*b*)

Figure 5 NDS example data for freeway diverge areas:

(*a*) time-series report; and (*b*) forward-view video.

For freeway work zones, in addition to the time-series data (i.e., speeds), radar data (i.e., time gap) and video clips of the forward roadway were obtained for each trip. As the radar data dictionary file stated in **Table 5**, the headway collected from the radar is actually gap in seconds which equals the distance between the target rear bumper and participant vehicle front bumper divided by the participant's vehicle speed. Space headway is defined as the distance between the same points of two consecutive vehicles following each other (Mathew and Rao 2006). Thus, an average vehicle length of 15 ft (Sellén, 2021) was added to the space gap, so that the time headway was counted from the lead vehicle's front bumper to the participant vehicle's front bumper. The example data is provided in **Figure 6**. To eliminate the potential distraction or impact by non-work zone elements, only trips that occurred during daylight time with a clear vision in good weather conditions on the dry pavement were selected. To reduce the impact of interchanges near work

zones that might potentially influence driver performance, trips near interchanges (within or one lane next to auxiliary lanes) were also filtered to exclude the effects of merging and diverging maneuvers on driver behaviors. A total of 200 complete work zone trips traversed the entire work zone by 103 unique drivers were finally selected at four locations as presented in **Table 7**, which encompass nearly 1,100 VMT, 19 vehicle hours traveled (VHT), and over 675,000 data points at 0.1-s intervals.

vtti.timestamp	vtti.file_id	vtti.accel_x	vtti.pedal_brake_state	vtti.pedal_gas_position	vtti.speed_network	vtti.video_frame	LEADVEHICLE_HEADWAY
1182800	27185101	0	0	14.75	86.5475	17695	1.059582
1182900	27185101	0.0087	0	15.875	86.5675	17696.5	1.060143
1183000	27185101	0.0319	0	16.3	86.545	17698	1.059526
1183100	27185101	0.0087	0	16.875	86.6425	17699.5	1.059962
1183200	27185101	0.0232	0	17	86.6275	17701	1.060723
1183300	27185101	0.0406	0	17	86.572	17702.5	1.062516
1183400	27185101	0.0058	0	17.3	86.63	17704	1.060484
1183500	27185101	0.0232	0	17.25	86.475	17705.5	1.062394
1183600	27185101	0.0058	0	17	86.445	17707	1.064325
1183700	27185101	-0.0029	0	17	86.455	17708.5	1.064268
1183800	27185101	0.0203	0	17	86.45	17710	1.066142
1183900	27185101	0.0145	0	16.5	86.4125	17711.5	1.066949
1184000	27185101	0.0203	0	16.5	86.318	17713	1.069653
[illegible]	27185101	0.0203	0	16.5	86.34	17714.5	1.070163
1184200	27185101	0.0087	0	16.6	86.3025	17716	1.072527
1184300	27185101	0.0261	0	17	86.3125	17717.5	1.072611
1184400	27185101	0.0058	0	17.75	86.32	17719	1.073194
1184500	27185101	0.0145	0	20.125	86.3575	17720.5	1.073753

(a)

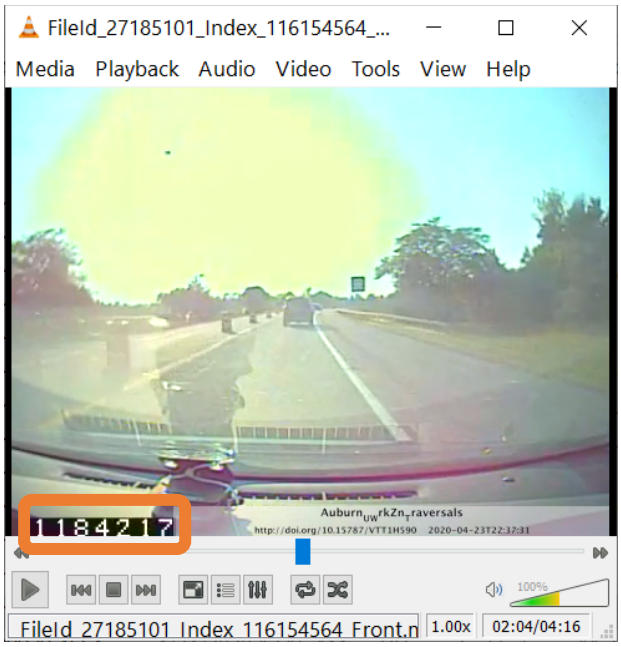

(*b*)

Figure 6 NDS example data for freeway work zones:

(*a*) time-series report; and (*b*) forward-view video.

3.2 Freeway Diverge Area

3.2.1 Site Description

Ten study locations, five one-lane exit with parallel-design deceleration lane locations (Locations 1P through 5P), and five one-lane exit with tapered-design deceleration lane locations (Locations 1T through 5T) are located on I-75 in Florida as shown in **Figure 7**. The 2018 *Green Book* design criterion for minimum deceleration lane lengths was compared with study locations to determine if they met the minimum requirement. **Table 6** lists site information, the type of interchange design, the type of deceleration lane design, the divergence angle, the length of every section (taper, deceleration lane, and off-ramp) in the diverge area, the minimum length determined in the *Green Book*, the number of trips, and the number of unique drivers.

Eight of 10 locations are diamond interchanges with relatively straight off-ramps. Two others are partial cloverleaf interchanges (Locations 3P and 5P) where the straight off-ramps were selected for reducing the impact on the speed by horizontal curvature (as presented in **Figures 2*e*** and **2*i***). For parallel-design locations, taper lengths are from 165 to 270 ft. Taper lengths of tapered-design locations were found to be shorter (130 to 205 ft). Deceleration lane lengths are in the range of 645 to 990 ft for parallel-design locations, which are longer than lengths in tapered-design locations (320 to 445 ft). For both types, off-ramp lengths vary from 940 to 1,725 ft. Most of the locations' off-ramp terminals are signalized intersections while three of them are under yield control (Locations 1T, 3P, and 5T). The speed limit on the freeway mainline is 70 mph for all locations. Off-ramp advisory speeds of 35 mph were posted at four locations (Locations 1P, 2P, 3P, and 4T). It should be noted that limited information is available on establishing advisory speeds for off-ramps that do not have horizontal curvatures (Venglar, et al. 2008). After comparing the actual deceleration lane length of each location with *Green Book* recommendations, lengths of deceleration lane from parallel-design locations are longer than the minimum length, while tapered-design locations are shorter.

Table 6 Site description, minimum deceleration lane length, and number of trips and drivers.

Site Locations	Interchange Design	Taper Length (ft)	Deceleration Lane Length (ft)	Off-Ramp Length (ft)	Green Book Minimum Deceleration Length (ft)	Design Status Compared to Green Book	Number of Trips	Number of Drivers
Location 1P: I-75/SW Archer Rd	Diamond	190	645	1475	490	**GREATER**	92	45
Location 1T: I-75/Clark Rd	Diamond	200	425	1595	615	**LESS**	102	30
Location 2P: I-75/SW County Highway 484	Diamond	195	735	990	490	**GREATER**	23	23
Location 2T: I-75/US 98	Diamond	150	320	940	615	**LESS**	59	48
Location 3P: I-75/FL 326	Parclo	165	775	1030	490	**GREATER**	46	32
Location 3T: I-75/US 98	Diamond	205	420	1170	615	**LESS**	202	56
Location 4P: I-75/CR 768	Diamond	200	700	1180	615	**GREATER**	28	6
Location 4T: I-75/SW College Rd	Diamond	150	445	1340	490	**LESS**	16	13
Location 5P: I-75/CR 765	Parclo	270	990	1690	615	**GREATER**	120	9
Location 5T: I-75/CR 769	Diamond	130	365	1725	615	**LESS**	21	10

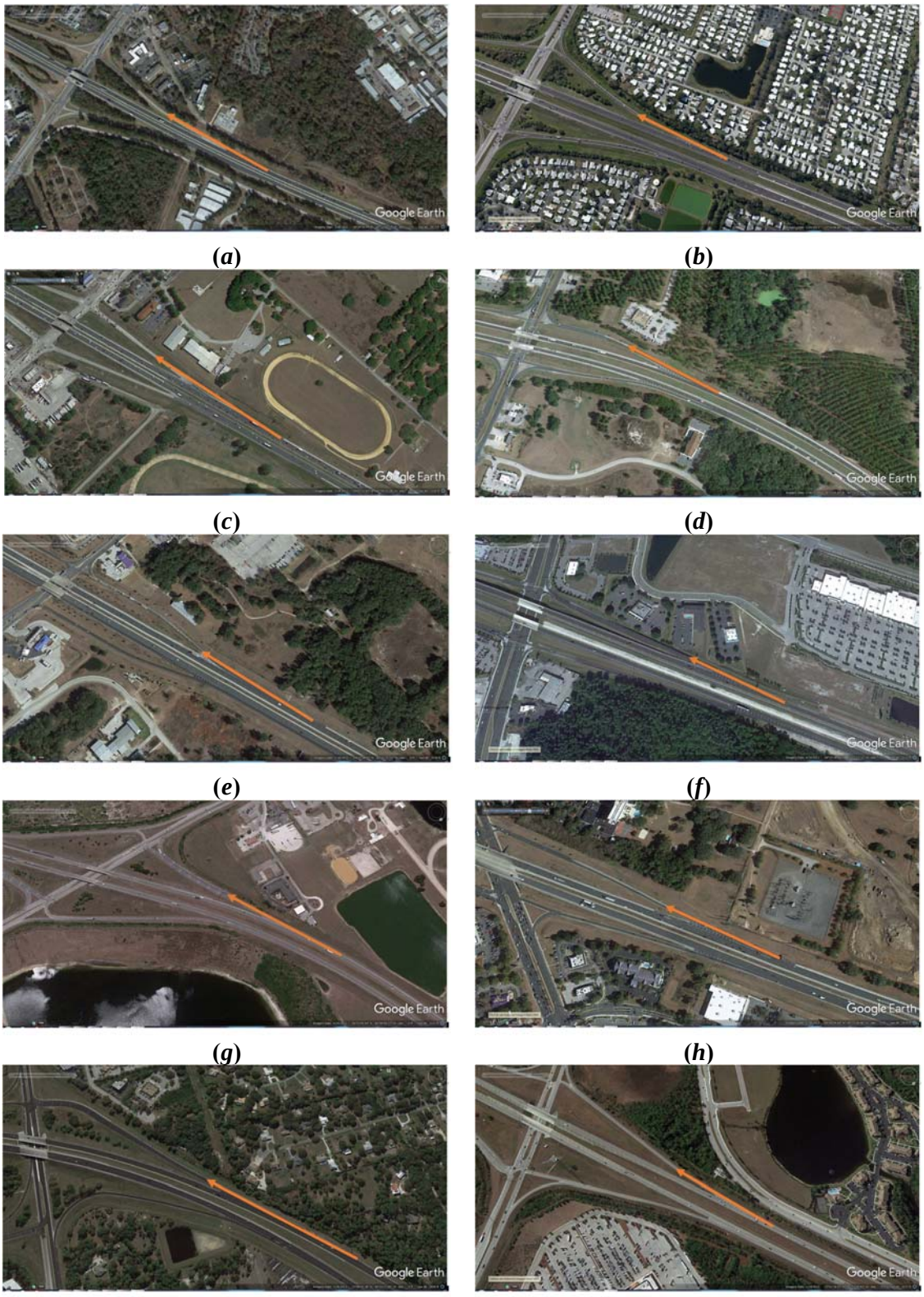

(*a*) (*b*)

(*c*) (*d*)

(*e*) (*f*)

(*g*) (*h*)

(*i*) (*j*)

Figure 7 Aerial photos of study locations: (*a*) Location 1P; (*b*) Location 1T; (*c*) Location 2P; (*d*) Location 2T; (*e*) Location 3P; (*f*) Location 3T; (*g*) Location 4P; (*h*) Location 4T; (*i*) Location 5P; and (*j*) Location 5T (Imagery © 2020 Google, Map data © 2020 Google).

3.2.2 Data Analysis

Data analysis was performed from three aspects: (1) speed distributions on deceleration lanes and off-ramps; (2) driver behaviors in terms of the brake pedal usage and the deceleration rates, and (3) methods on estimating minimum deceleration lane length based on naturalistic driving speeds and deceleration rates.

Reviewing videos was the first step in the data analysis. Observers recorded the video frame number (the timestamp) at critical points in the video. Taper start point, deceleration lane start point, deceleration lane endpoint (physical gore), and off-ramp endpoint (stop bar at the terminal) on each location were considered critical points for this analysis. The frame number allowed for correlation to the data in the time-series report (speed, acceleration/deceleration rate, brake pedal status, etc.). Thus, the timestamp of each critical point in the time-series table was tagged to help determine the speed distribution (i.e., maximum, 85th percentile, mean, and minimum speed; and their standard deviations) of every section on the deceleration lane and off-ramp. In **Table 6**, the lengths of different sections (taper, deceleration lane, and off-ramp) at each study location are presented.

3.2.2.1 Polynomial Regression

The speed distributions on the taper, the deceleration lane, and the off-ramp were calculated by applying polynomial regression models, which were estimated using the NDS trips and speed data at 0.1-second intervals. The polynomial regression method minimizes the sum-of-squared residuals between measured and simulated quantities. The least-squares method is used to estimate unknown parameters (Gill, Murray and Wright 2019):

$$v = \beta_0 + \beta_1 L + \beta_2 L^2 + \beta_3 L^3 + \cdots + \beta_n L^n + \varepsilon \quad (6)$$

Where, L = The distance from the starting point of the taper along the deceleration lane and off-ramp (ft)

v = Vehicle speed (mph)

β_n = Estimated parameters

ε = The error of the specification

Four best-fitted models using NDS speed data, maximum speed, 85th percentile speed, mean speed, and minimum speed distributions, were developed for each study location by using the statistical computing software R. R software provides a variety of statistical (linear and nonlinear modeling, classical statistical tests, time-series analysis, classification, clustering, etc.) and graphical techniques (R Core Team 1993). The residual standard error was used as a measure of goodness-of-fit to evaluate and determine the quality of the fitted model.

3.2.2.2 Critical Speed Changepoint Detection

The changepoint detection estimates the point at which the statistical properties of a sequence of observations change (Killick and Eckley 2014). It has been widely used in various application areas, including climatology, bioinformatic applications, finance, oceanography, and medical imaging (Reeves, et al. 2007, Erdman and Emerson 2008, Zeileis, Shah and Patnaik 2010, R. Killick, et al. 2010, Nam, Aston and Johansen 2012). By applying this method, speed time series data is defined as: $V_{1:n} = (V_1, V_2, \dots, V_n)$. A changepoint may occur within this set when there exists a time, $\tau \in \{1, \dots, n-1\}$, where the statistical properties of $\{V_1, \dots, V_\tau\}$ and $\{V_{\tau+1}, \dots, V_n\}$ are different in some way (R Core Team 1993). The aim of the analysis is to estimate the location of the changepoint efficiently and accurately by minimizing the following equation:

$$\sum_{i=1}^{m+1} \left[C\left(V_{(\tau_{i_1}+1):\tau_i} \right) \right] + \beta f(m) \tag{7}$$

Where, C = A cost function for a segment (e.g., negative log-likelihood)

m = The number of changepoints

$\beta f(m)$ = A penalty to guard against overfitting

This method is used to identify the driver speed change position on the deceleration lane and off-ramp, so that the location where drivers take action to decelerate can be determined.

3.2.2.3 Driver Behavior

Driver behavior was identified by brake pedal usage and deceleration rate. Brake pedal status was coded as 0 or 1 in the time-series reports. The value of 0 indicates that the driver did not apply the brake at the certain 0.1-second interval, while 1 means he or she did. To find where drivers applied brakes most often, brake pedal usage was evaluated by the percentage of the drivers applying brakes in certain sections.

The time-series reports provided deceleration rates which can be used to calculate the mean and 85th percentile deceleration rates on the taper, deceleration lane, and off-ramp sections. The rates can also be determined by converting the distance-based speed model to the time-based one. The deceleration rate distribution was executed to find out the section where drivers mostly reduce their speeds so that the effective decelerating section could be found. When calculating deceleration rates, the *Green Book* recommended two methods (AASHTO 2018): one is based on a two-step process of deceleration, coasting (assumed 3 seconds) and braking; the other is based on a constant decelerating behavior on the deceleration lane which was validated by El-Basha et al. (El-Basha, Hassan and Sayed 2007). In this study, the deceleration rate was compared with the *Green Book* rates based on a constant decelerating behavior over the entire deceleration process. The minimum deceleration lane length can then be estimated based on the deceleration rate from NDS data and polynomial regression models by using **Equation 8**.

$$D = \frac{v_i^2 - v_f^2}{2d} \quad (8)$$

Where, D = Deceleration distance (ft)

v_i = Initial speed (ft/s)

v_f = Final speed (ft/s)

d = Deceleration rate (ft/s^2)

3.3 Freeway Work Zone Mobility

3.3.1 Site Description

According to the FHWA, lane closure and shoulder closure are the most common work zone configurations (FHWA 2020). Meanwhile, four- and six-lane divided highways are the most common types of roadways that occupy over 90% of the Interstate System mileage (FHWA 2017). Thus, four work zone configurations were selected in this study as presented in **Figure 8**. They are lane closure with lane reduction from two lanes to one lane (LC 2-1), lane closure with lane reduction from three lanes to two lanes (LC 3-2), shoulder closure with two lanes (SC 2-2), and shoulder closure with three lanes (SC 3-3). As defined in the MUTCD, a work zone typically consists of four consecutive sections: advance warning area, transition area, activity area, and termination area. In lane closure work zones (**Figure 8*a*** and**Figure** 8***b***), it is easy to define these four sections. But in shoulder closure work zones, the borders among transition area, activity area, and termination area are not clear according to the forward-view videos. In this study, only two areas were defined for shoulder closure work zones: advance warning area and work zone area (the combination of transition area, activity area, and termination area) as shown in **Figure 8*c*** and**Figure** 8***d***.

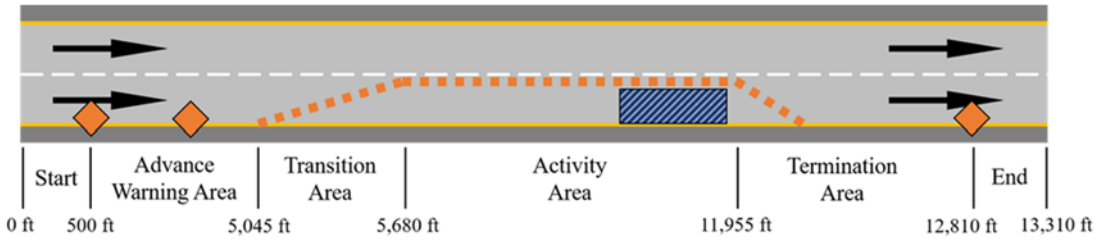

(*a*)

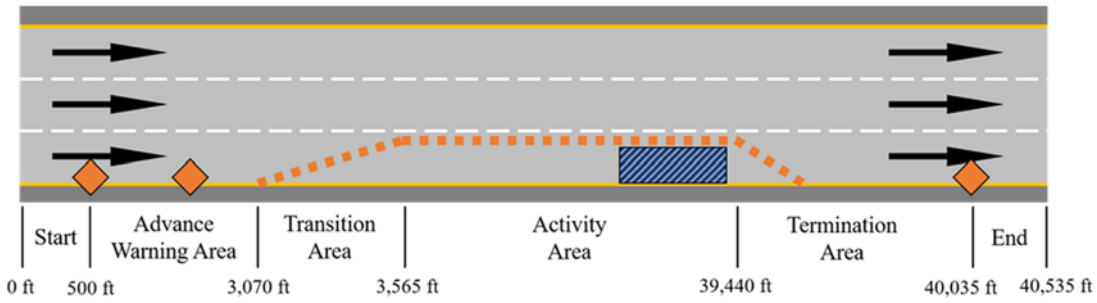

(*b*)

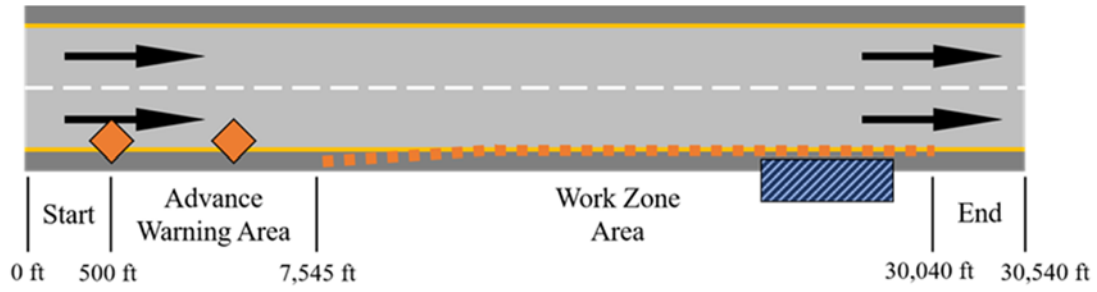

(*c*)

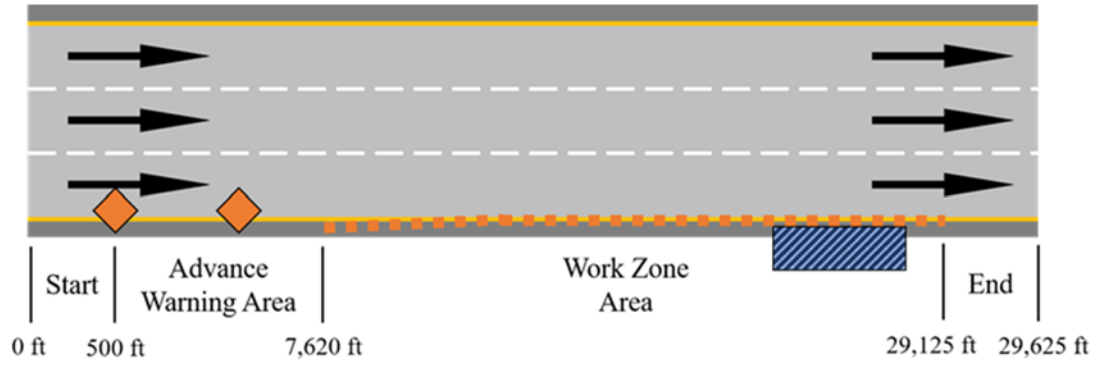

(*d*)

Figure 8 Four work zone configurations: (*a*) LC 2-1; (*b*) LC 3-2; (*c*) SC 2-2; and (*d*) SC 3-3.

All work zone configurations complied with the requirements of Temporary Traffic Control (TTC) zones in the Manual on Uniform Traffic Control Devices (MUTCD). The speed control methods were only applied at lane closure configurations with portable changeable message signs at the beginning of the transition area. Work zone speed limits that affect speed choice only appeared in the LC 2-1 location. There was no other law enforcement to affect speed reduction in the other three work zone locations. Only SC 2-2 appeared concrete barriers while drums were used as channelizing devices in the other three work zone configurations. **Table 7** summarizes numbers of unique drivers and trips at each work zone configuration (location) and their geographic locations. One LC 2-1 work zone is located in New York State, and the other three work zones are located in Florida.

Table 7. Summary of Final Dataset

Work Zone Configuration (Location)	Geographically Located	Number of Unique Drivers			Number of Trips
		Female	Male	Total	
LC 2-1	New York	11	9	20	50
LC 3-2	Florida	10	10	20	50
SC 2-2	Florida	10	14	24	50
SC 3-3	Florida	21	17	38	50

3.3.2 Data Analysis

Data analysis was performed with two objectives: (1) gap and headway selection tables based on different driver characteristics at four work zone configurations; and (2) speed analysis in terms of speed distribution and key speed change points identification at work zones.

The headway and gap distributions through the entire work zone were explored for the four different configurations. To identify the relationships between headway/gap selection and driver characteristics, all the drivers were categorized into different age groups: young, middle-aged, and senior groups. The mean headway and critical gap spacing, its 95% confidence interval, and the associated risk score were investigated. The analysis at different work zone sections was also performed to find out whether drivers adopted different headways and gap spacings.

3.3.2.1 Generalized Additive Model

To explore the driver's headway distribution through the entire work zone, the generalized additive model (GAM) was used to predict the best-fitted curve of headway profile of work zone consecutive sections to provide a better understanding of how driver negotiating the entire work zone, given the headway data from NDS. When compared with other techniques, GAM has three key advantages: (1) easy to interpret; (2) flexible predictor functions can uncover hidden patterns in the data; and (3) regularization of predictor functions help avoid overfitting (Larsen 2015). The GAM (Hastie and Tibshirani 1990, Wood 2017) allows non-linear functions of each variable, while maintaining the additivity of the model. This is achieved by replacing each linear component $\beta_j x_{ij}$ with a smooth non-linear function $f_j(x_{ij})$. A GAM can be written as **Equation 9**:

$$y_i = \beta_0 + \sum_{j=1}^{n} f_j(x_{ij}) + \varepsilon_i = \beta_0 + f_1(x_{i1}) + f_2(x_{i2}) + \cdots + f_n(x_{in}) + \varepsilon_i \quad (9)$$

Where, y_i = Dependent variable

x_{in} = Predictor variable

$f_n(x_{in})$ = Smooth non-linear function

GAM allows fitting a non-linear function f_j to each x_j that one does not need to manually try out numerous transformations on each of the predictor variables. Since GAM is an additive

model, one can examine the impact of each x_j on y_i individually. In this model, the smoothness of function f_j for the variable x_j is summarized via degrees of freedom. In GAM, the linear predictor predicts a known smooth monotonic function of the expected value of the response, and the response may follow any distribution (Wood 2017). To compare GAM with the other models such as the polynomial regression model, the Akaike information criterion (AIC) is an estimator of the relative quality of models for a given set of data. AIC uses a model's maximum likelihood estimation (log-likelihood) as a measure of fit. Typically, lower AIC values indicate a better-fit model. The R package 'mgcv' (Wood and Wood 2021) with the 'gam' function was applied to develop the GAM models.

3.3.2.2 Speed Analysis

A speed analysis was performed to explore the speed distribution and speed change over the entire work zone. To achieve this goal, GAM and change point detection techniques were applied. These two methods were described in the previous sections.

Chapter 4. Analysis and Results

This chapter summarizes the results from the freeway diverge area and work zone.

4.1 Freeway Diverge Area Results

The results are categorized into three parts: (1) polynomial regression of speed distribution on the deceleration lanes and off-ramps; (2) driver behavior in terms of brake pedal usage, deceleration rates, and a comparison with the *Green Book* assumptions; and (3) minimum lengths of deceleration lanes based on naturalistic driving speed and deceleration rates.

4.1.1 Speed Distribution

Four fitted speed distribution profiles by polynomial regression are presented in **Figure 9**, which shows speed distribution on the deceleration lane and the off-ramp in Locations 1P and 1T. The x-axis is the length (ft), and the y-axis is the speed (mph). The light blue lines are the speed data from NDS time-series reports, one trace coming from one traversal. The other four lines in the figure are fitted polynomial regression models, including the maximum speed distribution (maroon), the 85th percentile speed distribution (red), the mean speed distribution (orange), and the minimum speed distribution (pink). The critical points are also marked with estimated speeds.

For example, the 85th percentile speed distribution in Location 1P (**Figure 9*a***), the speed at the beginning of the taper was 74.02 mph. It was reduced to 72.67 mph when the vehicle entered the deceleration lane. The speed was further reduced to 63.39 mph after driving through the 645 ft deceleration lane, resulting in a 9.28 mph speed reduction on the deceleration lane. However, it was found that a great speed reduction occurred on the off-ramp, especially close to the off-ramp terminal where a signalized intersection exists. Finally, the 85th percentile speed was reduced to

23.88 mph. As for Location 1T as shown in **Figure 9*b***, the speed distribution was slightly different from Location 1P. Before the taper in Location 1T, an extra 210-ft segment before the taper section was counted to make the length equal to the total length of taper and deceleration lane in Location 1P. It was found that, in Location 1T, drivers decelerated on the mainline before entering the taper section. The 85th percentile speed at the taper start point was 69.64 mph, which is nearly 5 mph lower than that in Location 1P. When entering the deceleration lane, the speed was 68 mph. The 425-ft deceleration lane only helps reduce 3 mph considering the speed at the off-ramp start point being 64.49 mph. Similar to Location 1P, a significant speed reduction of 33.58 mph was observed on the off-ramp. The speed distribution of other study locations can be found in Appendix A.

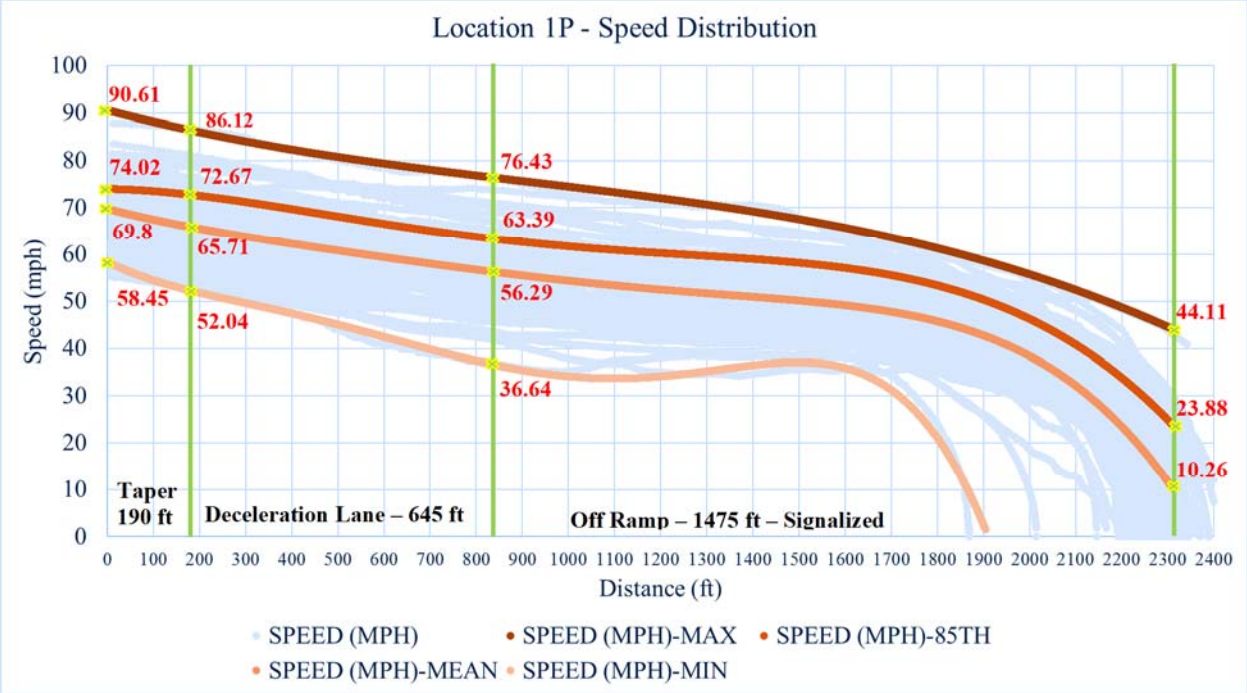

(*a*)

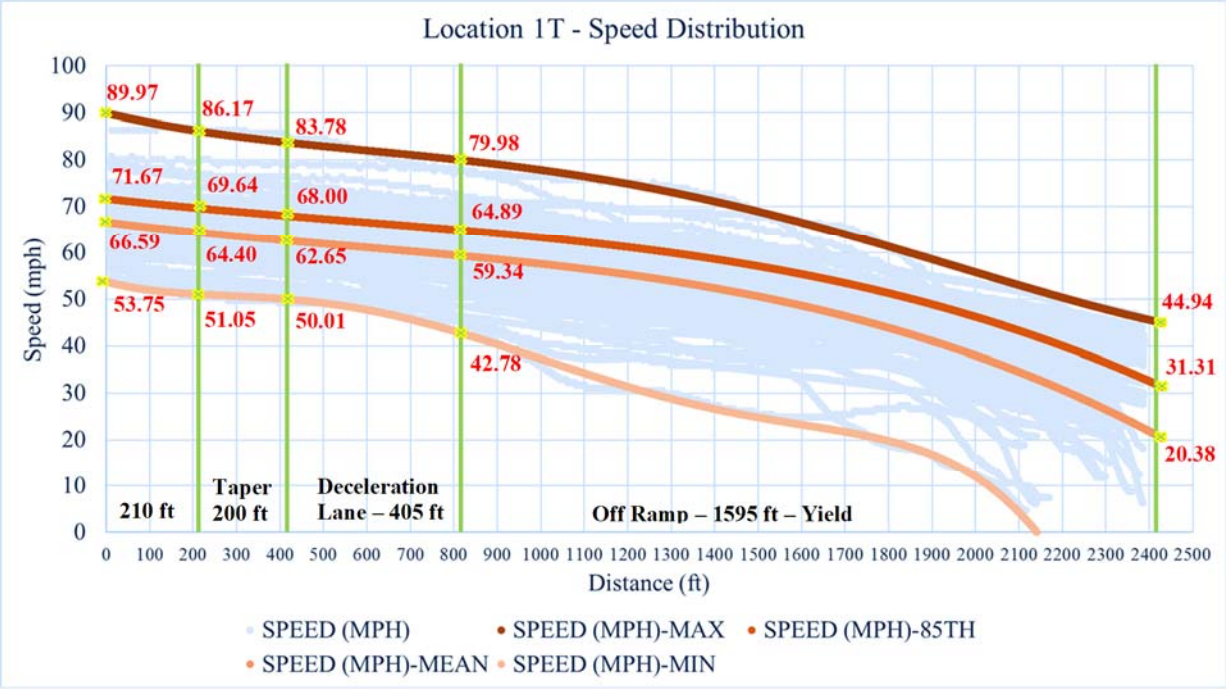

(*b*)

Figure 9 Speed distributions: (*a*) Location 1P; and (*b*) Location 1T.

Polynomial regression models and R-squared values of 85th percentile speed and mean speed distributions for Locations 1P and 1T are summarized as follows:

For Location 1P:

$$v_{1P-85^{th}} = -9.767 \times 10^{-12} {L_{1P}}^4 + 3.380 \times 10^{-8} {L_{1P}}^3 - 3.462 \times 10^{-5} {L_{1P}}^2 - 1.703 \times 10^{-3} \times L_{1P} + 74.02 \quad (10)$$

$$R^2 = 0.9981$$

$$v_{1P-Mean} = -6.646 \times 10^{-15} {L_{1P}}^5 + 2.697 \times 10^{-11} {L_{1P}}^4 - 3.978 \times 10^{-8} {L_{1P}}^3 + 2.997 \times 10^{-5} {L_{1P}}^2 - 2.594 \times 10^{-2} L_{1P} + 69.80 \quad (11)$$

$$R^2 = 0.9981$$

For Location 1T:

$$v_{1T-85^{th}} = -3.320 \times 10^{-9} {L_{1T}}^3 + 5.640 \times 10^{-6} {L_{1T}}^2 - 1.071 \times 10^{-2} L_{1T} + 71.67 \quad (12)$$

$$R^2 = 0.9980$$

$$v_{1T-Mean} = -3.968 \times 10^{-9} {L_{1T}}^3 + 6.610 \times 10^{-6} {L_{1T}}^2 - 1.165 \times 10^{-2} L_{1T} + 66.59 \quad (13)$$

$$R^2 = 0.9956$$

All study locations were performed four regressions. The equations and R-squared values can be found in Appendix A. All R-squared values are greater than 0.95, which indicates a very good fit. Generally, overfitting with polynomial regression occurs when the model is too complicated or has too many features. Thus, to avoid overfitting and obtain relatively accurate models, this study applied a two-step method. First, the R-squared value is examined to be greater than 0.95 so that a very good fit can be guaranteed. Second, the model should be consistent with the data distribution pattern. For example, by adding powers of the model, the regression distribution may not follow the data distribution pattern. Such a model should not be selected. It should be noted that all estimated parameters are statistically significant at the 99% confidence level. *L* is defined as the distance from the starting point of the taper to any points on the taper, deceleration lane, or off-ramp. *v* is the speed downstream from the taper start point.

From the models developed, only 85th percentile speeds and mean speeds at the taper start point, deceleration lane start point, deceleration lane endpoint, and off-ramp endpoint are summarized in **Table 8**. All speeds at critical points can be found in Appendix A. The speeds at parallel-design locations were 1-2 mph higher than that at tapered-design locations in taper and deceleration lane sections. However, the speeds upon vehicles entering the off-ramp for Locations 1T to 5T were typically 3 mph higher than parallel-design locations. When an advisory speed was

posted on the off-ramp, the operating speeds were not significantly affected by the advisory speed which is 35 mph for Locations 1P, 2P, 3P, and 4T. The mean speed for a 35-mph advisory speed location was approximately 55 mph, and the approximate speed was 58 mph without the advisory speed sign.

Table 8 A comparison of speed distribution and speed reduction percentage on the deceleration lane and off-ramp: (a) parallel-design locations; and (b) tapered-design locations.

(a)

Site		Speed (mph)				Speed Reduction Percentage*		
		Taper Start	Deceleration Lane Start	Deceleration Lane End	Off-Ramp End	Taper	Deceleration Lane	Off-Ramp
Location 1P 645 ft	85th	74.02	72.67	63.39	23.88	2.69%	18.51%	78.80%
	Mean	69.80	65.71	56.29	10.26	6.87%	15.82%	77.31%
Location 2P 735 ft	85th	72.53	70.14	60.04	31.48	5.82%	24.60%	69.57%
	Mean	64.59	65.70	53.14	17.71	-2.37%	26.79%	75.58%
Location 3P 775 ft	85th	68.09	65.12	55.92	19.31	6.09%	18.86%	75.05%
	Mean	61.97	58.84	47.13	11.50	6.20%	23.20%	70.60%
	85th	69.47	70.76	63.29	19.14	-2.56%	14.84%	87.72%

Location 4P 700 ft	Mean	63.03	64.57	55.95	13.95	-3.14%	17.56%	85.57%
Location 5P 990 ft	85th	75.07	73.87	69.81	29.00	2.60%	8.81%	88.58%
	Mean	69.26	68.36	62.18	22.50	1.92%	13.22%	84.86%
*Note: Speed reduction percentage=speed reduction/total speed reduction from deceleration lane start point to the off-ramp end point								

(b)

Site		Speed (mph)				Speed Reduction Percentage*		
		Taper Start	Deceleration Lane Start	Deceleration Lane End	Off-Ramp End	Taper	Deceleration Lane	Off-Ramp
Location 1T 425 ft	85th	69.64	68.00	64.89	31.31	4.28%	8.11%	87.61%
	Mean	64.40	62.65	59.34	20.38	3.98%	7.52%	88.51%
Location 2T 320 ft	85th	72.55	70.62	65.46	20.81	3.73%	9.97%	86.30%
	Mean	64.37	62.52	57.06	15.82	3.81%	11.25%	84.94%
Location 3T 420 ft	85th	67.14	65.47	61.58	28.29	4.30%	10.01%	85.69%
	Mean	61.30	59.45	54.59	19.62	4.44%	11.66%	83.90%
Location 4T 445 ft	85th	68.19	68.37	64.85	7.47	-0.30%	5.80%	94.50%
	Mean	64.37	63.63	58.75	0.00	1.15%	7.58%	91.27%

Location 5T 365 ft	85th	73.20	71.98	68.26	37.05	3.37%	10.29%	86.33%
	Mean	66.65	65.82	62.61	28.18	2.16%	8.34%	89.50%
*Note: Speed reduction percentage=speed reduction/total speed reduction from deceleration lane start point to the off-ramp end point								

The speed reduction percentage is the percentage of speed reduced at the taper, deceleration lane, and off-ramp section. As shown in **Table 8**, the high percentage of the speed reduction occurred on off-ramps, which revealed that speed reduction was more significant on off-ramps than deceleration lanes. However, NCHRP Report 730 made a different indication (Torbic, et al. 2012). It should be mentioned that NCHRP Report 730 did not include the speed and deceleration along the entire deceleration lane and off-ramp but only several points (Torbic, et al. 2012). The authors indicated that drivers were completing much of the required deceleration in the freeway lane upstream of the beginning of the taper when they found field-measured deceleration rates were less than the *Green Book* assumptions (Torbic, et al. 2012). This indication is very different from our results. For example, our results showed that Location 1P only had a 16% speed reduction in mean speed distribution on deceleration lanes and approximately 77% on off-ramps. When comparing parallel-design locations with tapered-design locations, it was found that tapered-design locations have higher speed reduction percentages on off-ramps in the range of 84% to 95%, while parallel-design locations have 70% to 88% speed reduction. The speed- reduction percentage on the deceleration lane and off-ramp indicated that drivers decelerated more on an off-ramp than on the deceleration lane. Also, some negative speed reduction percentages were observed, which implied that drivers may have accelerated on the taper section at three out of five parallel-design locations.

Moreover, longer deceleration lanes may not lead to higher speed reduction percentages. For both types of locations, the study sites with the longest deceleration lanes have the lowest speed reduction percentages. Location 5P with a 990-ft deceleration lane only had 8.81% speed reduction on it. Location 4T with a 445-ft deceleration lane only had 5.80% speed reduction on it. However, shorter deceleration lanes do not result in higher speed reduction percentages either. The locations with the highest speed reduction percentages are median lengths – Location 2P (735-ft deceleration lane) and Location 3T (420-ft deceleration lane).

4.1.2 Driver Braking Behavior

Driver braking behavior was interpreted by the brake pedal usage and deceleration rate distribution on the deceleration lane and off-ramp.

4.1.2.1 Brake Pedal Usage

The brake status (0 or 1) indicates whether the driver was applying the brake at the certain 0.1 seconds. The brake status distribution was performed based on the percentage of drivers who applied brakes at certain sections on the deceleration lane and off-ramp. **Figure 10** shows brake status distributions at Location 1P and Location 1T. At Location 1P, only 30% of drivers applied brakes when entering the taper section. An increase to 60% of drivers applied brakes when entering the deceleration lane while a decrease back to 30% happened after traversing the first half of the deceleration lane. More braking behavior was observed after the vehicle approached the off-ramp terminals. Similar results from Location 1T were presented in **Figure 10*b***. From ten study locations, the average brake percentages for taper, deceleration lane, and off-ramp sections are 21.42%, 30.30%, and 63.67% in parallel-design locations, respectively, and 25.23%, 32.51%, and 57.69% in tapered-design locations, respectively. The brake pedal usage was also performed in other study locations, which can be found in Appendix B.

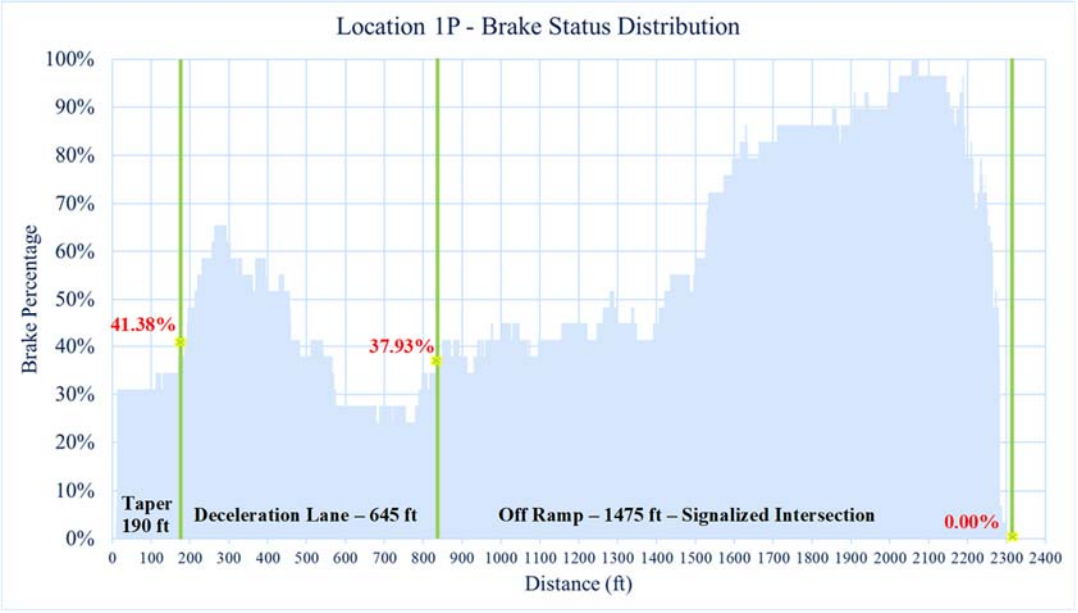

(*a*)

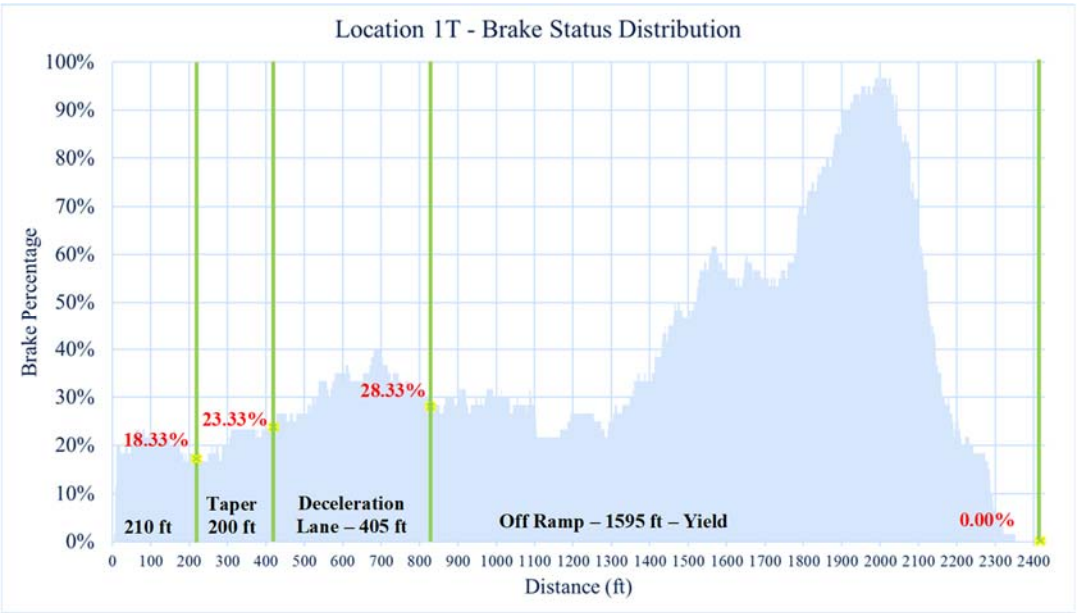

(*b*)

Figure 10 Brake status distribution: (*a*) Location 1P; and **(*b*) Location 1T.**

4.1.2.2 Deceleration Rate Distribution

To calculate the deceleration rates, the speed-distance-based model, for example, **Equations 10** to **13**, was first converted to the speed-time-based model as time can be calculated from the distance and speed. Then, the first derivative of this speed-time-based model was determined. This first derivative is the deceleration rate from speed regression. The mean and 85th percentile deceleration rates will be summarized. An extra step was taken to identify the critical speed changepoint on the off-ramp. As greater speed reductions and higher brake percentages were observed upstream from the off-ramp terminal, change point models were used to identify driver reaction point where most drivers decelerate very hard when approaching the ramp terminal. Two examples of critical speed changepoint analysis are presented in **Figure 11**. In Location 1P, drivers adjusted their speed 469-ft upstream of the off-ramp terminal (1,841 ft after the taper start point) from the 85th percentile speed distribution. For Location 1T as shown in **Figure 11*b***, this number was increased to 764 ft (1,666 ft after the taper start point). The average reaction points for parallel-design locations are 540.4 ft in 85th percentile speed and 541.6 ft in mean speed. For tapered-design locations, the critical speed changepoints are 646.8 ft in 85th percentile speed and 652.2 ft in mean speed upstream from the ramp terminal. The 85th percentile critical speed changepoint was calculated for each location, which can be found in Appendix C.

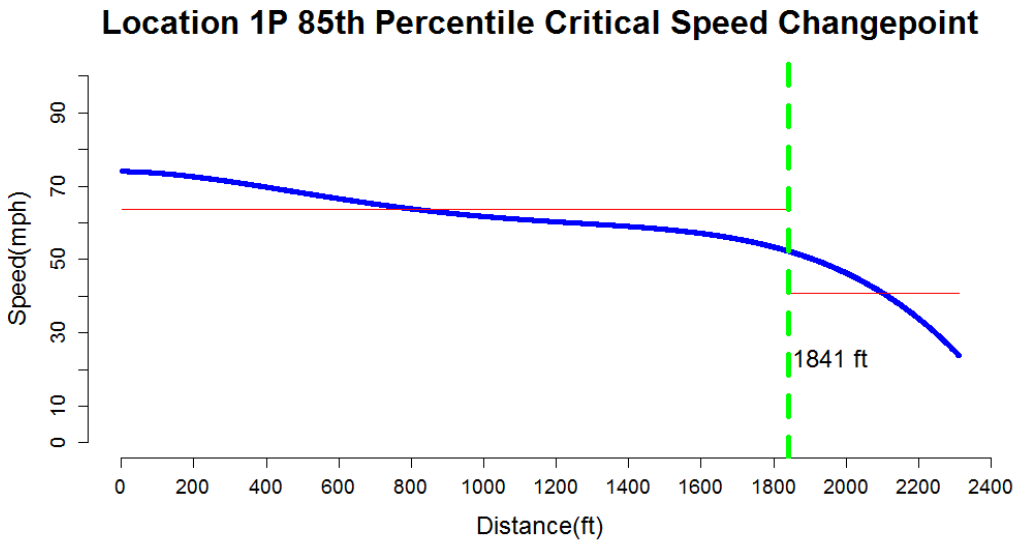

(*a*)

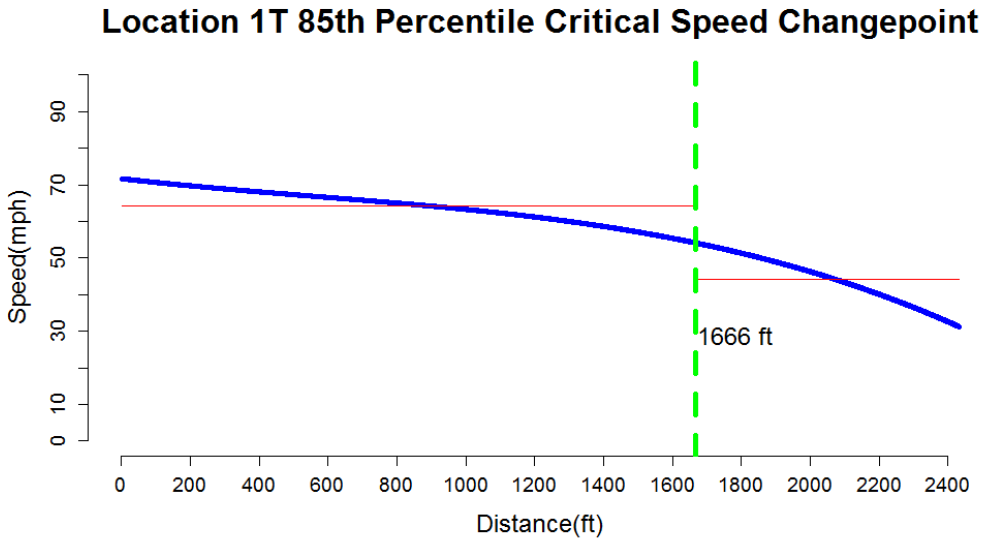

(*b*)

Figure 11 Critical speed changepoint: (*a*) Location 1P; and **(*b*) Location 1T.**

The R statistical package of changepoint was utilized for critical speed changepoint detection based on binary segmentation algorithms. After the changepoints are detected, the deceleration rate before and after the changepoint on the off-ramps can also be obtained. The mean and 85th percentile deceleration rates were compared with the *Green Book* criterion which assumes

a constant deceleration (AASHTO 2018). The *Green Book* deceleration rates were derived from recommended minimum deceleration lane lengths as summarized in NCHRP Report 730 (Torbic, et al. 2012). As shown in **Table 9**, most of the naturalistic driving deceleration rates were lower than the design deceleration rates in the *Green Book*. However, the deceleration rates after the changepoint on the off-ramp were relatively higher than other sections, and some of them were even greater than the design rates. For parallel-design deceleration lanes, the deceleration rates on the deceleration lane were slightly higher than that on the tapered-design locations. In NCHRP Report 730, however, the authors observed that parallel deceleration lanes had a substantially higher deceleration rate of more than twice than tapered-design ones especially on straight ramps (Torbic, et al. 2012). All deceleration rates on the deceleration lane were much smaller than the *Green Book* criterion. The mean deceleration rates on certain sections of parallel-design and tapered-design locations were summarized in the last four rows in **Table 9**. It can be found that the *Green Book* assumes that drivers are exiting the freeway with a constant deceleration rate, while the results of this study indicate that drivers' braking behavior on the taper section, deceleration lane section, and off-ramp section are different with different deceleration rates.

Table 9 Deceleration rates at study locations.

Deceleration Rate (ft/s^2)		Taper	Deceleration Lane d_D	Off Ramp d_R		GB Decel Rate* (ft/s^2)
				Before Changepoint	After Changepoint	
Location 1P 645 ft	85th	-1.63	-2.34	-2.12	-5.72	-5.41
	Mean	-3.61	-2.24	-1.88	-5.19	
Location 2P 735 ft	85th	-2.47	-2.41	-2.32	-6.46	-5.41
	Mean	-0.35	-2.57	-2.55	-4.52	

Location 3P 775 ft	85th	-2.87	-1.79	-2.76	-3.53	-5.41
	Mean	-2.67	-1.91	-2.20	-2.47	
Location 4P 700 ft	85th	0.18	-1.93	-2.89	-5.09	-5.88
	Mean	0.17	-1.95	-2.20	-4.20	
Location 5P 990 ft	85th	-0.98	-0.92	-2.15	-5.45	-5.88
	Mean	-0.52	-1.01	-1.77	-4.55	
Location 1T 425 ft	85th	-1.28	-1.12	-2.06	-2.94	-5.88
	Mean	-1.26	-1.10	-2.12	-2.69	
Location 2T 320 ft	85th	-2.08	-2.53	-3.77	-5.22	-5.88
	Mean	-1.78	-2.46	-3.35	-3.61	
Location 3T 420 ft	85th	-1.23	-1.27	-2.28	-4.48	-5.88
	Mean	-1.37	-1.48	-1.90	-4.12	
Location 4T 445 ft	85th	0.08	-1.90	-2.60	-7.03	-5.41
	Mean	-0.88	-1.63	-3.08	-5.40	
Location 5T 365 ft	85th	-1.50	-1.55	-1.50	-3.24	-5.88
	Mean	-0.96	-1.36	-1.62	-2.87	
Parallel-Design	85th	-1.55	-1.88	-2.45	-5.25	Note: *GB Decel Rate is the deceleration rate recommended in the *Green Book*.
	Mean	-1.40	-1.94	-2.12	-4.19	
Tapered-Design	85th	-1.20	-1.67	-2.44	-4.58	
	Mean	-1.25	-1.61	-2.41	-3.74	

4.1.3 Determination of the Minimum Length of Deceleration Lane

Equations 14 to **16** were developed to estimate the minimum deceleration lane length. The general idea of determining the minimum length for deceleration lane is to calculate the deceleration distance needed to decelerate from mainline speeds to ramp terminal speeds and subtract the certain off-ramp length. In other words, the minimum deceleration lane length is equal to the deceleration distance deducted by the off-ramp length. The minimum deceleration length can be determined by plugging in the deceleration rates from the deceleration lanes (d_D) and off-ramps (d_R and d_{RP}) sections in **Table 9**, entering speed for the deceleration lane (V_D), and estimating entering speed for the exit ramp (V_R'), the changepoint on the off-ramp (V_{RP}), and the first controlling feature on off-ramp (V_C) from regression models. The controlling feature represents whether ramp curvature or the crossroad terminal is the design element that controls vehicle deceleration (Torbic, et al. 2012). On the relatively straight ramps at locations described in this study, the first controlling feature usually is the crossroad terminal (signalized intersection).

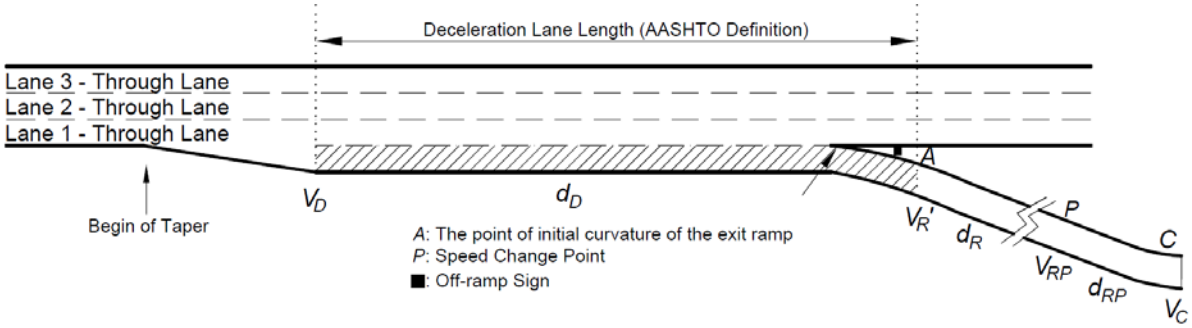

$$\begin{cases} L_{Decel} = L_Q, & V_D \le V_R' \\ L_{Decel} = \dfrac{(1.47V_R')^2 - (1.47V_D)^2}{2d_D} + L_Q, & V_D > V_R' \end{cases} \quad (14)$$

$$V_R' = \frac{\sqrt{(1.47V_{RP})^2 - 2d_R L_R}}{1.47} \quad (15)$$

$$V_{RP} = \frac{\sqrt{(1.47V_C)^2 - 2d_{RP}L_{RP}}}{1.47} \quad (16)$$

Where, L_{Decel} = Deceleration lane length, ft

L_Q = Queue length at the off-ramp terminal, ft

L_R = Length from deceleration lane endpoint to the critical speed changepoint upstream from the first controlling feature on the off-ramp, ft

L_{RP} = Length from the critical speed changepoint to the off-ramp terminal, ft

V_C = Speed at the first controlling feature on the off-ramp, mi/h

V_D = Entering speed for deceleration lane, mi/h

V_R' = Estimated entering speed for the off-ramp, assuming drivers decelerate on $L_R$with a constant deceleration rate on exit ramps (d_R), mi/h

V_{RP} = Speed at the changepoint on the off-ramp, mi/h

d_D = Deceleration rate on deceleration lane, ft/s^2

d_R = Deceleration rate on exit ramp, ft/s^2

d_{RP} = Deceleration rate after the critical speed changepoint on the off-ramp, mi/h

To determine the deceleration lane length, the key parameters are summarized in **Table 10**. For example, at parallel-design locations, the speed at the stop bar of the off-ramp terminal (V_C) should be 0 mph and the deceleration rate (d_{RP}) is estimated to be -5.25 ft/s^2 on the off-ramp after the changepoint. The distance between the stop bar and the changepoint (L_{RP}) is 540 ft as mentioned previously. By applying Equation 12, the speed at the changepoint (V_{RP}) is 51.22 mph. When the total length of the off-ramp is 1,550 ft ($L_R = 1550 - 540 = 1010\ ft$), drivers would be able to comfortably reduce all the required speed on the off-ramp ($V_R' = 70mph = V_D$). For tapered-design locations, the final speed should also be 0 mph ($V_C = 0\ mph$) and the deceleration rate is -4.58 ft/s^2 after the changepoint ($d_{RP} = -4.58\ ft/s^2$). Following the same steps, it can be

determined that no deceleration lane will be required for decelerating purpose with a 1,540 ft off-ramp. The proposed minimum deceleration lane lengths of study locations are presented in

Table 11. As a result, Locations 1T, 5P, and 5T do not require a deceleration lane serving decelerating functions.

Table 10 Summary of key parameters to determine the deceleration lane length.

Key Parameters		Parallel-Design		Tapered-Design	
		Minimum (85th)	Mean	Minimum (85th)	Mean
Deceleration Lane (ft/s^2) d_D		-1.88	-1.94	-1.67	-1.61
Off Ramp	Before Changepoint (ft/s^2) d_R	-2.45	-2.12	-2.44	-2.41
	After Changepoint (ft/s^2) d_{RP}	-5.25	-4.19	-4.58	-3.74
Speed Entering Dec.Lane (mph) V_D		70.00	65.00	69.00	63.00
Speed at the Changepoint on Off-Ramp (mph) V_{RP}		51.22	45.74	52.49	47.43
Speed at the 1st Controlling Feature (mph) V_C		0.00	0.00	0.00	0.00
Length from Changepoint to Off-Ramp terminal (ft) L_{RP}		540		650	

Table 11 Comparison of proposed deceleration lane length and design length

Site Locations	Proposed Minimum Length (ft) (85th) L_{Decel}	Actual Deceleration Lane Length (ft)	Green Book Minimum Deceleration Length (ft)	Off-Ramp Length (ft) L_R+L_{RP}
Location 1P: I-75/SW Archer Rd	75	645	490	1475
Location 1T: I-75/Clark Rd	NA[1]	425	615	1595
Location 2P: I-75/SW County Highway 484	560	735	490	990
Location 2T: I-75/US 98	600	320	615	940
Location 3P: I-75/FL 326	520	775	490	1030
Location 3T: I-75/US 98	370	420	615	1170
Location 4P: I-75/CR 768	370	700	615	1180

Location 4T: I-75/SW College Rd	200	445	490	1340
Location 5P: I-75/CR 765	NA[1]	990	615	1690
Location 5T: I-75/CR 769	NA[1]	365	615	1725
Note: [1]NA indicates that the deceleration lane is not required for decelerating purpose.				

4.2 Freeway Work Zone Mobility Analysis

This section describes how the SHRP 2 NDS data led to the freeway work zone mobility evaluation. First, the gap and headway selection tables based on the driver characteristics and work zone configurations were developed. Second, speed analysis in terms of speed distributions and speed changepoint detection along the entire work zone consecutive sections was performed.

4.2.1 Gap and Headway Distribution

Time and space gap together with time headway distribution were studied based on driver characteristics (i.e., gender, age group, and risk perception) at four work zone configurations.

4.2.1.1 Driver characteristics

Driver characteristics include gender (female and male), age group (younger than 24, 25 to 59, and older than 60), and mean risk perception score. A higher perception score indicates that the driver is conservative and a lower score represents an aggressive driver. As presented in **Figure 12*a***, 60% of drivers in the dataset have a risk perception score greater than 160, which indicates

that these participants have good risk perceptions and tend to be cautious and obedient to traffic rules. It was found that risk perception distributions in female and male drivers are very different in **Figure 12*b*** and **12*c***. Approximate 80% of female drivers' risk perceptions fall into the interval between 140 and 200, while only 55% of male drivers scored within that interval. 25% of male drivers' risk perceptions fall into the interval between 200 and 220. In other words, male drivers were self-reported to have higher risk perceptions than the participating female drivers. In total, there were 52 female drivers and 50 male drivers. As shown in **Table 12**, the numbers of young, middle-aged, and senior drivers are 52, 28, and 22, respectively. Despite two cases with very low risk perceptions, the risk perceptions of female and male drivers range from 120 to 220. Female drivers obtain higher risk perception scores than male drivers in the same age group. It is interesting to find that regardless of gender, the risk perception score increases with the increase of driver's age. Please note that there was one participant who left demographic info blank, and thus it was not included in the headway distribution analysis.

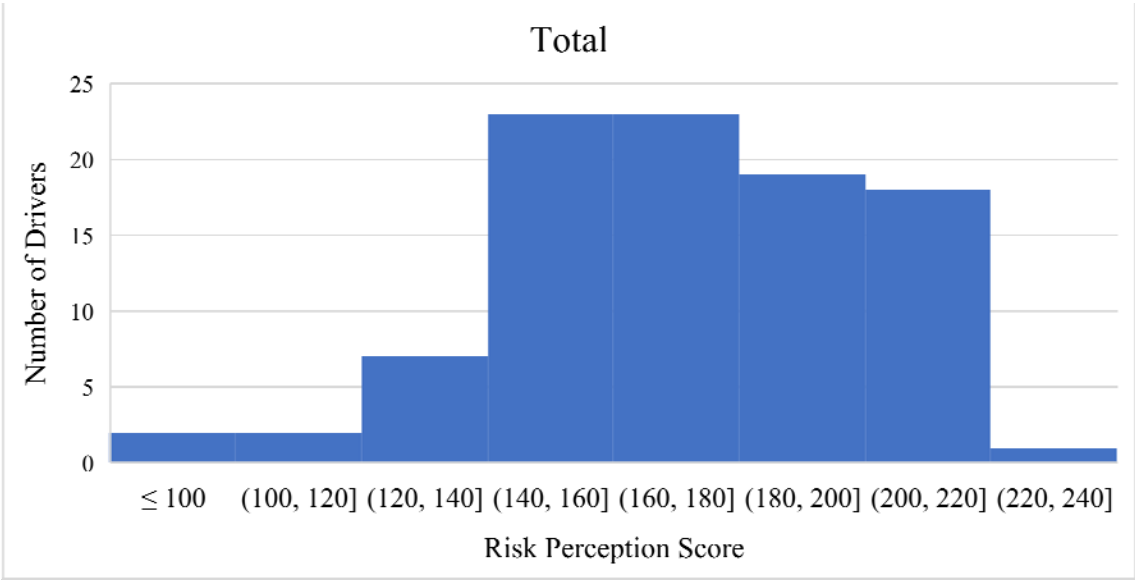

(a)

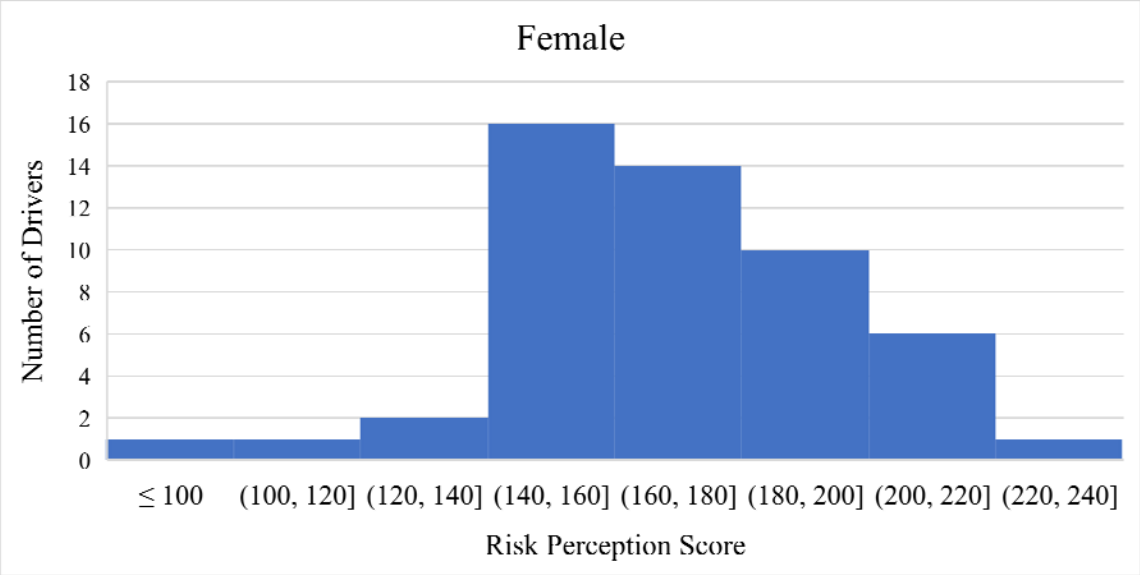

(*b*)

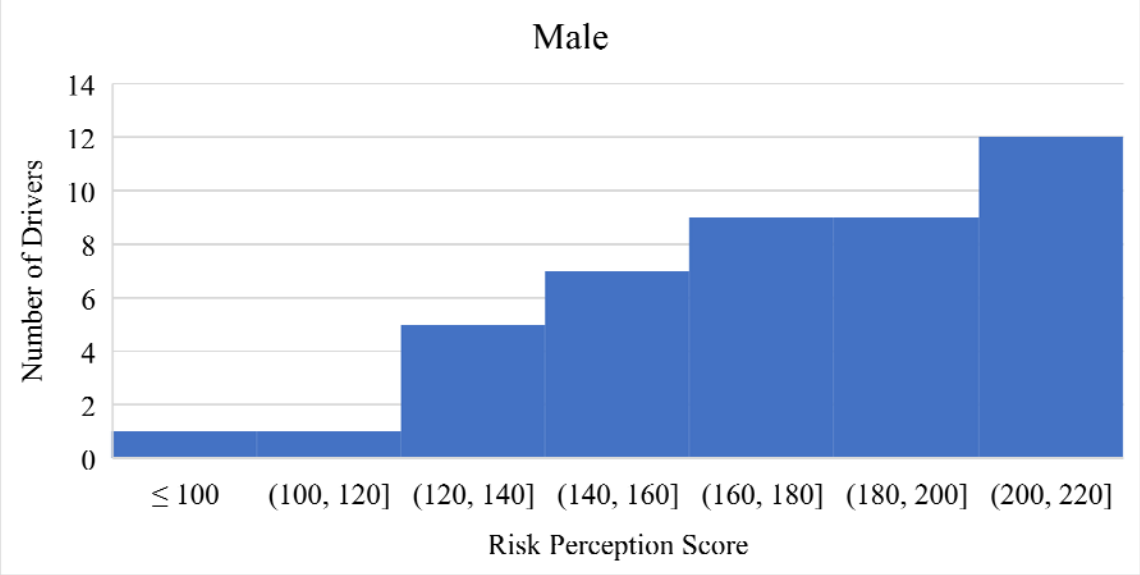

(*c*)

Figure 12 Driver Risk Perception Distribution:

(*a*) Total Drivers; (*b*) Female Drivers; and (*c*) Male Drivers.

Table 12 Summary of Driver Risk Perception and Demographic Info

Age	Female		Male	
	Sample Size	Risk Perception*	Sample Size	Risk Perception*
≤ 24	32	(120, 198)	20	(112, 192)
25 - 59	11	(150, 205)	17	(123, 206)
≥ 60	9	(164, 221)	13	(147, 219)
*Note: a higher risk perception score indicates a higher cautious level.				

4.2.1.2 Gap and headway profiles by driver types

Figure 13 presents the gap and headway profile by driver types at the LC 2-1 work zone. The gap and headway profile at other locations can be found in Appendix D. It was stated that young drivers are more aggressive and have higher risks to be involved in fatal crashes when compared with other age groups (Lambert-Bélanger, et al. 2012), which is consistent with lower risk perception score (more aggressive driver) from young drivers. Interestingly, young drivers maintained a longer gap and headway than middle-aged drivers. From four work zone configurations in this study, middle-aged drivers typically maintained the shortest time gap and headway among all age groups. Please note that space headway equals to gap spacing plus 15 ft (which is the vehicle length). Thus, space headway was not presented in **Figure 13**.

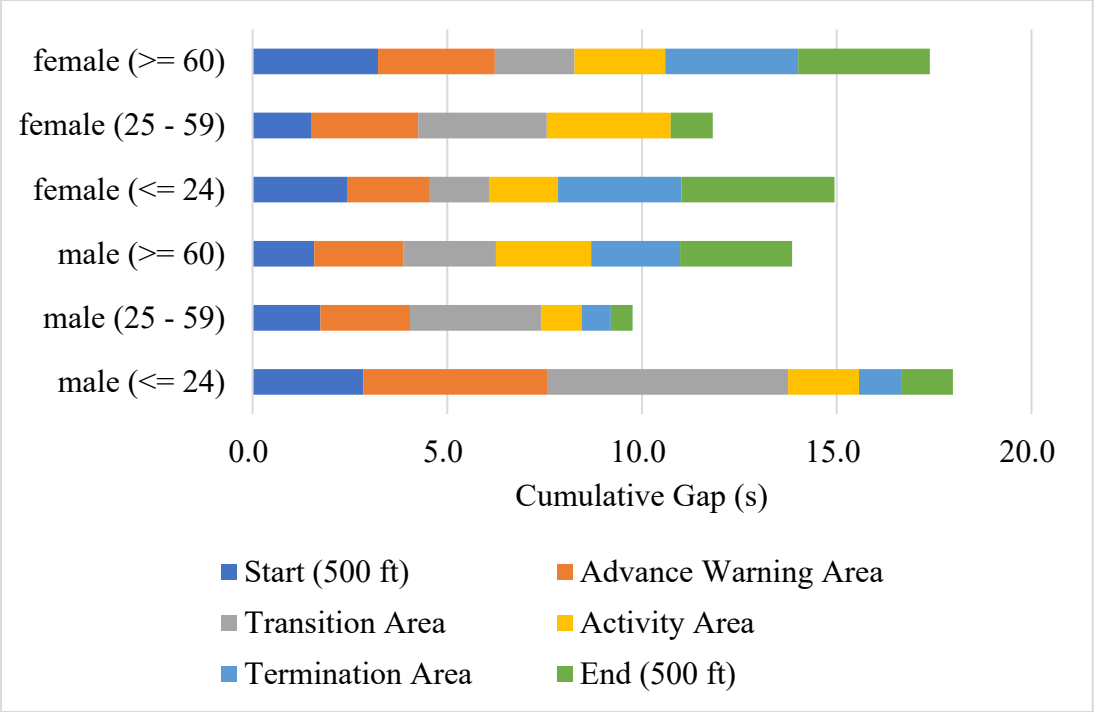
female (>= 60)
female (25 - 59)
female (<= 24)
male (>= 60)
male (25 - 59)
male (<= 24)
0.0
5.0
10.0
15.0
20.0
Cumulative Gap (s)
Start (500 ft)
Advance Warning Area
Transition Area
Activity Area
Termination Area
End (500 ft)

(a)

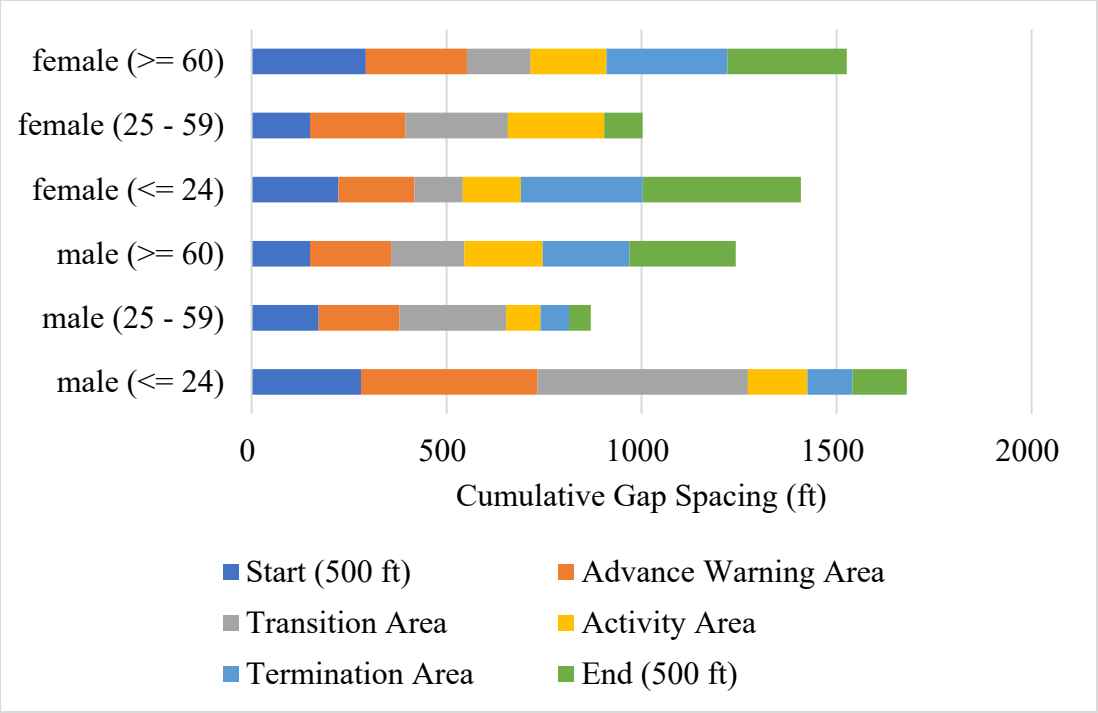
female (>= 60)
female (25 - 59)
female (<= 24)
male (>= 60)
male (25 - 59)
male (<= 24)
0
500
1000
1500
2000
Cumulative Gap Spacing (ft)
Start (500 ft)
Advance Warning Area
Transition Area
Activity Area
Termination Area
End (500 ft)

(b)

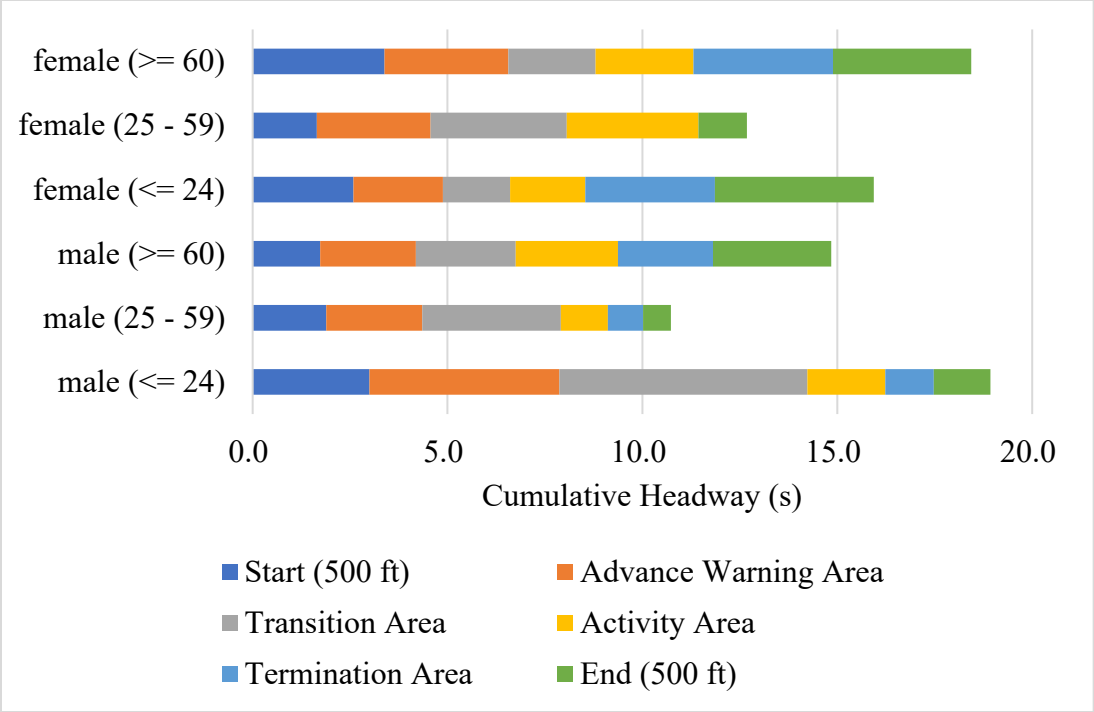

(*c*)

Figure 13 Gap and headway profile by driver types at LC 2-1:

(*a*) gap; (*b*) gap spacing; and (*c*) headway.

Gap and headway selection tables before, during, and after work zone by different driver types at four selected work zone configurations (LC 2-1, LC 3-2, SC 2-2, and SC 3-3) were developed, which can be found in Appendix E. **Table 13** summarized the details of gap and headway distribution and driver characteristics (gender, age group, and driver risk perceptions) at the LC 2-1 work zone. It includes the 95% confidence interval, mean values of risk perception scores, and gap and headways from drivers by age group and gender.

The time and space gap distributions from different drivers traversing various work zones can improve ACC spacing policies for the automotive industry. Taking driver characteristics into consideration when developing spacing policies contributes to the similarity of human driver's spacing behavior in the ACC systems, and thus, would be able to enhance comfort for drivers. It

can further improve driver's acceptance and system utilization by introducing driver characteristics.

The headway distributions from different drivers traversing various work zone can improve work zone capacity models. The desired time headway parameter (CC1) in VISSIM is static through all work zone consecutive sections, although it was suggested that desired time headway should be modeled as a distribution rather than a static value when data are available (Dong, et al. 2015). Thus, if headway distribution models built for different driver characteristics are used in lieu of a static value in VISSIM, a more accurate capacity estimation can be captured.

Table 13 Gap and headway selection table by driver characteristics at LC 2-1.

	Gender	Age	Mean Gap (s)	95% CI of Gap (s)	Mean Gap Spacing (ft)	95% CI of Gap Spacing (ft)	Mean Headway (s)	95% CI of Headway (s)	Mean Risk Score
Start (500 ft)	Female	Subtotal	2.7	(1.3, 4.2)	251	(121, 380)	2.9	(1.4, 4.3)	176
		≤ 24	2.4	(2.3, 2.5)	223	(218, 228)	2.6	(2.5, 2.7)	142
		25 - 59	1.5	(1.2, 1.8)	150	(120, 180)	1.6	(1.3, 2.0)	161
		≥ 60	3.2	(1.7, 4.7)	293	(155, 431)	3.4	(1.9, 4.9)	186
	Male	Subtotal	1.9	(0.8, 2.9)	181	(81, 281)	2.0	(0.9, 3.1)	191
		≤ 24	2.8	(2.0, 3.7)	281	(191, 371)	3.0	(2.1, 3.9)	146
		25 - 59	1.7	(1.0, 2.5)	172	(99, 244)	1.9	(1.1, 2.7)	190
		≥ 60	1.6	(0.5, 2.6)	150	(58, 241)	1.7	(0.7, 2.8)	208
	Grand Total		2.4	(1.0, 3.8)	225	(101, 349)	2.6	(1.2, 3.9)	182

	Gender	Age	Mean Gap (s)	95% CI of Gap (s)	Mean Gap Spacing (ft)	95% CI of Gap Spacing (ft)	Mean Headway (s)	95% CI of Headway (s)	Mean Risk Score
Advance Warning Area	Female	Subtotal	2.9	(1.5, 4.2)	249	(125, 374)	3.0	(1.6, 4.4)	174
		≤ 24	2.1	(1.7, 2.5)	194	(149, 240)	2.3	(1.9, 2.7)	142
		25 - 59	2.8	(1.7, 2.5)	245	(126, 364)	2.9	(1.4, 4.4)	167
		≥ 60	3.0	(1.6, 4.4)	259	(128, 391)	3.2	(1.8, 4.6)	182
	Male	Subtotal	2.6	(1.3, 4.2)	240	(94, 386)	2.8	(1.2, 4.4)	185
		≤ 24	4.7	(3.6, 5.8)	453	(356, 549)	4.9	(3.8, 6.0)	146
		25 - 59	2.3	(0.7, 3.9)	207	(72, 342)	2.5	(0.8, 4.1)	167
		≥ 60	2.3	(1.0, 3.6)	208	(93, 323)	2.5	(1.2, 3.7)	207
	Grand Total		2.8	(1.3, 4.2)	246	(114, 378)	2.9	(1.5, 4.4)	178
	Gender	Age	Mean Gap (s)	95% CI of Gap (s)	Mean Gap Spacing (ft)	95% CI of Gap Spacing (ft)	Mean Headway (s)	95% CI of Headway (s)	Mean Risk Score
Transition Area	Female	Subtotal	2.4	(1.1, 3.7)	190	(88, 292)	2.6	(1.3, 3.9)	170
		≤ 24	1.5	(1.5, 1.6)	124	(122, 127)	1.7	(1.7, 1.8)	142
		25 - 59	3.3	(1.4, 5.2)	262	(112, 412)	3.5	(1.6, 5.4)	165
		≥ 60	2.0	(1.5, 2.6)	163	(120, 206)	2.2	(1.7, 2.8)	177
	Male	Subtotal	3.1	(0.8, 5.4)	253	(60, 445)	3.3	(1.0, 5.6)	192
		≤ 24	6.2	(5.9, 6.5)	539	(513, 566)	6.4	(6.1, 6.7)	146
		25 - 59	3.4	(0.8, 6.8)	273	(68, 542)	3.6	(0.9, 7.0)	174
		≥ 60	2.4	(1.0, 3.8)	188	(77, 299)	2.6	(1.1, 4.0)	207

	Grand Total		2.7	(0.9, 4.4)	213	(68, 359)	2.8	(1.1, 4.6)	179
Activity Area	Gender	Age	Mean Gap (s)	95% CI of Gap (s)	Mean Gap Spacing (ft)	95% CI of Gap Spacing (ft)	Mean Headway (s)	95% CI of Headway (s)	Mean Risk Score
	Female	Subtotal	2.4	(1.0, 3.9)	200	(79, 322)	2.6	(1.2, 4.1)	174
		≤ 24	1.8	(0.6, 3.4)	149	(53, 297)	1.9	(0.8, 3.6)	142
		25 - 59	3.2	(0.8, 5.5)	247	(62, 432)	3.4	(1.0, 5.7)	163
		≥ 60	2.3	(1.4, 3.3)	195	(107, 282)	2.5	(1.5, 3.5)	181
	Male	Subtotal	2.1	(0.6, 3.6)	174	(54, 294)	2.3	(0.8, 3.8)	196
		≤ 24	1.8	(0.5, 3.2)	152	(37, 268)	2.0	(0.6, 3.4)	146
		25 - 59	1.0	(0.8, 1.2)	88	(69, 108)	1.2	(1.0, 1.4)	202
		≥ 60	2.4	(0.9, 4.0)	201	(77, 325)	2.6	(1.1, 4.2)	207
	Grand Total		2.3	(0.8, 3.8)	191	(70, 313)	2.5	(1.0, 4.0)	181
Termination Area	Gender	Age	Mean Gap (s)	95% CI of Gap (s)	Mean Gap Spacing (ft)	95% CI of Gap Spacing (ft)	Mean Headway (s)	95% CI of Headway (s)	Mean Risk Score
	Female	Subtotal	3.4	(1.8, 5.0)	310	(162, 459)	3.5	(1.9, 5.1)	177
		≤ 24	3.2	(2, 4.40)	313	(196, 429)	3.3	(2.1, 4.5)	141
		25 - 59	NA	NA	NA	NA	NA	NA	NA
		≥ 60	3.4	(1.8, 5.1)	310	(158, 462)	3.6	(1.9, 5.2)	182
	Male	Subtotal	1.7	(0.4, 3.1)	163	(31, 297)	1.8	(0.5, 3.3)	191
		≤ 24	1.1	(1.0, 1.2)	115	(105, 126)	1.2	(1.2, 1.3)	146
		25 - 59	0.8	(0.4, 1.2)	73	(30, 119)	0.9	(0.5, 1.4)	202

		≥ 60	2.3	(0.5, 4.0)	222	(65, 379)	2.4	(0.7, 4.2)	204
	Grand Total		2.8	(1.1, 4.6)	262	(103, 422)	3.0	(1.2, 4.7)	181
End (500 ft)	Gender	Age	Mean Gap (s)	95% CI of Gap (s)	Mean Gap Spacing (ft)	95% CI of Gap Spacing (ft)	Mean Headway (s)	95% CI of Headway (s)	Mean Risk Score
	Female	Subtotal	2.9	(1.2, 4.6)	267	(108, 425)	3.1	(1.4, 4.8)	181
		≤ 24	3.9	(3.9, 4.0)	405	(403, 408)	4.1	(4.0, 4.1)	141
		25 - 59	1.1	(0.9, 1.2)	99	(81, 116)	1.2	(1.1, 1.4)	171
		≥ 60	3.4	(1.7, 5.0)	306	(154, 458)	3.5	(1.9, 5.2)	186
	Male	Subtotal	2.1	(0.5, 3.9)	198	(49, 364)	2.2	(0.6, 4.1)	191
		≤ 24	1.3	(1.3, 1.3)	139	(135, 144)	1.4	(1.4, 1.5)	146
		25 - 59	0.6	(0.5, 0.6)	56	(52, 60)	0.7	(0.7, 0.7)	202
		≥ 60	2.9	(0.8, 5.0)	273	(91, 455)	3.0	(0.9, 5.1)	203
	Grand Total		2.6	(0.8, 4.4)	242	(78, 407)	2.8	(1.0, 4.6)	185

4.2.1.3 Gap comparison

The gap spacing distributions by different work zone consecutive sections are illustrated in **Figure 14**. Boxplots were utilized to detect potential outliers, which were filtered if they were beyond the upper limit or lower limit. It can be found that vehicles maintain different gap spacings in different work zone sections and configurations. For instance, at work zone configuration LC 2-1 as presented in **Figure 14*a***, the mean gap spacings from start section to end section (**Table 13**) are 225, 246, 213, 191, 262, and 242 ft, respectively. The lower quartile (25%) can be treated as the critical gap spacing that most drivers would maintain a gap that is longer than that. From the boxplots, the range of the upper quartile (75%) and lower quartile (25%) in mean gap spacing tend to decrease as vehicles move from the start section to transition area. The mean gap spacing began to increase after traversing the activity area. While for LC 3-2 (**Figure 14*b***), the mean gap spacing throughout the entire work zone remained focused – from 166 to 190 ft (**Table E- 2**). As for shoulder closure, the mean gap spacings from the start to the end at SC 2-2 are 225, 179, 162, and 184 ft (**Table E- 3**). At SC 3-3, headways were stable with minor changes ranging from 142 to 172 ft traversing work zones (**Table E- 4**). This might be indicating that with more through lanes, work zone activity will have fewer impacts on drivers.

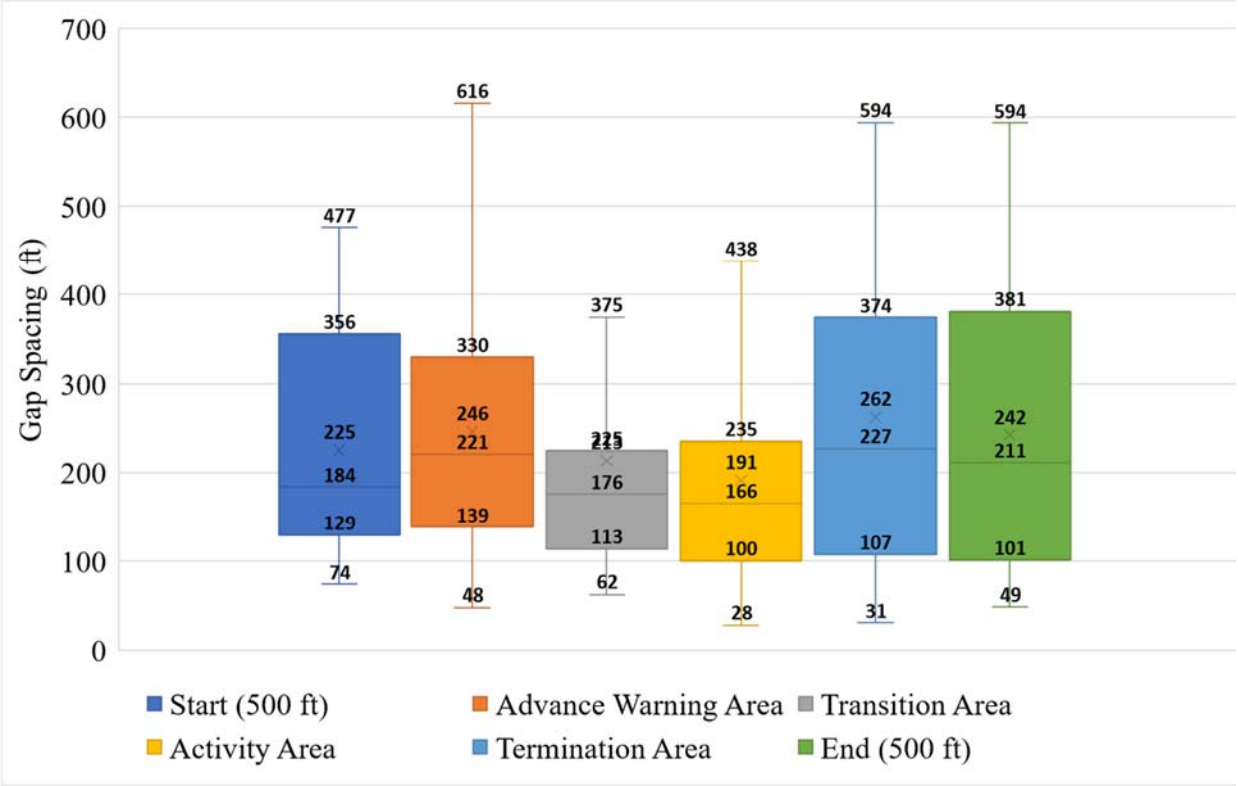
Gap Spacing (ft)
700
600
500
400
300
200
100
0
477
356
225
184
129
74
616
330
246
221
139
48
375
225
176
113
62
438
235
191
166
100
28
594
374
262
227
107
31
594
381
242
211
101
49
Start (500 ft)
Advance Warning Area
Transition Area
Activity Area
Termination Area
End (500 ft)

(*a*)

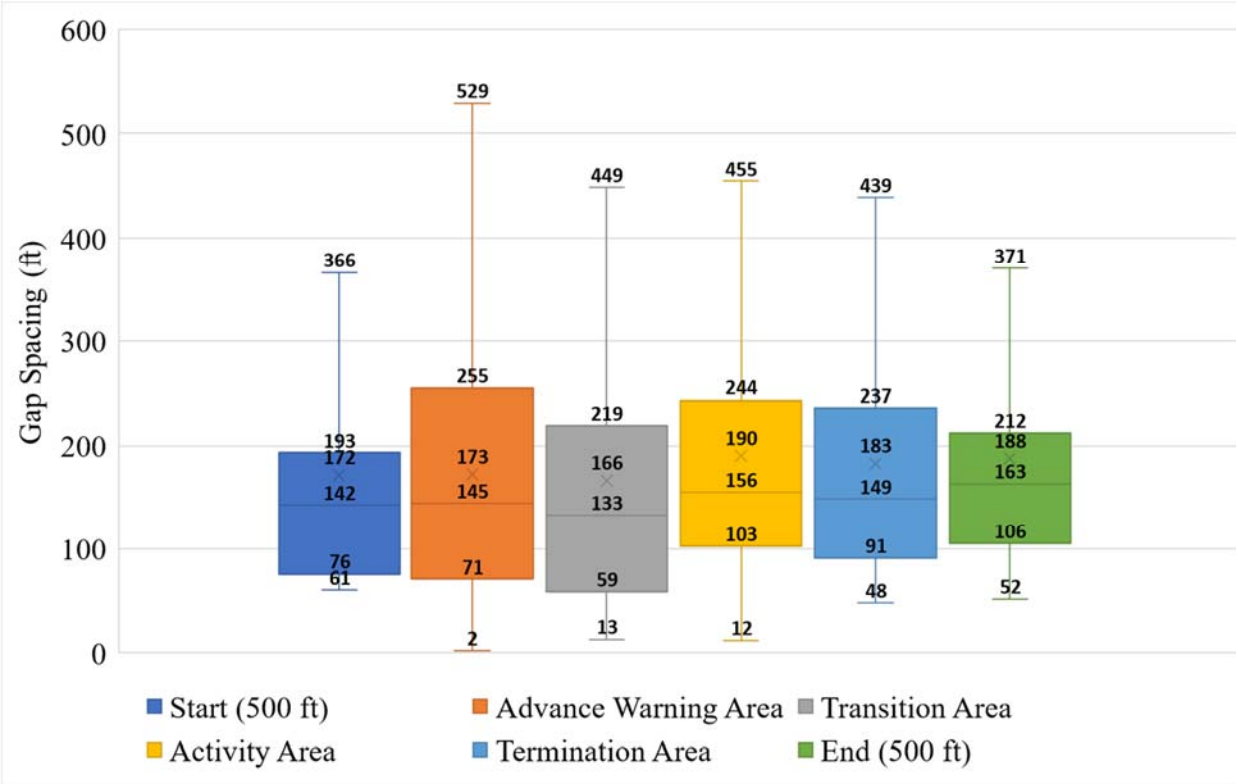
Gap Spacing (ft)
600
500
400
300
200
100
0
366
193
172
142
76
61
529
255
173
145
71
2
449
219
166
133
59
13
455
244
190
156
103
12
439
237
183
149
91
48
371
212
188
163
106
52
Start (500 ft)
Advance Warning Area
Transition Area
Activity Area
Termination Area
End (500 ft)

(*b*)

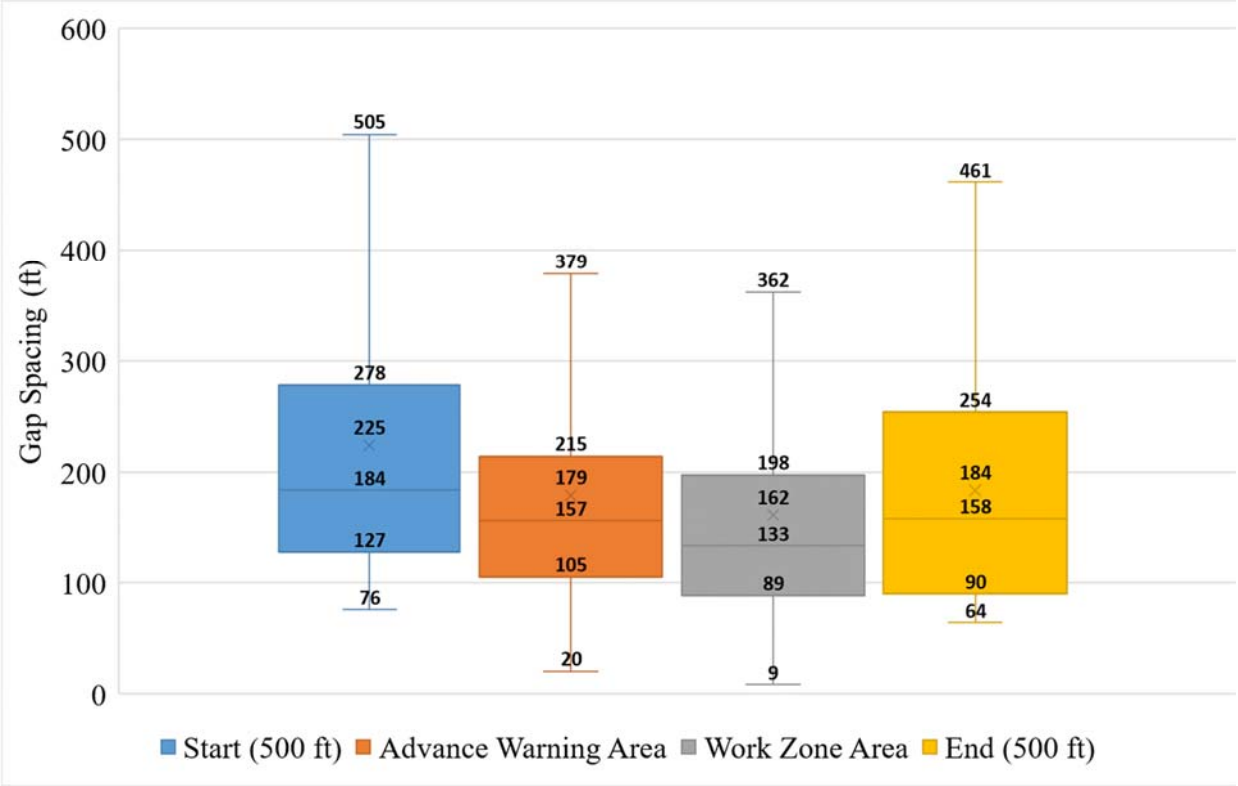
600
500
400
300
200
100
0
Gap Spacing (ft)
505
278
225
184
127
76
379
215
179
157
105
20
362
198
162
133
89
9
461
254
184
158
90
64
Start (500 ft)
Advance Warning Area
Work Zone Area
End (500 ft)

(c)

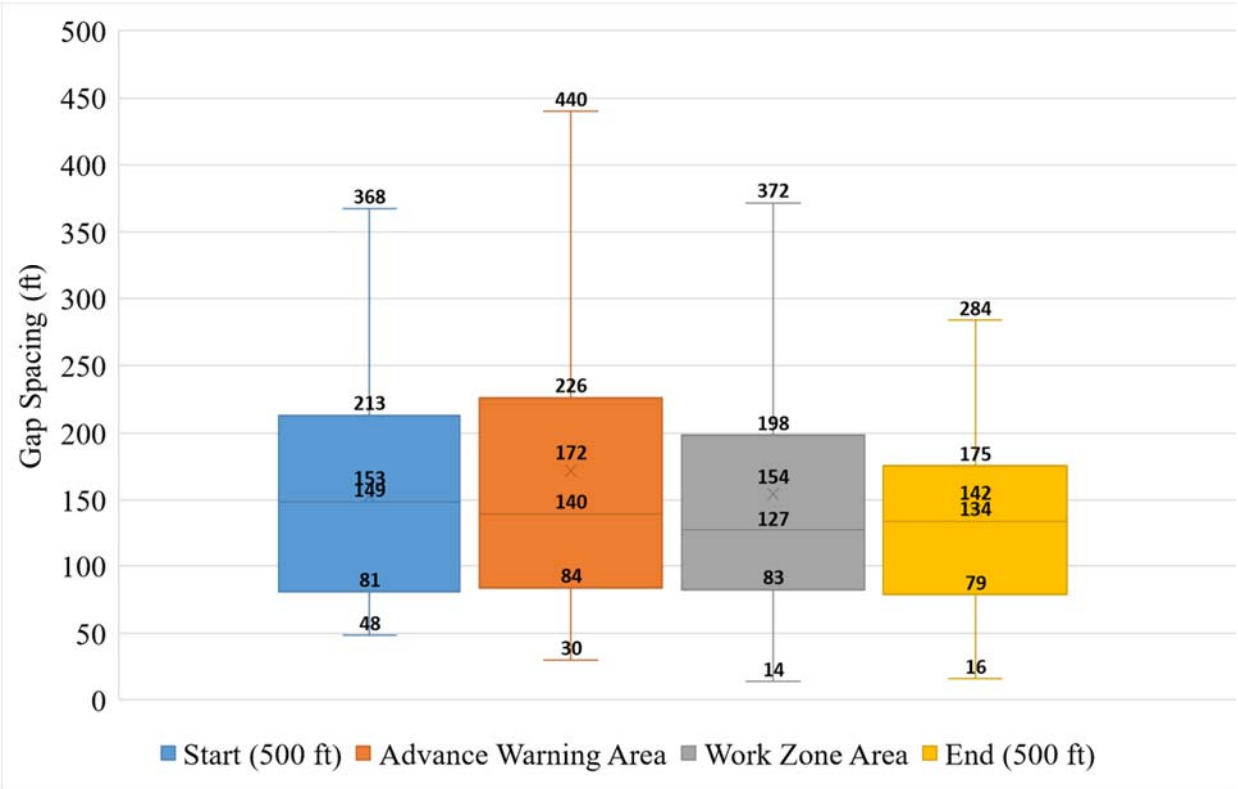
500
450
400
350
300
250
200
150
100
50
0
Gap Spacing (ft)
368
213
153
149
81
48
440
226
172
140
84
30
372
198
154
127
83
14
284
175
142
134
79
16
Start (500 ft)
Advance Warning Area
Work Zone Area
End (500 ft)

(*d*)

Figure 14. Gap spacing distribution by work zone areas:

(*a*) LC 2-1; (*b*) LC 3-2; (*c*) SC 2-2; and (*d*) SC 3-3.

4.2.1.4 Headway Estimation

As shown in **Figure 15**, GAM estimated the best-fitted curves of time headway throughout the work zone at four work zone configurations. **Figure 15*a*** presents the time headway estimation for LC 2-1. The time headway tends to increase when drivers approach advance warning area. It starts to decrease when drivers are in the advance warning area. The decreasing trend continues until drivers are at the end of activity area. The smallest time headway occurs in activity area. The time headway quickly increases after drivers enter termination area. For LC 3-2 (**Figure 15*b***), fluctuations are expected before activity area. The time headway tends to consistently decrease when drivers approach activity area. The smallest headway was estimated in activity area. The time headway started to increase in termination area where drums are removed.

Figure 15*c* presents the estimated headway for SC 2-2. The overall trend illustrates that time headway decreases until drivers start to leave the work zone. For SC 3-3 (**Figure 15*d***), two smallest headway points were observed. The first one occurs at where the shoulder has been fully closed with limited shoulder clearance. The second one can be found where drivers approach activity area. A decreasing trend in time headway can be noticed before these two points and an increasing trend shows up after.

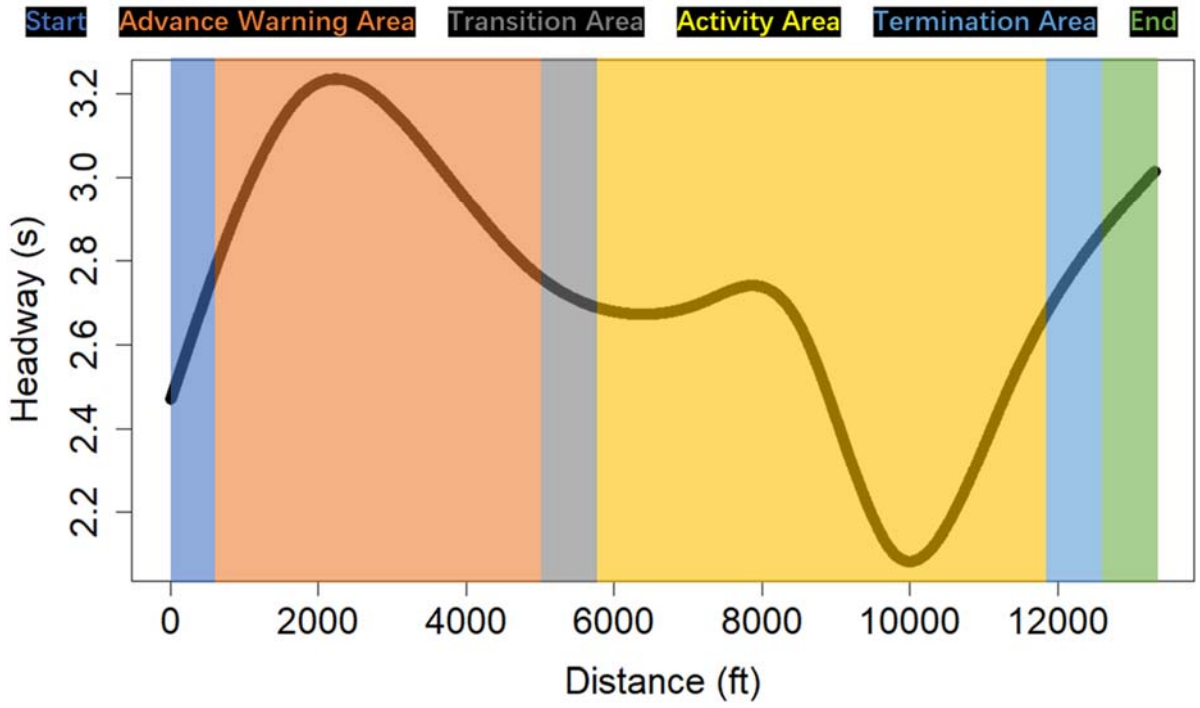
Start
Advance Warning Area
Transition Area
Activity Area
Termination Area
End
Headway (s)
2.2
2.4
2.6
2.8
3.0
3.2
0
2000
4000
6000
8000
10000
12000
Distance (ft)

(*a*)

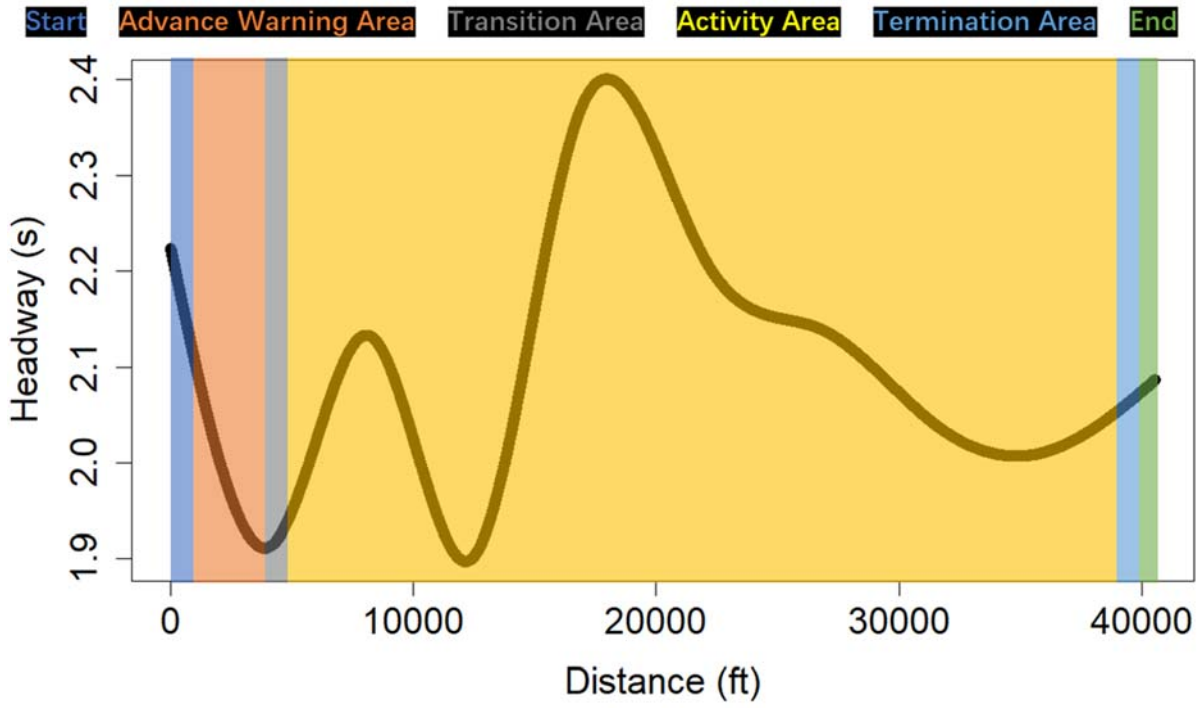
Start
Advance Warning Area
Transition Area
Activity Area
Termination Area
End
Headway (s)
1.9
2.0
2.1
2.2
2.3
2.4
0
10000
20000
30000
40000
Distance (ft)

(*b*)

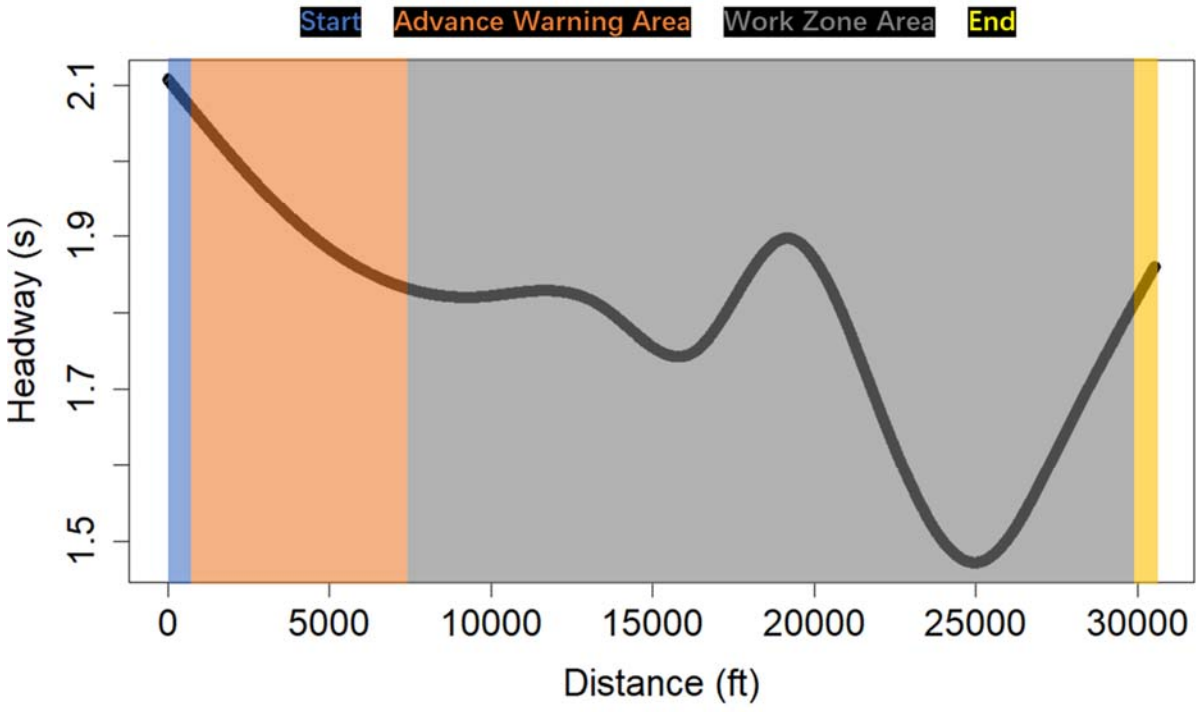
Start
Advance Warning Area
Work Zone Area
End
Headway (s)
2.1
1.9
1.7
1.5
0
5000
10000
15000
20000
25000
30000
Distance (ft)

(*c*)

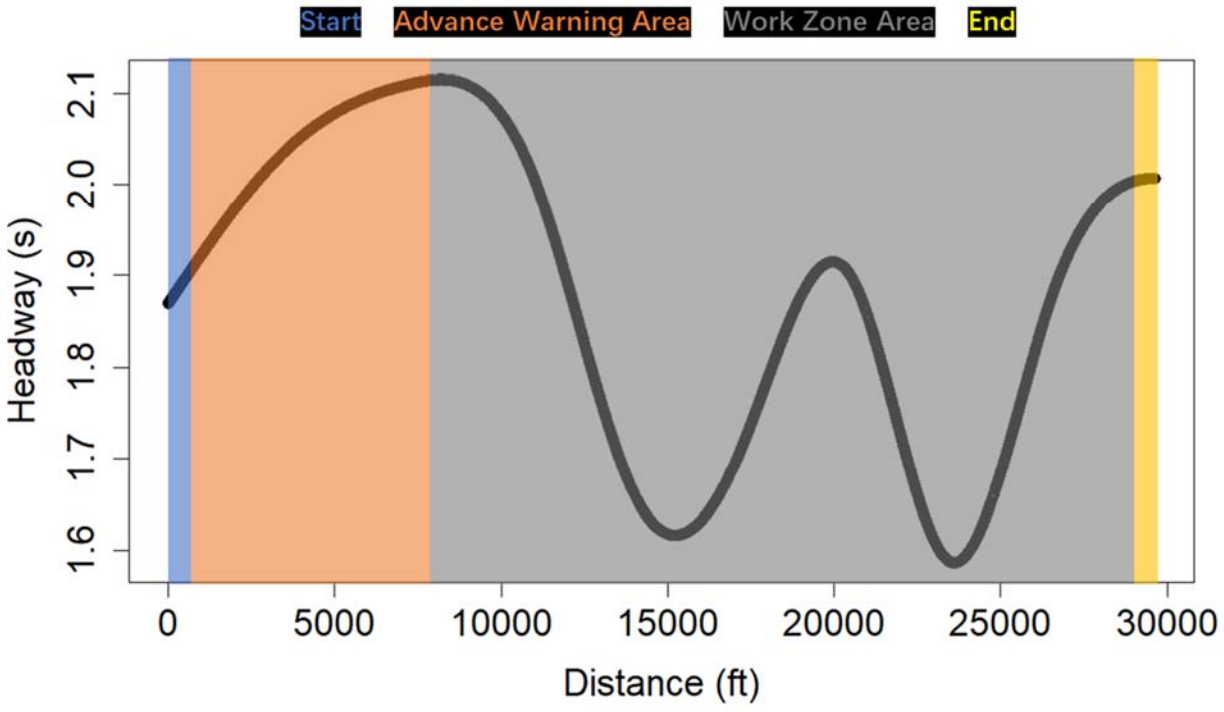

(*d*)

Figure 15 Headway estimation by work zone sections:

(*a*) LC 2-1; (*b*) LC 3-2; (*c*) SC 2-2; and (*d*) SC 3-3.

4.2.2 Speed Analysis

4.2.2.1 Speed profile

Speed profiles by GAM are presented in **Figure 16**, which shows speed distributions in the entire work zone at four configurations. The x-axis is the length (ft) and the y-axis is the speed (mph). The black dots are the speed data from SHRP 2 NDS time-series reports, one trace coming from one traversal. The red lines are the best-fitted curves by using GAM. After reviewing the forward-view videos, it was found that the reduced speed limit sign (55 mph) only appeared at LC 2-1 configuration. From **Figure 16*a***, it is observed that at LC 2-1 work zone, speeds decreased

when approaching the work zone, but drivers were only compliant with the 55 mph speed limit during transition area. Their speeds increased when entering activity area. At SC 2-2 work zone, there is a speed reduction between 10,000 and 20,000 ft, which was due to the presence of concrete barriers instead of drums. The other two configurations did not observe significant speed changes during the entire work zone traversal. Additionally, speed profiles by different driver types can be found in Appendix F.

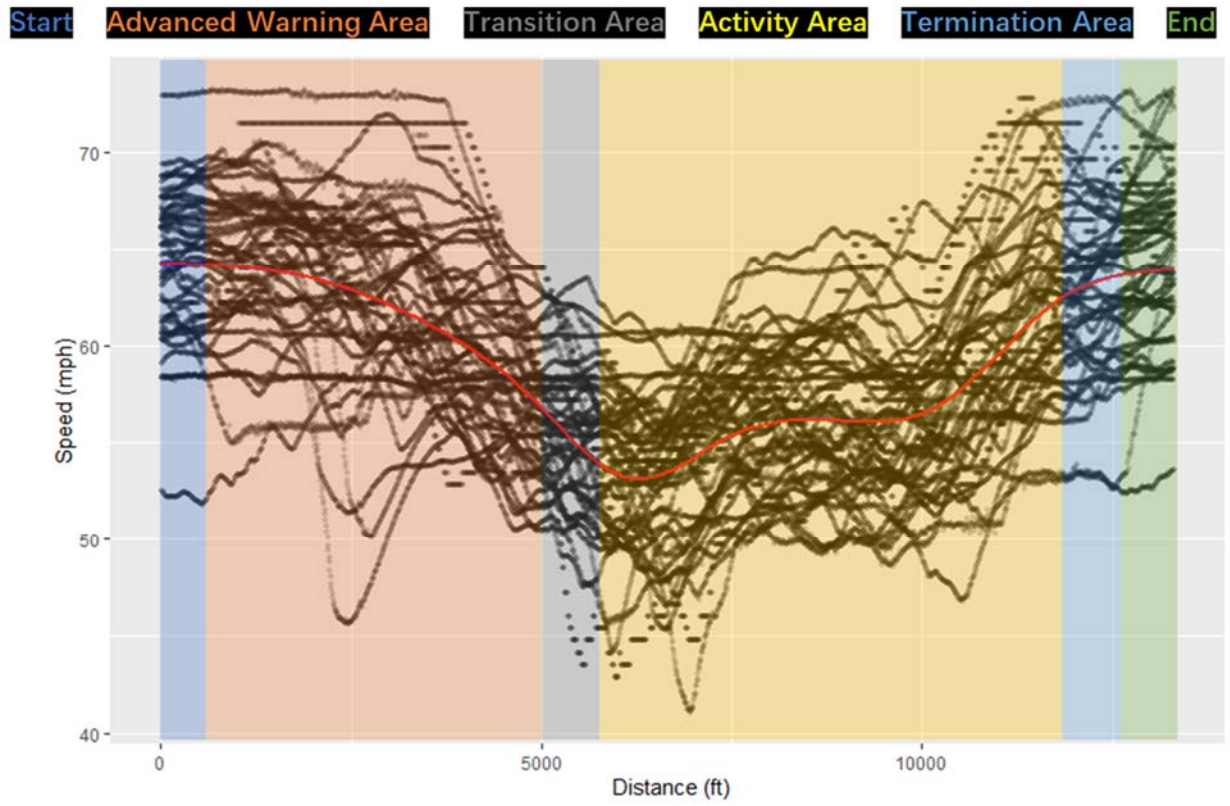

(a)

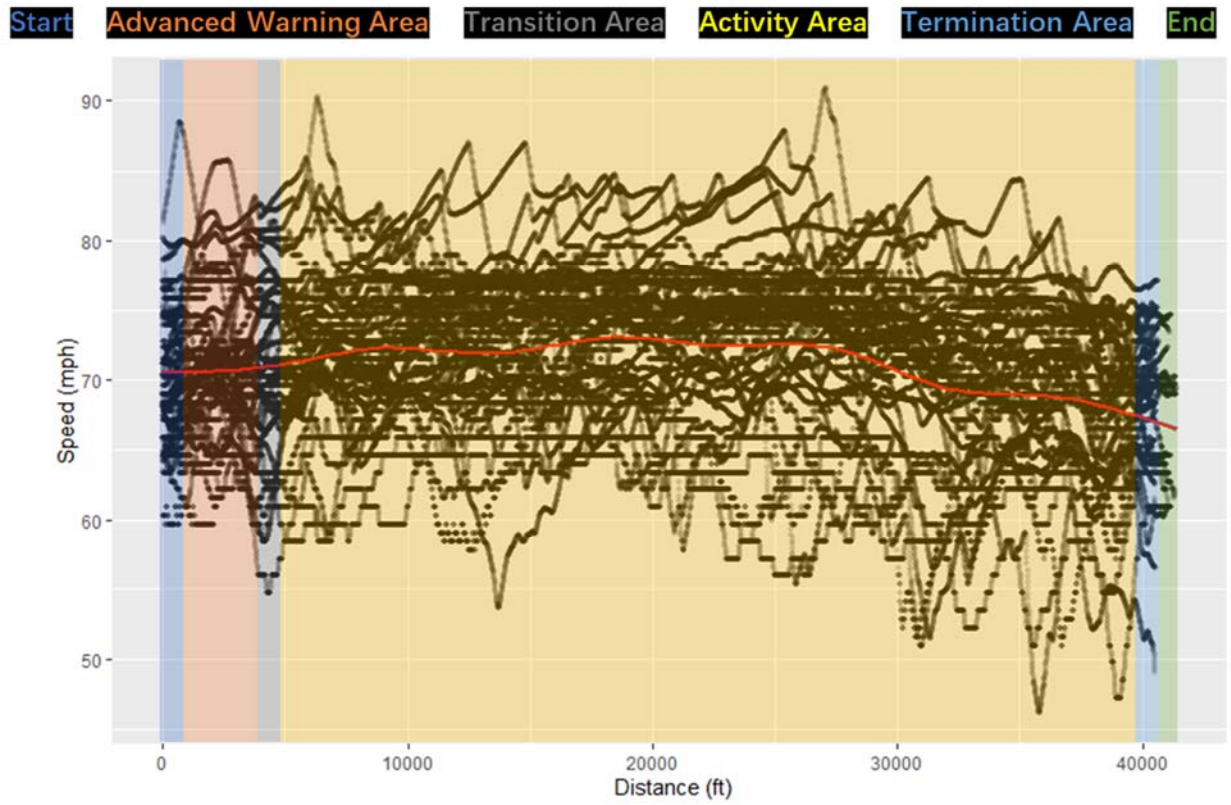
Start
Advanced Warning Area
Transition Area
Activity Area
Termination Area
End
Speed (mph)
90
80
70
60
50
0
10000
20000
30000
40000
Distance (ft)

(b)

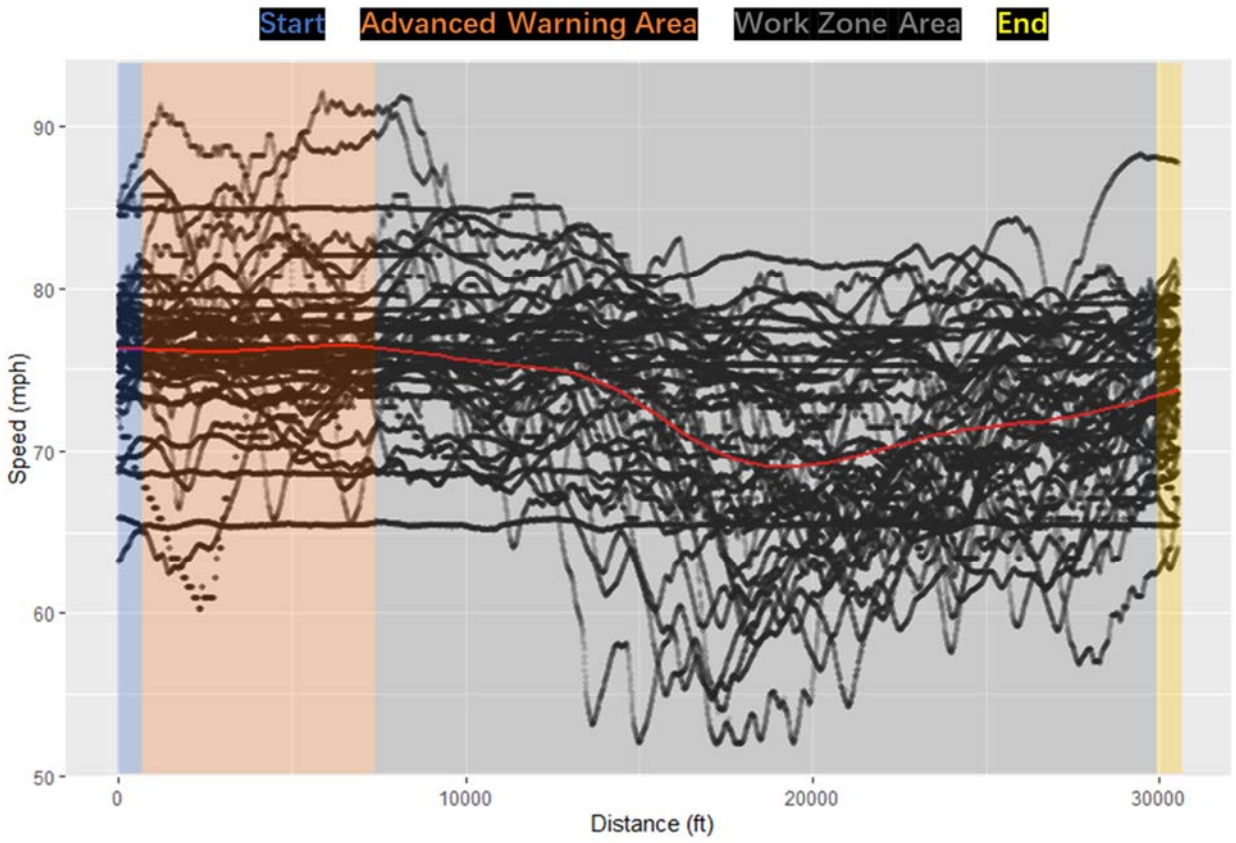
Start
Advanced Warning Area
Work Zone Area
End
90
80
70
60
50
Speed (mph)
0
10000
20000
30000
Distance (ft)

(*c*)

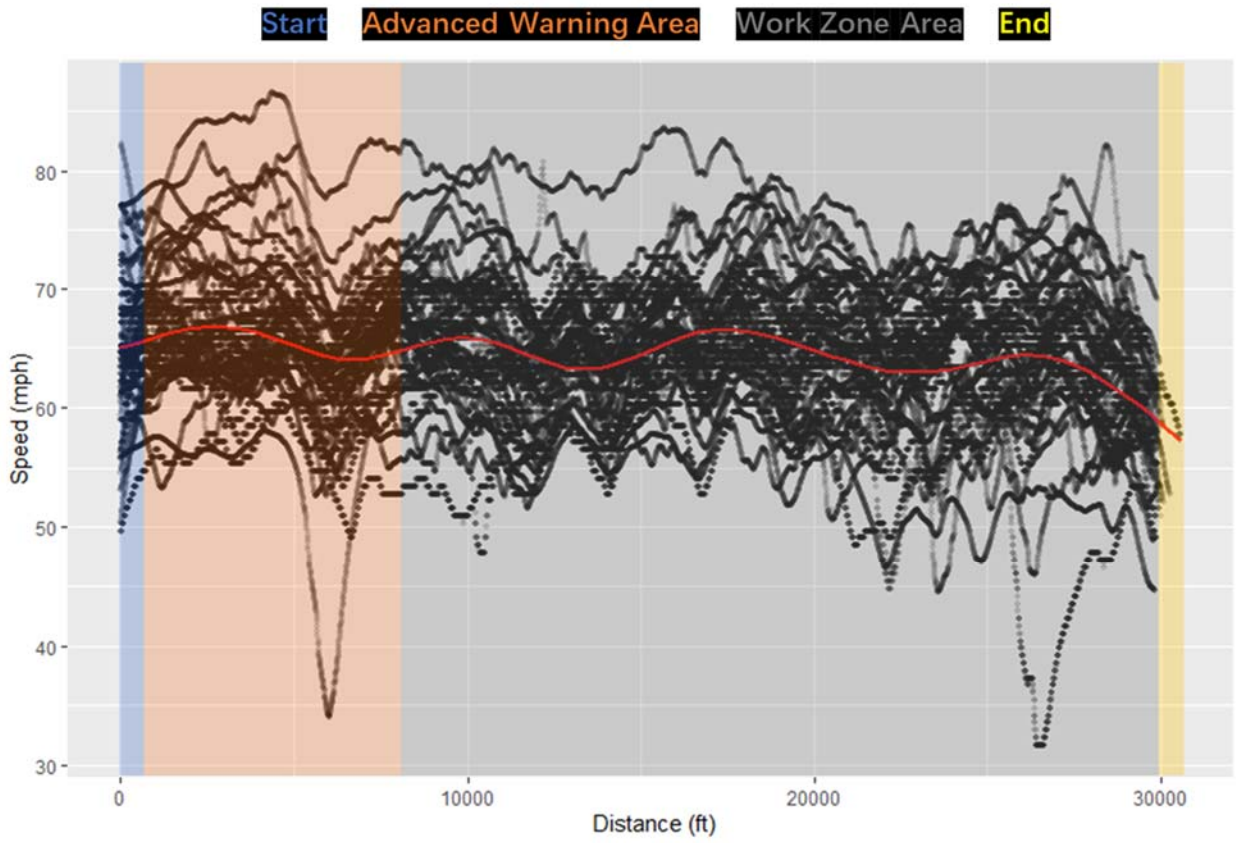

(d)

Figure 16 Speed Distribution: (a) LC 2-1; (b) LC 3-2; (c) SC 2-2; and (d) SC 3-3.

4.2.2.2 Speed change point

Speed change point detection was used to identify points where both mean and variance of speeds had significant changes. **Figure 17** presents speed change points at four work zone configurations. The x-axis is the data point index and the y-axis is the speed (mph). The red arrow indicates the location of a speed change point in work zones. As aforementioned, only LC 2-1 presented the speed reduction requirement from the reduced speed limit sign. It was found, in **Figure 17*a***, that the mean speed began to decrease by 8 mph after entering advance warning area and increased back to initial speeds after drivers saw the end of work zone drums. At LC 3-2 (**Figure 17 *b***), it was observed a slight speed increase (2 mph on average) after the transition area.

This might be caused by the driver accelerating to merge to the left two lanes. The mean speed then decreased by 4 mph when drivers reached the activity area. No reduced speed limit sign was installed at the LC 3-2 location. For SC 2-2 (**Figure 17*c***), the mean speed was significantly reduced by 5 mph where concrete barriers narrowed shoulder clearance. It increased by 2 mph near the end of work zone area. The slight speed decreases (2-3 mph) at SC 3-3 (**Figure 17*d***) were observed which was likely led by the downstream merging behavior from downstream freeway on-ramps.

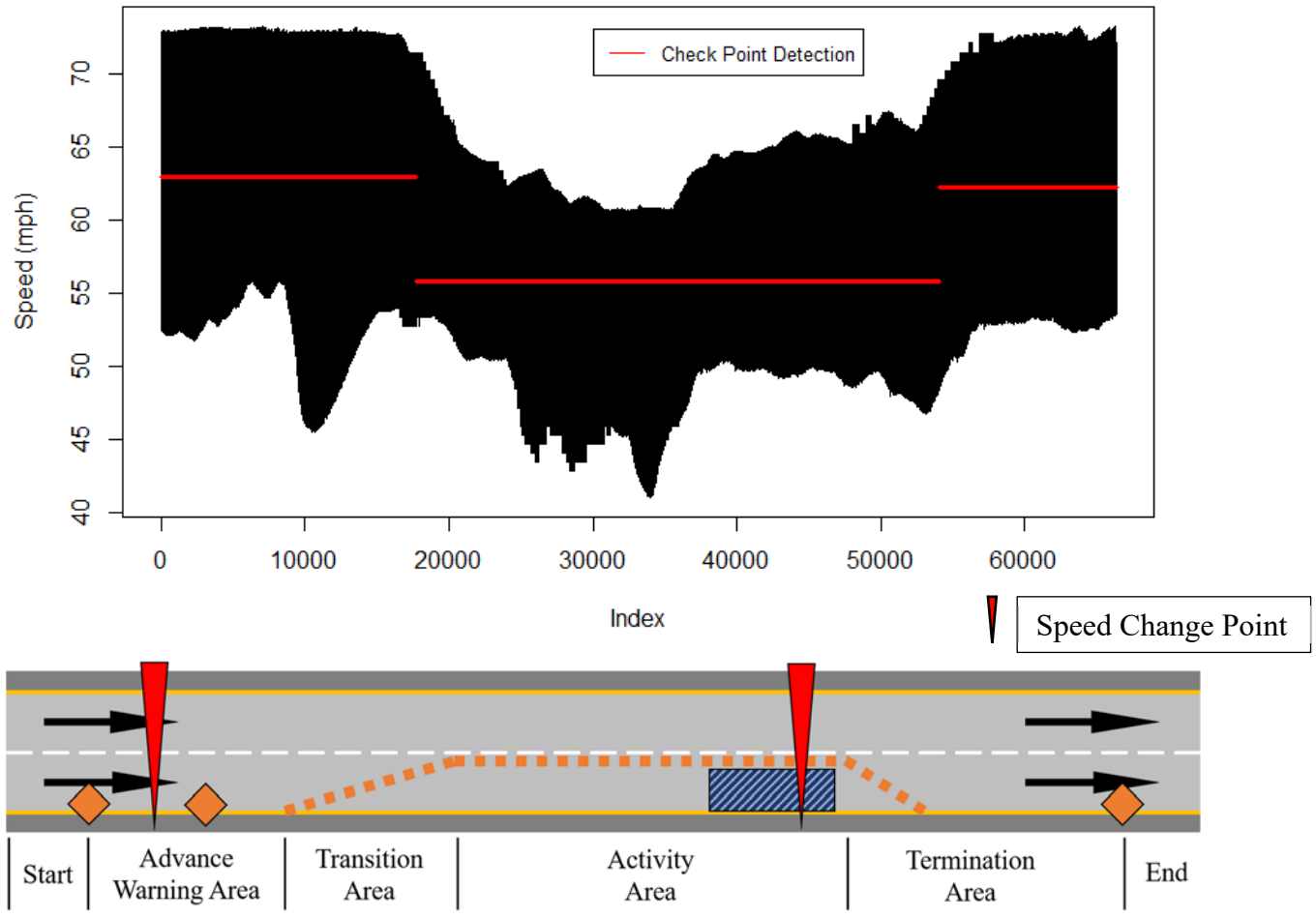

(a)

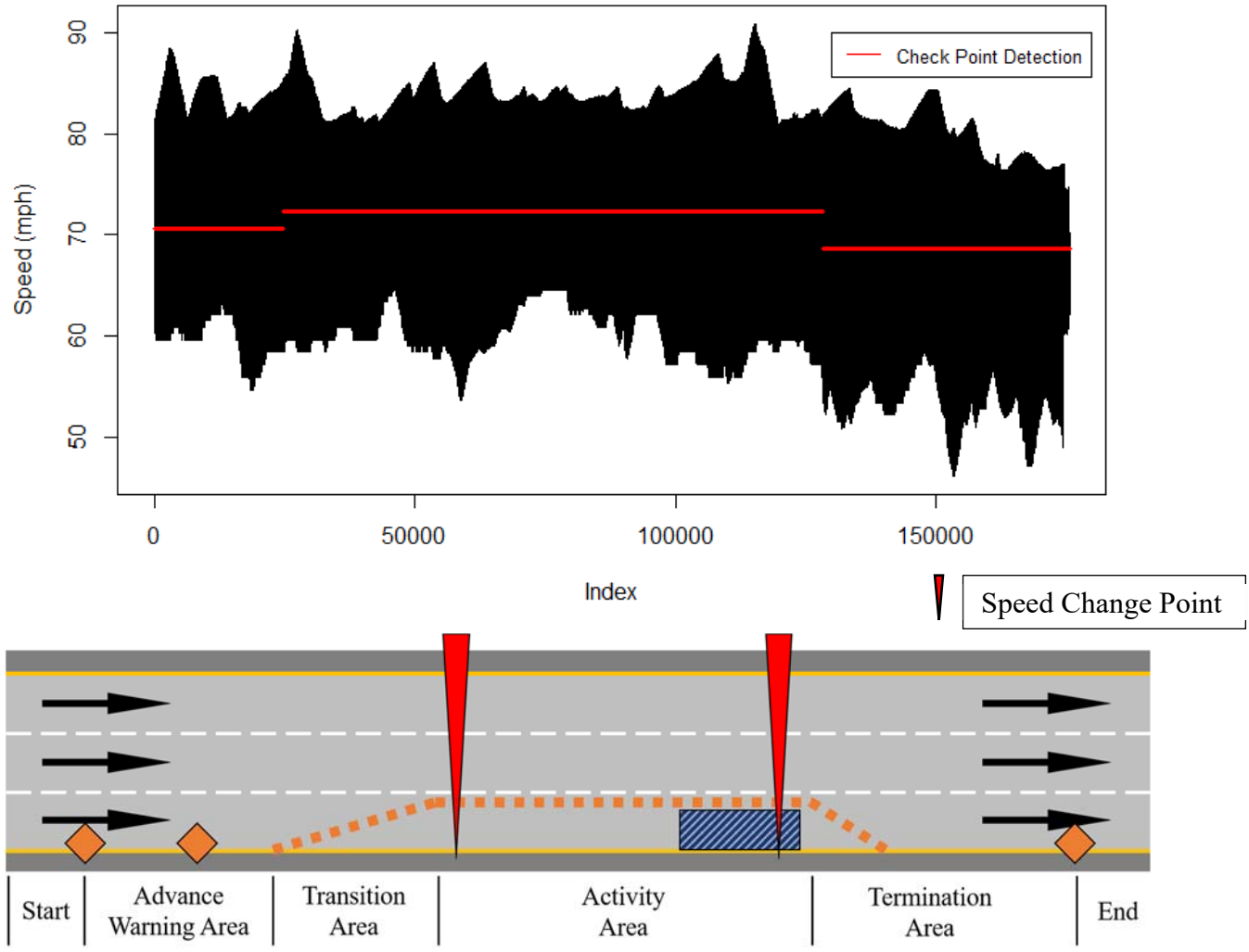
Check Point Detection
Speed (mph)
90
80
70
60
50
0
50000
100000
150000
Index
Speed Change Point
Start
Advance Warning Area
Transition Area
Activity Area
Termination Area
End

(b)

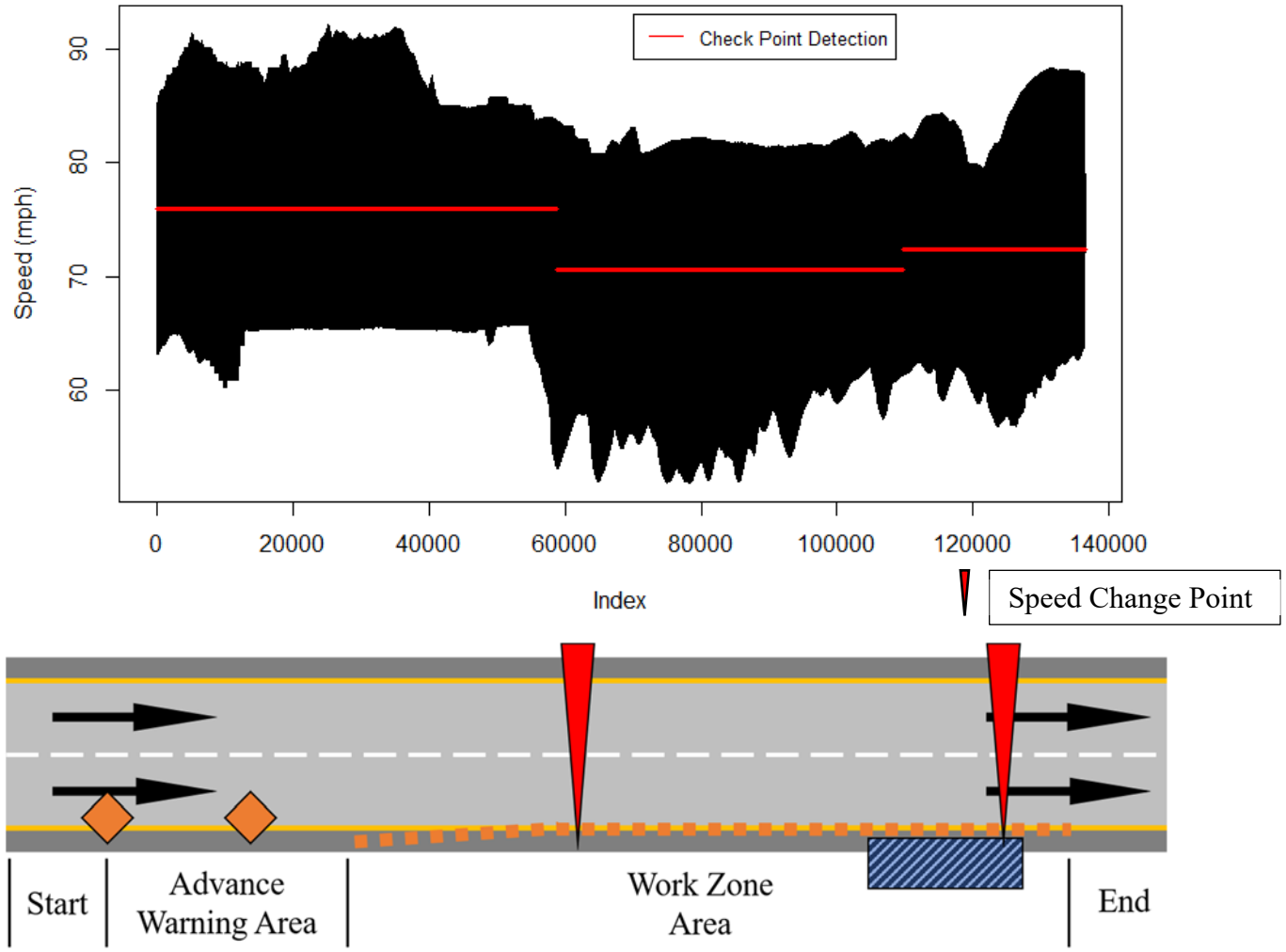
Check Point Detection
Speed (mph)
90
80
70
60
0
20000
40000
60000
80000
100000
120000
140000
Index
Speed Change Point
Start
Advance Warning Area
Work Zone Area
End

(*c*)

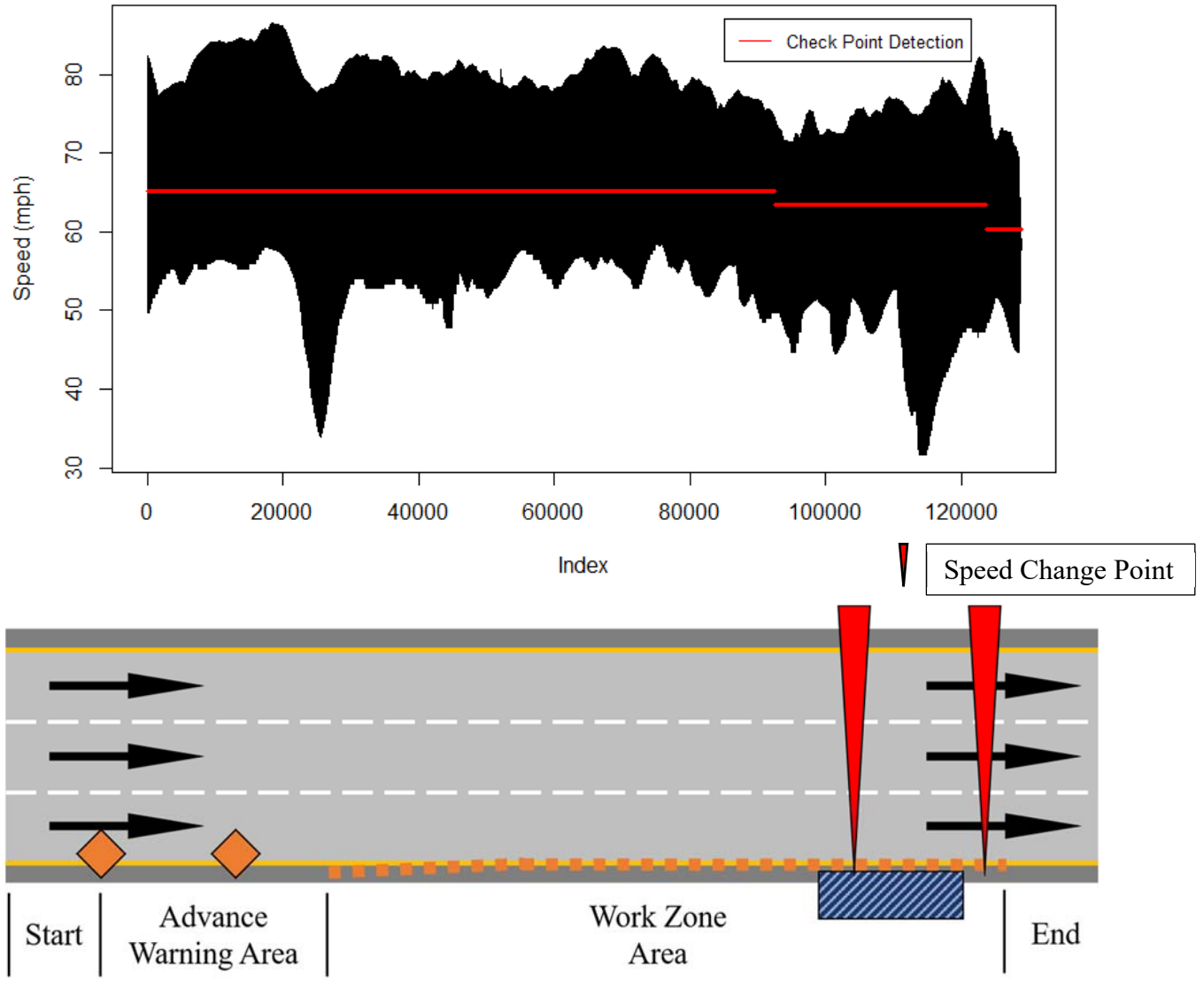

(*d*)

Note: Red Arrow = Speed Change Point

Figure 17 Speed Change Point Detection:

(*a*) LC 2-1; (*b*) LC 3-2; (*c*) SC 2-2; and (*d*) SC 3-3.

Chapter 5. Conclusions

This research conducted a first-ever study to investigate two innovative applications of SHRP 2 NDS data to improve freeway interchange deceleration lane design and analyze work zone mobility. Transportation agencies can utilize findings from this study to better design freeway diverge areas and evaluate work zone mobility.

For freeway diverge areas, this dissertation proposed a new method to determine the minimum deceleration lane lengths based on naturalistic driving speeds and deceleration rates. The results can be used to improve new freeway diverge areas and modify existing ones. Some key findings are concluded as follows:

1. The operating speeds were much higher than the *Green Book* assumptions. The *Green Book* indicates that on a freeway with a 70-mph design speed, drivers will enter the deceleration lane at 58 mph. In the five parallel-design locations, the speed distribution, however, showed that the speed was 65 mph on average when vehicles entered the deceleration lane. The *Green Book* also assumed that the speed reached the end of deceleration lane with a ramp of 35 mph design speed should be 30 mph, which instead was 55 mph on average based on this study.
2. Drivers were not effectively using the deceleration lane regarding the speed reduction. From speed distribution results, for parallel-design locations, the speed reduction on the deceleration lane is approximately 15% to 25%. The percentage of the speed reduced on the off-ramp is 75% to 85% which indicates that the speed reduced much more after vehicles approached the off-ramp terminal. For tapered-design locations, the speeds reduced on the deceleration lane were even lower, 10% speed reduction on deceleration lanes and 85% to 90% on off-ramps.

3. The brake status distribution further emphasized that the effective deceleration segment is on the off-ramp rather than the deceleration lane. The average brake pedal usage on off-ramps is higher than that on deceleration lanes on average (26.01% for taper section, 36.83% for the deceleration lane section, and 53.72% for the off-ramp section).
4. The results from critical speed changepoint models also implied that drivers' reaction points of sharp deceleration were on the off-ramp upstream of the ramp terminal. The average distances of reaction points from the terminal are 540 ft for parallel-design locations and 650 ft for tapered-design locations.
5. The calculated mean and 85th percentile deceleration rates were dynamic while the *Green Book* criterion assumes constant values for the entire decelerating maneuver. It was found that the deceleration rates on the deceleration lane were much lower than those on the off-ramp after the critical speed changepoint. Most of the deceleration rates on the deceleration lane and off-ramp at study locations were lower than constants provided by the *Green Book*, however, some were higher after the critical speed changepoint.
6. Based on the speed and deceleration rate distribution, a new method was developed to determine the minimum length of the deceleration lane. The results indicated that a deceleration lane may not be required for serving decelerating purpose on both parallel- and tapered-design deceleration lane locations when the ramp length is more than 1,550 ft. This number is specific to the diamond interchange (or interchanges with relatively straight off-ramps) with 70 mph speed limit on the mainline with the assumption of a stop is required at the off-ramp terminal. For off-

ramps that have relatively high volume, the queue length can be added to the original design length to provide a queue storage function.

In addition to the original objectives of this work, this study enabled the following observations. The advisory speeds posted on off-ramps were not able to significantly impact drivers' operating speeds. For locations with a 35-mph advisory speed, the average 85th percentile speed and mean speed are 63 mph and 55 mph, respectively. For those without advisory speeds, the 85th percentile speed is 65 mph and the mean speed is 58 mph. Thus, based on the speed distribution and speed change, the speed advisory sign can be installed before the critical speed change point on off-ramps to guide the drivers to reduce their speeds accordingly.

For freeway work zones, this dissertation developed gap and headway selection tables based on driver characteristics and studied speed distributions during the entire work zone areas. The results can be used to enhance work zone planning and simulation models and improve ACC spacing policies in work zones. Some key findings are summarized as follows:

1. Gap and headway selection tables revealed that car-following behaviors are highly variable among different drivers. The time and space gap distributions from different drivers traversing various work zone areas can be useful to improve ACC spacing policies for the automotive industry. Further studies are needed to understand drivers' acceptance of current ACC gap settings at work zones. This study found that mean headways change through work zone consecutive sections. These findings suggest that separate headway distributions should be used for different work zone areas when modeling work zone traffic control using simulation or planning tools.

2. Speed data analysis indicated that speeds decrease when drivers approach transition area and increase when they are near termination area for lane closure conditions. The mean speed at LC 2-1 was reduced by 8 mph from 63 mph to 55 mph (speed limit) when entering advance warning area and the speed increased back to initial speeds after activity area. At LC 3-2, the 4 mph mean speed reduction from 72 mph to 68 mph was observed when drivers were approaching activity area. For SC 2-2, the mean speed was reduced by 5 mph from 76 mph to 71 mph by the concrete barriers that narrowed shoulder clearance. The shoulder closure typically does not have significant impacts on speeds under non-breakdown conditions. There was no significant speed change at SC 3-3.

Chapter 6. Future Study

This study applied SHRP 2 NDS data to explore freeway deceleration lane and off-ramp designs based on naturalistic driving speeds and deceleration rates at 10 freeway diverge areas; and to develop gap and headway selection tables based on driver characteristics and establish speed profiles in four work zone configurations. The needs of future studies are pointed out as follows:

For freeway diverge areas:

Future studies could expand the sample size by requesting more NDS data on locations with different types of interchanges and off-ramps. The same procedure can be followed to further summarize the design methods for other types of interchanges and off-ramps.

For freeway work zones:

Future studies could investigate the headway and gap distributions under other types of weather and lighting conditions. It is also suggested to collect more NDS data to further validate the gap and headway selection and speed distribution by different driver types for more work zone configurations with additional work zone trips by more unique drivers. This would also be helpful for understanding drivers' acceptance of current ACC gap settings at work zones.

References

AASHTO. (1965). *A Policy on Geometric Design of Rural Highways.* Washington, D.C.: American Association of State Highway and Transportation Officials.

AASHTO. (1965). *A Policy on Geometric Design of Rural Highways.* Washington, D.C.: American Association of State Highway and Transportation Officials.

AASHTO. (2004). *A Policy on Geometric Design of Highways and Streets.* Washington, D.C.: American Association of State Highway and Transportation Officials.

AASHTO. (2011). *A Policy on Geometric Design of Highways and Streets.* Washington, D.C.: American Association of State Highway and Transportation Officials.

AASHTO. (2018). *A Policy on Geometric Design of Highways and Streets.* Washington, D.C.: American Association of State Highway and Transportation Officials.

Abdelnaby, A. (2014). Probabilistic analysis of freeway deceleration speed-change lanes. *Transportation Research Record: Journal of the Transportation Research Board*, 27-37.

Adeli, A. (2014). *Work Zone Speed Analysis using Driving Simulator Data.* Baltimore, MD: Morgan State University.

Adeli, H., & Jiang, X. (2003). Neuro-Fuzzy Logic Model for Freeway Work Zone Capacity Estimation. *Journal of Transportation Engineering*, 129 (5): 484-493.

Ahmed, M. M., & Ghasemzadeh, A. (2018). The Impacts of Heavy Rain on Speed and Headway Behaviors: an Investigation using the SHRP2 Naturalistic Driving Study Data. . *Transportation Research Part C: Emerging Technologies*, 91: 371-384.

Alexiadis, V., Jeannotte, K., & Chandra, A. (2004). *Traffic Analysis Toolbox Volume I: Traffic Analysis Tools Primer.* Mclean, VA: Federal Highway Administration. Office of Research, Development, and Technology.

Ali, E. M., Ahmed, M. M., & Yang, G. (2020). Normal and Risky Driving Patterns Identification in Clear and Rainy Weather on Freeway Segments using Vehicle Kinematics Trajectories and Time Series Cluster Analysis. *IATSS Research*.

Al-Kaisy, A., & Hall, F. (2003). Guidelines for Estimating Capacity at Freeway Reconstruction Zones. *Journal of Transportation Engineering*, 129 (5): 572-577.

Al-Kaisy, A., Zhou, M., & Hall, F. (2000). New Insights into Freeway Capacity at Work Zones: Empirical Case Study. *Transportation Research Record: Journal of the Transportation Research Board*, 1710: 154-160.

Antin, J., Lee, S., Hankey, J., & Dingus, T. (2011). *Design of the In-Vehicle Driving Behavior and Crash Risk Study: In Support of the SHRP 2 Naturalistic Driving Study.* Washington, D.C.: Transportation Research Board.

Antin, J., Lee, S., Perez, M. A., Dingus, T. A., Hankey, J. M., & Brach, A. (2019). Second Strategic Highway Research Program Naturalistic Driving Study Methods. *Safety Science*, 119: 2-10.

Avrenli, K. A., Benekohal, R., & Ramezani, H. (2011). Determining Speed-Flow Relationship and Capacity for Freeway Work Zone with No Lane Closure. *90th Annual Meeting of the Transportation Research Board.* Washington, D.C.: Transportation Research Board.

Bageshwar, V. L., Garrard, W. L., & Rajamani, R. (2004). Model Predictive Control of Transitional Maneuvers for Adaptive Cruise Control Vehicles. *IEEE Transactions on Vehicular Technology*, 53(5): 1573-1585.

Bared, J., Giering, G., & Warren, D. (1999). Safety Evaluation of Aceleration and Deceleration Lane Lengths. *ITE Journal*, 69: 50-54.

Barnard, Y., Utesch, F., van Nes, N., Eenink, R., & Baumann, M. (2016). The study design of UDRIVE: the naturalistic driving study across Europe for cars, trucks and scooters. *European Transport Research Review*, 8:14.

Bauer, K. M., & Harwood, D. W. (1998). *Statistical models of accidents on interchange ramps and speed-change lanes.* Federal Highway Administration.

Benekohal, R. F., Kaja-Mohideen, A. Z., & Chitturi, M. V. (2003). *Evaluation of Counstruction Work Zone Operational Issues: Capacity, Queue, and Delay.* Rantoul: Illinois Transportation Research Center.

Benekohal, R., Kaja-Mohideen, A. Z., & Chitturi, M. (2004). Methodology for Estimating Operating Speed and Capacity in Work Zone. *Transportation Research Record: Journal of the Transportation Research Board*, 1833: 103-111.

Bham, G. H., & Mohammadi, M. A. (2011). *Evaluation of Work Zone Speed Limits: An Objective and Subjective Analysis of Work Zones in Missouri.* Mid-America Transportation Center.

Bharadwaj, N., Edara, P., & Sun, C. (2019). Risk Factors in Work Zone Safety Events: A Naturalistic Driving Study Analysis. *Transportation Research Record: Journal of the Transportation Research Board*, 2673 (1): 379-387.

Bharadwaj, N., Edara, P., Sun, C., Brown, H., & Chang, Y. (2018). Traffic Flow Modeling of Diverse Work Zone Activities. *Transportation Research Record: Journal of the Transportation Research Board*, 2676 (16): 23-34.

Brewer, M. A., & Stibbe, J. (2019). Investigation of Design Speed Characteristics on Freeway Ramps using SHRP 2 Naturalistic Driving Data. *Transportation Research Record: Journal of Transportation Research Board*, 2673 (3): 247-258.

Căilean, A. M., & Dimian, M. (2017). Current Challenges for Visible Light Communications Usage in Vehicle Applications: A Survey. *IEEE Communications Surveys & Tutorials*, 19(4): 2681-2703.

Calvi, A., Bella, F., & D'Amico, F. (2015). Diverging Driver Performance Along Deceleration Lanes. *Transportation Research Record: Journal of Transportation Research Board*, 2518: 95-103.

Calvi, A., Benedetto, A., & De Blasiis, M. R. (2012). A Driving Simulator Study of Driver Performance on Deceleration Lanes. *Accident Analysis and Prevention*, 45: 195-203.

Calvi, A., D'Amico, F., Ferrante, C., & Ciampoli, L. B. (2020). A Driving Simulator Validation Study for Evaluating the Driving Performance on Deceleration and Acceleration Lanes. *Advances in Transportation Studies*, 50: 67-80.

Campbell, K. L. (2012). The SHRP 2 Naturalistic Driving Study: Addressing Driver Performance and Behavior in Traffic Safety. *Transportation Research News*, 282: 30-35.

Cascetta, E. (2013). *Transportation Systems Engineering: Theory and Methods.* Berlin: Springer Science & Business Media.

Chang, Y., & Edara, P. (2017). Predicting Hazardous Events in Work Zones using Naturalistic Driivng Data. *IEEE 20th International Conference on Intelligent Transportation Systems* (pp. 1-6). IEEE.

Chatterjee, I., Edara, P., Menneni, S., & Sun, C. (2009). Replication of Work Zone Capacity Values in a Simulation Model. *Transportation Research Record: Journal of the Transportation Research Board*, 2130: 138-148.

Chehardoli, H., & Homaeinezhad, M. R. (2018). Third-Order Leader-Following Consensus Protocol of Traffic Flow formed by Cooperative Vehicular Platoons by Considering Time

Delay: Constant Spacing Strategy. *Proceedings of the Institution of Mechanical Engineers, Part I: Journal of Systems and Control Engineering*, 232(3): 285-298.

Chen, H., Liu, P., Lu, J. J., & Behzadi, B. (2009). Evaluating the Safety Impacts of the Number and Arrangement of Lanes on Freeway Exit Ramps. *Accident Analysis & Prevention*, 41(3): 543-551.

Chen, H., Zhou, H., & Lin, P. S. (2014). Freeway Deceleration Lane Lengths Effects on Traffic Safety and Operation. *Safety Science*, 64: 39-49.

Chen, H., Zhou, H., Zhao, J., & Hsu, P. (2011). Safety Performance Evaluation of Left-Side Off-Ramps at Freeway Diverge Areas. *Accident Analysis and Prevention*, 43 (3): 605-612.

Chitturi, M. V., & Benekohal, R. F. (2005). Effect of Lane Width on Speeds of Cars and Heavy Vehicles in Work Zones. *Transportation Research Record: Journal of the Transportation Research Board*, 1920 (1): 41-48.

Cirillo, J. (1970). The relationship of accidents to length of speed-change lanes and weaving areas on interstate highways. *Highway Research Record*, 17-32.

Corder, G. W., & Foreman, D. I. (2014). *Nonparametric Statistics: A Step-by-Step Approach.* New York: John Wiley & Sons, Inc.

Cowan, R. J. (1975). Useful Headway Models. *Transportation Research*, 9 (6): 371-375.

Critial Analysis Reporting Enviornment (CARE) (Computer Software). (2018, June 15). Retrieved from https://www.caps.ua.edu/software/care/

Darbha, S., & Rajagopal, K. R. (1999). Intelligent Cruise Control Systems and Traffic Flow Stability. *Transportation Research Part C: Emerging Technologies*, 7(6): 329-352.

Darbha, S., Rajagopal, K. R., & Tyagi, V. (2008). A Review of Mathematical Models for the Flow of Traffic and Some Recent Results. *Nonlinear Analysis: Theory, Methods & Applications*, 69(3): 950-970.

Dingus, T. A., Hankey, J. M., Antin, J. F., Lee, S. E., Eichelberger, L., Stulce, K. E., . . . Stowe, L. (2015). *Naturalistic Driving Study: Technical Coordination and Quality Control.* Federal Higwhay Administration, U. S. Department of Transportation.

Dong, J., Houchin, A. J., Shafieirad, N., Lu, C., Hawkins, N. R., & Knickerbocker, S. (2015). *VISSIM Calibration for Urban Freeways.* Ames: Iowa State University. Institute for Transportation.

Dowling, R., Skabardonis, A., & Alexiadis, V. (2004). *Traffic Analysis Toolbox Volume III: Guidelines for Applying Traffic Microsimulation Modeling Software.* McLean, VA: Federal Highway Administration. Office of Research, Development, and Technology.

El-Basha, R. H., Hassan, Y., & Sayed, T. A. (2007). Modeling Freeway Diverging Behavior on Deceleration Lanes. *Transportation Research Record: Journal of the Transportation Research Board*, 2012: 30-37.

Erdman, C., & Emerson, J. W. (2008). A Fast Bayesian Change Point Analysis for the Segmentation of Microarray Data. *Bioinformatics (Oxford, England)*, 24 (19): 2143-2148.

Fancher, P., Bareket, Z., & Ervin, R. (2001). Human-Centered Design of an ACC-With-Braking and Forward-Crash-Warning System. *Vehicle System Dynamics*, 36(2-3): 203-223.

Fancher, P., Bareket, Z., Peng, H., & Ervin, R. (2003). *Research on Desirable Adaptive Cruise Control Behavior in Traffic Streams.* Ann Arbor: The University of Michigan Transportation Research Instisute.

Farnam, A., & Sarlette, A. (2019). About String Stability of a Vehicle Chain with Unidirectional Controller. *European Journal of Control*, 50: 138-144.

FHWA. (2017, June 17). *The Interstate System: Size of the Job*. Retrieved January 5, 2021, from https://www.fhwa.dot.gov/infrastructure/50size.cfm

FHWA. (2020, November 16). *FHWA Road Closure and Lane Closure*. Retrieved January 5, 2021, from https://ops.fhwa.dot.gov/wz/construction/full_rd_closures.htm

FHWA Work Zone Facts and Statistics. (2019, March 5). Retrieved from Work Zone Management Program, Federal Highway Administration: https://ops.fhwa.dot.gov/wz/resources/facts_stats.htm

Fitzpatrick, K., Chrysler, S. T., & Brewer, M. (2012). Deceleration Lengths for Exit Terminals. *Journal of Transportation Engineering*, 768-775.

Fitzpatrick, K., Chrysler, S. T., & Brewer, M. (2012). Deceleration Lengths for Exit Terminals. *Journal of Transportation Engineering*, 138 (6): 768-775.

Flannagan, C. A., Baykas, P. B., Leslie, A., Kovaceva, J., & Thomson, R. (2019). *Analysis of SHRP2 Data to Understand Normal and Abnormal Driving Behavior in Work Zones.* Mclean, VA: Federal Higwhay Administration. Research, Development, and Technology.

Gao, Z., Yan, W., Hu, H., & Li, H. (2015). Human-Centered Headway Control for Adaptive Cruise-Controlled Vehicles. *Advances in Mechanical Engineering*, 7(11).

Garcia, A., & Romero, A. R. (2006). Experimental Observation of Vehicle Evolution on Deceleration Lanes with Different Lengths. *Compendium of 85th Transportation Research Board Annual Meeting.* Washington, D.C.

Gerdes, J. C., & Hedrick, J. K. (1996). Vehicle Speed and Spacing Control via Coordinated Throttle and Brake Actuation. *IFAC Proceedings Volumes*, 29(1): 7879-7884.

Gill, P. E., Murray, W., & Wright, M. H. (2019). *Practical Optimization.* Society for Industrial and Applied Mathematics.

Goswamy, A. (2019). *Evaluation of Work Zone Safety using the SHRP2 Naturalistic Driving Study Data.* Ames, IA: Iowa State Universtiy.

Greenberg, I. (1966). The Log-Normal Distribution of Headways. *Australian Road Research*, 2 (7): 14-18.

Hall, F. L. (1992). Traffic Stream Characteristics. In N. H. Gartner, C. J. Messer, & A. Rathi, *Revised Monograph on Traffic Flow Theory* (pp. 2: 1-36). Federal Higwhay Administration.

Hallmark, S. L., Tyner, S., Oneyear, N., Carney, C., & McGehee, D. (2015). Evaluation of Driving Behavior on Rural 2-Lane Curves using the SHRP 2 Naturalistic Driving Study Data. *Journal of Safety Research*, 54: 17-27.

Hankey, J., Perez, M., & McClafferty, J. (2016). *Description of the SHRP2 Naturalistic Database and the Crash, Near-Crash, and Baseline Data Sets.*

Hao, H., Li, Y. E., Medina, A., Gibbons, R. B., & Wang, L. (2020). Understanding Crashes Involving Roadway Objects with SHRP 2 Naturalistic Driving Study Data. *Journal of Safety Research*, 73: 199-209.

Harwood, D., & Graham, J. (1983). Rehabilitation of Existing Freeway-Arterial Highway Interchanges. *Transportation Research Record*, 923: 18-26.

Hastie, T. J., & Tibshirani, R. J. (1990). *Generalized Additive Models.* CRC Press.

Heaslip, K., Jain, M., & Elefteriadou, L. (2011). Estimation of Arterial Work Zone Capacity using Simulation. *Transportation Letters*, 3(2): 123-134.

Heaslip, K., Kondyli, A., Arguea, D., Elefteriadou, L., & Sullivan, F. (2009). Estimation of Freeway Work Zone Capacity through Simulation and Field Data. *Transportation Research Record: Journal of the Transportation Research Board*, 2130: 16-24.

Hoogendoorn, S. P., & Bovy, P. H. (1998). A New Estimation Technique for Vehicle-Type Specific Headway Distributions. *Transportation Research Record: Journal of the Transportation Research Board*, 1646: 18-28.

Ishimaru, J., & Hallenbeck, M. (2019). *QUEWZ Work Zone Software: Literature Search and Methodology Review.* Olympia, WA: Washington State Department of Transportation.

Kan, X., Ramezani, H., & Benekohal, R. (2014). Calibration of VISSIM for Freeway Work Zones with Time Varying Capacity. *93rd Annual Meeting of the Transportation Research Board.* Washington, D.C.: Transportation Research Board.

Karim, A., & Adeli, H. (2003). Radial Basis Function Neural Network for Work Zone Capacity and Queue Estimation. *Journal of Transportation Engineering*, 129 (5): 494-503.

Kesting, A., & Treiber, M. (2008). Calibrating Car-Following Models by Using Trajectory Data: Methodological Study. *Transportation Research Record: the Journal of Transportation Research Board*, 2088(1): 148-156.

Khan, M. N., Das, A., & Ahmed, M. M. (2020). Non-Parametric Association Rules Mining and Parametric Ordinal Logistic Regression for an In-Depth Investigation of Driver Speed Selection Behavior in Adverse Weather using SHRP2 Naturalistic Driving Study Data. *Transportation Research Record: Journal of the Transportation Research Board*.

Killick, R., & Eckley, I. (2014). Changepoint: An R Package for Changepoint Analysis. *Journal of Statistical Software*, 58 (3): 1-19.

Killick, R., Eckley, I. A., Ewans, K., & Jonathan, P. (2010). Detection of Changes in Variance of Oceanographic Time-Series Using Changepoint Analysis. *Ocean Engineering*, 37 (13): 1120-1126.

Kim, T., Lovell, D. J., Hall, M., & Paracha, J. (2000). A New Methodology to Estimate Capacity for Freeway Work Zones. *80th Annual Meeting of the Transportation Research Board.* Washington, D.C.: Transportation Research Board.

Krammes, R. A., & Lopez, G. O. (1994). Updated Capacity Values for Short-Term Freeway Work Zone Lane Closures. *Transportation Research Record: Journal of the Transportation Research Board*, 1442: 49-56.

Lambert-Bélanger, A., Dubois, S., Weaver, B., Mullen, N., & Bedard, M. (2012). Aggressive Driving Behaviour in Young Drivers (Aged 16 Through 25) Involved in Fatal Crashes. *Journal of Safety Research*, 43(5-6): 333-338.

Larsen, K. (2015, July 30). *GAM: The Predictive Modeling Silver Bullet*. Retrieved January 5, 2021, from https://multithreaded.stitchfix.com/blog/2015/07/30/gam/

Li, Y., & Bai, Y. (2008). Comparison of Characteristics Between Fatal and Injury Accidents in the Highway Construction Zones. *Journal of Safety Science*, 46: 646-660.

Lin, T. W., Hwang, S. L., Su, J. M., & Chen, W. H. (2008). The Effects of In-Vehicle Tasks and Time-Gap Selection while Reclaiming Control from Adaptive Cruise Control (ACC) with Bus Simulator. *Accident Analysis & Prevention*, 40(3):1164-1170.

Lord, D., & Bonneson, J. (2005). Calibration of Predictive Models for Estimating Safety of Ramp. *Transportation Research Record: Journal of the Transportation Research Board*, 1908: 88-95.

Lu, C., Dong, J., Sharma, A., Huang, T., & Knickerbocker, S. (2018). Predicting Freeway Work Zone Capacity Distribution Based on Logistic Speed-Density Models. *Journal of Advanced Transportation*.

Lu, J. J., Lu, L., Liu, P., Chen, H., & Guo, T. (2010). *Safety and Operational Performance of Four Types of Exit Ramps on Florida's Freeways.* Tampa: University of South Florida, Florida Department of Transportation.

Lundy, R. (1965). *The Effect of Ramp Type and Geometry on Accidents.* Washington, D.C.: Highway Research Board.

Ma, Y., Zhang, W., Gu, X., & Zhao, J. (2019). Impacts of Experimental Advisory Exit Speed Sign on Traffic Speeds for Freeway Exit Ramp. *PLoS ONE*, 14(11): e0225203.

Mackinnon, D. (1975). High Capacity Personal Rapid Transit System Developments. *IEEE Transactions on Vehicular Technology*, 24(1): 8-14.

Mahmassani, H. S., Sbayti, H., & Zhou, X. (2004). *DYNASMART-P Version 1.0 User's Guide.* College Park, MD: Maryland Transportation Initiative.

Marsden, G., cDonald, M., & Brackstone, M. (2001). Towards an Understanding of Adaptive Cruise Control. *Transportation Research Part C: Emerging Technologies*, 9(1): 33-51.

Mathew, T. V., & Rao, K. K. (2006, October 19). *Introduction to Transportation Engineering.* Retrieved July 5, 2020, from Civil Engineering - Transportation Engineering: http://www.cdeep. iitb. ac. in/nptel/Civil% 20Engineering

May, A. D. (1990). *Traffic Flow Fundamentals.* Englewood Cliffs, NJ: Prentice Hall.

McCartt, A., Northrup, V., & Retting, R. (2004). Types and characteristics of ramp-related motor vehicle crashes on urban interstate roadways in Northern Virginia. *Journal of Safety Research*, 107-114.

McMahon, D. H., Hedrick, J. K., & Shladover, S. E. (1990). Vehicle Modelling and Control for Automated Highway Systems. *American Control Conference*, (pp. 297-303). San Diego.

Migletz, J., Graham, J. L., Anderson, I. B., Harwood, D. W., & Bauer, K. M. (1999). Work Zone Speed Limit Procedure. *Transportation Research Record: Journal of the Transportation Research Board*, 1657 (1): 24-30.

Migletz, J., Graham, J., Hess, B., Anderson, I., Harwood, D., & K., B. (1998). *Effectiveness and Implementability of Procedures for Setting Work Zone Speed Limits.* Independence, MO: Graham-Migletz Enterprises.

Missouri DOT. (2017). *Interchanges and Intersections*. Retrieved 9 10, 2017, from http://www.modot.org/InterchangesandIntersections.htm

Moon, S., & Yi, K. (2008). Human Driving Data-Based Design of a Vehicle Adaptive Cruise Control Algorithm. *Vehicle System Dynamics*, 46(8): 661-690.

Moon, S., Kang, H. J., & Yi, K. (2010). Multi-Vehicle Target Selection for Adaptive Cruise Control. *Vehicle System Dynamics*, 48(11): 1325-1343.

Nam, C. F., Aston, J. A., & Johansen, A. M. (2012). Quantifying the Uncertainty in Change Points. *Journal of Time Series Analysis*, 33 (5): 807-823.

Naranjo, J. E., González, C., García, R., & De Pedro, T. (2006). ACC+ Stop&Go Maneuvers with Throttle and Brake Fuzzy Control. *IEEE Transactions on Intelligent Transportation Systems*, 7(2): 213-225.

Noel, E. C., Dudek, C. L., Pendleton, O. J., & Sabra, Z. A. (1988). Speed Control through Freeway Work Zones: Techniques Evaluation. *Transportation Research Record: Journal of the Transportation Research Board*, 1163: 31-42.

Oppenlander, J., & Dawson, R. (1970). Chapter 9 Interchanges. In J. Oppenlander, & R. Dawson, *Traffic Control & Roadway Elements - Their Relationship to Highway Safety/Revised* (p. 11 p.). Washington, D.C.: Highway Users Federation for Safety and Mobility.

Pesti, G., & McCoy, P. T. (2001). Long-Term Effectiveness of Speed Monitoring Displays in Work Zones on Rural Interstate Highways. *Transportation Research Record: Jornal of the Transportation Research Board*, 1754 (1): 21-30.

Pisarski, A., & Reno, A. (2015). *2015 AASHTO bottom line report.* American Association of State Highway and Transportation Officials.

R Core Team. (1993, August). *What is R?* Retrieved July 2, 2018, from https://www.r-project.org/about.html

Racha, S., Chowdhury, M., Sarasua, W., & Ma, Y. (2008). Analysis of Work Zone Traffic Behavior for Planning Applications. *Transportation Planning and Technology*, 31 (2): 183-199.

Ramezani, H., & Benekohal, R. F. (2012). Work Zones as a Series of Bottlenecks. *Transportation Research Record: Journal of the Transportation Research Board*, 2272: 67-77.

Reeves, J. J., Chen, J., Wang, X. L., Lund, R., & Lu, Q. Q. (2007). A Review and Comparison of Changepoint Detection Techniques for Climate Data. *Journal of Applied Meteorology and Climatology*, 46 (6): 900-915.

Santhanakrishnan, K., & Rajamani, R. (2003). On Spacing Policies for Highway Vehicle Automation. *IEEE Transactions on Intelligent Transportation Systems*, 4(4): 198-204.

Sarasua, W. A., Davis, W. J., Chowdhury, M. A., & Ogle, J. (2006). Estimating Interstate Highway Capacity for Short-Term Work Zone Lane Closures: Development of Methodology. *Transportation Research Record: Journal of the Transportation Research Board*, 1948: 45-57.

Schagen, I. v., Welsh, R., Backer-Grøndahl, A., Hoedemaeker, M., Lotan, T., Morris, A., . . . and Winkelbauer, M. (2011). *Towards a large-scale European Naturalistic Driving study: final report of PROLOGUE: deliverable D4.2.* SWOV Institute for Road Safety Research.

Seiler, P., Pant, A., & Hedrick, K. (2004). Disturbance Propagation in Vehicle Strings. *IEEE Transactions on Automatic Control*, 49(10): 1835-1842.

Sellén, M. (2021, September 9). *How Long Is The Average Car?* Retrieved September 2021, from https://mechanicbase.com/cars/average-car-length/

Sheikholeslam, S., & Desoer, C. A. (1990). Longitudinal Control of a Platoon of Vehicles. *American Control Conference*, (pp. 291-296). San Diego.

Shladover, S. E., Nowakowski, C., Lu, X. Y., & Ferlis, R. (2015). Cooperative Adaptive Cruise Control: Definitions and Operating Concepts. *Transportation Research Record: the Journal of Transportation Research Board*, 2489(1): 145-152.

Strategic Highway Research Program. (2014, May 15). *SHRP 2 Products Chart.* Retrieved August 29, 2020, from The national Academies of Sciences, Engineering, and Medicine: http://onlinepubs.trb.org/onlinepubs/shrp2/SHRP2ProductsChart.pdf

Stüdli, S., Seron, M. M., & Middleton, R. H. (2017). From Vehicular Platoons to General Networked Systems: String Stability and Related Concepts. *Annual Reviews in Control*, 44: 157-172.

Sun, D., & Benekohal, R. F. (2006). Analysis of Work Zone Gaps and Rear-End Collision Probability. *Journal of Transportation and Statistics*, 8 (2): 71-86.

Swaroop, D., & Huandra, R. (1998). Intelligent Cruise Control System Design based on a Traffic Flow Specification. *Vehicle System Dynamics*, 30(5): 319-344.

Swaroop, D., & Rajagopal, K. R. (2001). A Review of Constant Time Headway Policy for Automatic Vehicle Following. *IEEE Intelligent Transportation Systems*, (pp. 65-69). Oakland.

The National Academies of Sciences, Enginerring, and Medicine. (2020). *The second Strategic Highway Research Program (2006-2015)*. Retrieved August 29, 2020, from http://www.trb.org/StrategicHighwayResearchProgram2SHRP2/Blank2.aspx#:~:text=SHRP%202%20%7C%20Strategic%20Highway%20Research%20Program%202%20(SHRP%202)&text=SHRP%202%20was%20created%20to,for%20renewing%20roads%20and%20bridges.

Tomizuka, M., & KARL HEDRICK, J. (1995). Advanced Control Methods for Automotive Applications. *Vehicle System Dynamics*, 24(6-7): 449-468.

Torbic, D. J., Hutton, J. M., Bokenkroger, C. D., Harwood, D. W., Gilmore, D. K., Knoshaug, M. M., . . . Stanley, J. (2012). *Design Guidance for Freeway Mainline Ramp Terminals.* Washting, D.C.: Transportation Research Board.

Transportation Research Board. (2013, April 3). *The 2nd Strategic Highway Research Program Naturalistic Driving Study Dataset*. Retrieved July 5, 2020, from https://insight.shrp2nds.us

Transportation Research Board. (2016). *Highway Capacity Manual 6th Edition: A Guide for Multimodal Mobility Analysis.* Washington, D. C.

Transportation Research Board. (2016). *Highway Capacity Manual 6th Edition: A Guide for Multimodal Mobility Analysis.* Washington, D.C.: The National Academies Press.

Transportation Research Board of the National Academies of Science. (2020). *The 2nd Strategic Highway Research Program Naturalistic Driving Study Dataset*. Retrieved July 5, 2020, from http://insight.shrp2nds.us

Trask, L., Aghdashi, B., Schroeder, B., & Rouphail, N. (2015). *FREEVAL-WZ Users Guide.* Raleigh: North Carolina State University.

Twomey, J. M., Heckman, M. L., Hayward, J. C., & Zuk, R. J. (1993). Accidents and Safety Associated with Interchanges. *Transportation Research Record: Jornal of Transportation Research Board*, 1385: 100-105.

U.S. Food & Drug Administration. (2019, April 18). *Institutional Review Boards Frequently Asked Questions: Guidance for Institutional Review Boards and Clinical Investigators*. Retrieved September 15, 2020, from https://www.fda.gov/regulatory-information/search-fda-guidance-documents/institutional-review-boards-frequently-asked-questions

van der Heijden, R., Lukaseder, T., & Kargl, F. (2017). Analyzing Attacks on Cooperative Adaptive Cruise Control (CACC). *IEEE Vehicular Networking Conference (VNC)*, (pp. 45-52). New York.

Van-Schagen, W. I., Backer-Grondahl, A., Hoedemaeker, M., Lotan, T., Morris, A., & Sagberg, F. (2011). *Towards a Large-Scale European Naturalistic Driving Study: A Final Report of PROLOGUE.* Leidschendam, Netherlands: SWOV Institute for Road Safety Research.

Venglar, S. P., Porter, R. J., Obeng-Boampong, K. O., & Kuchangi, S. (2008). *Establishing Advisory Speeds on Non Direct-Connect Ramps: Technical Report.* College Station: Texas Transportation Institute, Texas Department of Transportation.

Victor, T., Dozza, M., Bärgman, J., Boda, C., Engström, J., Flannagan, C., . . . Markkula, G. (2015). *Analysis of Naturalistic Driving Study Data: Safer Glances, Driver Inattention, and Crash Risk.* Washington, D.C.: Transportation Research Board.

Wang, J., & Rajamani, R. (2004). Should Adaptive Cruise-Control Systems be Designed to Maintain a Constant Time Gap between Vehicles? *IEEE Transactions on Vehicular Technology*, 53(5): 1480-1490.

Wang, Z., Chen, H., & Lu, J. J. (2009). Exploring Impacts of Factors Contributing to Injury Severity at Freeway Diverge Areas. *Transportation Research Record: Journal of Transportation Research Board*, 2102: 43-52.

Weng, J., & Meng, Q. (2011). Decision Tree-Based Model for Estimation of Work Zone Capacity. *Transportation Research Record: Journal of the Transportation Research Board*, 2257: 40-50.

Weng, J., & Meng, Q. (2012). Ensemble Tree Approach to Estimating Work Zone Capacity. *Transportation Research Record: Journal of the Transportation Research Board*, 2286: 56-67.

Weng, J., & Meng, Q. (2015). Incorporating Work Zone Configuration Factors into Speed-Flow and Capacity Models. *Journal of Advanced Transportation*, 49(3): 371-384.

Weng, J., Meng, Q., & Fwa, T. F. (2014). Vehicle Headway Distribution in Work Zones. *Transportmetrica A: Transport Science*, 10 (4): 285-303.

Weng, J., & Meng, Q. (2013). Estimating Capacity and Traffic Delay in Work Zones: An Overview. *Transportation Research Part C: Emerging Technologies*, 35: 34-45.

Wood, S. N. (2017). *Generalized Additive Models: An Introduction with R.* CRC Press.

Wood, S., & Wood, M. S. (2021, February 16). *Package 'mgcv'*. Retrieved February 20, 2021, from https://cran.uib.no/web/packages/mgcv/mgcv.pdf

Wu, J., & Xu, H. (2017). Driver Behavior Analysis for Right-Turn Drivers at Signalized Intersections using SHRP 2 Naturalistic Driving Study Data. *Journal of Safety Research*, 63: 177-185.

Wu, K. F., & Lin, Y. J. (2019). Exploring the Effects of Critical Driving Situations on Driver Perception Time (PT) using SHRP2 Naturalistic Driving Study Data. . *Accident Analysis & Prevention*, 128: 94-102.

Xiao, L., & Gao, F. (2010). A Comprehensive Review of the Development of Adaptive Cruise Control Systems. *Vehicle System Dynamics*, 48(10): 1167-1192.

Xiao, L., Gao, F., & Wang, J. (2009). On Scalability of Platoon of Automated Vehicles for Leader-Predecessor Information Framework. *IEEE Intelligent Vehicles Symposium*, 1103-1108.

Yau, C. (2013). *Non-parametric Methods. R Tutorial: An R Introduction to Statistics*. Retrieved March 5, 2019, from http://www.r-tutor.com/elementary-statistics/non-parametric-methods

Ye, F., & Zhang, Y. (2009). Vehicle Type–Specific Headway Analysis Using Freeway Traffic Data. *Transportation Research Record: Journal of the Transportation Research Board*, 2124 (1): 222-230.

Yeom, C., Rouphail, N., & Rasdorf, W. (2015). Simulation Guidance for Freeway Lane Closure Capacity Calibration. *Transportation Research Record: Journal of the Transportation Research Board*, 2553: 82-89.

Zeileis, A., Shah, A., & Patnaik, I. (2010). Testing, Monitoring, and Dating Structural Changes in Exchange Rate Regimes. *Computational Statistics & Data Analysis*, 54 (6): 1696-1706.

Zhang, L., Chen, C., Zhang, J., Fang, S., You, J., & Guo, J. (2018). Modeling Lane-Changing Behavior in Freeway Off-Ramp Areas from the Shanghai Naturalistic Driving Study. *Journal of Advanced Transportation*.

Zhang, L., Morallos, D., Jeannotte, K., & Strasser, J. (2012). *Traffic Analysis Toolbox Volume XII: Work Zone Traffic Analysis–Applications and Decision Framework.* Washington D.C.: Federal Highway Administration. Office of Operations.

Zhou, H. H., Turochy, R., & Xu, D. (2019). *Evaluation of Work Zone Mobility by Utilizing Naturalistic Driving Study Data.* Gainesville, FL: Southeastern Transportation Research, Innovation, Development and Education Center (STRIDE), University of Florida Tranportation Institute.

Zhou, J., & Peng, H. (2005). Range Policy of Adaptive Cruise Control Vehicles for Improved Flow Stability and String Stability. *IEEE Transactions on Intelligent Transportation Systems*, 6(2): 229-237.

Zou, X., & Levinson, D. (2002). Evaluation of Impacts of Adaptive Cruise Control on Mixed Traffic Flow. *International Conference of Traffic and Transportation Studies*, (pp. 762-769). Guilin.

Appendix A: Freeway Diverge Area Speed Distribution and Regression

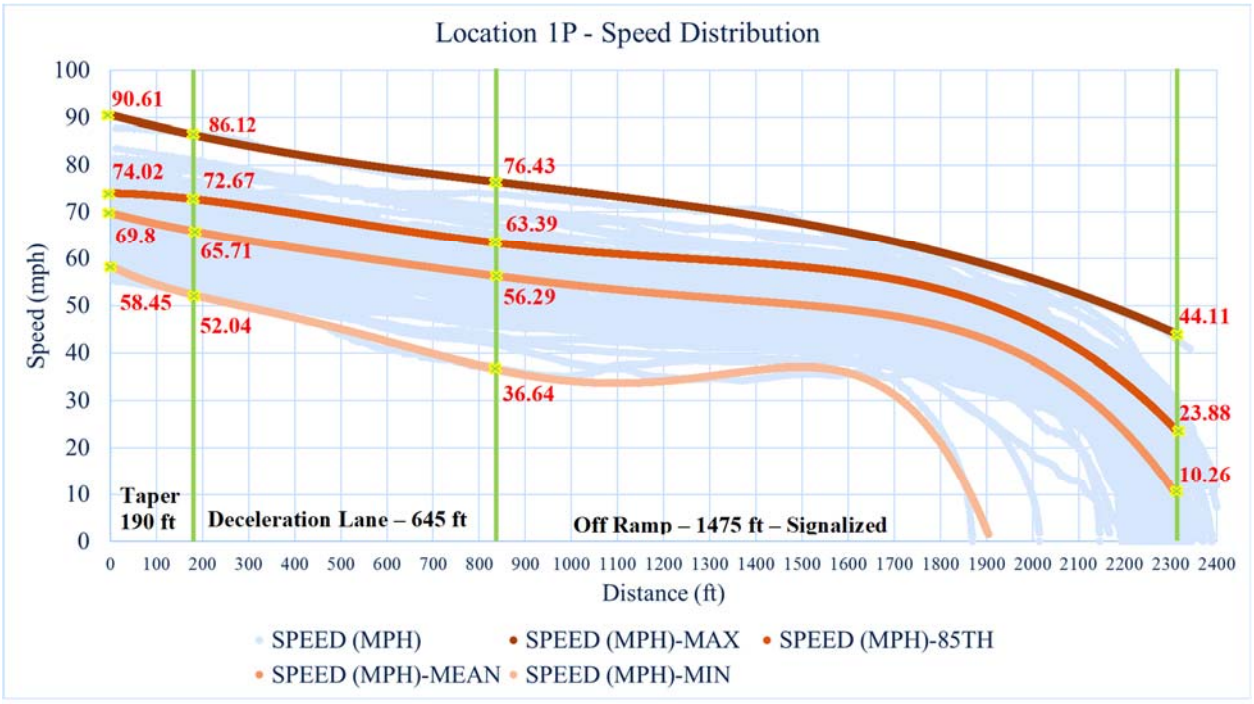

(*a*)

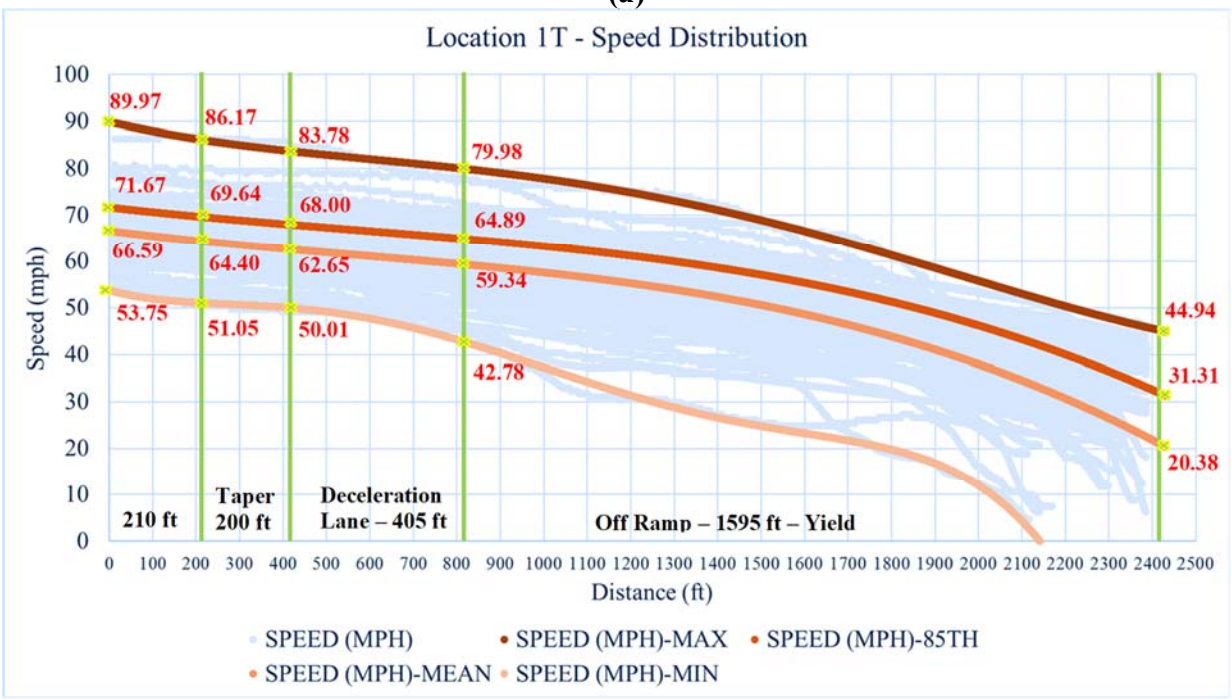

(*b*)

Figure A- 1 Speed distributions: (*a*) Location 1P; and (*b*) Location 1T.

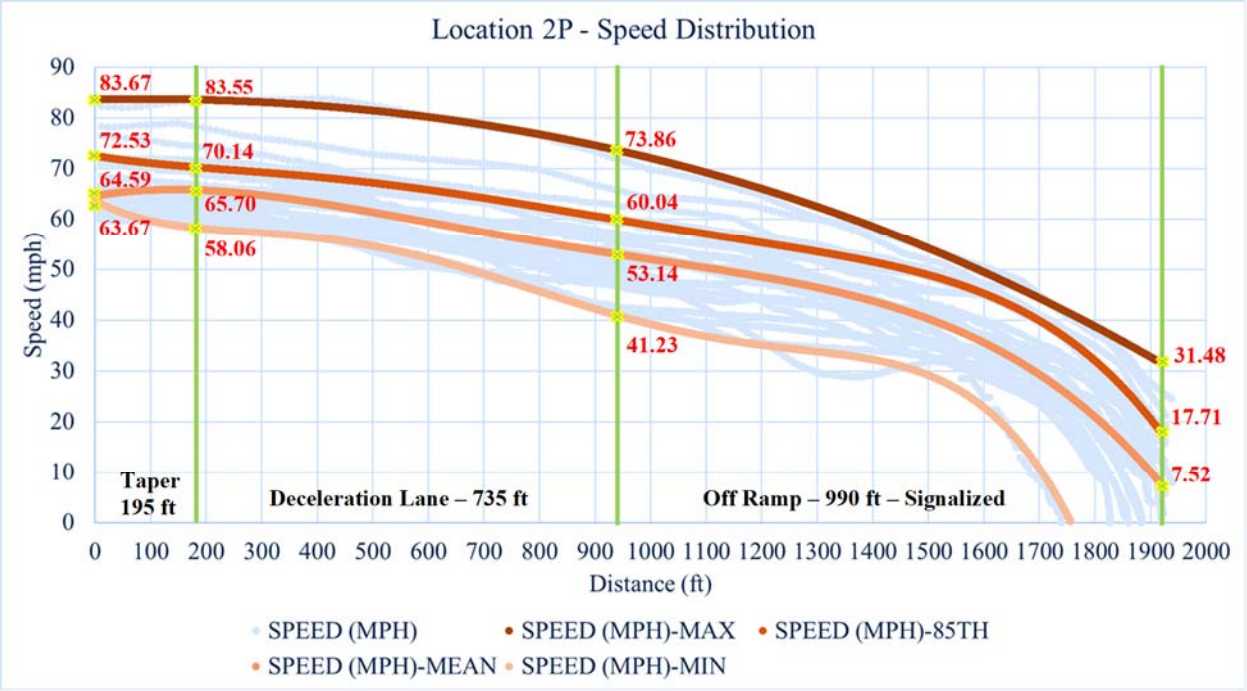

(*a*)

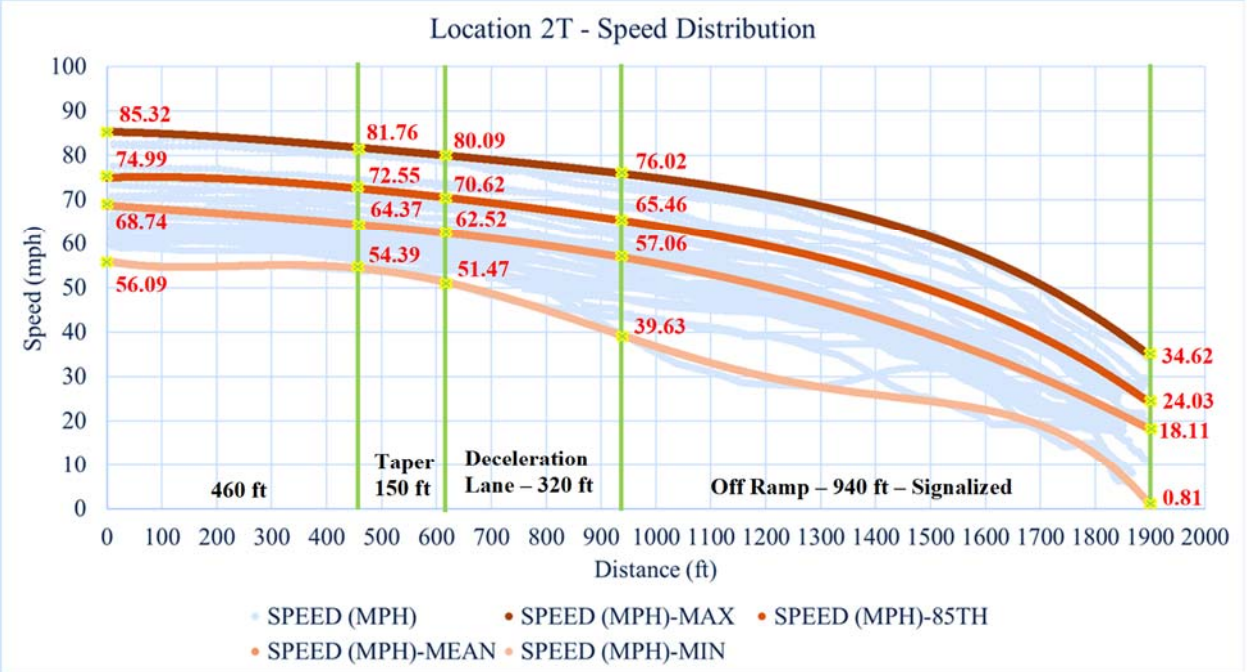

(*b*)

Figure A- 2 Speed distributions: (*a*) Location 2P; and (*b*) Location 2T.

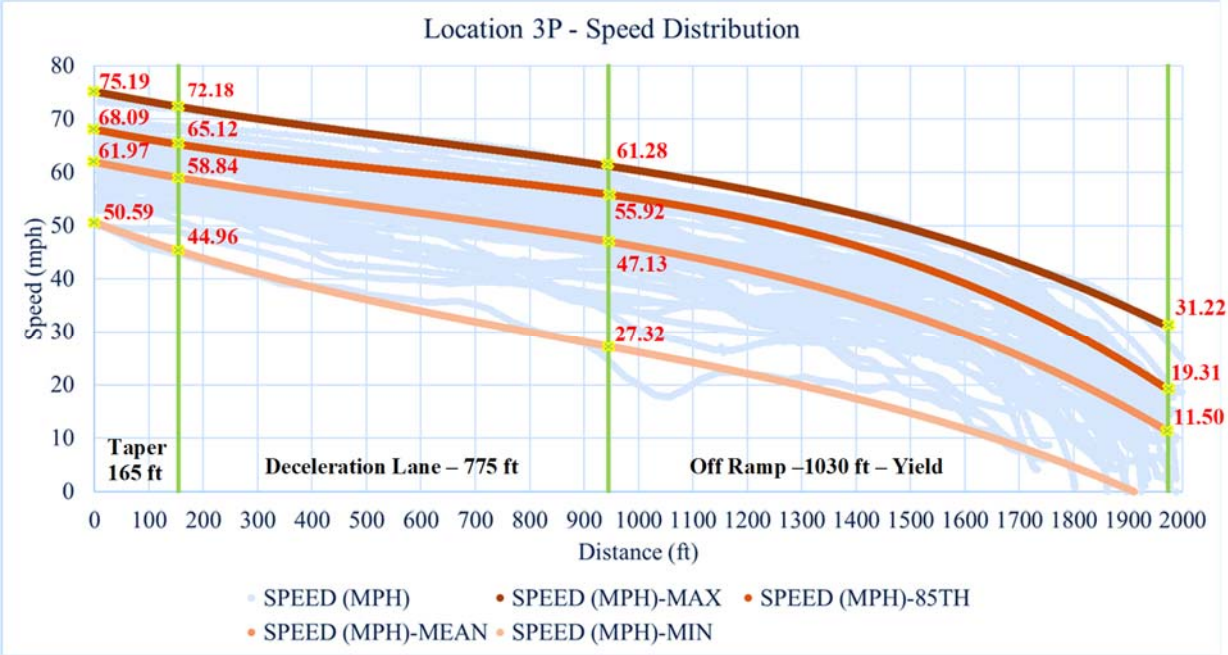

(*a*)

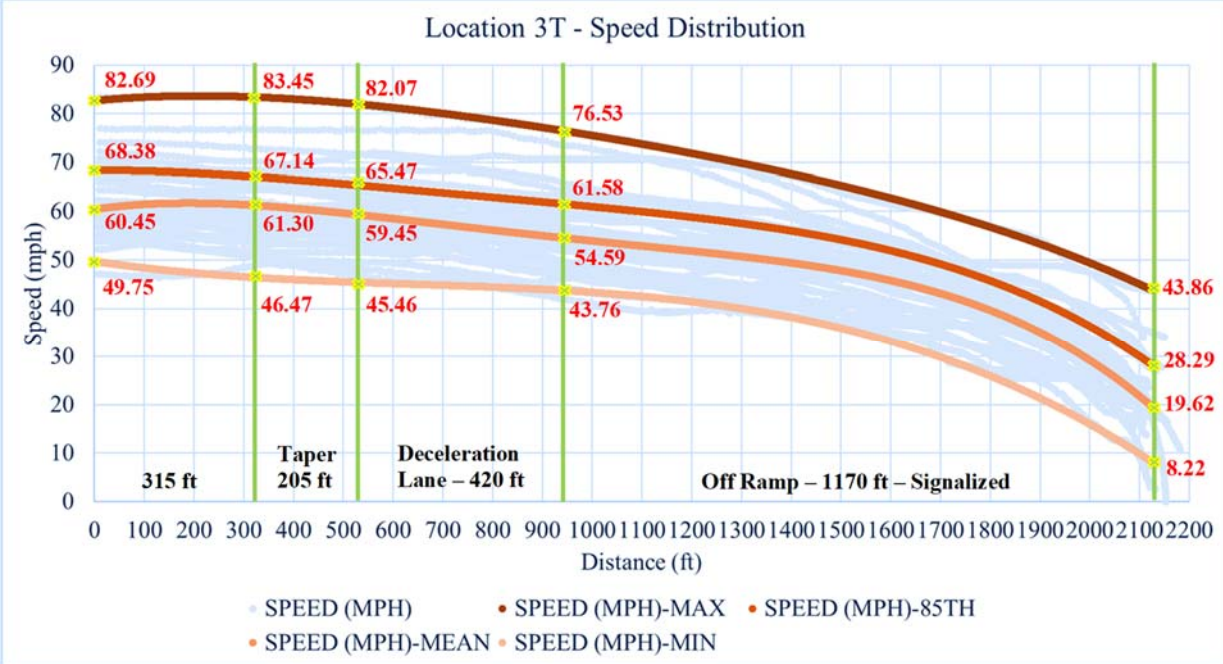

(*b*)

Figure A- 3 Speed distributions: (*a*) Location 3P; and (*b*) Location 3T.

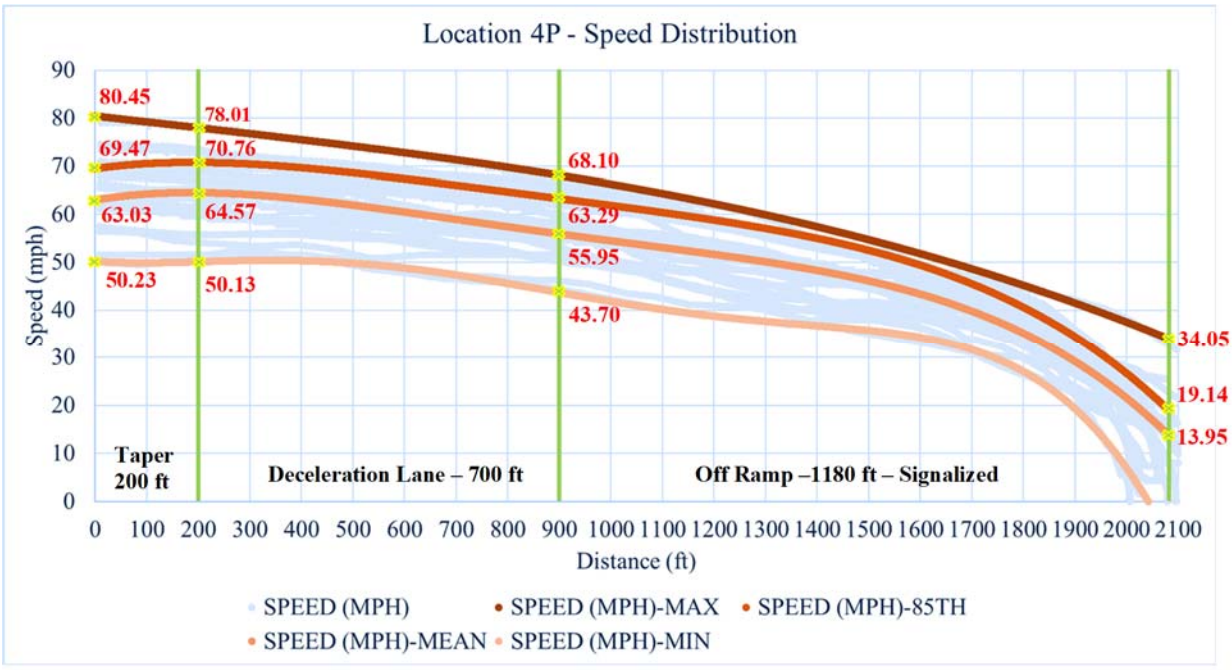

(*a*)

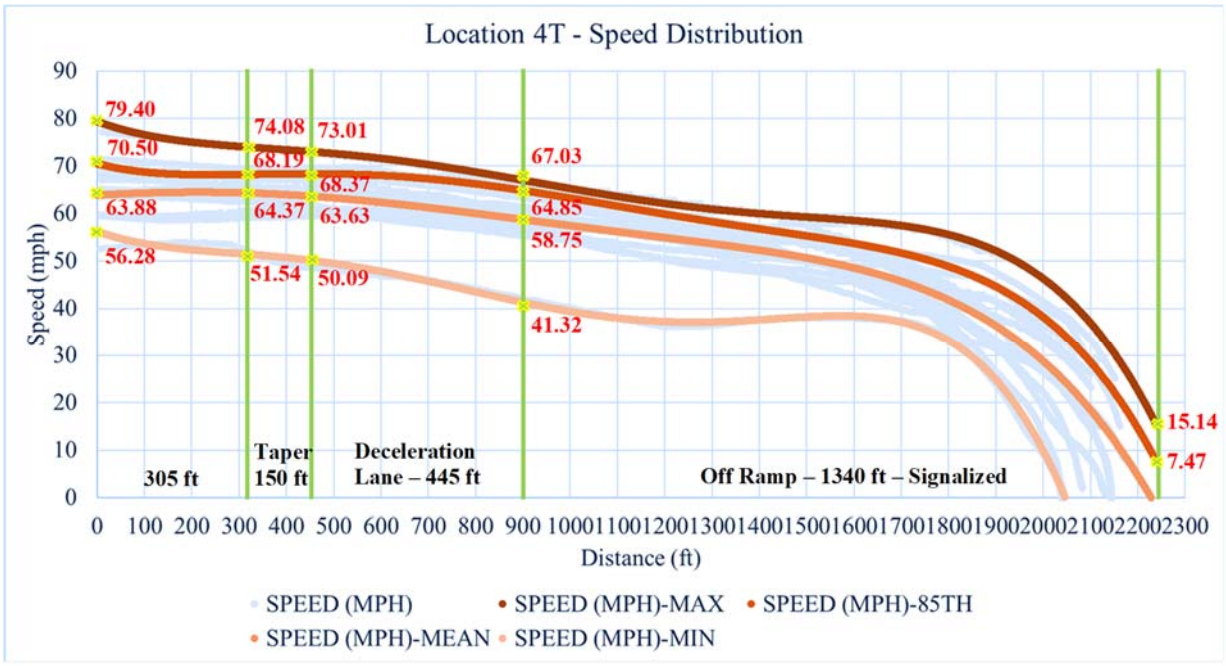

(*b*)

Figure A- 4 Speed distributions: (*a*) Location 4P; and (*b*) Location 4T.

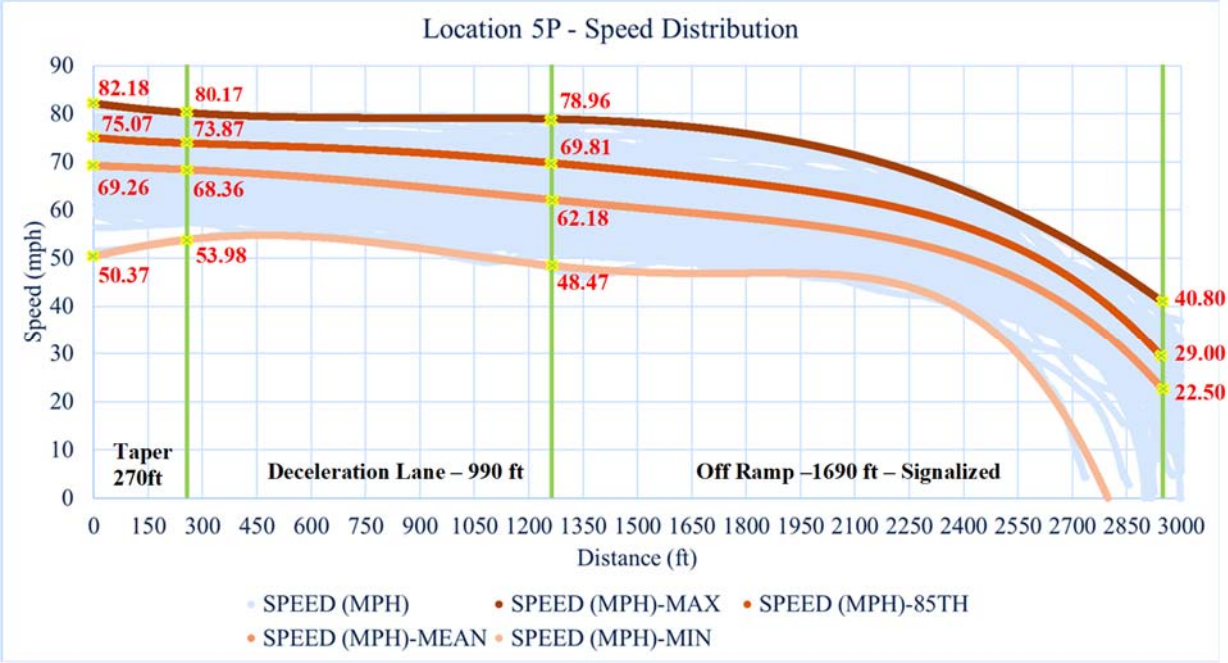

(*a*)

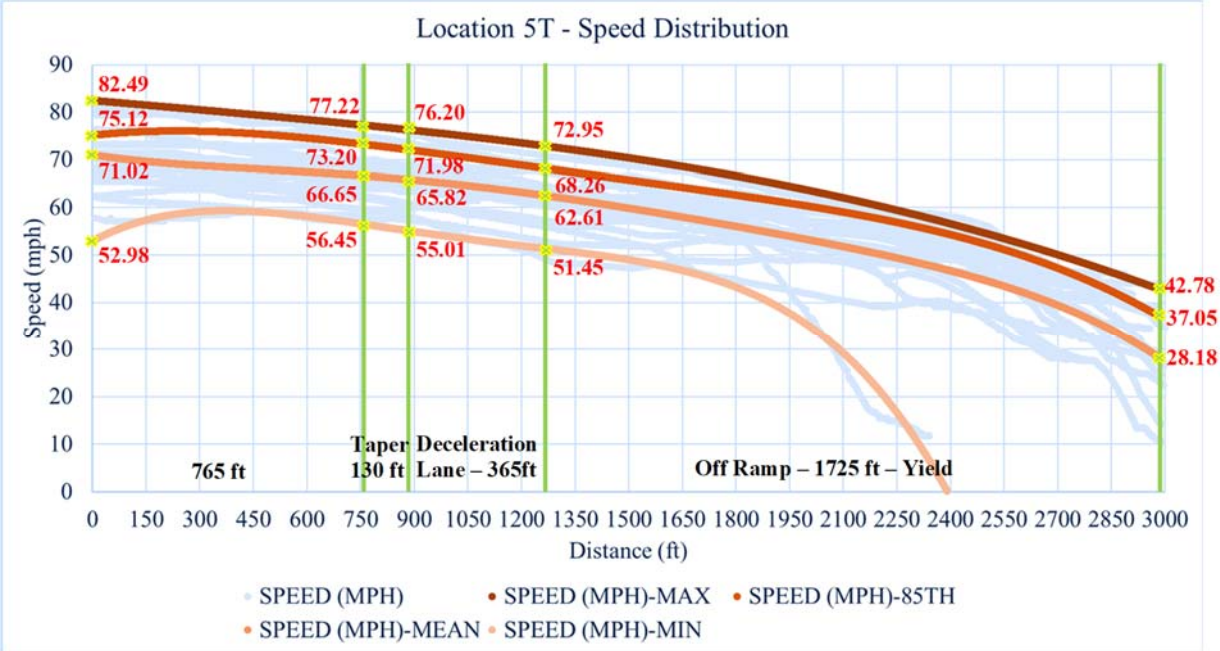

(*b*)

Figure A- 5 Speed distributions: (*a*) Location 5P; and (*b*) Location 5T.

Table A- 1 Max, 85th percentile, mean, and min speed distributions at critical points.

Site	Speed (mph)					
			Taper Start	Deceleration Lane Start	Deceleration Lane End	Off-Ramp End
Location 1P	Max	-	90.61	86.18	76.43	44.11
	85th	-	74.02	72.67	63.39	23.88
	Mean	-	69.80	65.71	56.29	10.26
	Min	-	58.45	52.04	36.64	0.00
		210ft				
Location 1T	Max	89.97	86.17	83.78	79.98	44.94
	85th	71.67	69.64	68.00	64.89	31.31
	Mean	66.59	64.40	62.65	59.34	20.38
	Min	53.75	51.05	50.01	42.78	0.00
Location 2P	Max	-	83.67	83.55	73.86	31.48
	85th	-	72.53	70.14	60.04	17.71
	Mean	-	64.59	65.70	53.14	7.52
	Min	-	63.67	58.06	41.23	0.00
		460ft				
Location 2T	Max	85.32	81.76	80.09	76.02	34.62
	85th	74.99	72.55	70.62	65.46	24.03
	Mean	68.74	64.37	62.52	57.06	18.11

	Min	56.09	54.39	51.47	39.63	0.81
Location 3P	Max	-	75.19	72.18	61.28	31.22
	85th	-	68.09	65.12	55.92	19.31
	Mean	-	61.97	58.84	47.13	11.50
	Min	-	50.59	44.96	27.32	0.00
		315ft				
Location 3T	Max	82.69	83.45	82.07	76.53	43.86
	85th	68.38	67.14	65.47	61.58	28.29
	Mean	60.45	61.30	59.45	54.59	19.62
	Min	49.75	46.47	45.46	43.76	8.22
Location 4P	Max	-	80.45	78.01	68.10	34.05
	85th	-	69.47	70.76	63.29	19.14
	Mean	-	63.03	64.57	55.95	13.95
	Min	-	50.23	50.13	43.70	0.00
		305ft				
Location 4T	Max	79.40	74.08	73.01	67.03	15.14
	85th	70.50	68.19	68.37	64.85	7.47
	Mean	63.88	64.37	63.63	58.75	0.00
	Min	56.28	51.54	50.09	41.32	0.00
Location 5P	Max	-	82.18	80.17	78.96	40.80
	85th	-	75.07	73.87	69.81	29.00
	Mean	-	69.26	68.36	62.18	22.50

	Min	-	50.37	53.98	48.47	0.00
		765ft				
Location 5T	Max	82.49	77.22	76.20	72.95	42.78
	85th	75.12	73.20	71.98	68.26	37.05
	Mean	71.02	66.65	65.82	62.61	28.18
	Min	52.98	56.45	55.01	51.45	0.00

Regression models

For Location 1P:

$$v_{1P-Max} = -5.633 \times 10^{-9} {L_{1P}}^3 + 1.558 \times 10^{-5} {L_{1P}}^2 - 2.606 \times 10^{-2} \times L_{1P} + 90.61$$

$$R^2 = 0.9963$$

$$v_{1P-85^{th}} = -9.767 \times 10^{-12} {L_{1P}}^4 + 3.380 \times 10^{-8} {L_{1P}}^3 - 3.462 \times 10^{-5} {L_{1P}}^2 - 1.703 \times 10^{-3} \times L_{1P} + 74.02$$

$$R^2 = 0.9981$$

$$v_{1P-Mean} = -6.646 \times 10^{-15} {L_{1P}}^5 + 2.697 \times 10^{-11} {L_{1P}}^4 - 3.978 \times 10^{-8} {L_{1P}}^3 + 2.997 \times 10^{-5} {L_{1P}}^2 - 2.594 \times 10^{-2} L_{1P} + 69.80$$

$$R^2 = 0.9981$$

$$v_{1P-Min} = -4.970 \times 10^{-14} {L_{1P}}^5 + 1.866 \times 10^{-10} {L_{1P}}^4 - 2.340 \times 10^{-7} {L_{1P}}^3 + 1.226 \times 10^{-4} {L_{1P}}^2 - 4.982 \times 10^{-2} L_{1P} + 58.45$$

$$R^2 = 0.9600$$

For Location 1T:

$$v_{1T-Max} = 3.664 \times 10^{-12} {L_{1T}}^4 - 1.877 \times 10^{-8} {L_{1T}}^3 + 2.570 \times 10^{-5} {L_{1T}}^2 - 2.272 \times 10^{-2} \times L_{1T} + 89.97$$

$$R^2 = 0.9877$$

$$v_{1T-85^{th}} = -3.320 \times 10^{-9} {L_{1T}}^3 + 5.640 \times 10^{-6} {L_{1T}}^2 - 1.071 \times 10^{-2} L_{1T} + 71.67$$

$$R^2 = 0.9980$$

$$v_{1T-Mean} = -3.968 \times 10^{-9} {L_{1T}}^3 + 6.610 \times 10^{-6} {L_{1T}}^2 - 1.165 \times 10^{-2} L_{1T} + 66.59$$

$$R^2 = 0.9956$$

$$v_{1T-Min} = -2.108 \times 10^{-14} {L_{1T}}^5 + 1.012 \times 10^{-10} {L_{1T}}^4 - 1.630 \times 10^{-7} {L_{1T}}^3 + 9.239 \times 10^{-5} {L_{1T}}^2 - 2.597 \times 10^{-2} L_{1T} + 53.75$$

$$R^2 = 0.9922$$

For Location 2P:

$$v_{2P-Max} = -1.892 \times 10^{-9} {L_{2P}}^3 - 1.141 \times 10^{-5} {L_{2P}}^2 + 1.701 \times 10^{-3} \times L_{2P} + 83.67$$

$$R^2 = 0.9932$$

$$v_{2P-85^{th}} = -1.958 \times 10^{-14} {L_{2P}}^5 + 7.472 \times 10^{-11} {L_{2P}}^4 - 9.974 \times 10^{-8} {L_{2P}}^3 + 4.947 \times 10^{-5} {L_{2P}}^2 - 1.863 \times 10^{-2} \times L_{2P} + 72.53$$

$$R^2 = 0.9968$$

$$v_{2P-Mean} = -2.261 \times 10^{-11} {L_{2P}}^4 + 7.285 \times 10^{-8} {L_{2P}}^3 - 8.193 \times 10^{-5} {L_{2P}}^2 + 1.906 \times 10^{-2} L_{2P} + 64.59$$

$$R^2 = 0.9970$$

$$v_{2P-Min} = -8.148 \times 10^{-14} {L_{2P}}^5 + 3.177 \times 10^{-10} {L_{2P}}^4 - 4.281 \times 10^{-7} {L_{2P}}^3 + 2.262 \times 10^{-4} {L_{2P}}^2 - 5.882 \times 10^{-2} L_{2P} + 63.67$$

$$R^2 = 0.9825$$

For Location 2T:

$$v_{2T-Max} = -8.369 \times 10^{-12} {L_{2T}}^4 + 1.891 \times 10^{-8} {L_{2T}}^3 - 1.848 \times 10^{-5} {L_{2T}}^2 - 2.432 \times 10^{-3} \times L_{2T} + 85.32$$

$$R^2 = 0.9971$$

$$v_{2T-85^{th}} = -8.131 \times 10^{-12} {L_{2T}}^4 + 2.220 \times 10^{-8} {L_{2T}}^3 - 2.916 \times 10^{-5} {L_{2T}}^2 + 4.214 \times 10^{-3} L_{2T} + 74.99$$

$$R^2 = 0.9962$$

$$v_{2T-Mean} = -5.557 \times 10^{-9} {L_{2T}}^3 + 1.200 \times 10^{-6} {L_{2T}}^2 - 8.866 \times 10^{-3} L_{2T} + 68.74$$

$$R^2 = 0.9962$$

$$v_{2T-Min} = -5.084 \times 10^{-14} {L_{2T}}^5 + 2.176 \times 10^{-10} {L_{2T}}^4 - 3.091 \times 10^{-7} {L_{2T}}^3 + 1.486 \times 10^{-4} {L_{2T}}^2 - 2.555 \times 10^{-2} L_{2T} + 56.09$$

$$R^2 = 0.9917$$

For Location 3P:

$$v_{3P-Max} = -6.522 \times 10^{-9} {L_{3P}}^3 + 1.167 \times 10^{-5} {L_{3P}}^2 - 2.000 \times 10^{-2} \times L_{3P} + 75.19$$

$$R^2 = 0.9906$$

$$v_{3P-85^{th}} = -9.955 \times 10^{-9} {L_{3P}}^3 + 1.750 \times 10^{-5} {L_{3P}}^2 - 2.060 \times 10^{-2} \times L_{3P} + 68.09$$

$$R^2 = 0.9932$$

$$v_{3P-Mean} = -7.536 \times 10^{-9} {L_{3P}}^3 + 1.239 \times 10^{-5} {L_{3P}}^2 - 2.078 \times 10^{-2} L_{3P} + 61.97$$

$$R^2 = 0.9965$$

$$v_{3P-Min} = -7.934 \times 10^{-9} {L_{3P}}^3 + 2.085 \times 10^{-5} {L_{3P}}^2 - 3.734 \times 10^{-2} L_{3P} + 50.59$$

$$R^2 = 0.9612$$

For Location 3T:

$$v_{3T-Max} = -3.299 \times 10^{-12} {L_{3T}}^4 + 1.362 \times 10^{-8} {L_{3T}}^3 - 2.723 \times 10^{-5} {L_{3T}}^2 + 9.745 \times 10^{-3} \times L_{3T} + 82.69$$

$$R^2 = 0.9973$$

$$v_{3T-85^{th}} = -5.794 \times 10^{-12} {L_{3T}}^4 + 1.708 \times 10^{-8} {L_{3T}}^3 - 1.931 \times 10^{-5} {L_{3T}}^2 + 6.374 \times 10^{-4} L_{3T} + 68.38$$

$$R^2 = 0.9953$$

$$v_{3T-Mean} = -1.110 \times 10^{-11} {L_{3T}}^4 + 3.937 \times 10^{-8} {L_{3T}}^3 - 4.952 \times 10^{-5} {L_{3T}}^2 + 1.475 \times 10^{-2} L_{3T} + 60.45$$

$$R^2 = 0.9977$$

$$v_{3T-Min} = -9.707 \times 10^{-9} {L_{3T}}^3 + 1.864 \times 10^{-5} {L_{3T}}^2 - 1.532 \times 10^{-2} L_{3T} + 49.75$$

$$R^2 = 0.9738$$

For Location 4P:

$$v_{4P-Max} = -2.724 \times 10^{-9} {L_{4P}}^3 + 8.403 \times 10^{-7} {L_{4P}}^2 - 1.227 \times 10^{-2} \times L_{4P} + 80.45$$

$$R^2 = 0.9965$$

$$v_{4P-85^{th}} = -1.144 \times 10^{-11} {L_{4P}}^4 + 3.867 \times 10^{-8} {L_{4P}}^3 - 4.975 \times 10^{-5} {L_{4P}}^2 + 1.493 \times 10^{-2} \times L_{4P} + 69.47$$

$$R^2 = 0.9976$$

$$v_{4P-Mean} = -1.379 \times 10^{-11} {L_{4P}}^4 + 4.858 \times 10^{-8} {L_{4P}}^3 - 6.145 \times 10^{-5} {L_{4P}}^2 + 1.814 \times 10^{-2} L_{4P} + 63.03$$

$$R^2 = 0.9957$$

$$v_{4P-Min} = -2.555 \times 10^{-14} {L_{4P}}^5 + 1.051 \times 10^{-10} {L_{4P}}^4 - 1.430 \times 10^{-7} {L_{4P}}^3 + 6.331 \times 10^{-5} {L_{4P}}^2 - 8.255 \times 10^{-3} L_{4P} + 50.23$$

$$R^2 = 0.9939$$

For Location 4T:

$$v_{4T-Max} = -2.033 \times 10^{-14} {L_{4T}}^5 + 9.842 \times 10^{-11} {L_{4T}}^4 - 1.548 \times 10^{-7} {L_{4T}}^3 + 1.032 \times 10^{-4} {L_{4T}}^2 - 3.702 \times 10^{-2} \times L_{4T} + 79.40$$

$$R^2 = 0.9953$$

$$v_{4T-85^{th}} = -1.844 \times 10^{-14} {L_{4T}}^5 + 8.800 \times 10^{-11} {L_{4T}}^4 - 1.487 \times 10^{-7} {L_{4T}}^3 + 9.779 \times 10^{-5} {L_{4T}}^2 - 2.589 \times 10^{-2} L_{4T} + 70.50$$

$$R^2 = 0.9973$$

$$v_{4T-Mean} = -7.229 \times 10^{-15} {L_{4T}}^5 + 2.393 \times 10^{-11} {L_{4T}}^4 - 2.094 \times 10^{-8} {L_{4T}}^3 - 7.380 \times 10^{-6} {L_{4T}}^2 + 5.196 \times 10^{-3} L_{4T} + 63.88$$

$$R^2 = 0.9955$$

$$v_{4T-Min} = -3.888 \times 10^{-14} {L_{4T}}^5 + 1.622 \times 10^{-10} {L_{4T}}^4 - 2.273 \times 10^{-7} {L_{4T}}^3 + 1.234 \times 10^{-4} {L_{4T}}^2 - 3.630 \times 10^{-2} L_{4T} + 56.28$$

$$R^2 = 0.9924$$

For Location 5P:

$$v_{5P-Max} = -4.382 \times 10^{-9} {L_{5P}}^3 + 1.166 \times 10^{-5} {L_{5P}}^2 - 1.029 \times 10^{-2} \times L_{5P} + 82.18$$

$$R^2 = 0.9982$$

$$v_{5P-85^{th}} = -1.516 \times 10^{-15} {L_{5P}}^5 + 8.509 \times 10^{-12} {L_{5P}}^4 - 1.768 \times 10^{-8} {L_{5P}}^3 + 1.415 \times 10^{-5} {L_{5P}}^2 - 1.732 \times 10^{-3} \times L_{5P} + 75.07$$

$$R^2 = 0.9977$$

$$v_{5P-Mean} = -1.206 \times 10^{-15} {L_{5P}}^5 + 5.515 \times 10^{-12} {L_{5P}}^4 - 7.754 \times 10^{-9} {L_{5P}}^3 + 1.588 \times 10^{-6} {L_{5P}}^2 - 3.306 \times 10^{-3} L_{5P} + 69.26$$

$$R^2 = 0.9990$$

$$v_{5P-Min} = -4.204 \times 10^{-15} {L_{5P}}^5 + 1.815 \times 10^{-11} {L_{5P}}^4 - 1.753 \times 10^{-8} {L_{5P}}^3 + 1.383 \times 10^{-5} {L_{5P}}^2 + 1.804 \times 10^{-2} L_{5P} + 50.37$$

$$R^2 = 0.9841$$

For Location 5T:

$$v_{5T-Max} = -8.728 \times 10^{-10} {L_{5T}}^3 + 3.841 \times 10^{-7} {L_{5T}}^2 - 6.672 \times 10^{-3} \times L_{5T} + 82.49$$

$$R^2 = 0.9949$$

$$v_{5T-85^{th}} = -1.941 \times 10^{-12} {L_{5T}}^4 + 1.048 \times 10^{-8} {L_{5T}}^3 - 2.105 \times 10^{-5} {L_{5T}}^2 + 8.325 \times 10^{-3} L_{5T} + 75.12$$

$$R^2 = 0.9936$$

$$v_{5T-Mean} = -1.221 \times 10^{-15} {L_{5T}}^5 + 8.262 \times 10^{-12} {L_{5T}}^4 - 2.044 \times 10^{-8} {L_{5T}}^3 + 1.892 \times 10^{-5} {L_{5T}}^2 - 1.151 \times 10^{-2} L_{5T} + 71.02$$

$$R^2 = 0.9895$$

$$v_{5T-Min} = -1.348 \times 10^{-11} {L_{5T}}^4 + 5.531 \times 10^{-8} {L_{5T}}^3 - 8.135 \times 10^{-5} {L_{5T}}^2 + 4.044 \times 10^{-2} L_{5T} + 52.98$$

$$R^2 = 0.9727$$

Appendix B: Freeway Diverge Area Driver Brake Pedal Usage

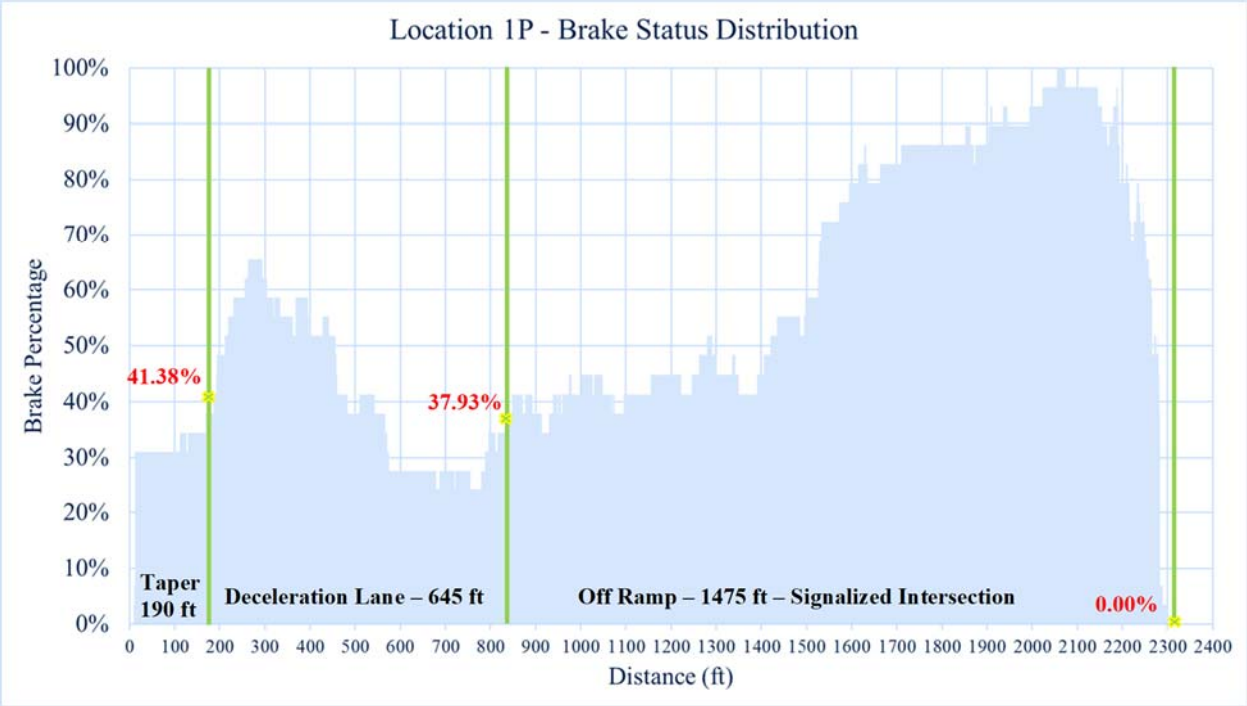

(*a*)

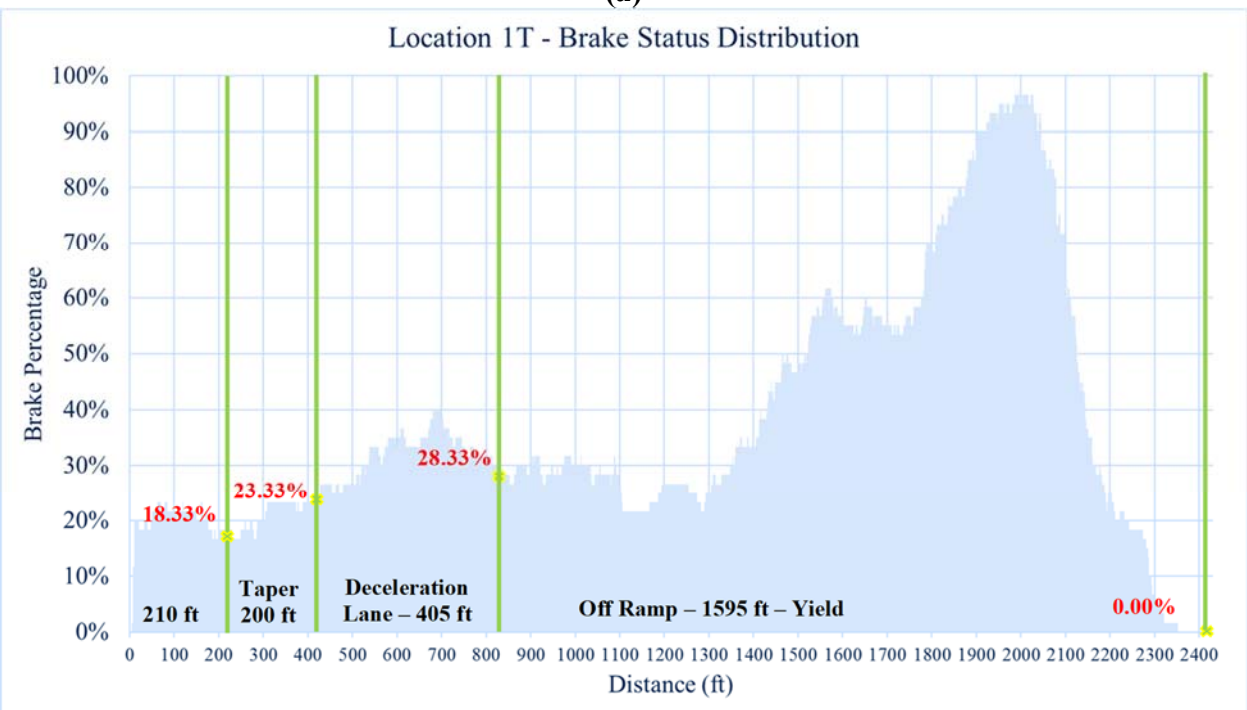

(*b*)

Figure B- 1 Brake status distribution: (*a*) Location 1P; and (*b*) Location 1T.

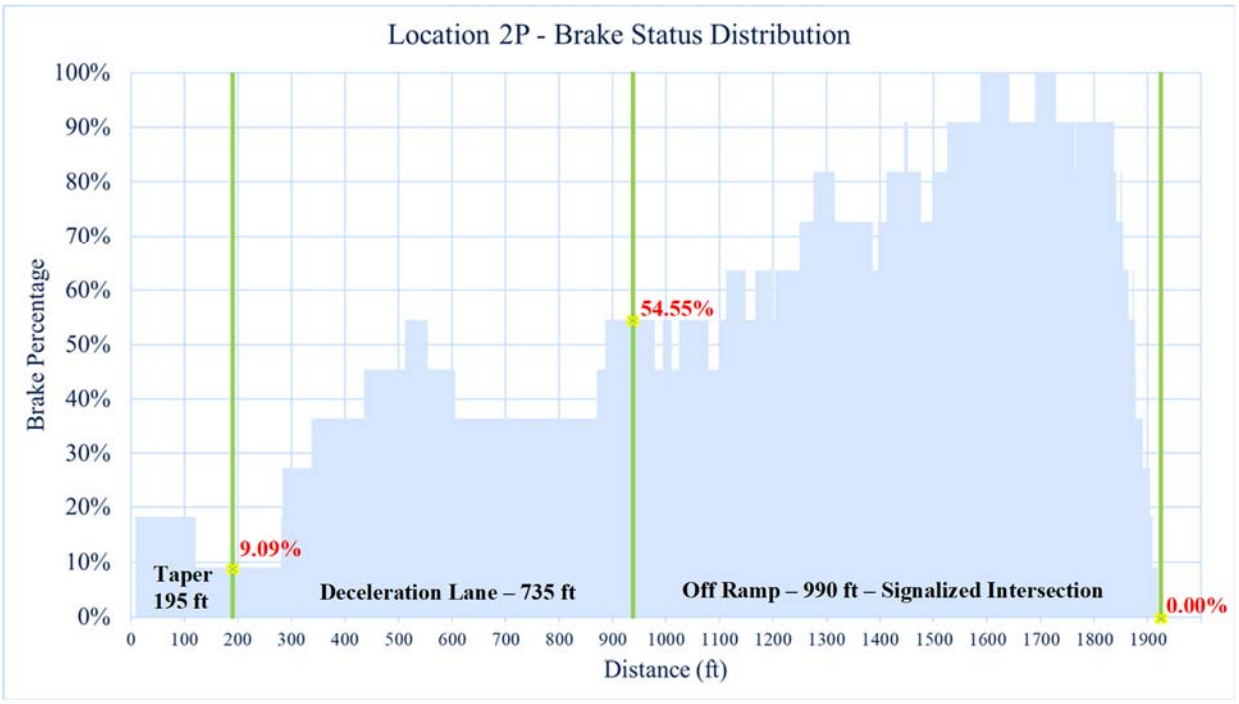

(*a*)

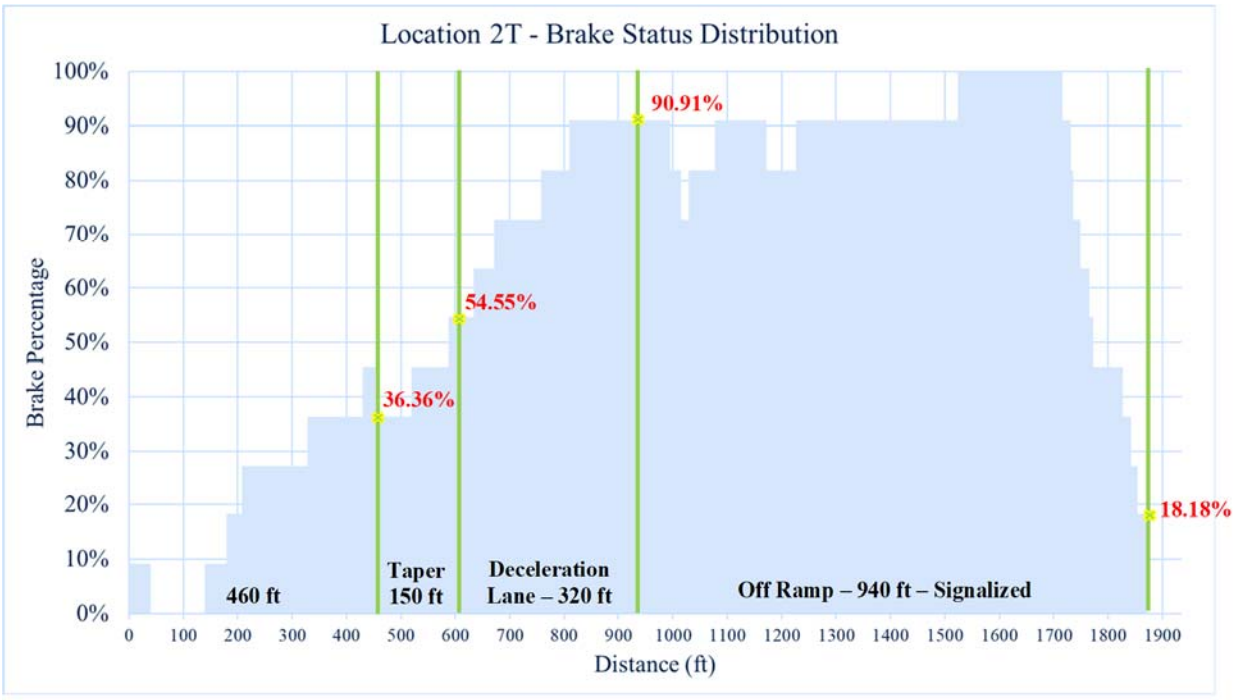

(*b*)

Figure B- 2 Brake status distribution: (*a*) Location 2P; and (*b*) Location 2T.

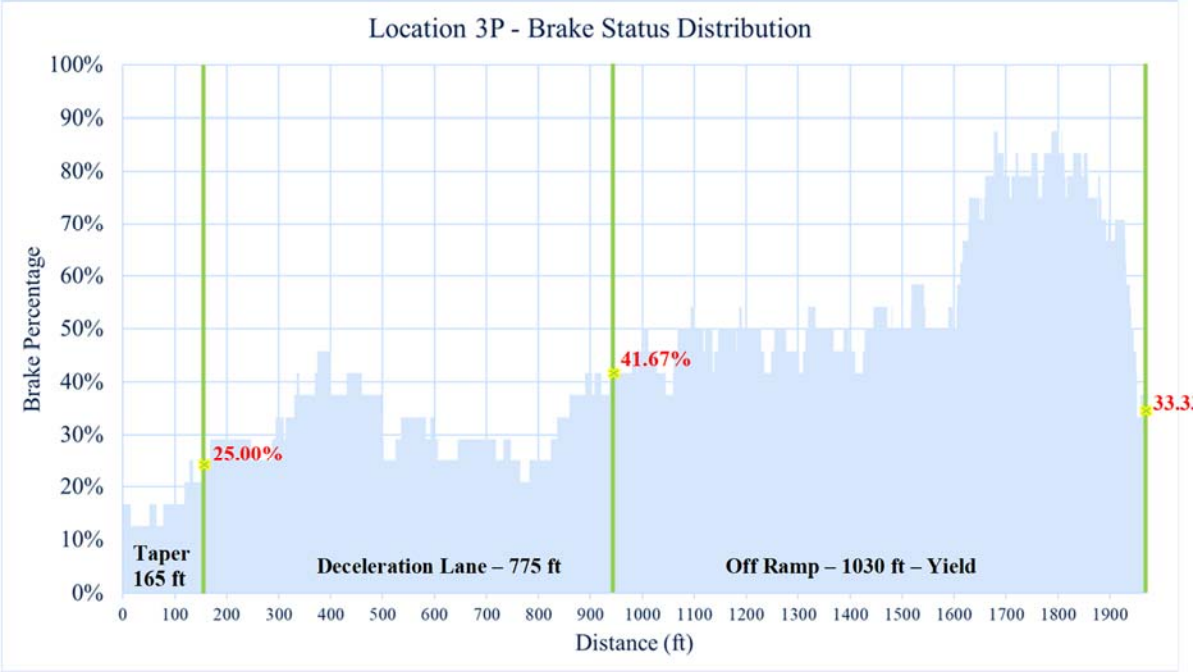

(*a*)

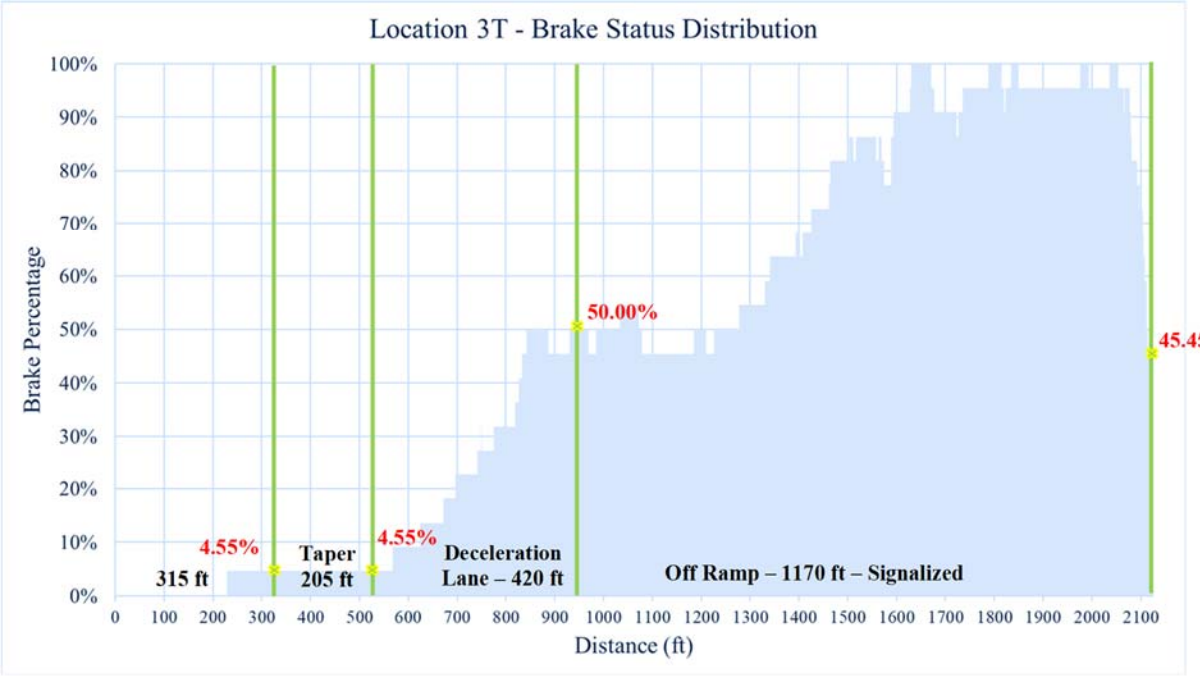

(*b*)

Figure B- 3 Brake status distribution: (*a*) Location 3P; and (*b*) Location 3T.

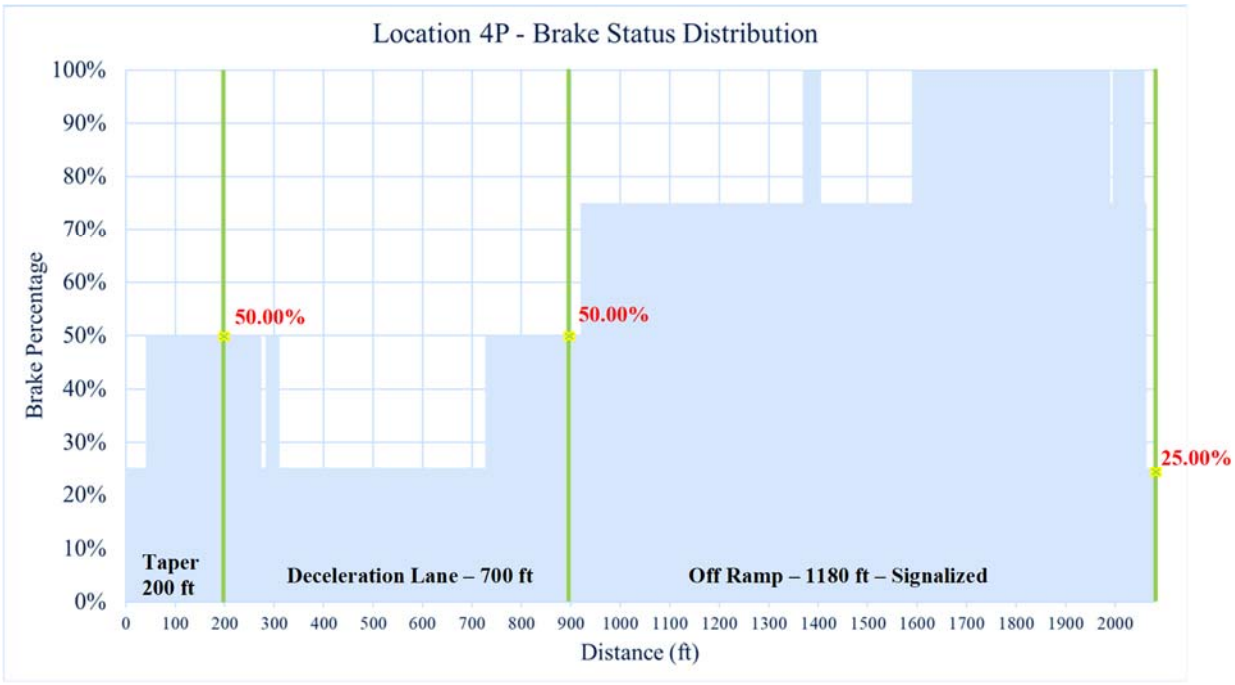

(*a*)

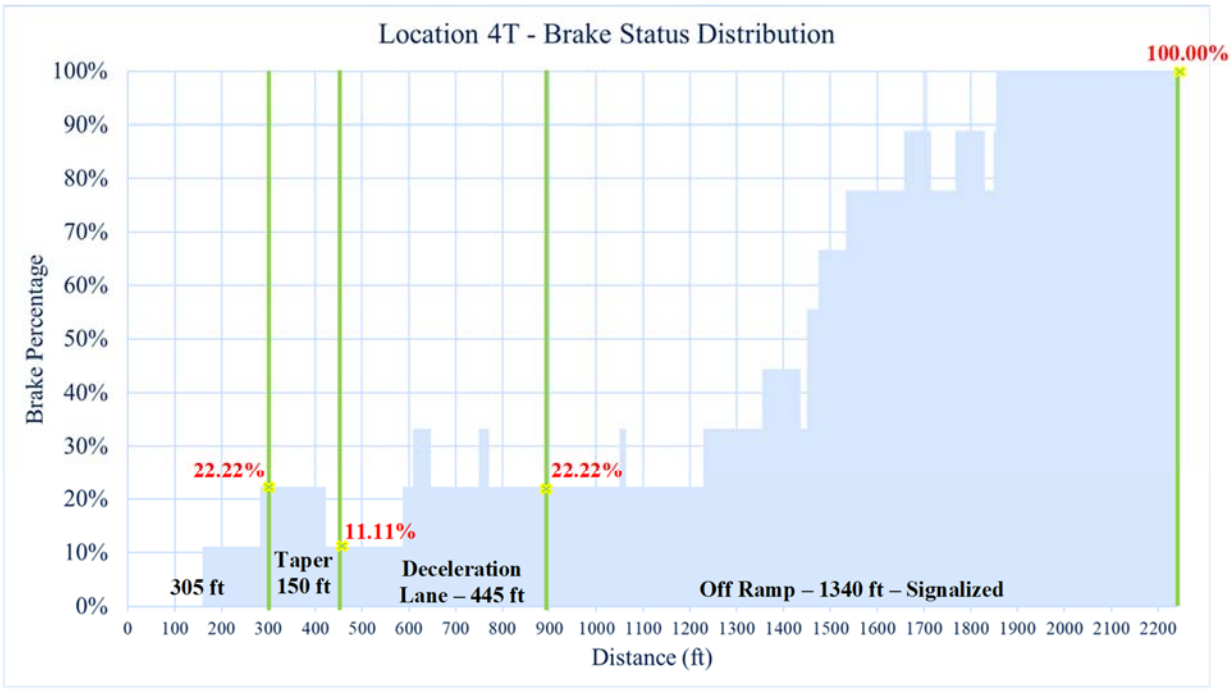

(*b*)

Figure B- 4 Brake status distribution: (*a*) Location 4P; and (*b*) Location 4T.

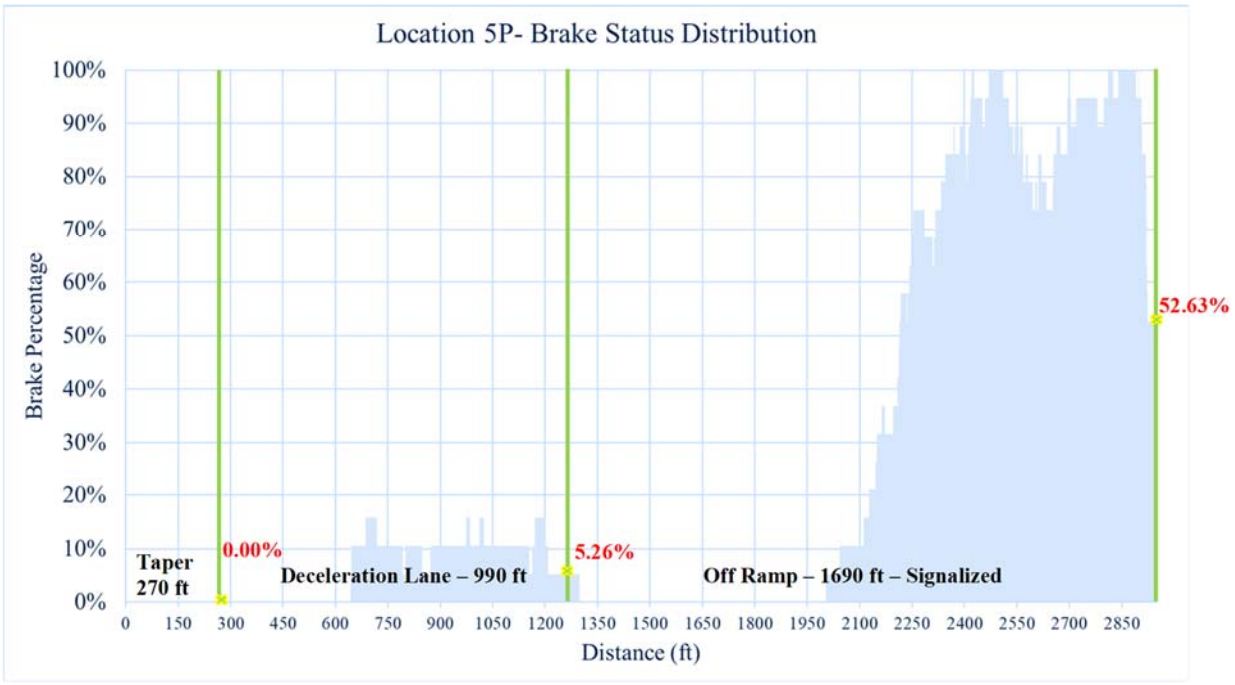

(*a*)

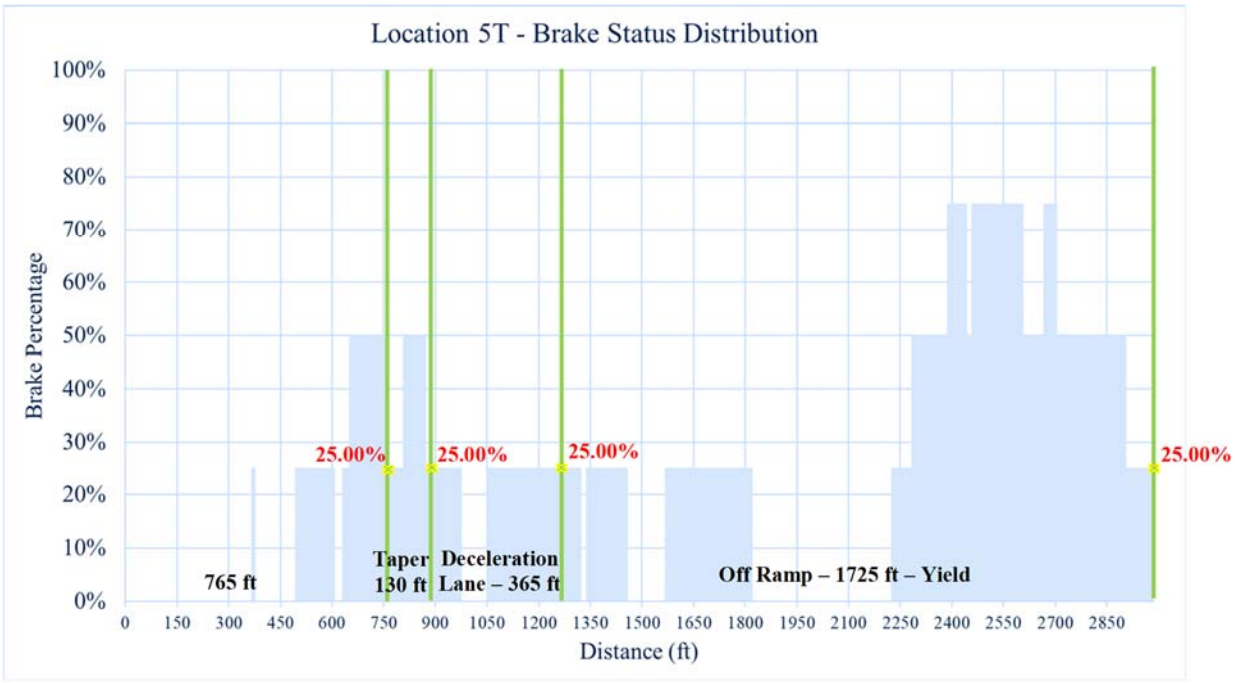

(*b*)

Figure B- 5 Brake status distribution: (*a*) Location 5P; and (*b*) Location 5T.

Table B- 1 Brake pedal usage at critical points.

Site	Brake Usage (%)				
		Taper Start	Deceleration Lane Start	Deceleration Lane End	Off-Ramp End
Location 1P	-	0.00	41.38	37.93	0.00
	210ft				
Location 1T	0.00	18.33	23.33	28.33	0.00
Location 2P	-	0.00	9.09	54.55	0.00
	460ft				
Location 2T	9.09	36.36	54.55	90.91	18.18
Location 3P	-	16.67	25.00	41.67	33.33
	315ft				
Location 3T	0.00	4.55	4.55	50.00	25.00
Location 4P	-	25.00	50.00	50.00	34.05
	305ft				
Location 4T	0.00	22.22	11.11	22.22	100.00
Location 5P	-	0.00	0.00	5.26	52.63
	765ft				
Location 5T	0.00	25.00	25.00	25.00	25.00

Appendix C: Freeway Diverge Area Critical Speed Changepoint

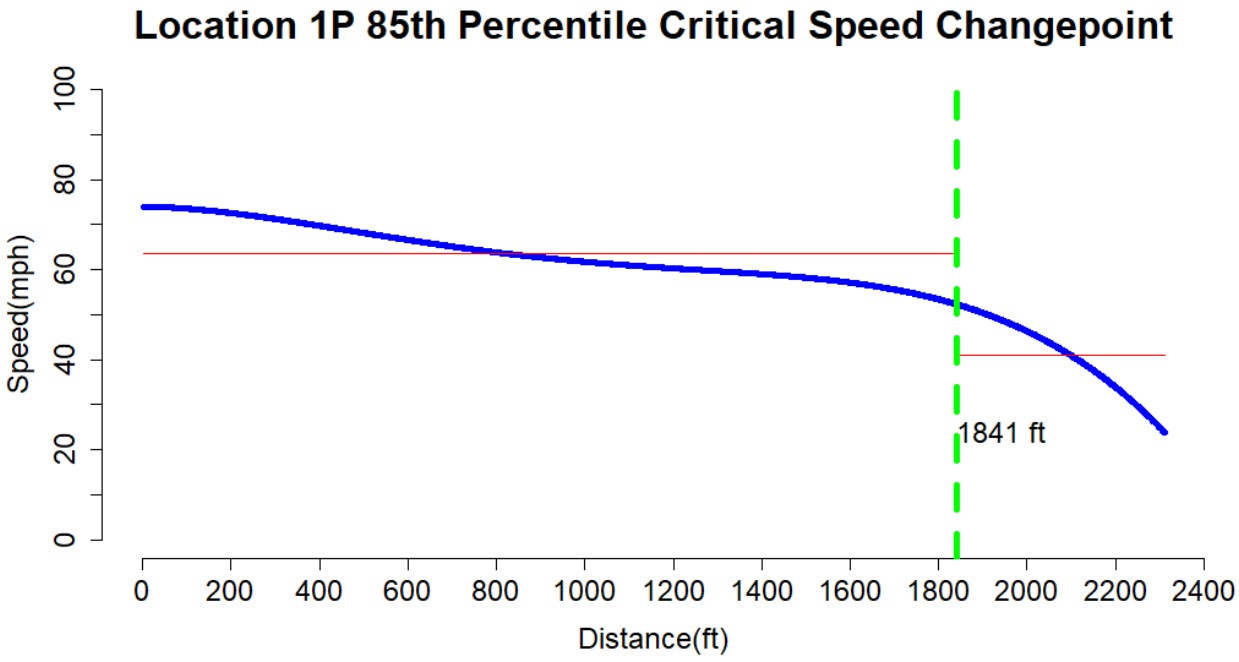

(*a*)

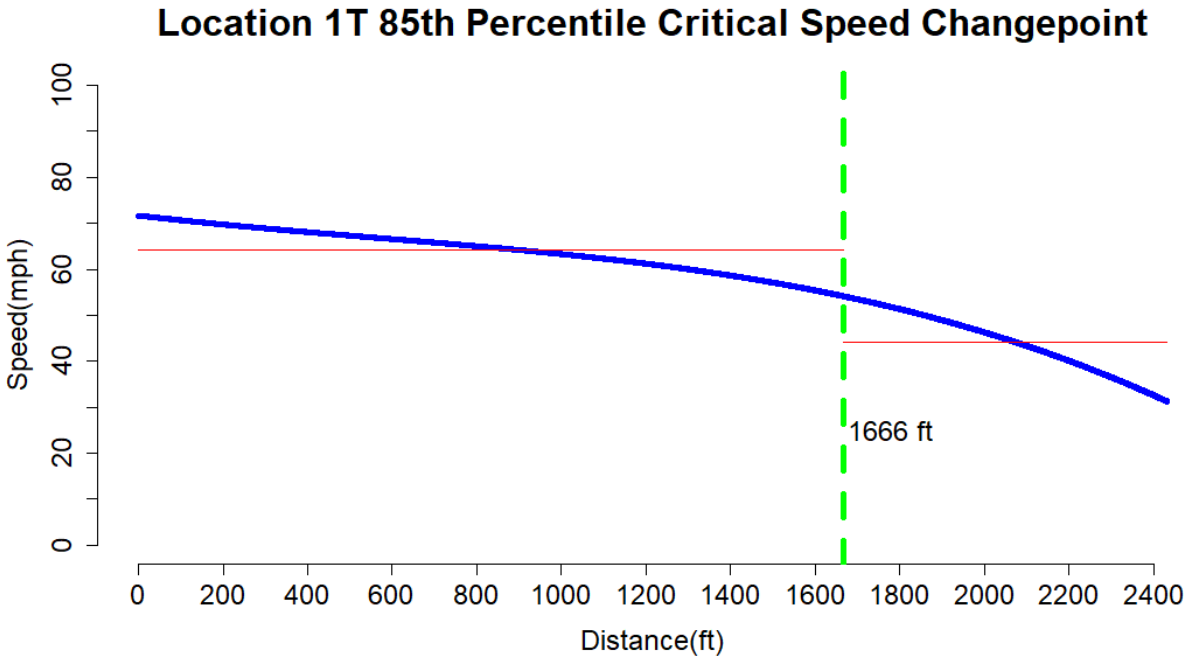

(*b*)

Figure C- 1 Critical speed changepoint: (*a*) Location 1P; and (*b*) Location 1T.

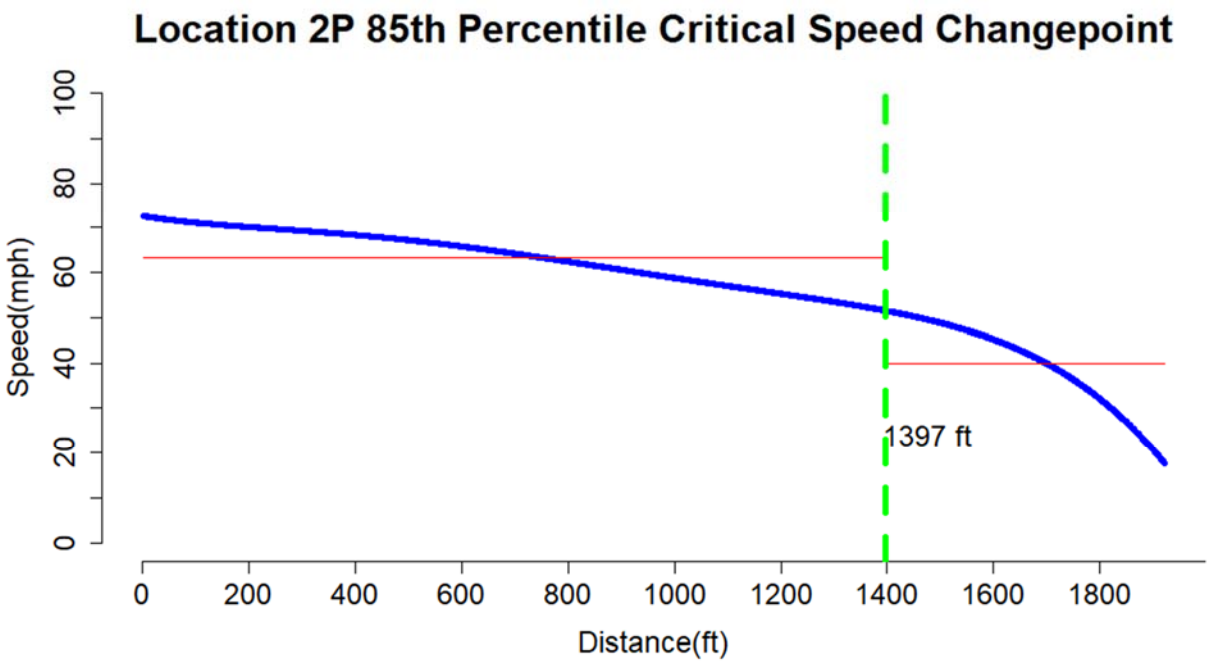

(*a*)

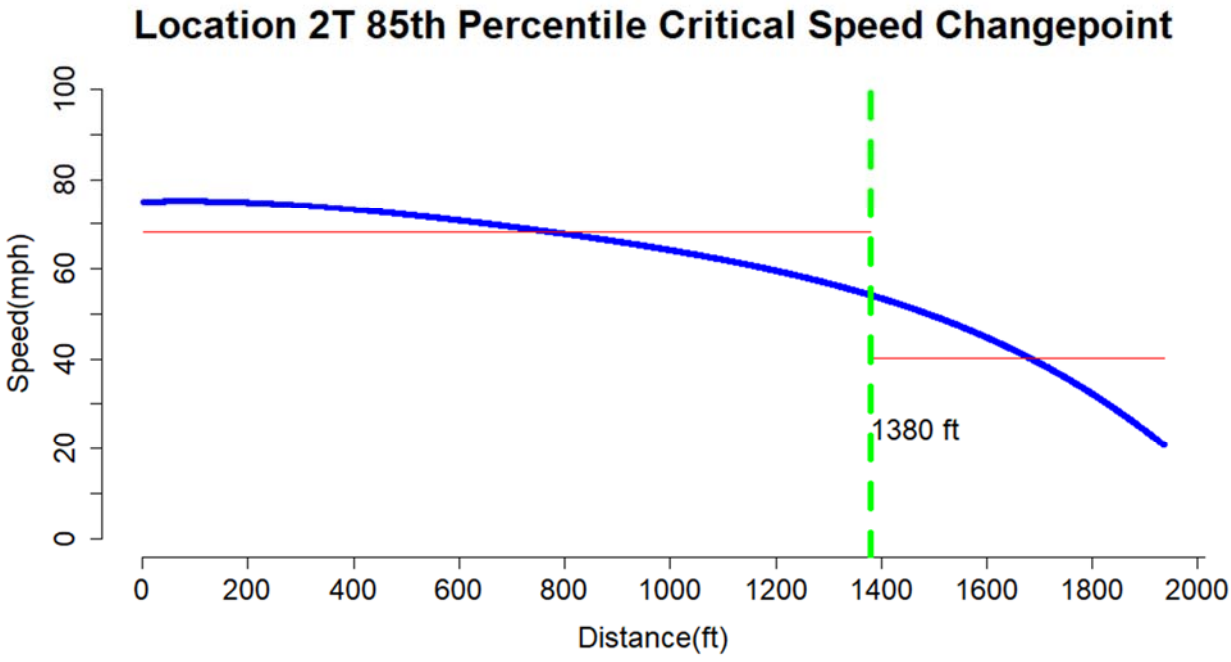

(*b*)

Figure C- 2 Critical speed changepoint: (*a*) Location 2P; and (*b*) Location 2T.

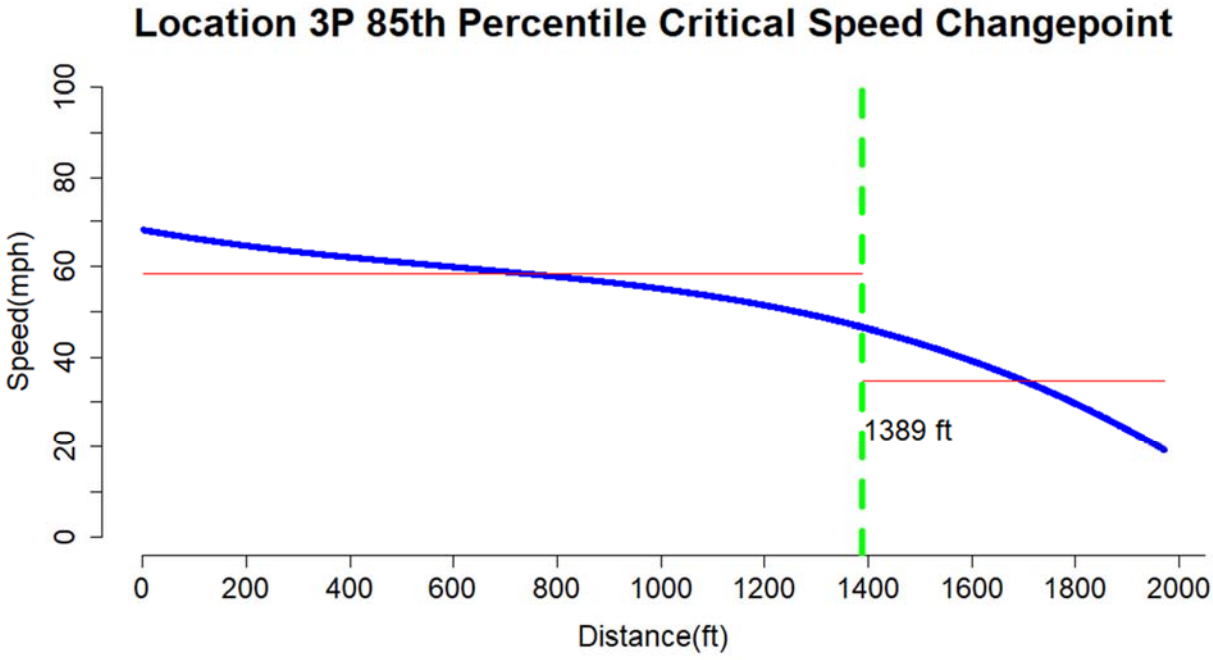

(*a*)

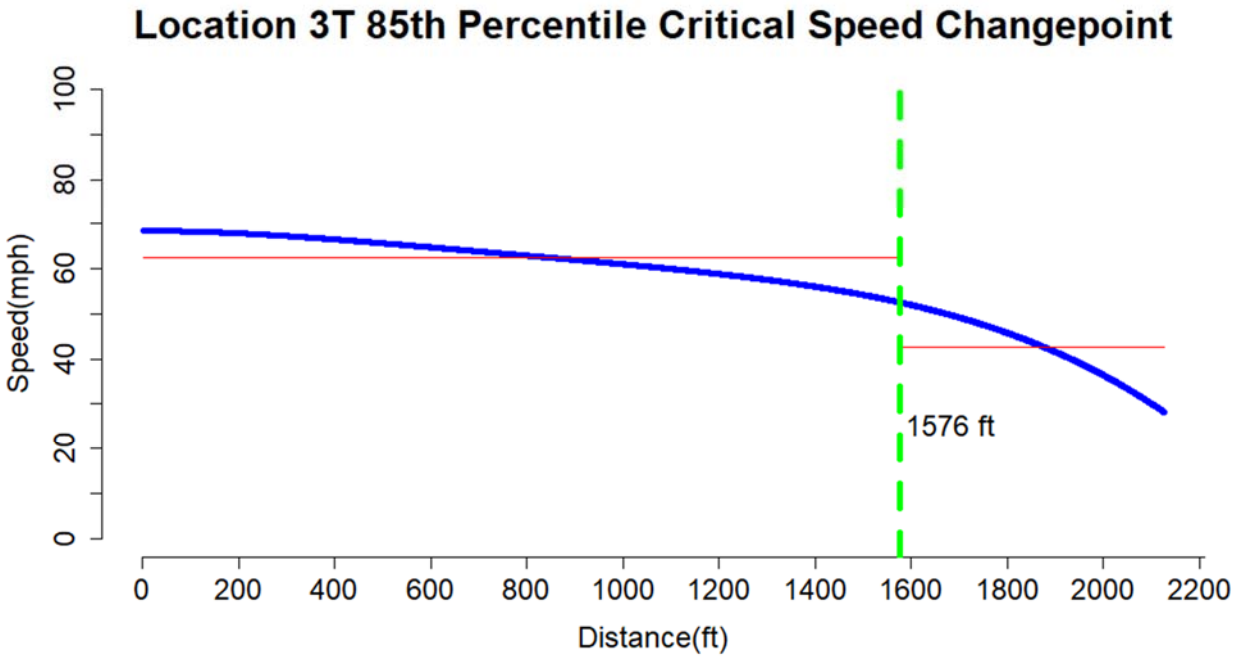

(*b*)

Figure C- 3 Critical speed changepoint: (*a*) Location 3P; and (*b*) Location 3T.

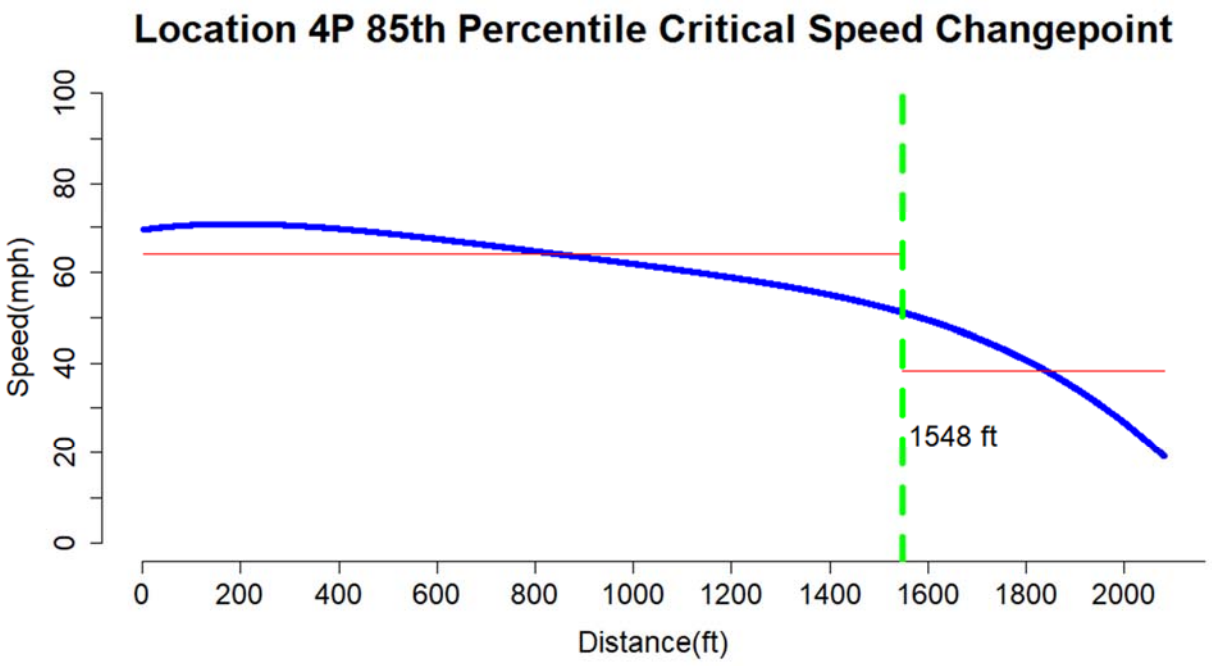

(*a*)

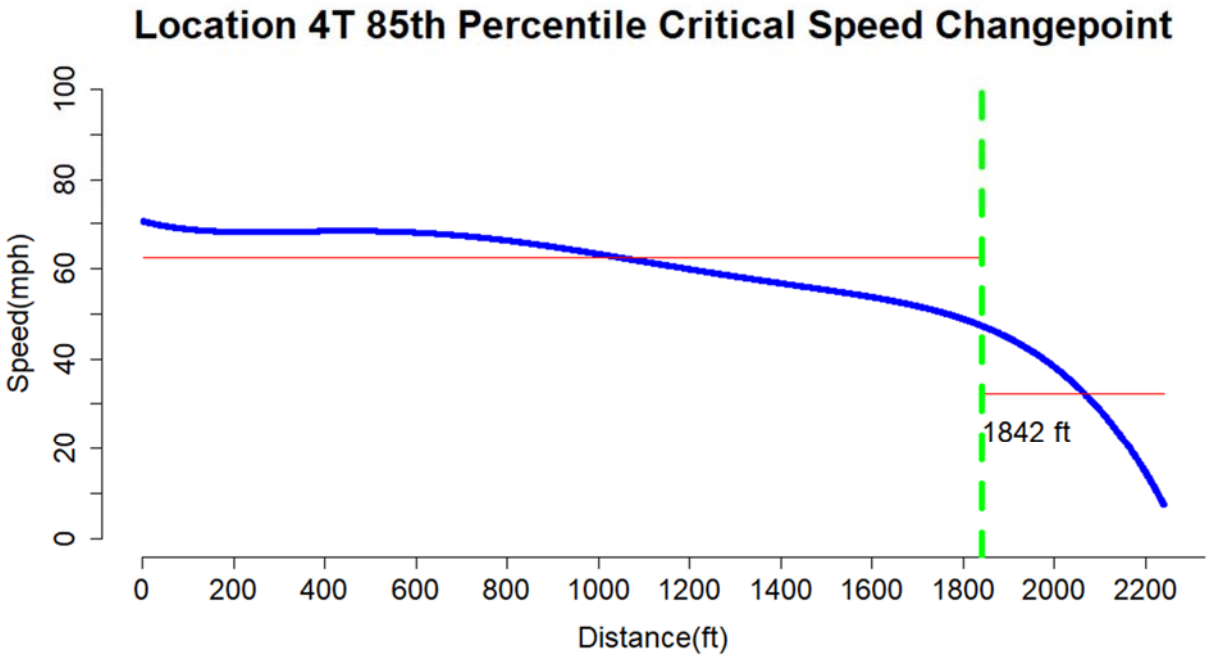

(*b*)

Figure C- 4 Critical speed changepoint: (*a*) Location 4P; and (*b*) Location 4T.

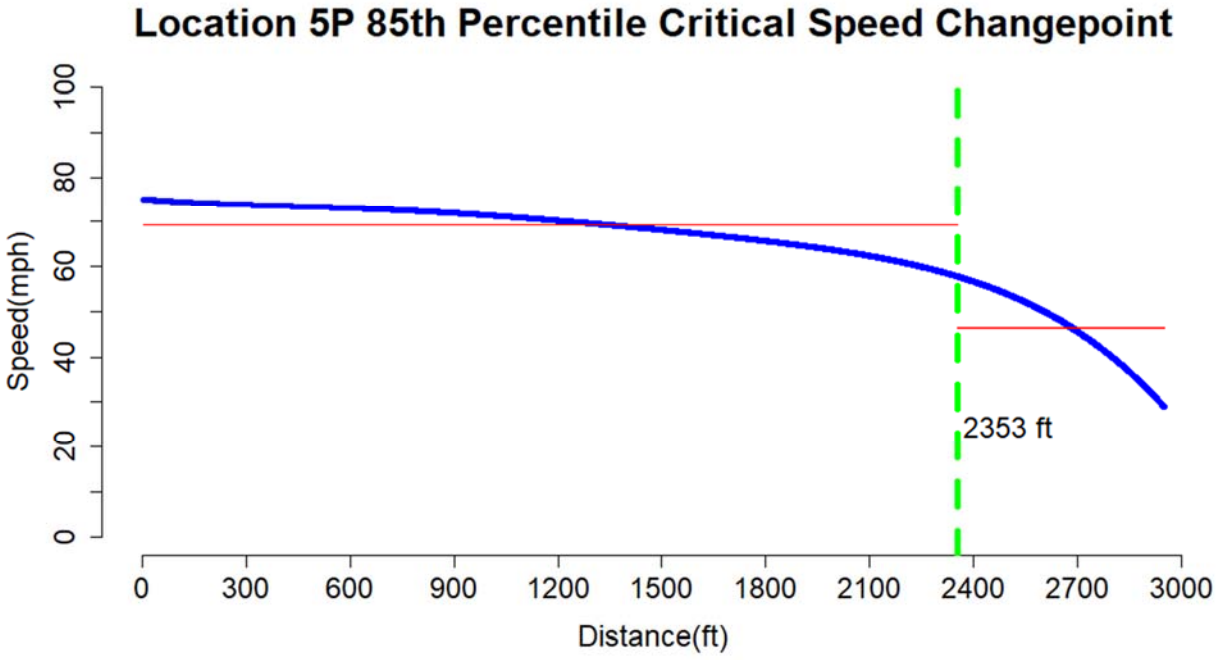

(*a*)

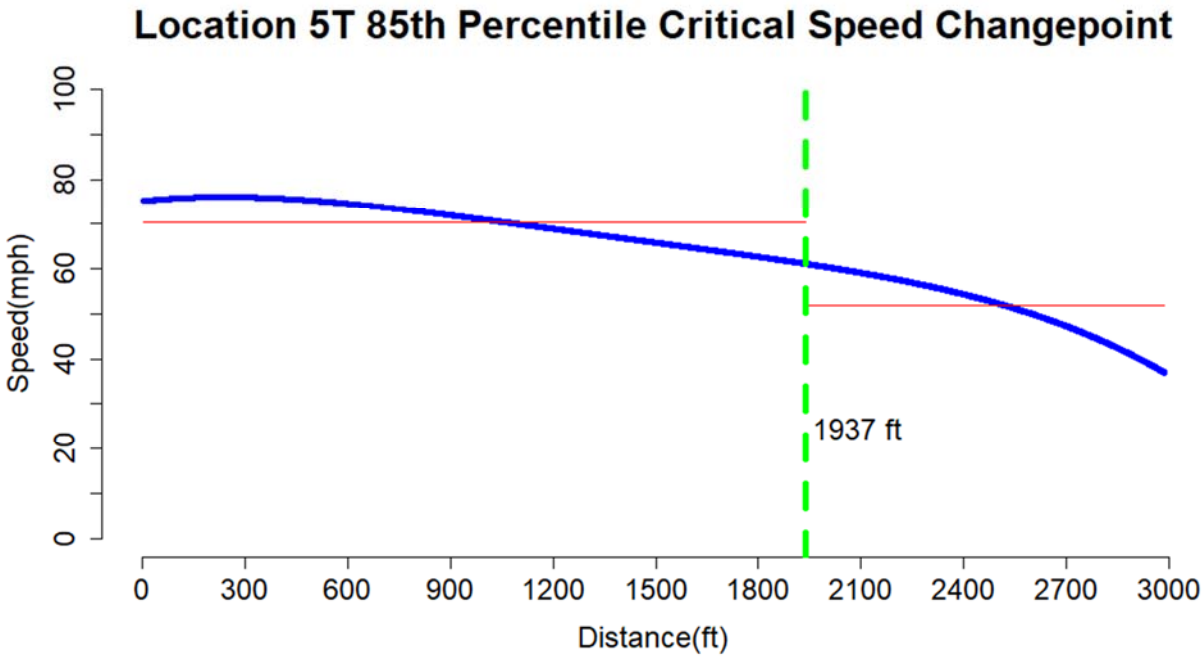

(*b*)

Figure C- 5 Critical speed changepoint: (*a*) Location 5P; and (*b*) Location 5T.

Table C- 1 Critical speed change point summary.

Site	Change Point (ft)			
	Distance from Taper		Distance from Terminal	
	85th	Mean	85th	Mean
Location 1P	1841	1889	469	421
Location 1T	1666	1685	764	745
Location 2P	1397	1423	523	497
Location 2T	1380	1309	490	561
Location 3P	1389	1305	581	665
Location 3T	1576	1615	534	495
Location 4P	1548	1541	532	539
Location 4T	1842	1817	398	423
Location 5P	2353	2364	597	586
Location 5T	1937	1948	1048	1037
Parallel-Design	1421	1420	450	451
Tapered-Design	1400	1396	539	544

Appendix D: Freeway Work Zone Gap and Headway Distribution

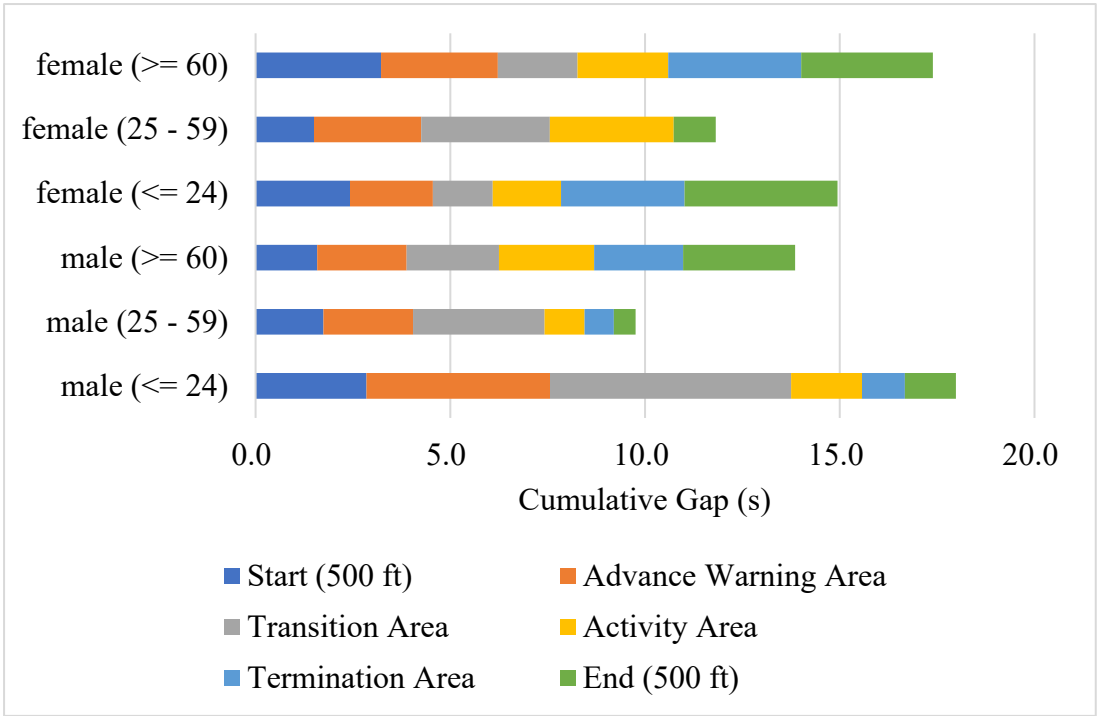

(a)

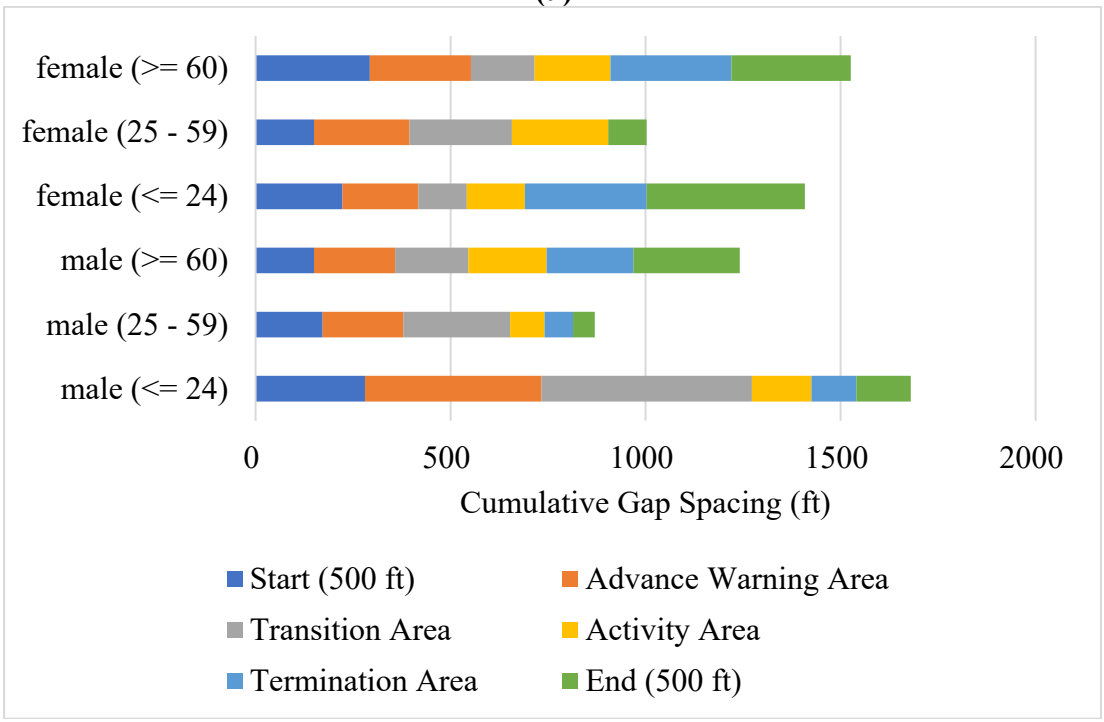

(b)

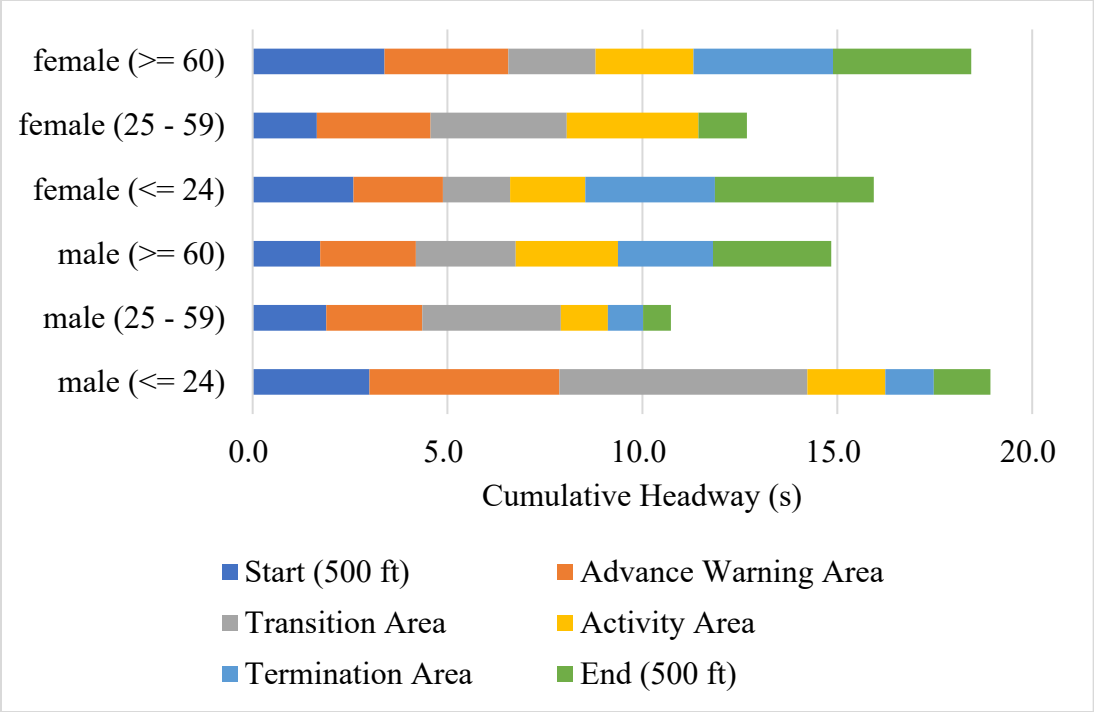

(*c*)

Figure D- 1 Gap and headway profile by driver types at LC 2-1:

(*a*) gap; (*b*) gap spacing; and (*c*) headway.

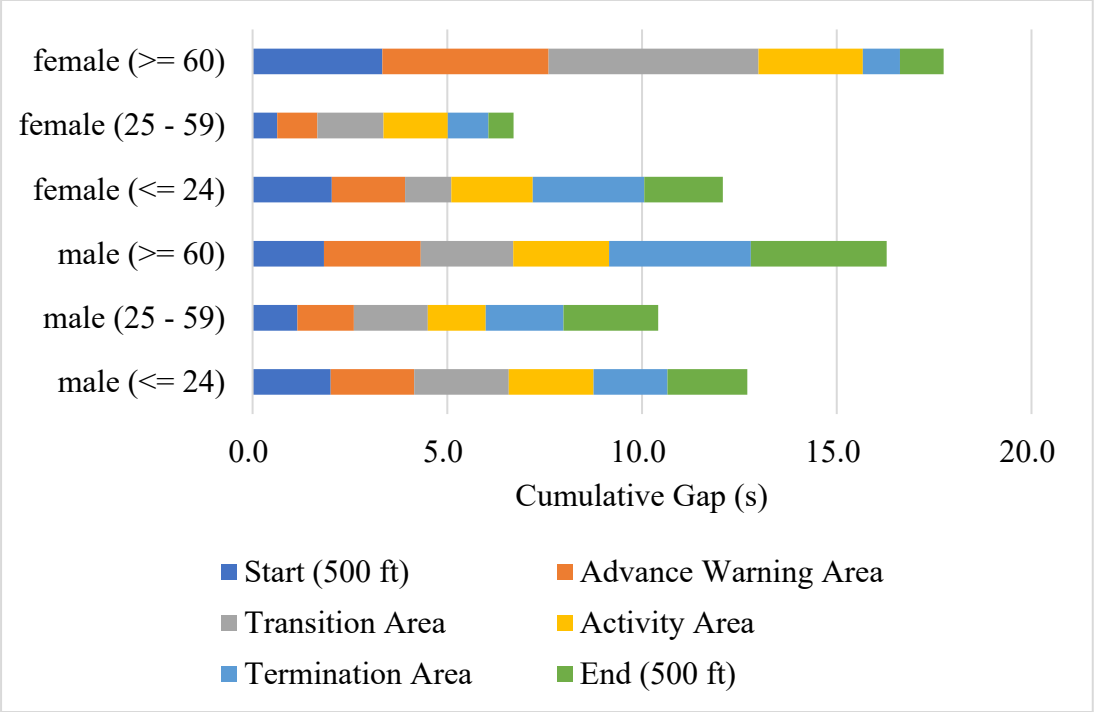
female (>= 60)
female (25 - 59)
female (<= 24)
male (>= 60)
male (25 - 59)
male (<= 24)
0.0
5.0
10.0
15.0
20.0
Cumulative Gap (s)
Start (500 ft)
Advance Warning Area
Transition Area
Activity Area
Termination Area
End (500 ft)

(a)

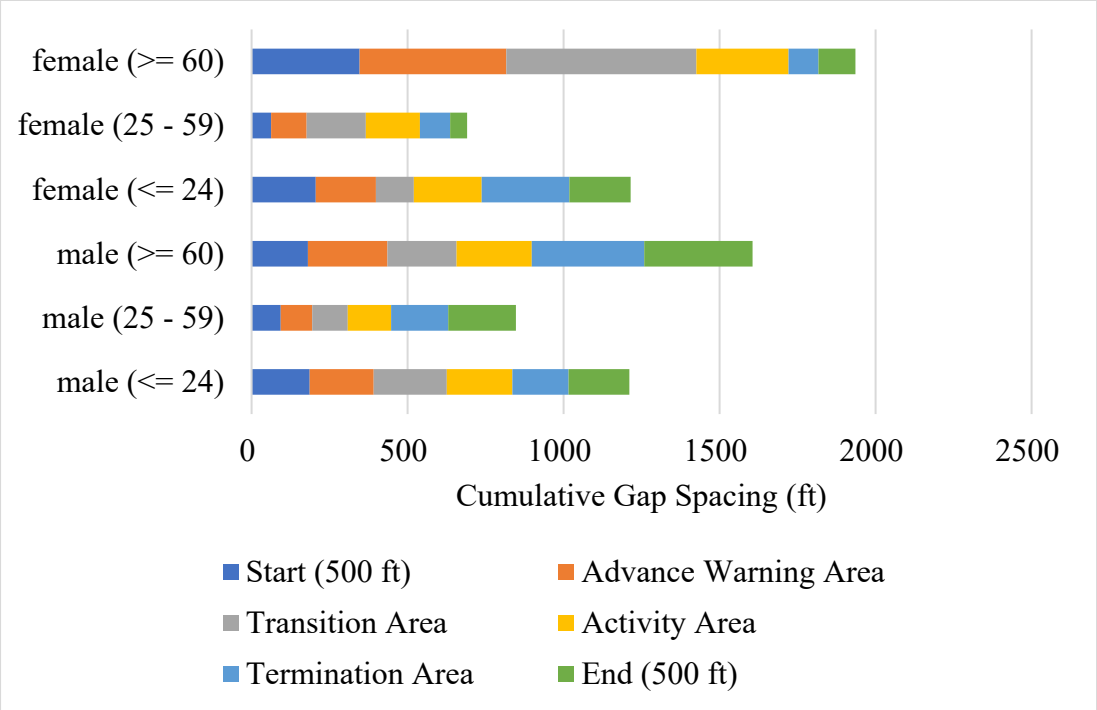
female (>= 60)
female (25 - 59)
female (<= 24)
male (>= 60)
male (25 - 59)
male (<= 24)
0
500
1000
1500
2000
2500
Cumulative Gap Spacing (ft)
Start (500 ft)
Advance Warning Area
Transition Area
Activity Area
Termination Area
End (500 ft)

(b)

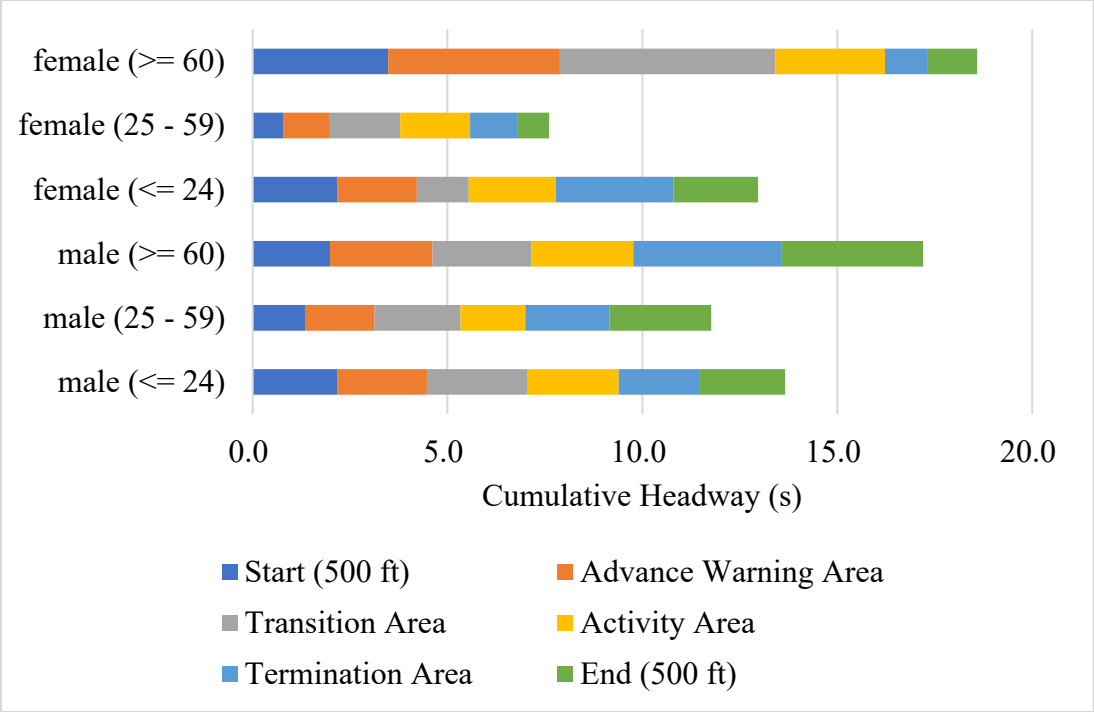

(*c*)

Figure D- 2 Gap and headway profile by driver types at LC 3-2:

(*a*) gap; (*b*) gap spacing; and (*c*) headway.

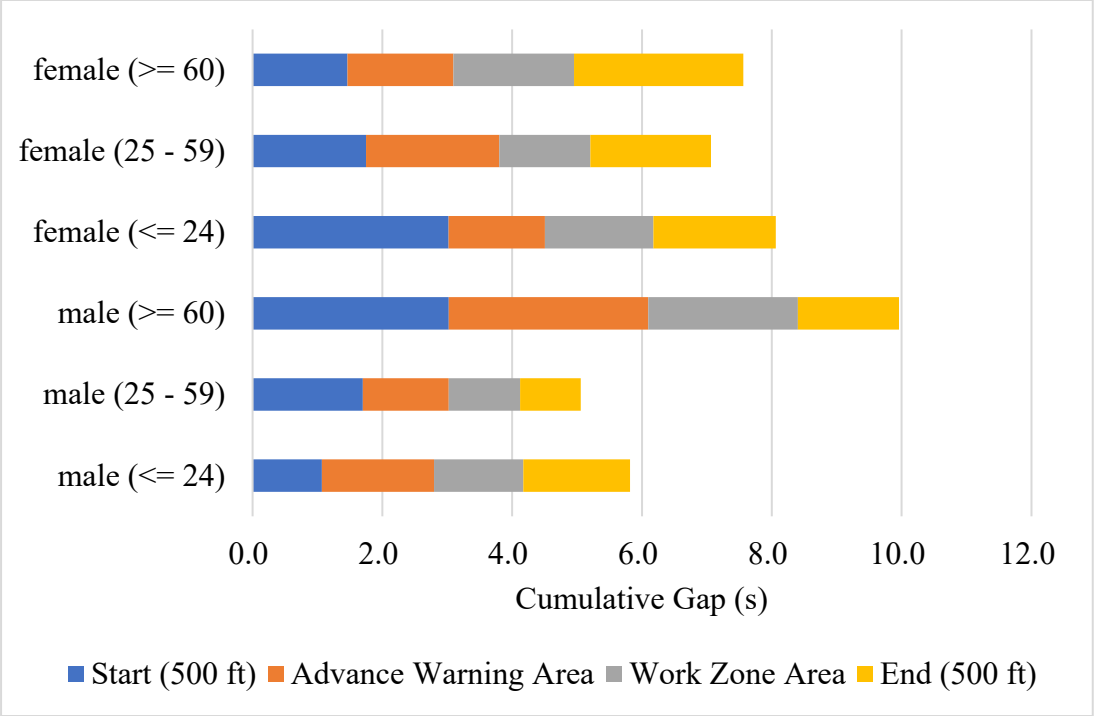
female (>= 60)
female (25 - 59)
female (<= 24)
male (>= 60)
male (25 - 59)
male (<= 24)
0.0
2.0
4.0
6.0
8.0
10.0
12.0
Cumulative Gap (s)
Start (500 ft)
Advance Warning Area
Work Zone Area
End (500 ft)

(a)

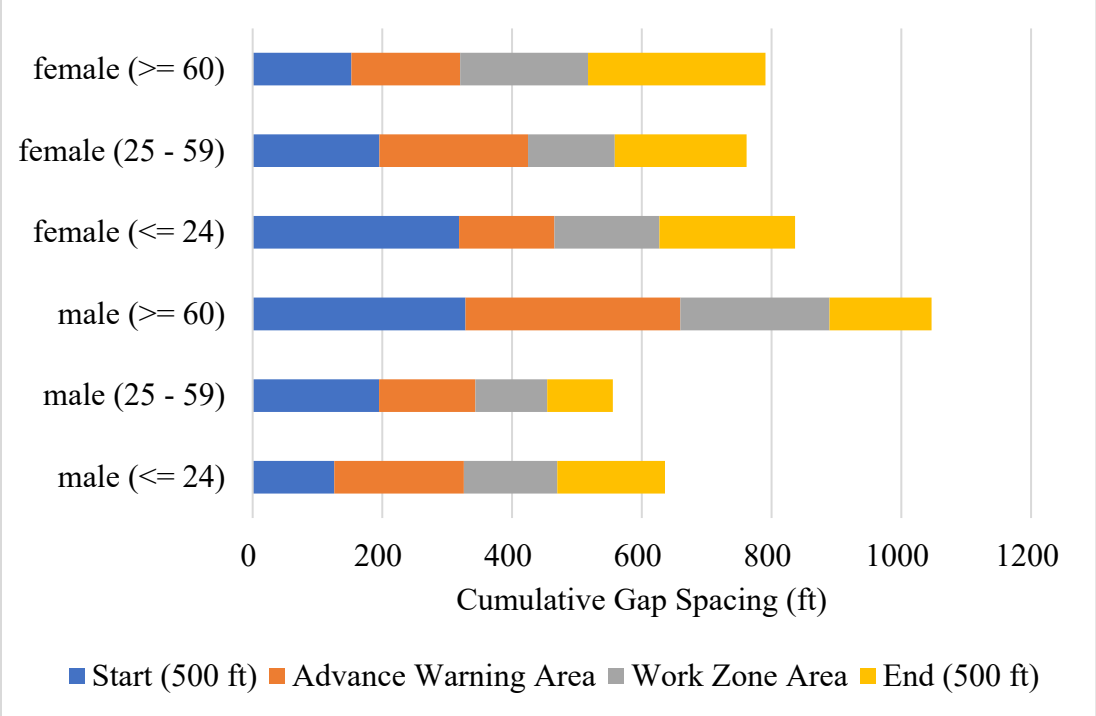
female (>= 60)
female (25 - 59)
female (<= 24)
male (>= 60)
male (25 - 59)
male (<= 24)
0
200
400
600
800
1000
1200
Cumulative Gap Spacing (ft)
Start (500 ft)
Advance Warning Area
Work Zone Area
End (500 ft)

(b)

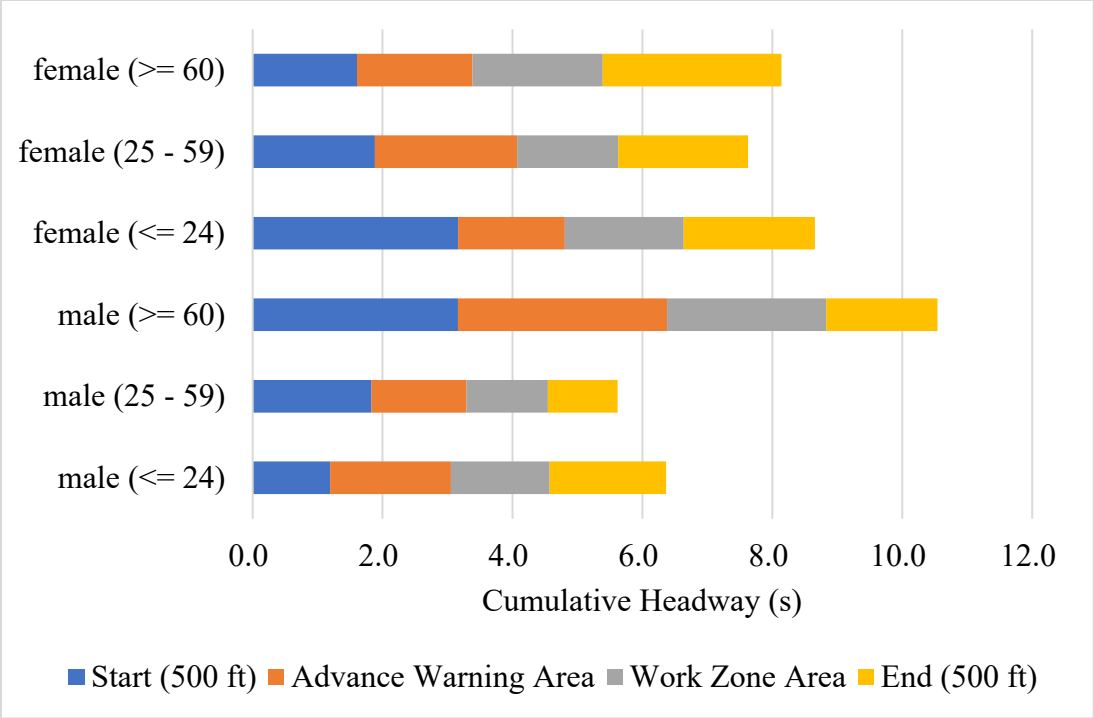

(*c*)

Figure D- 3 Gap and headway profile by driver types at SC 2-2:

(*a*) gap; (*b*) gap spacing; and (*c*) headway.

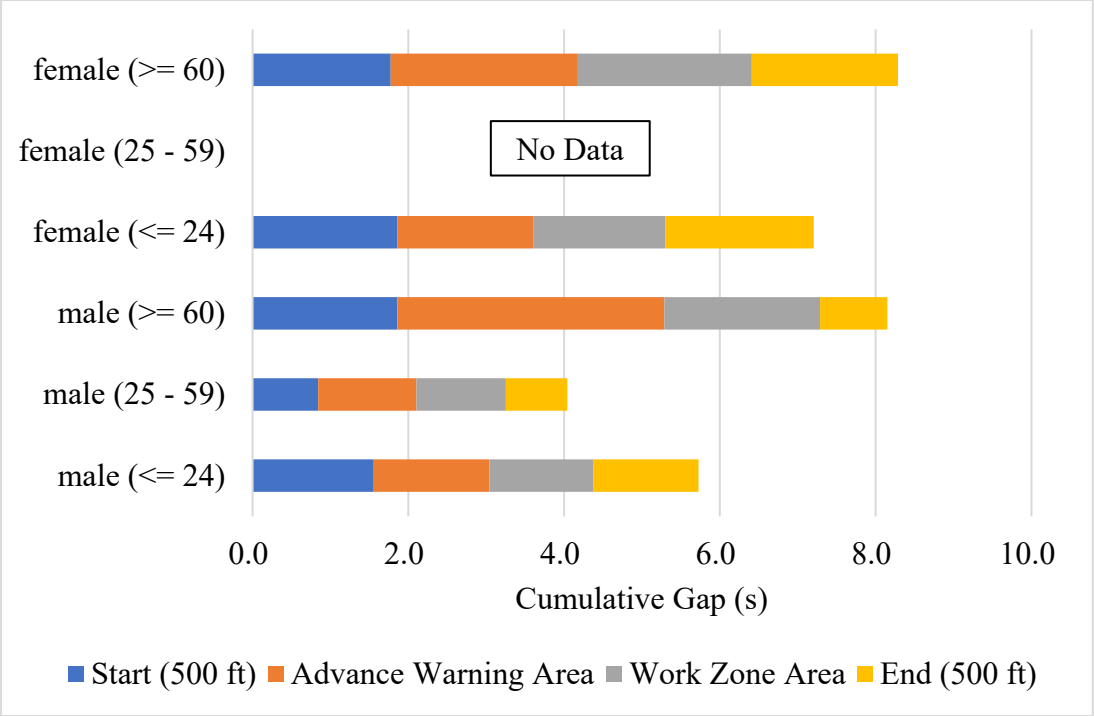
female (>= 60)
female (25 - 59)
female (<= 24)
male (>= 60)
male (25 - 59)
male (<= 24)
No Data
0.0
2.0
4.0
6.0
8.0
10.0
Cumulative Gap (s)
Start (500 ft)
Advance Warning Area
Work Zone Area
End (500 ft)

(a)

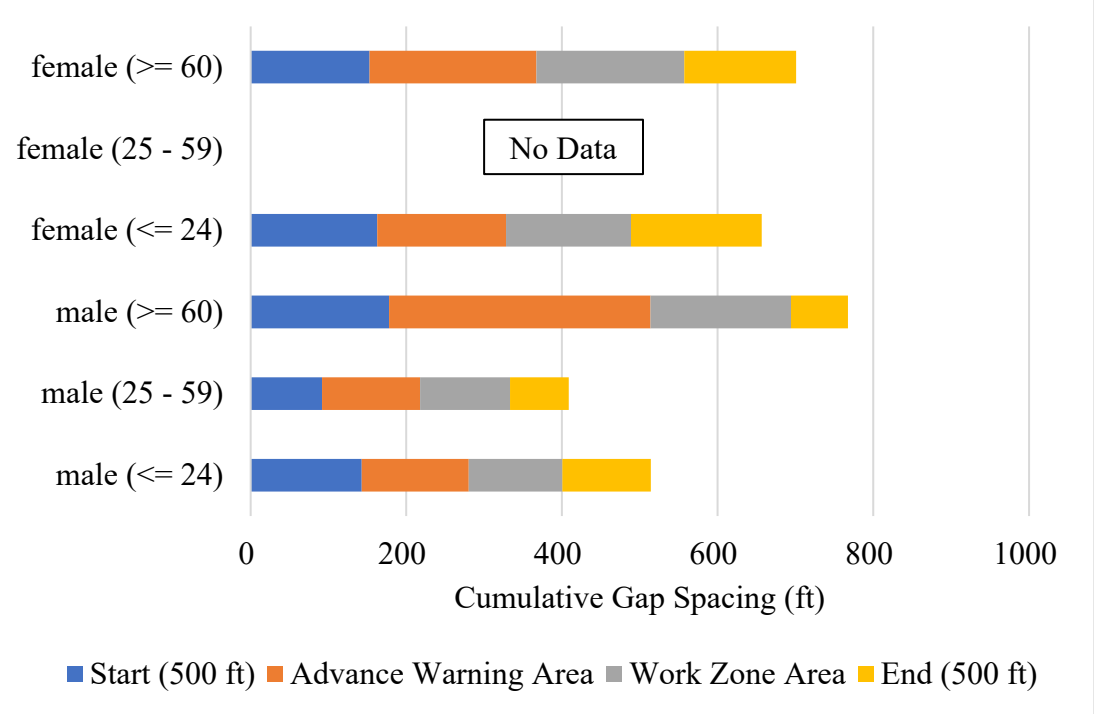
female (>= 60)
female (25 - 59)
female (<= 24)
male (>= 60)
male (25 - 59)
male (<= 24)
No Data
0
200
400
600
800
1000
Cumulative Gap Spacing (ft)
Start (500 ft)
Advance Warning Area
Work Zone Area
End (500 ft)

(b)

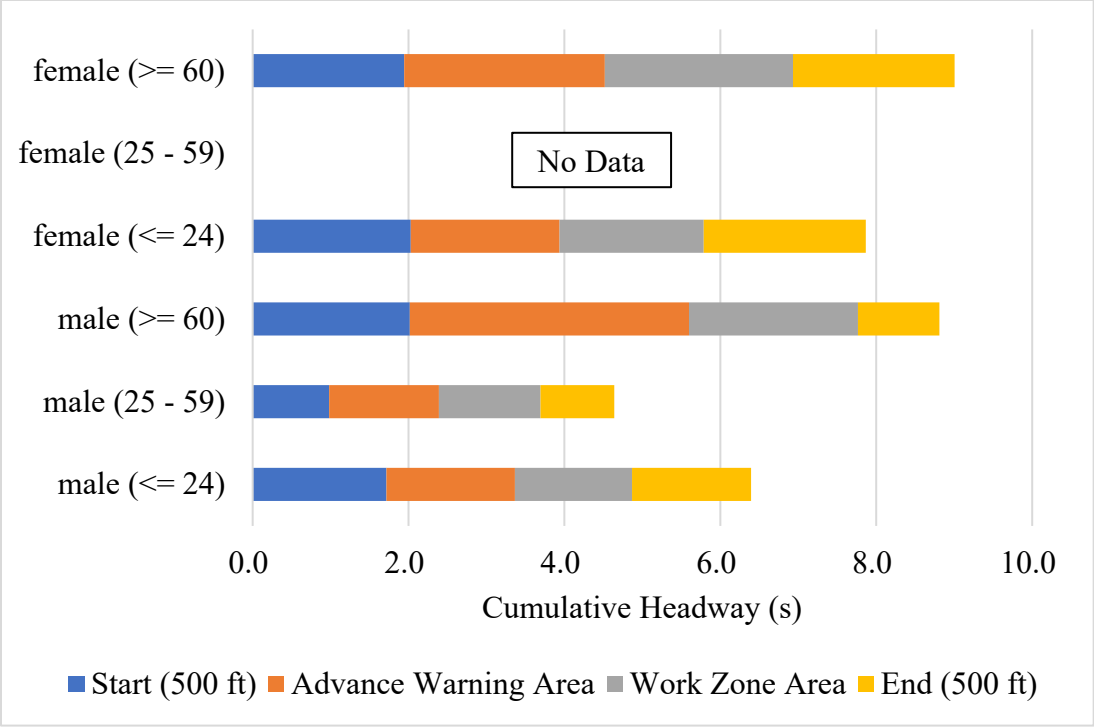

(*c*)

Figure D- 4 Gap and headway profile by driver types at SC 3-3:

(*a*) gap; (*b*) gap spacing; and (*c*) headway.

Appendix E: Freeway Work Zone Gap and Headway Selection Table

Table E- 1 Gap and headway selection table by driver characteristics at LC 2-1.

	Gender	Age	Mean Gap (s)	95% CI of Gap (s)	Mean Gap Spacing (ft)	95% CI of Gap Spacing (ft)	Mean Headway (s)	95% CI of Headway (s)	Mean Risk Score
Start (500 ft)	Female	Subtotal	2.7	(1.3, 4.2)	251	(121, 380)	2.9	(1.4, 4.3)	176
		≤ 24	2.4	(2.3, 2.5)	223	(218, 228)	2.6	(2.5, 2.7)	142
		25 - 59	1.5	(1.2, 1.8)	150	(120, 180)	1.6	(1.3, 2.0)	161
		≥ 60	3.2	(1.7, 4.7)	293	(155, 431)	3.4	(1.9, 4.9)	186
	Male	Subtotal	1.9	(0.8, 2.9)	181	(81, 281)	2.0	(0.9, 3.1)	191
		≤ 24	2.8	(2.0, 3.7)	281	(191, 371)	3.0	(2.1, 3.9)	146
		25 - 59	1.7	(1.0, 2.5)	172	(99, 244)	1.9	(1.1, 2.7)	190
		≥ 60	1.6	(0.5, 2.6)	150	(58, 241)	1.7	(0.7, 2.8)	208
	Grand Total		2.4	(1.0, 3.8)	225	(101, 349)	2.6	(1.2, 3.9)	182
	Gender	Age	Mean Gap (s)	95% CI of Gap (s)	Mean Gap Spacing (ft)	95% CI of Gap Spacing (ft)	Mean Headway (s)	95% CI of Headway (s)	Mean Risk Score
Advance Warning Area	Female	Subtotal	2.9	(1.5, 4.2)	249	(125, 374)	3.0	(1.6, 4.4)	174
		≤ 24	2.1	(1.7, 2.5)	194	(149, 240)	2.3	(1.9, 2.7)	142
		25 - 59	2.8	(1.7, 2.5)	245	(126, 364)	2.9	(1.4, 4.4)	167
		≥ 60	3.0	(1.6, 4.4)	259	(128, 391)	3.2	(1.8, 4.6)	182
	Male	Subtotal	2.6	(1.3, 4.2)	240	(94, 386)	2.8	(1.2, 4.4)	185

		≤ 24	4.7	(3.6, 5.8)	453	(356, 549)	4.9	(3.8, 6.0)	146
		25 - 59	2.3	(0.7, 3.9)	207	(72, 342)	2.5	(0.8, 4.1)	167
		≥ 60	2.3	(1.0, 3.6)	208	(93, 323)	2.5	(1.2, 3.7)	207
	Grand Total		2.8	(1.3, 4.2)	246	(114, 378)	2.9	(1.5, 4.4)	178
Transition Area	Gender	Age	Mean Gap (s)	95% CI of Gap (s)	Mean Gap Spacing (ft)	95% CI of Gap Spacing (ft)	Mean Headway (s)	95% CI of Headway (s)	Mean Risk Score
	Female	Subtotal	2.4	(1.1, 3.7)	190	(88, 292)	2.6	(1.3, 3.9)	170
		≤ 24	1.5	(1.5, 1.6)	124	(122, 127)	1.7	(1.7, 1.8)	142
		25 - 59	3.3	(1.4, 5.2)	262	(112, 412)	3.5	(1.6, 5.4)	165
		≥ 60	2.0	(1.5, 2.6)	163	(120, 206)	2.2	(1.7, 2.8)	177
	Male	Subtotal	3.1	(0.8, 5.4)	253	(60, 445)	3.3	(1.0, 5.6)	192
		≤ 24	6.2	(5.9, 6.5)	539	(513, 566)	6.4	(6.1, 6.7)	146
		25 - 59	3.4	(0.8, 6.8)	273	(68, 542)	3.6	(0.9, 7.0)	174
		≥ 60	2.4	(1.0, 3.8)	188	(77, 299)	2.6	(1.1, 4.0)	207
	Grand Total		2.7	(0.9, 4.4)	213	(68, 359)	2.8	(1.1, 4.6)	179
Activity Area	Gender	Age	Mean Gap (s)	95% CI of Gap (s)	Mean Gap Spacing (ft)	95% CI of Gap Spacing (ft)	Mean Headway (s)	95% CI of Headway (s)	Mean Risk Score
	Female	Subtotal	2.4	(1.0, 3.9)	200	(79, 322)	2.6	(1.2, 4.1)	174
		≤ 24	1.8	(0.6, 3.4)	149	(53, 297)	1.9	(0.8, 3.6)	142
		25 - 59	3.2	(0.8, 5.5)	247	(62, 432)	3.4	(1.0, 5.7)	163
		≥ 60	2.3	(1.4, 3.3)	195	(107, 282)	2.5	(1.5, 3.5)	181

	Male	Subtotal	2.1	(0.6, 3.6)	174	(54, 294)	2.3	(0.8, 3.8)	196
		≤ 24	1.8	(0.5, 3.2)	152	(37, 268)	2.0	(0.6, 3.4)	146
		25 - 59	1.0	(0.8, 1.2)	88	(69, 108)	1.2	(1.0, 1.4)	202
		≥ 60	2.4	(0.9, 4.0)	201	(77, 325)	2.6	(1.1, 4.2)	207
	Grand Total		2.3	(0.8, 3.8)	191	(70, 313)	2.5	(1.0, 4.0)	181
Termination Area	Gender	Age	Mean Gap (s)	95% CI of Gap (s)	Mean Gap Spacing (ft)	95% CI of Gap Spacing (ft)	Mean Headway (s)	95% CI of Headway (s)	Mean Risk Score
	Female	Subtotal	3.4	(1.8, 5.0)	310	(162, 459)	3.5	(1.9, 5.1)	177
		≤ 24	3.2	(2, 4.40)	313	(196, 429)	3.3	(2.1, 4.5)	141
		25 - 59	NA	NA	NA	NA	NA	NA	NA
		≥ 60	3.4	(1.8, 5.1)	310	(158, 462)	3.6	(1.9, 5.2)	182
	Male	Subtotal	1.7	(0.4, 3.1)	163	(31, 297)	1.8	(0.5, 3.3)	191
		≤ 24	1.1	(1.0, 1.2)	115	(105, 126)	1.2	(1.2, 1.3)	146
		25 - 59	0.8	(0.4, 1.2)	73	(30, 119)	0.9	(0.5, 1.4)	202
		≥ 60	2.3	(0.5, 4.0)	222	(65, 379)	2.4	(0.7, 4.2)	204
	Grand Total		2.8	(1.1, 4.6)	262	(103, 422)	3.0	(1.2, 4.7)	181
End (500 ft)	Gender	Age	Mean Gap (s)	95% CI of Gap (s)	Mean Gap Spacing (ft)	95% CI of Gap Spacing (ft)	Mean Headway (s)	95% CI of Headway (s)	Mean Risk Score
	Female	Subtotal	2.9	(1.2, 4.6)	267	(108, 425)	3.1	(1.4, 4.8)	181
		≤ 24	3.9	(3.9, 4.0)	405	(403, 408)	4.1	(4.0, 4.1)	141
		25 - 59	1.1	(0.9, 1.2)	99	(81, 116)	1.2	(1.1, 1.4)	171

		≥ 60	3.4	(1.7, 5.0)	306	(154, 458)	3.5	(1.9, 5.2)	186
	Male	Subtotal	2.1	(0.5, 3.9)	198	(49, 364)	2.2	(0.6, 4.1)	191
		≤ 24	1.3	(1.3, 1.3)	139	(135, 144)	1.4	(1.4, 1.5)	146
		25 - 59	0.6	(0.5, 0.6)	56	(52, 60)	0.7	(0.7, 0.7)	202
		≥ 60	2.9	(0.8, 5.0)	273	(91, 455)	3.0	(0.9, 5.1)	203
	Grand Total		2.6	(0.8, 4.4)	242	(78, 407)	2.8	(1.0, 4.6)	185

Table E- 2 Gap and headway selection table by driver characteristics at LC 3-2.

	Gender	Age	Mean Gap (s)	95% CI of Gap (s)	Mean Gap Spacing (ft)	95% CI of Gap Spacing (ft)	Mean Headway (s)	95% CI of Headway (s)	Mean Risk Score
Start (500 ft)	Female	Subtotal	2.3	(1.0, 3.5)	230	(96, 364)	2.4	(1.1, 3.7)	170
		≤ 24	2.0	(0.9, 3.2)	206	(84, 328)	2.2	(1.0, 3.4)	150
		25 - 59	0.6	(0.6, 0.6)	62	(62, 63)	0.8	(0.8, 0.8)	196
		≥ 60	3.3	(2.7, 3.9)	346	(272, 420)	3.5	(2.9, 4.1)	203
	Male	Subtotal	1.7	(1.0, 2.3)	150	(78, 221)	1.8	(1.2, 2.5)	148
		≤ 24	2.0	(1.3, 2.7)	186	(115, 258)	2.2	(1.5, 2.9)	152
		25 - 59	1.2	(0.9, 1.4)	94	(59, 128)	1.3	(1.1, 1.6)	165
		≥ 60	1.8	(1.8, 1.9)	180	(177, 184)	2.0	(1.9, 2.0)	192
	Grand Total		1.8	(0.9, 2.7)	172	(72, 271)	2.0	(1.1, 2.9)	154
	Gender	Age	Mean Gap (s)	95% CI of Gap (s)	Mean Gap Spacing (ft)	95% CI of Gap Spacing (ft)	Mean Headway (s)	95% CI of Headway (s)	Mean Risk Score
Advance Warning Area	Female	Subtotal	1.8	(0.5, 3.2)	192	(51, 332)	2.0	(0.6, 3.4)	172
		≤ 24	1.9	(0.6, 3.2)	192	(63, 322)	2.0	(0.7, 3.4)	163
		25 - 59	1.0	(0.2, 1.8)	114	(23, 205)	1.2	(0.4, 2.0)	196
		≥ 60	4.3	(3.9, 4.6)	470	(413, 527)	4.4	(4.0, 4.8)	203
	Male	Subtotal	1.9	(1.0, 2.8)	165	(60, 270)	2.1	(1.2, 3.0)	152
		≤ 24	2.1	(1.3, 3.0)	205	(117, 293)	2.3	(1.4, 3.2)	153
		25 - 59	1.5	(0.7, 2.2)	101	(17, 190)	1.8	(0.9, 2.7)	165

		≥ 60	2.5	(1.8, 3.1)	255	(191, 319)	2.6	(2.0, 3.3)	104
	Grand Total		1.9	(0.8, 2.9)	173	(56, 289)	2.1	(1.0, 3.1)	158
Transition Area	Gender	Age	Mean Gap (s)	95% CI of Gap (s)	Mean Gap Spacing (ft)	95% CI of Gap Spacing (ft)	Mean Headway (s)	95% CI of Headway (s)	Mean Risk Score
	Female	Subtotal	1.4	(0.3, 2.6)	152	(25, 280)	1.6	(0.4, 2.7)	164
		≤ 24	1.2	(0.4, 2.0)	122	(37, 206)	1.3	(0.5, 2.2)	156
		25 - 59	1.7	(1.0, 2.4)	190	(127, 253)	1.8	(1.1, 2.5)	196
		≥ 60	5.4	(5.4, 5.4)	609	(606, 612)	5.5	(5.5, 5.6)	203
	Male	Subtotal	2.2	(0.2, 4.2)	174	(49, 300)	2.4	(0.4, 4.4)	162
		≤ 24	2.4	(1.4, 3.5)	235	(130, 340)	2.6	(1.5, 3.6)	147
		25 - 59	1.9	(0.5, 4.5)	114	(13, 225)	2.2	(0.6, 4.9)	170
		≥ 60	2.4	(0.9, 3.8)	221	(88, 355)	2.5	(1.1, 4.0)	190
	Grand Total		1.9	(0.3, 3.7)	166	(39, 293)	2.1	(0.5, 3.9)	163
Activity Area	Gender	Age	Mean Gap (s)	95% CI of Gap (s)	Mean Gap Spacing (ft)	95% CI of Gap Spacing (ft)	Mean Headway (s)	95% CI of Headway (s)	Mean Risk Score
	Female	Subtotal	2.0	(0.7, 3.4)	212	(73, 351)	2.2	(0.8, 3.5)	169
		≤ 24	2.1	(0.7, 3.5)	217	(73, 361)	2.2	(0.8, 3.6)	158
		25 - 59	1.7	(0.7, 2.6)	173	(75, 272)	1.8	(0.9, 2.7)	193
		≥ 60	2.7	(1.2, 4.2)	295	(130, 461)	2.8	(1.3, 4.3)	203
	Male	Subtotal	1.9	(0.8, 3.0)	181	(66, 295)	2.1	(0.9, 3.2)	154
		≤ 24	2.2	(1.1, 3.3)	210	(100, 321)	2.3	(1.3, 3.4)	140

		25 - 59	1.5	(0.5, 2.5)	139	(34, 244)	1.7	(0.6, 2.7)	167
		≥ 60	2.5	(1.4, 3.5)	241	(135, 347)	2.6	(1.6, 3.6)	156
	Grand Total		1.9	(0.7, 3.1)	190	(67, 314)	2.1	(0.9, 3.3)	159
Termination Area	Gender	Age	Mean Gap (s)	95% CI of Gap (s)	Mean Gap Spacing (ft)	95% CI of Gap Spacing (ft)	Mean Headway (s)	95% CI of Headway (s)	Mean Risk Score
	Female	Subtotal	1.6	(0.7, 2.6)	161	(63, 259)	1.8	(0.8, 2.8)	184
		≤ 24	2.9	(2.4, 3.3)	281	(228, 333)	3.0	(2.6, 3.5)	158
		25 - 59	1.0	(0.5, 1.5)	97	(52, 142)	1.2	(0.7, 1.7)	191
		≥ 60	1.0	(0.6, 1.3)	96	(65, 127)	1.1	(0.8, 1.4)	203
	Male	Subtotal	2.0	(0.8, 3.3)	190	(69, 312)	2.2	(0.9, 3.4)	141
		≤ 24	1.9	(0.8, 3.0)	180	(63, 296)	2.1	(1.0, 3.2)	138
		25 - 59	2.0	(0.6, 3.4)	183	(63, 304)	2.2	(0.8, 3.5)	164
		≥ 60	3.6	(3.6, 3.7)	360	(356, 365)	3.8	(3.7, 3.8)	192
	Grand Total		1.9	(0.7, 3.1)	183	(66, 299)	2.1	(0.9, 3.3)	160
End (500 ft)	Gender	Age	Mean Gap (s)	95% CI of Gap (s)	Mean Gap Spacing (ft)	95% CI of Gap Spacing (ft)	Mean Headway (s)	95% CI of Headway (s)	Mean Risk Score
	Female	Subtotal	1.5	(0.9, 2.1)	151	(96, 206)	1.7	(1.1, 2.3)	180
		≤ 24	2.0	(1.6, 2.5)	196	(155, 237)	2.2	(1.7, 2.6)	154
		25 - 59	0.6	(0.6, 0.7)	54	(53, 56)	0.8	(0.8, 0.8)	179
		≥ 60	1.1	(0.8, 1.4)	119	(90, 147)	1.3	(1.0, 1.6)	203
	Male	Subtotal	2.2	(0.9, 3.5)	205	(74, 336)	2.4	(1.1, 3.7)	154

		≤ 24	2.1	(0.7, 3.4)	195	(62, 328)	2.2	(0.9, 3.6)	146
		25 - 59	2.4	(1.2, 3.7)	217	(90, 343)	2.6	(1.4, 3.9)	164
		≥ 60	3.5	(3.4, 3.6)	347	(341, 353)	3.6	(3.6, 3.7)	192
	Grand Total		2.0	(0.8, 3.2)	188	(73, 303)	2.1	(1.0, 3.3)	162

Table E- 3 Gap and headway selection table by driver characteristics at SC 2-2.

	Gender	Age	Mean Gap (s)	95% CI of Gap (s)	Mean Gap Spacing (ft)	95% CI of Gap Spacing (ft)	Mean Headway (s)	95% CI of Headway (s)	Mean Risk Score
Start (500 ft)	Female	Subtotal	2.1	(0.7, 3.6)	226	(81, 371)	2.3	(0.9, 3.7)	177
		≤ 24	3.0	(1.2, 4.9)	318	(132, 505)	3.2	(1.3, 5.0)	154
		25 - 59	1.7	(1.6, 1.9)	196	(183, 208)	1.9	(1.8, 2.0)	192
		≥ 60	1.5	(1.2, 1.7)	152	(121, 184)	1.6	(1.3, 1.9)	193
	Male	Subtotal	2.0	(0.8, 3.1)	222	(91, 352)	2.1	(0.9, 3.3)	185
		≤ 24	1.1	(1.0, 1.1)	126	(121, 131)	1.2	(1.2, 1.2)	191
		25 - 59	1.7	(0.7, 3.0)	195	(76, 349)	1.8	(0.8, 3.1)	201
		≥ 60	3.0	(2.9, 3.2)	328	(300, 357)	3.2	(3.0, 3.3)	156
	Grand Total		2.1	(0.7, 3.4)	225	(84, 365)	2.2	(0.9, 3.6)	179
	Gender	Age	Mean Gap (s)	95% CI of Gap (s)	Mean Gap Spacing (ft)	95% CI of Gap Spacing (ft)	Mean Headway (s)	95% CI of Headway (s)	Mean Risk Score
Advance Warning Area	Female	Subtotal	1.6	(0.9, 2.3)	166	(89, 242)	1.8	(1.1, 2.4)	181
		≤ 24	1.5	(0.8, 2.2)	147	(65, 229)	1.6	(0.9, 2.4)	158
		25 - 59	2.1	(1.2, 2.9)	229	(136, 322)	2.2	(1.4, 3.0)	192
		≥ 60	1.6	(1.0, 2.2)	168	(102, 233)	1.8	(1.2, 2.4)	192
	Male	Subtotal	1.8	(0.5, 3.1)	200	(59, 342)	1.9	(0.7, 3.2)	194
		≤ 24	1.7	(0.9, 2.6)	200	(107, 292)	1.9	(1.0, 2.7)	188
		25 - 59	1.3	(0.5, 2.2)	149	(41, 256)	1.5	(0.6, 2.4)	201

		≥ 60	3.1	(1.4, 4.8)	331	(140, 522)	3.2	(1.5, 4.9)	188
	Grand Total		1.7	(0.7, 2.6)	179	(71, 288)	1.8	(0.9, 2.8)	186
Work Zone Area	Gender	Age	Mean Gap (s)	95% CI of Gap (s)	Mean Gap Spacing (ft)	95% CI of Gap Spacing (ft)	Mean Headway (s)	95% CI of Headway (s)	Mean Risk Score
	Female	Subtotal	1.8	(0.7, 2.8)	183	(72, 294)	1.9	(0.9, 3.0)	181
		≤ 24	1.7	(0.5, 2.8)	162	(44, 280)	1.8	(0.7, 3.0)	158
		25 - 59	1.4	(0.7, 2.1)	134	(71, 196)	1.6	(0.8, 2.3)	192
		≥ 60	1.9	(0.8, 2.9)	197	(87, 307)	2.0	(1.0, 3.0)	192
	Male	Subtotal	1.4	(0.5, 2.3)	141	(43, 238)	1.5	(0.6, 2.5)	194
		≤ 24	1.4	(0.5, 2.3)	144	(41, 246)	1.5	(0.6, 2.4)	188
		25 - 59	1.1	(0.4, 1.8)	111	(34, 187)	1.3	(0.5, 2.0)	188
		≥ 60	2.3	(1.4, 3.2)	230	(140, 321)	2.5	(1.5, 3.4)	201
	Grand Total		1.6	(0.6, 2.6)	162	(55, 268)	1.7	(0.7, 2.7)	187
End (500 ft)	Gender	Age	Mean Gap (s)	95% CI of Gap (s)	Mean Gap Spacing (ft)	95% CI of Gap Spacing (ft)	Mean Headway (s)	95% CI of Headway (s)	Mean Risk Score
	Female	Subtotal	2.4	(1.5, 3.4)	255	(158, 352)	2.5	(1.6, 3.5)	181
		≤ 24	1.9	(1.4, 2.4)	209	(146, 272)	2.0	(1.5, 2.5)	158
		25 - 59	1.9	(1.8, 1.9)	203	(202, 204)	2.0	(1.9, 2.0)	192
		≥ 60	2.6	(1.6, 3.6)	274	(168, 379)	2.8	(1.7, 3.8)	192
	Male	Subtotal	1.2	(0.6, 1.9)	125	(64, 192)	1.3	(0.7, 2.0)	194
		≤ 24	1.6	(1.4, 1.8)	166	(155, 177)	1.8	(1.6, 2.0)	188

		25 - 59	0.9	(0.6, 1.4)	101	(64, 148)	1.1	(0.7, 1.5)	201
		≥ 60	1.6	(0.9, 2.8)	157	(86, 284)	1.7	(1.0, 2.9)	188
	Grand Total		1.7	(0.7, 2.8)	184	(79, 289)	1.9	(0.9, 2.9)	183

Table E- 4 Gap and headway selection table by driver characteristics at SC 3-3.

	Gender	Age	Mean Gap (s)	95% CI of Gap (s)	Mean Gap Spacing (ft)	95% CI of Gap Spacing (ft)	Mean Headway (s)	95% CI of Headway (s)	Mean Risk Score
Start (500 ft)	Female	Subtotal	1.8	(0.9, 2.8)	160	(73, 247)	2.0	(1.0, 3.0)	171
		≤ 24	1.9	(1.0, 2.8)	163	(83, 243)	2.0	(1.1, 2.9)	168
		25 - 59	NA	NA	NA	NA	NA	NA	NA
		≥ 60	1.8	(0.6, 3.0)	153	(48, 258)	1.9	(0.7, 3.1)	181
	Male	Subtotal	1.5	(0.7, 2.3)	143	(70, 216)	1.7	(0.9, 2.5)	162
		≤ 24	1.6	(0.7, 2.4)	143	(68, 218)	1.7	(0.9, 2.6)	153
		25 - 59	0.8	(0.5, 1.6)	92	(57, 176)	1.0	(0.6, 1.7)	166
		≥ 60	1.9	(1.8, 1.9)	178	(169, 187)	2.0	(1.9, 2.1)	189
	Grand Total		1.7	(0.8, 2.6)	153	(71, 235)	1.9	(0.9, 2.8)	167
	Gender	Age	Mean Gap (s)	95% CI of Gap (s)	Mean Gap Spacing (ft)	95% CI of Gap Spacing (ft)	Mean Headway (s)	95% CI of Headway (s)	Mean Risk Score
Advance Warning Area	Female	Subtotal	1.9	(0.7, 3.2)	179	(63, 296)	2.1	(0.9, 3.3)	174
		≤ 24	1.8	(0.6, 2.9)	166	(58, 273)	1.9	(0.8, 3.1)	170
		25 - 59	NA	NA	NA	NA	NA	NA	NA
		≥ 60	2.4	(1.1, 3.7)	215	(85, 345)	2.6	(1.2, 3.9)	184
	Male	Subtotal	1.6	(0.5, 2.8)	152	(44, 264)	1.8	(0.6, 2.9)	166
		≤ 24	1.5	(0.7, 2.3)	137	(68, 207)	1.6	(0.9, 2.4)	158
		25 - 59	1.3	(0.4, 2.7)	126	(44, 265)	1.4	(0.5, 2.8)	193

		≥ 60	3.4	(1.6, 5.3)	336	(187, 518)	3.6	(1.7, 5.4)	194
	Grand Total		1.8	(0.6, 3.1)	172	(56, 288)	2.0	(0.8, 3.2)	172
Work Zone Area	Gender	Age	Mean Gap (s)	95% CI of Gap (s)	Mean Gap Spacing (ft)	95% CI of Gap Spacing (ft)	Mean Headway (s)	95% CI of Headway (s)	Mean Risk Score
	Female	Subtotal	1.8	(0.6, 3.0)	167	(58, 276)	2.0	(0.8, 3.1)	173
		≤ 24	1.7	(0.5, 2.9)	160	(45, 276)	1.8	(0.7, 3.0)	168
		25 - 59	NA	NA	NA	NA	NA	NA	NA
		≥ 60	2.2	(1.4, 3.1)	190	(112, 268)	2.4	(1.5, 3.3)	191
	Male	Subtotal	1.4	(0.6, 2.2)	128	(55, 201)	1.6	(0.8, 2.3)	168
		≤ 24	1.3	(0.6, 2.0)	120	(55, 185)	1.5	(0.8, 2.2)	161
		25 - 59	1.2	(0.4, 1.9)	116	(40, 191)	1.3	(0.6, 2.0)	170
		≥ 60	2.0	(1.1, 2.9)	180	(95, 266)	2.2	(1.3, 3.1)	198
	Grand Total		1.7	(0.6, 2.7)	154	(54, 255)	1.8	(0.8, 2.9)	171
End (500 ft)	Gender	Age	Mean Gap (s)	95% CI of Gap (s)	Mean Gap Spacing (ft)	95% CI of Gap Spacing (ft)	Mean Headway (s)	95% CI of Headway (s)	Mean Risk Score
	Female	Subtotal	1.9	(1.0, 2.8)	166	(79, 253)	2.1	(1.2, 3.0)	175
		≤ 24	1.9	(1.0, 2.8)	168	(82, 254)	2.1	(1.2, 3.0)	173
		25 - 59	NA	NA	NA	NA	NA	NA	NA
		≥ 60	1.9	(0.7, 3.1)	144	(50, 237)	2.1	(0.9, 3.3)	198
	Male	Subtotal	1.1	(0.4, 1.8)	92	(35, 150)	1.2	(0.5, 1.9)	173
		≤ 24	1.3	(0.9, 1.8)	114	(77, 150)	1.5	(1.1, 2.0)	168

		25 - 59	0.8	(0.6, 0.9)	75	(58, 93)	0.9	(0.8, 1.1)	171
		≥ 60	0.9	(0.2, 1.9)	73	(16, 161)	1.0	(0.4, 2.1)	181
	Grand Total		1.6	(0.7, 2.6)	142	(56, 228)	1.8	(0.9, 2.8)	174

Appendix F: Freeway Work Zone Speed Profile by Driver Types

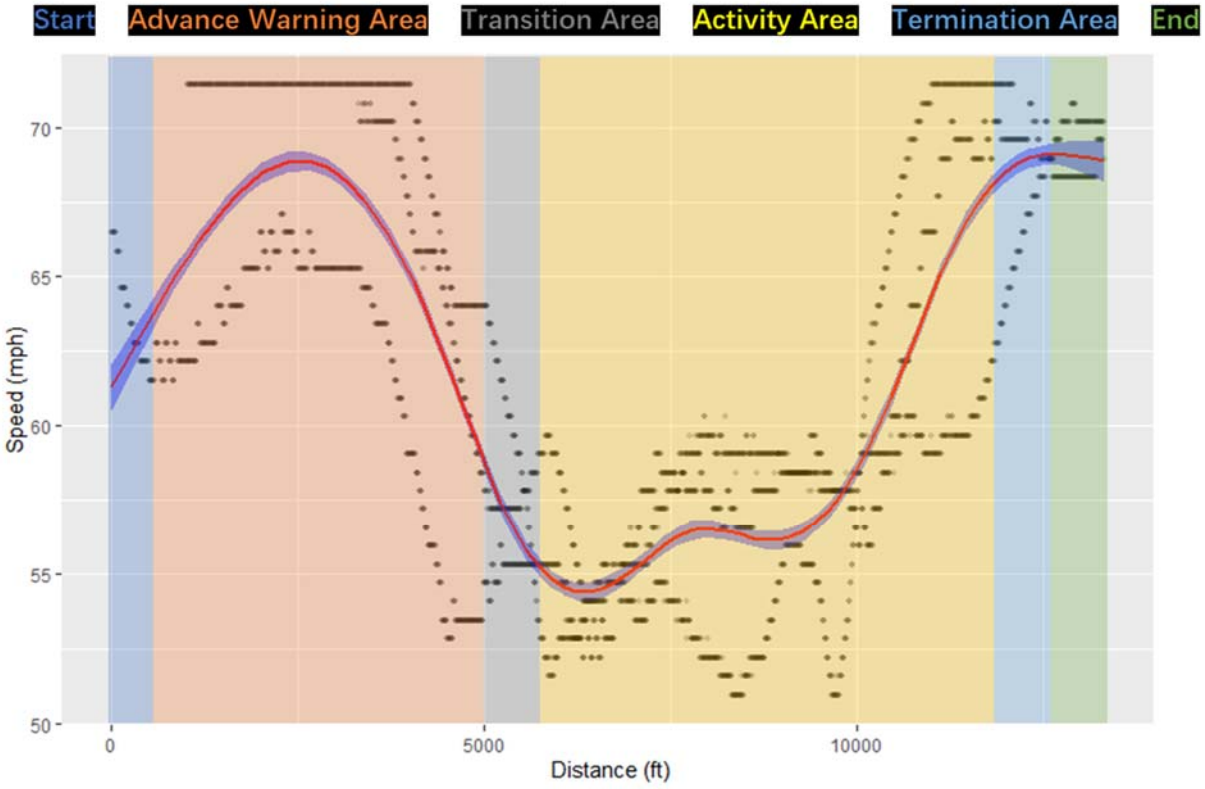

(a)

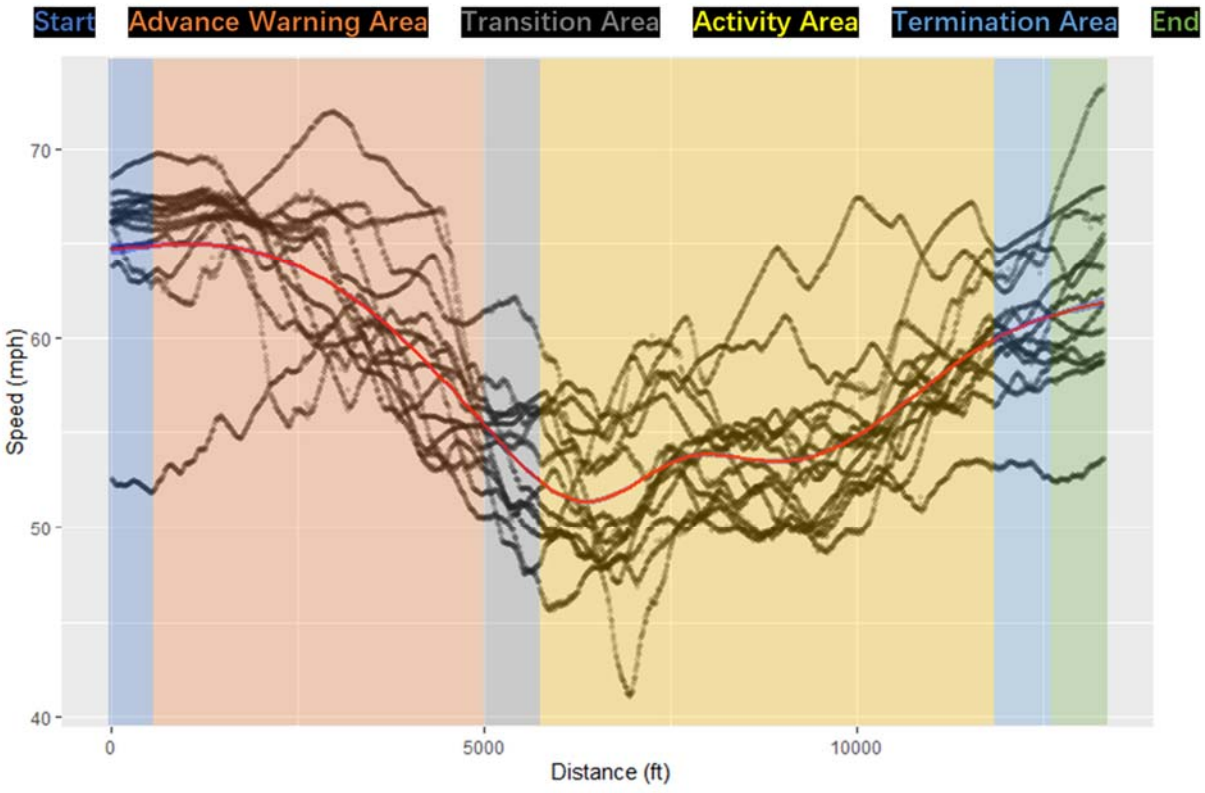
Start
Advance Warning Area
Transition Area
Activity Area
Termination Area
End
70
60
50
40
Speed (mph)
0
5000
10000
Distance (ft)

(b)

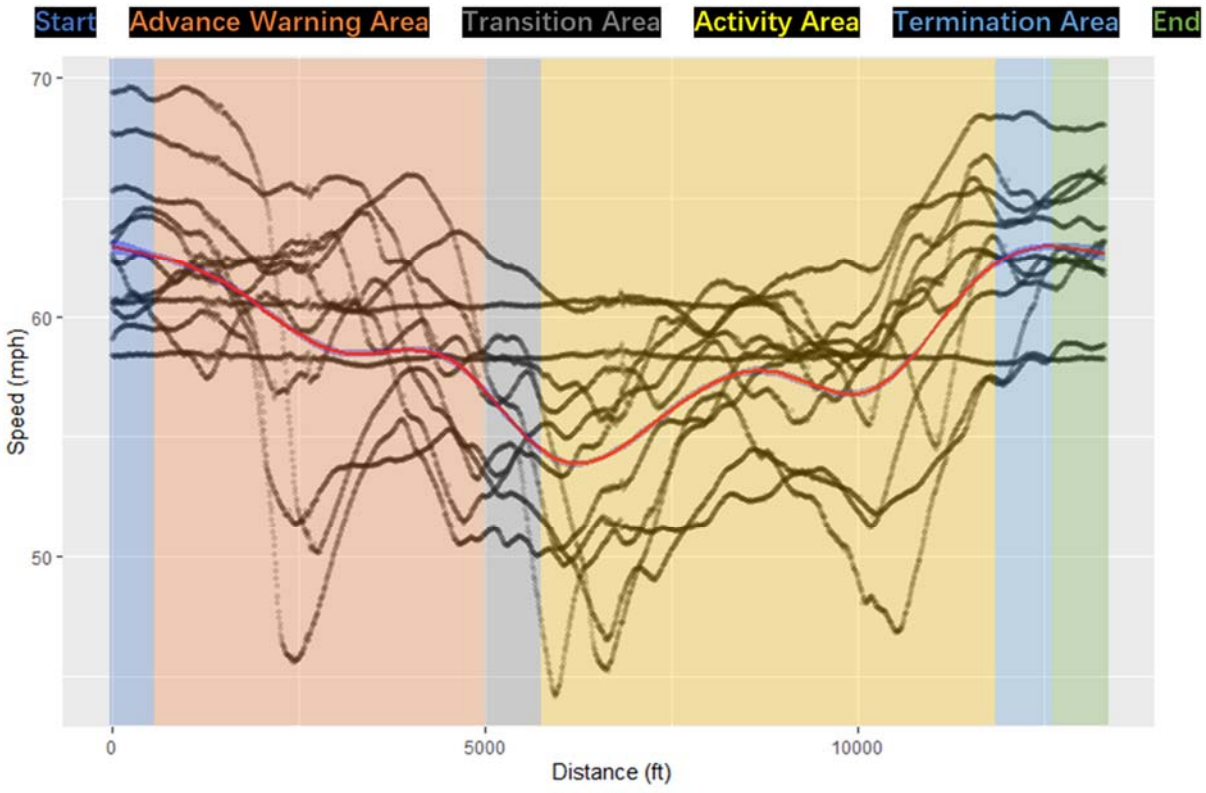
Start
Advance Warning Area
Transition Area
Activity Area
Termination Area
End
70
60
50
Speed (mph)
0
5000
10000
Distance (ft)

(c)

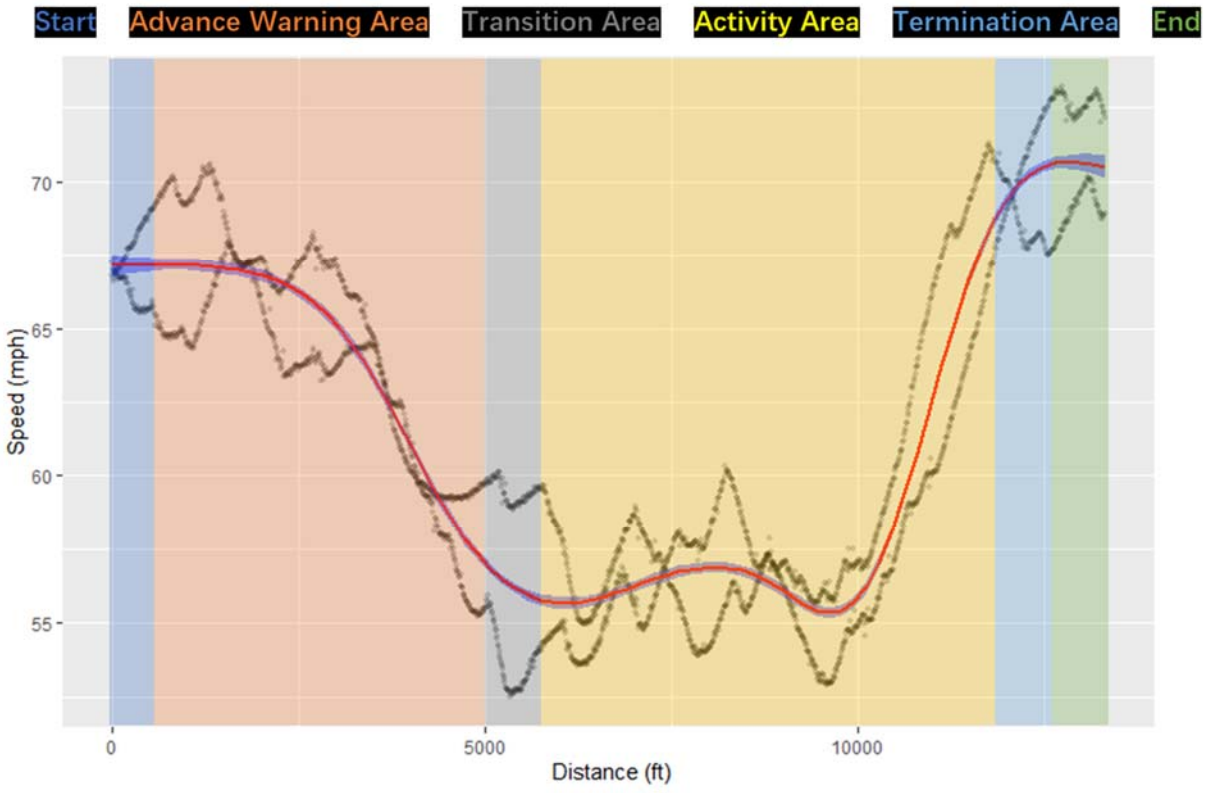
Start
Advance Warning Area
Transition Area
Activity Area
Termination Area
End
70
65
60
55
Speed (mph)
0
5000
10000
Distance (ft)

(d)

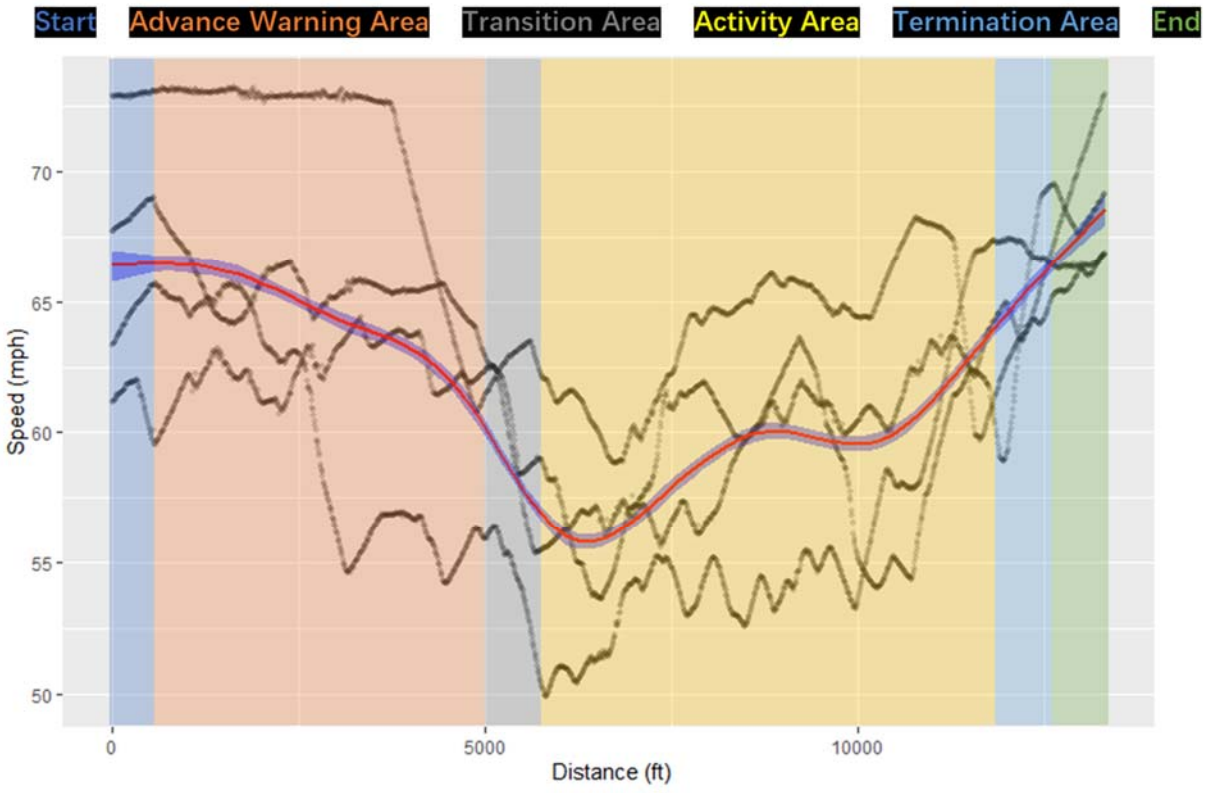
Start
Advance Warning Area
Transition Area
Activity Area
Termination Area
End
70
65
60
55
50
Speed (mph)
0
5000
10000
Distance (ft)

(e)

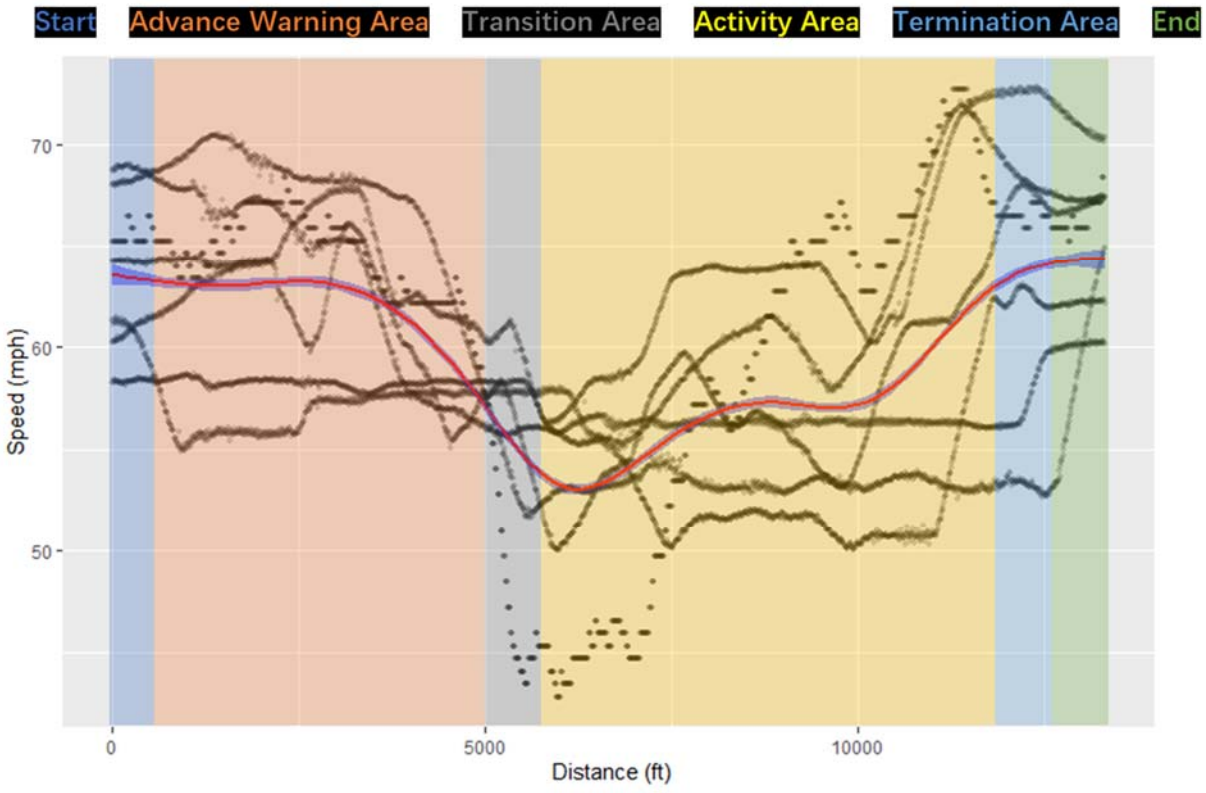
Start
Advance Warning Area
Transition Area
Activity Area
Termination Area
End
70
60
50
Speed (mph)
0
5000
10000
Distance (ft)

(*f*)

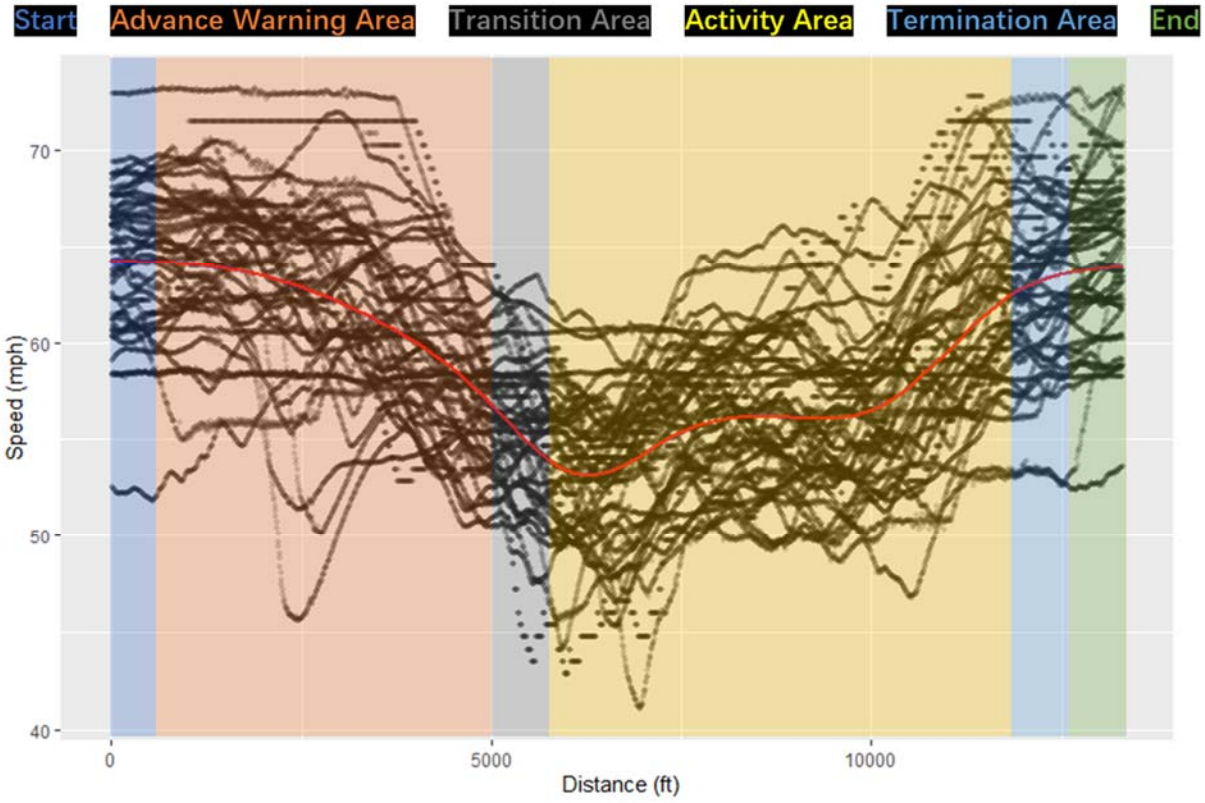

(*g*)

Figure F- 1 Speed profile at LC 2-1: (*a*) young female drivers; (*b*) middle-aged female drivers; (*c*) senior female drivers; (*d*) young male drivers; (*e*) middle-aged male drivers; (*f*) senior female drivers; and (*g*) all drivers.

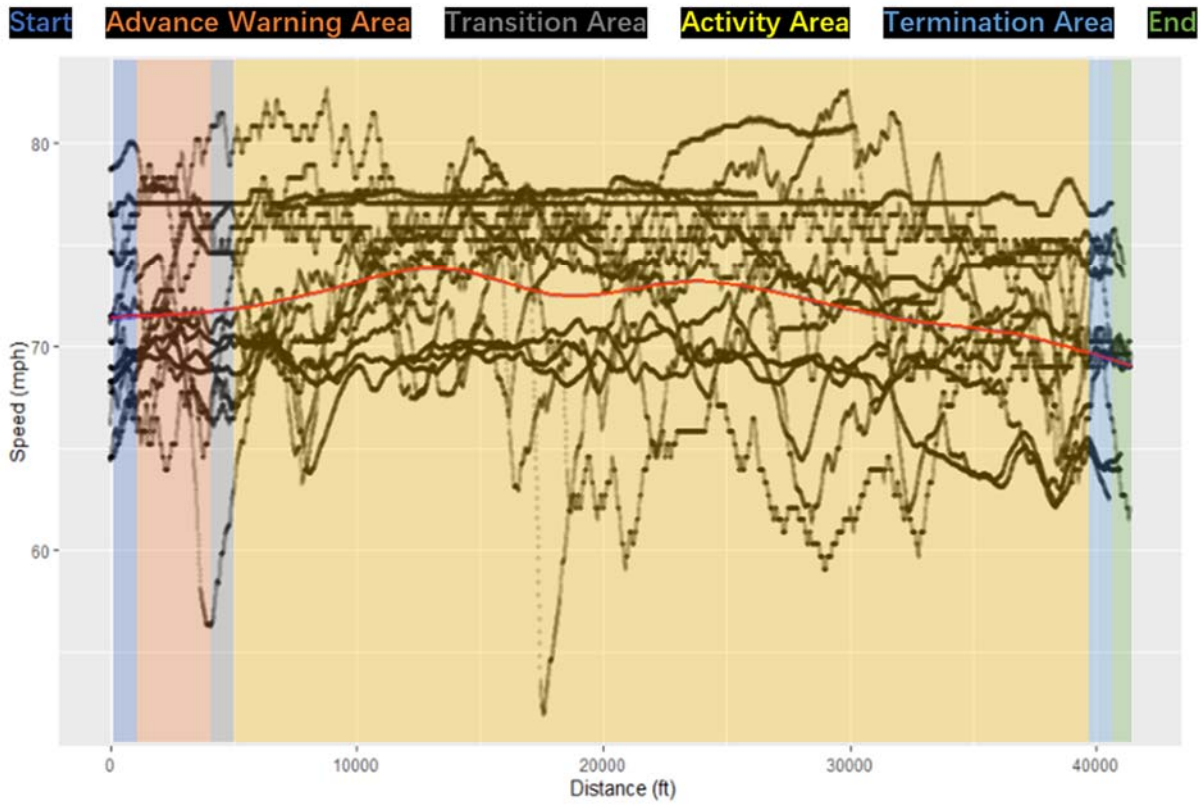
Start
Advance Warning Area
Transition Area
Activity Area
Termination Area
End
80
70
60
Speed (mph)
0
10000
20000
30000
40000
Distance (ft)

(*a*)

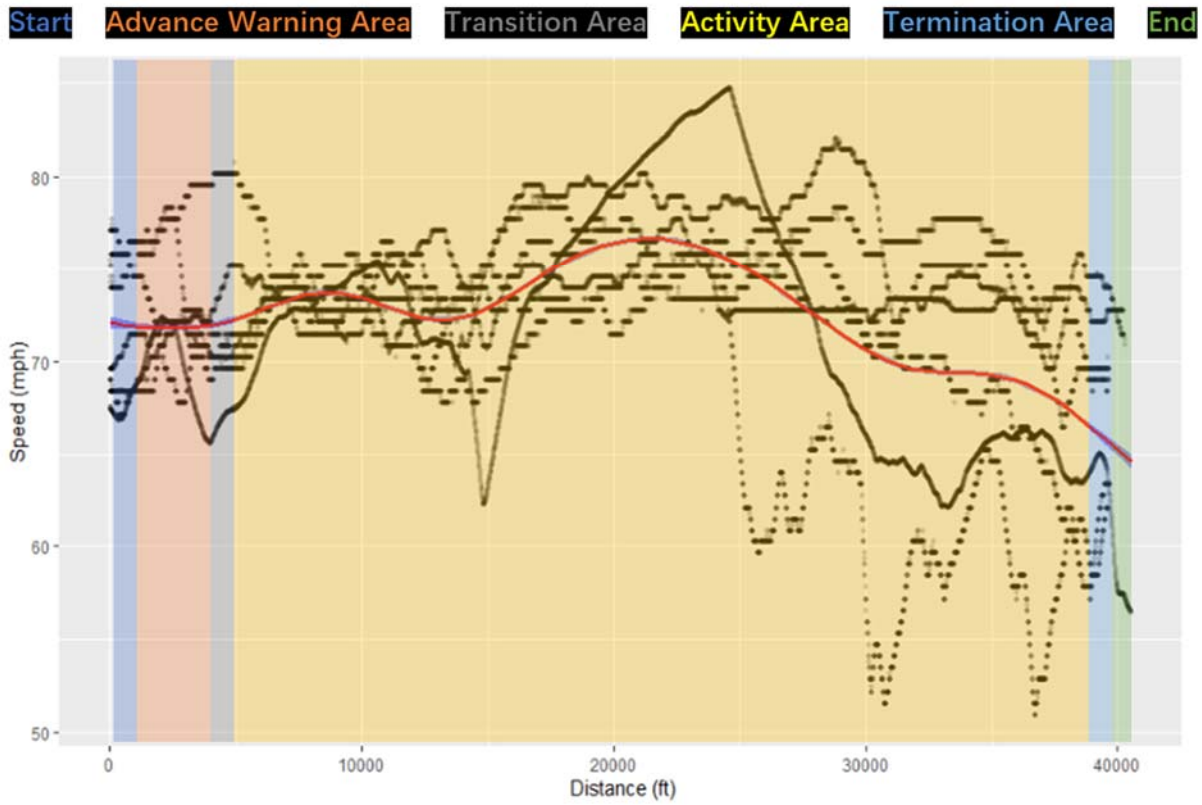
Start
Advance Warning Area
Transition Area
Activity Area
Termination Area
End
Speed (mph)
80
70
60
50
0
10000
20000
30000
40000
Distance (ft)

(b)

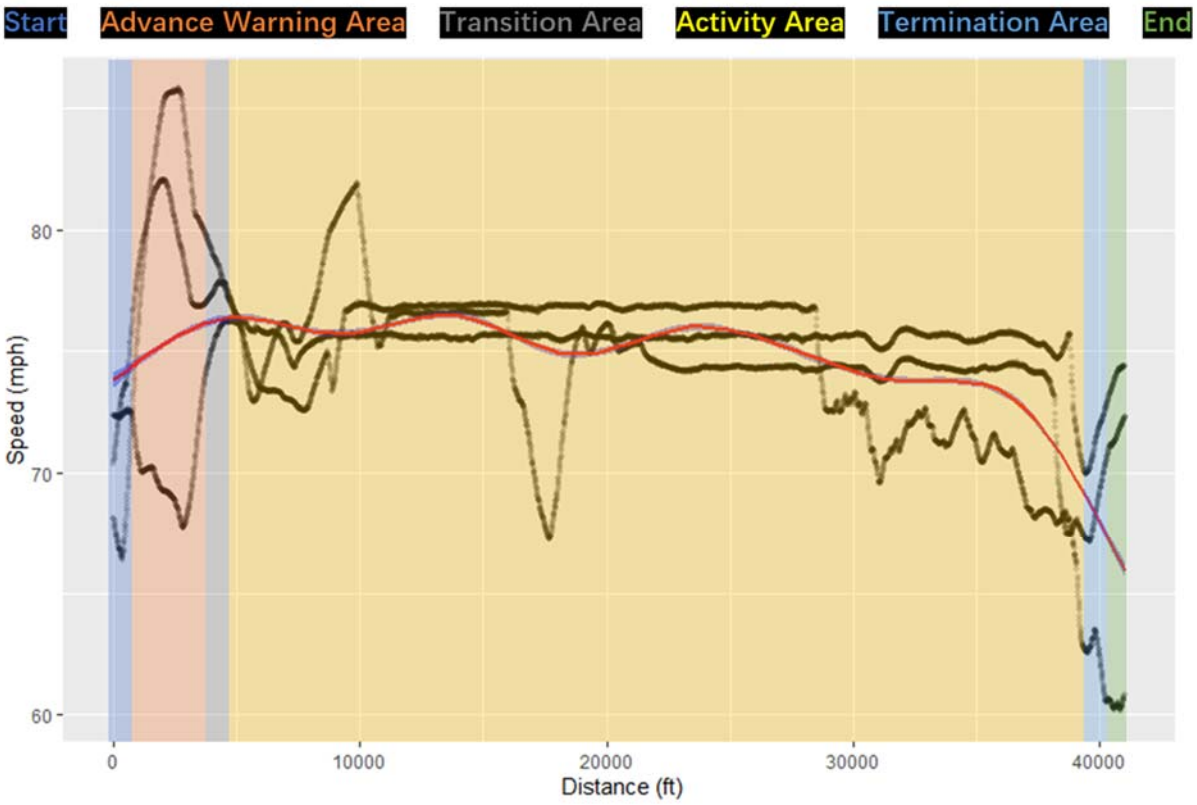
Start
Advance Warning Area
Transition Area
Activity Area
Termination Area
End
80
70
60
Speed (mph)
0
10000
20000
30000
40000
Distance (ft)

(*c*)

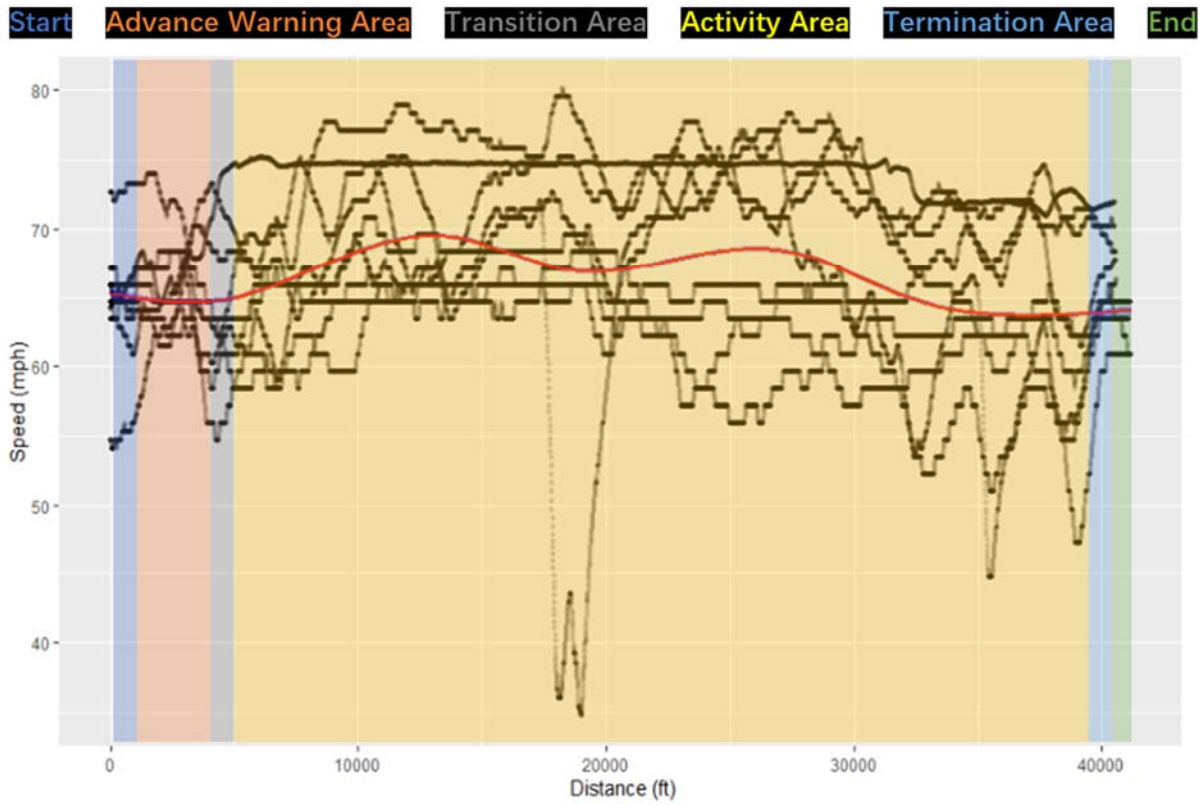
Start
Advance Warning Area
Transition Area
Activity Area
Termination Area
End
80
70
60
50
40
Speed (mph)
0
10000
20000
30000
40000
Distance (ft)

(d)

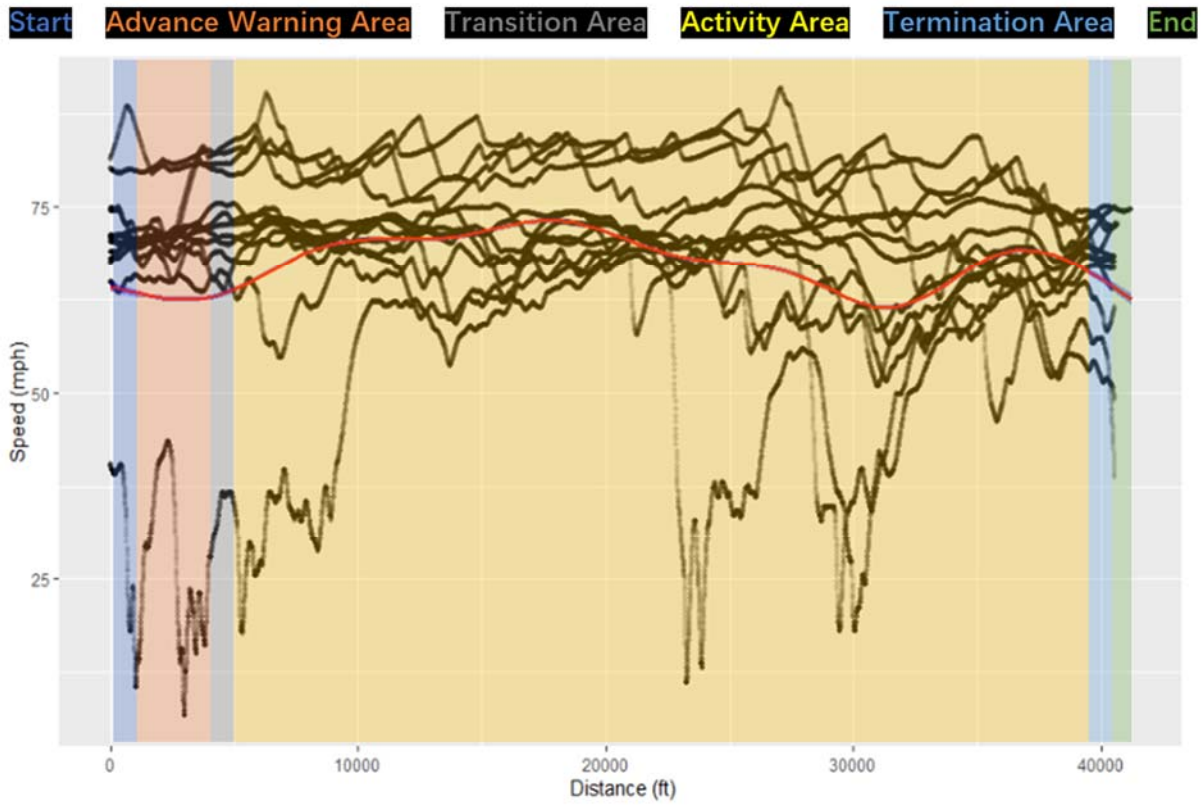
Start
Advance Warning Area
Transition Area
Activity Area
Termination Area
End
75
50
25
Speed (mph)
0
10000
20000
30000
40000
Distance (ft)

(e)

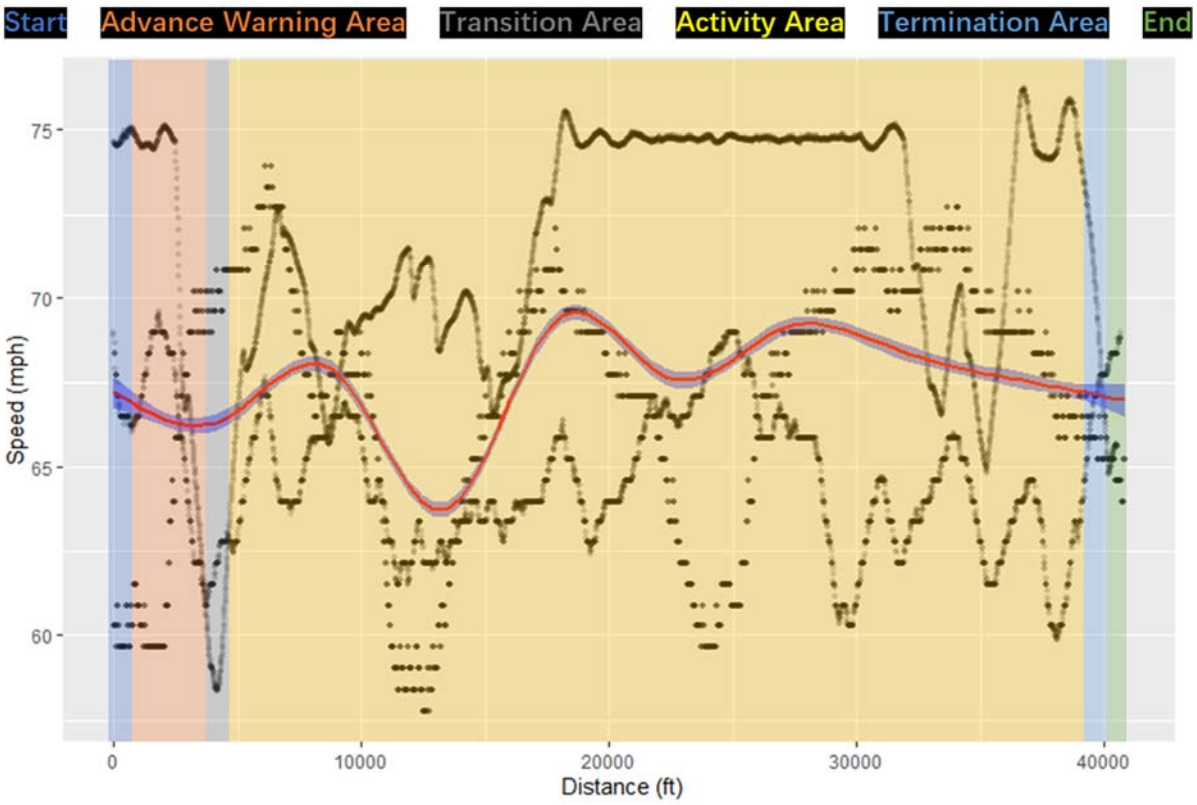
Start
Advance Warning Area
Transition Area
Activity Area
Termination Area
End
75
70
65
60
Speed (mph)
0
10000
20000
30000
40000
Distance (ft)

(*f*)

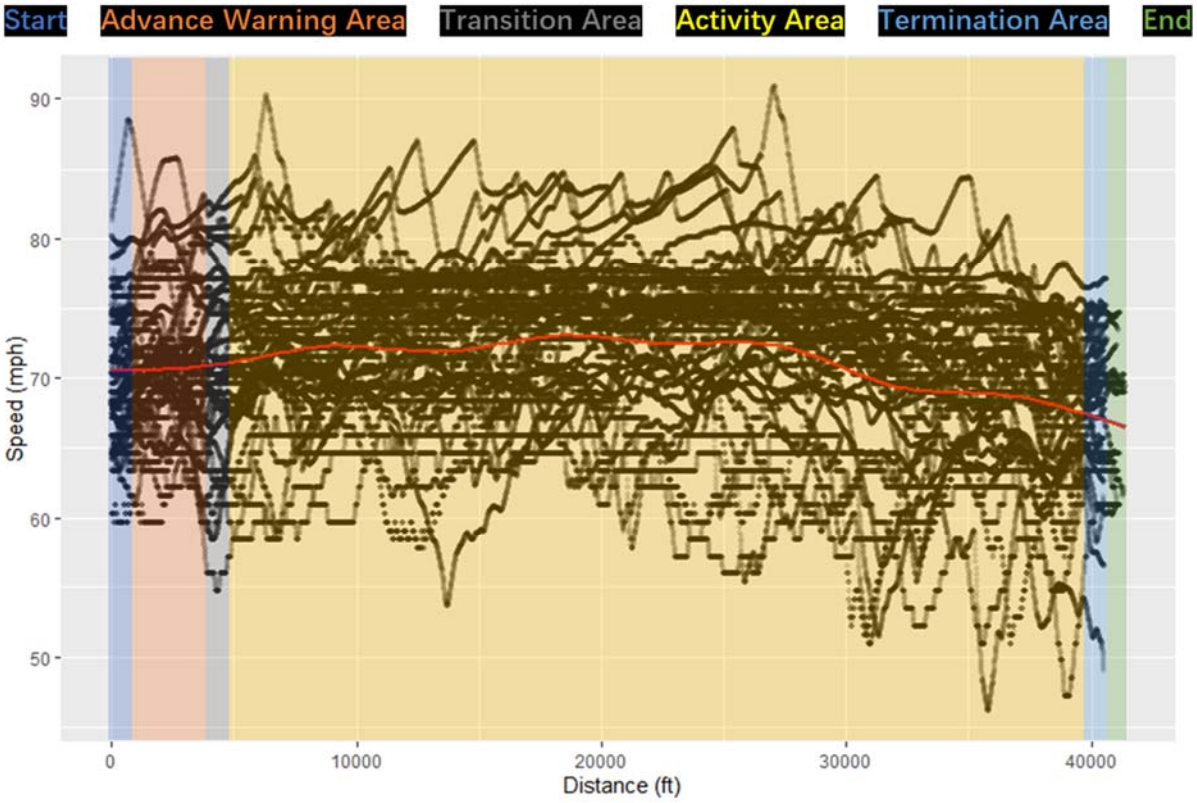

(*g*)

Figure F- 2 Speed profile at LC 3-2: (*a*) young female drivers; (*b*) middle-aged female drivers; (*c*) senior female drivers; (*d*) young male drivers; (*e*) middle-aged male drivers; (*f*) senior female drivers; and (*g*) all drivers.

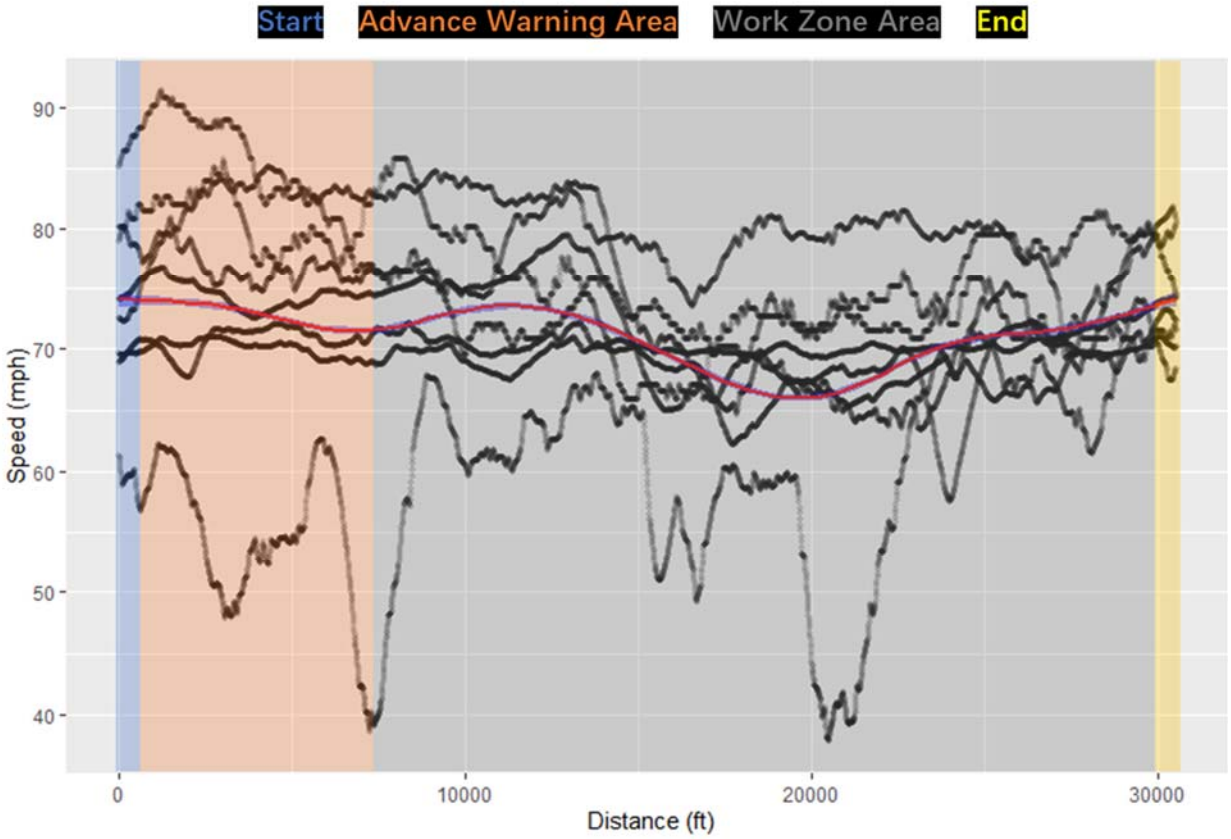
Start
Advance Warning Area
Work Zone Area
End
90
80
70
60
50
40
Speed (mph)
0
10000
20000
30000
Distance (ft)

(a)

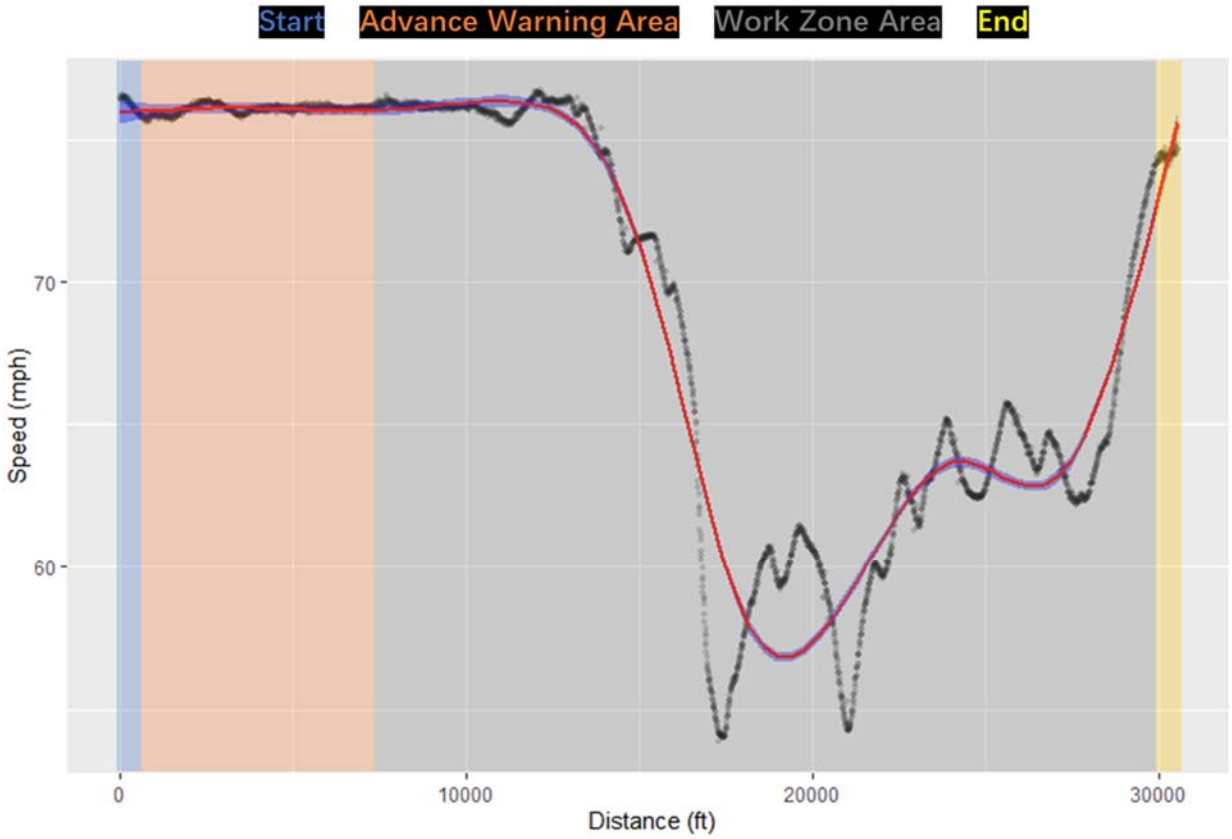
Start
Advance Warning Area
Work Zone Area
End
70
60
Speed (mph)
0
10000
20000
30000
Distance (ft)

(b)

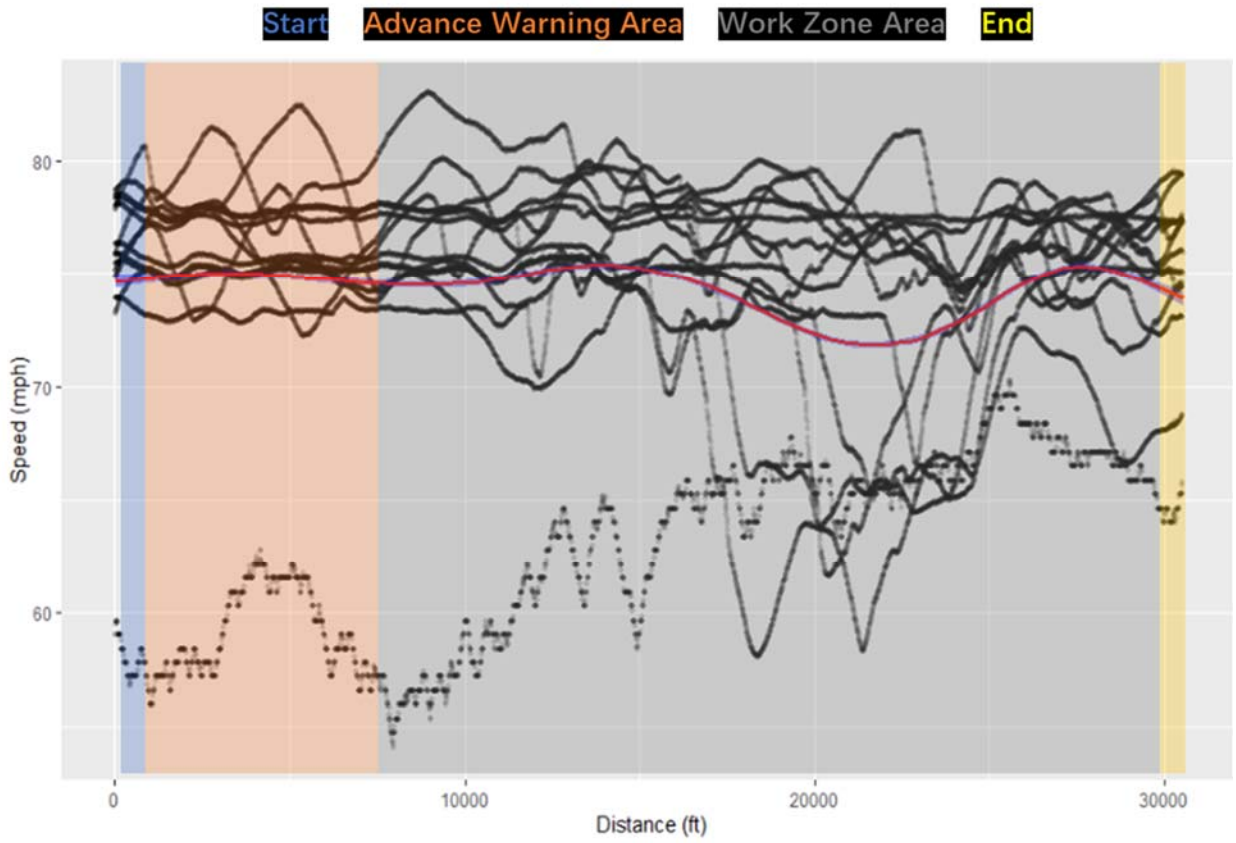
Start
Advance Warning Area
Work Zone Area
End
80
70
60
Speed (mph)
0
10000
20000
30000
Distance (ft)

(*c*)

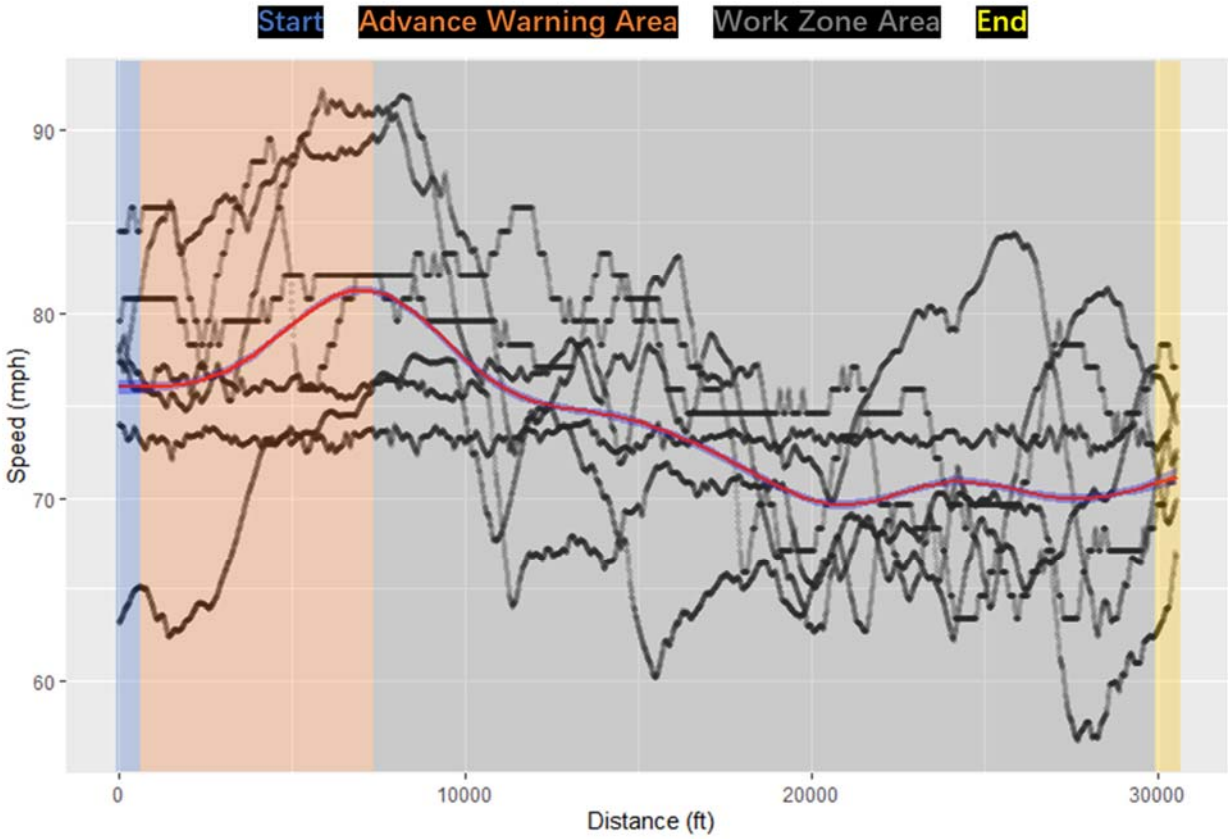
Start
Advance Warning Area
Work Zone Area
End
90
80
70
60
Speed (mph)
0
10000
20000
30000
Distance (ft)

(d)

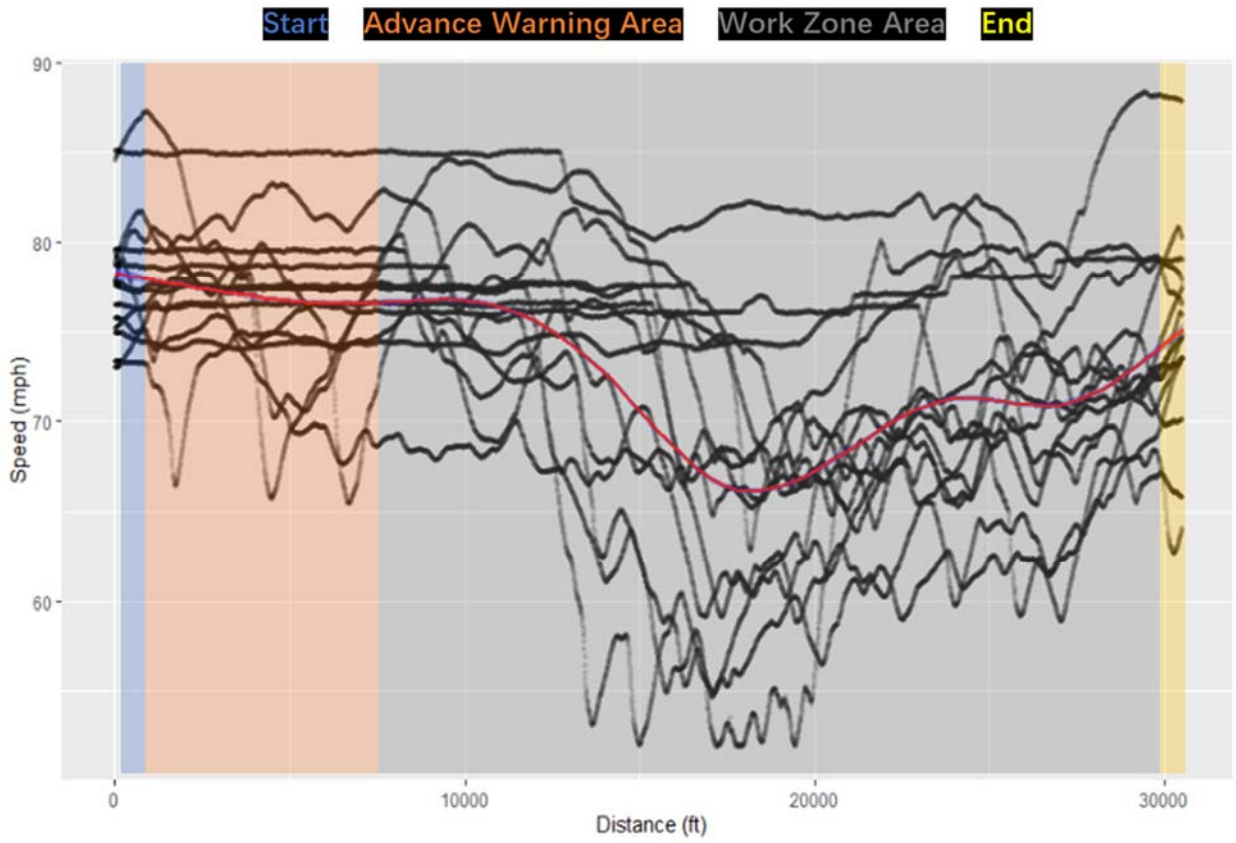
Start
Advance Warning Area
Work Zone Area
End
90
80
70
60
Speed (mph)
0
10000
20000
30000
Distance (ft)

(*e*)

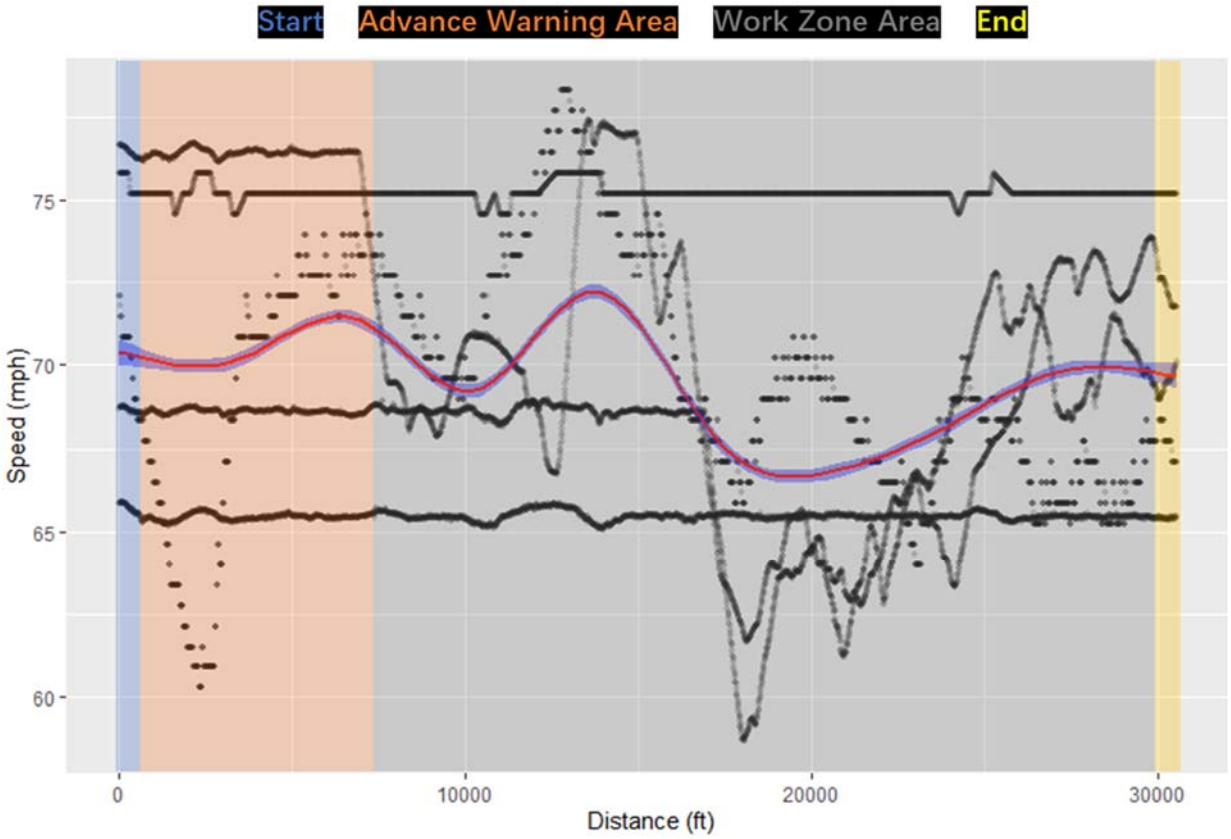
Start
Advance Warning Area
Work Zone Area
End
75
70
65
60
Speed (mph)
0
10000
20000
30000
Distance (ft)

(*f*)

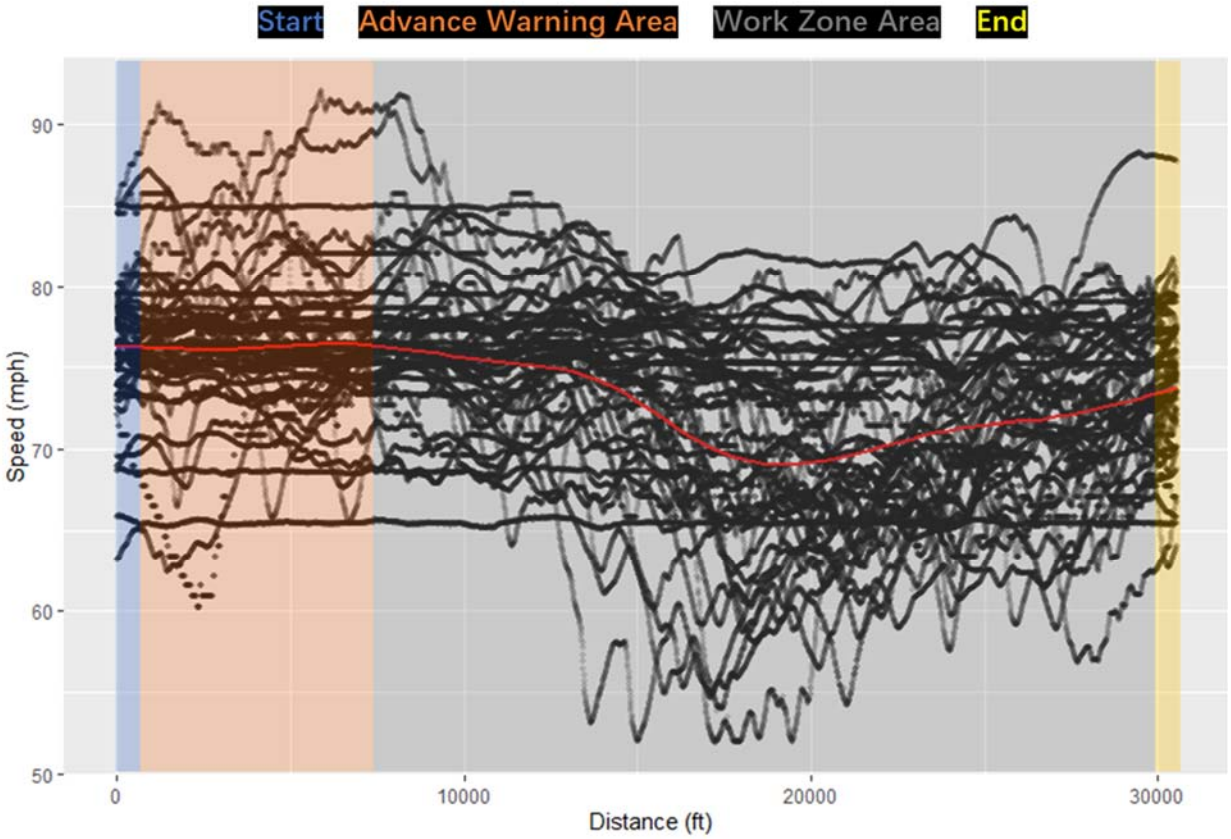

(*g*)

Figure F- 3 Speed profile at SC 2-2: (*a*) young female drivers; (*b*) middle-aged female drivers; (*c*) senior female drivers; (*d*) young male drivers; (*e*) middle-aged male drivers; (*f*) senior female drivers; and (*g*) all drivers.

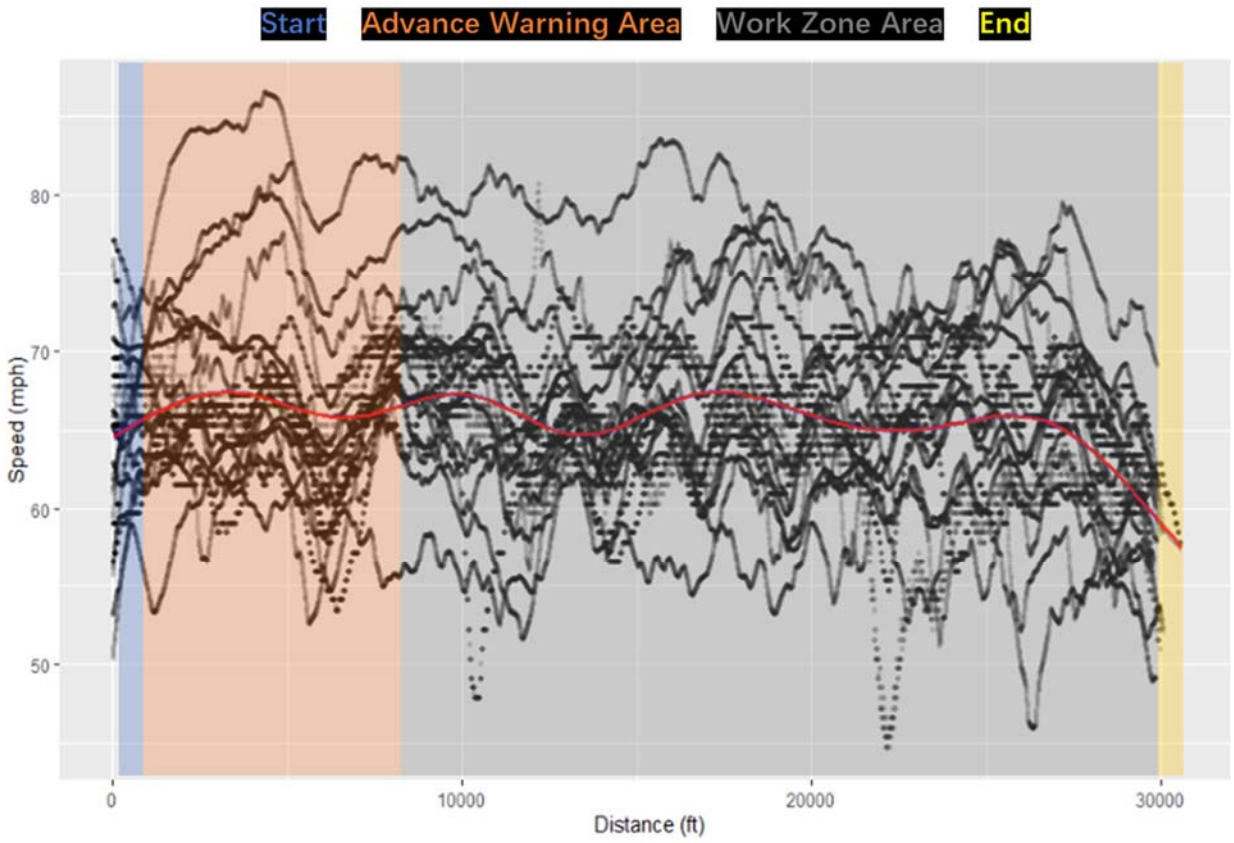
Start
Advance Warning Area
Work Zone Area
End
80
70
60
50
Speed (mph)
0
10000
20000
30000
Distance (ft)

(a)

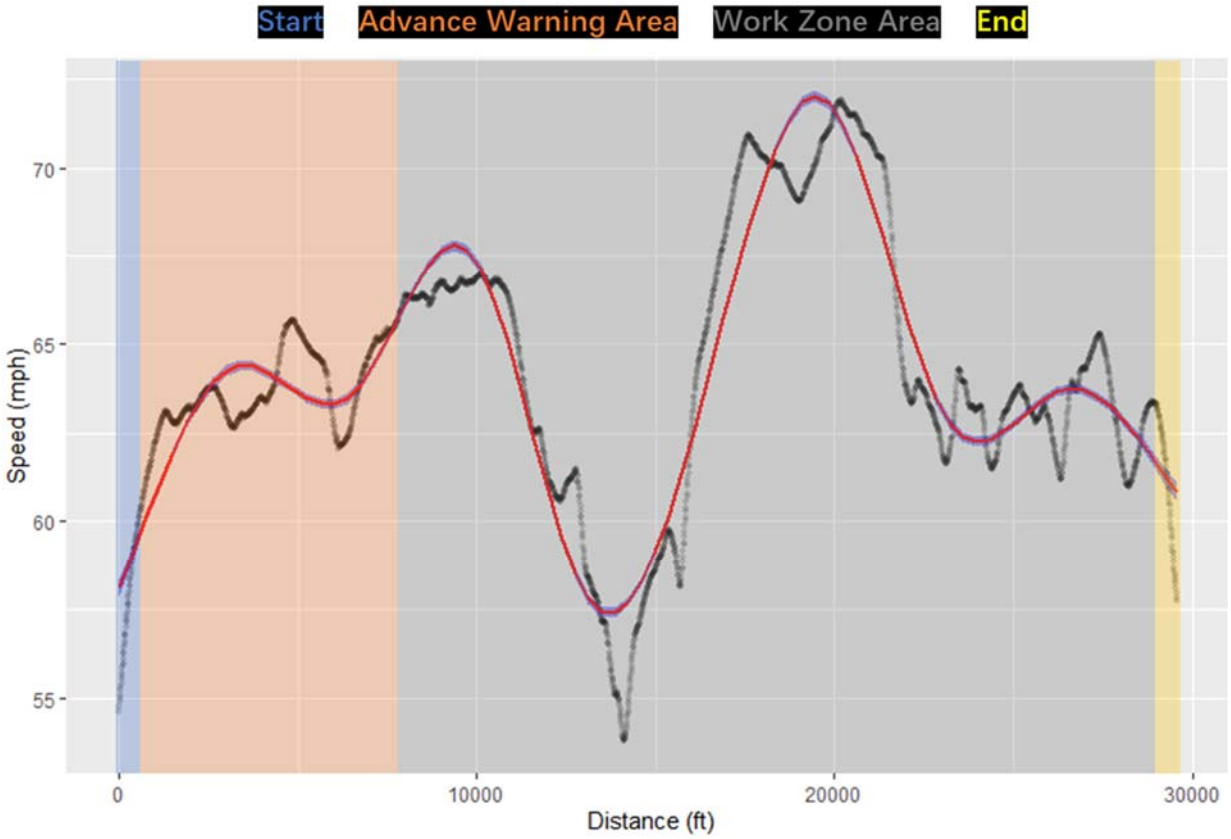
Start
Advance Warning Area
Work Zone Area
End
70
65
60
55
Speed (mph)
0
10000
20000
30000
Distance (ft)

(b)

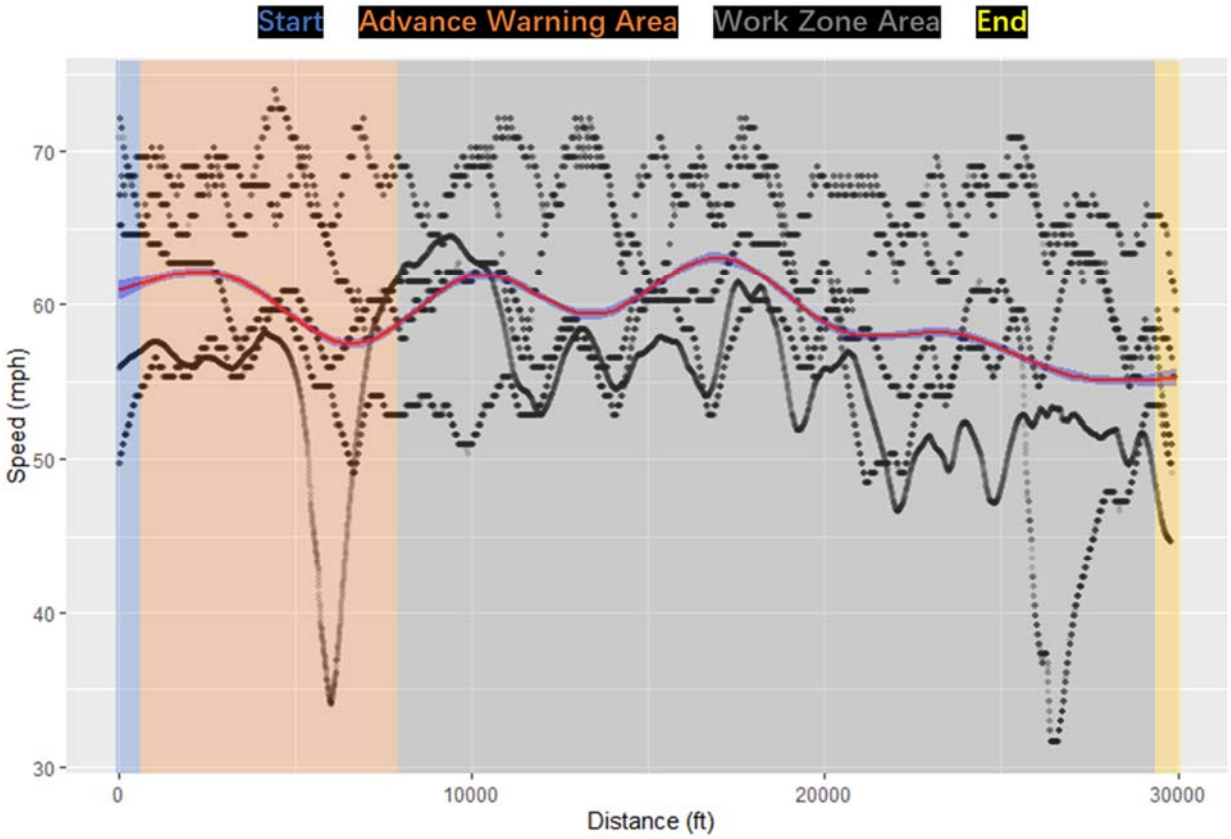
Start
Advance Warning Area
Work Zone Area
End
70
60
50
40
30
Speed (mph)
0
10000
20000
30000
Distance (ft)

(*c*)

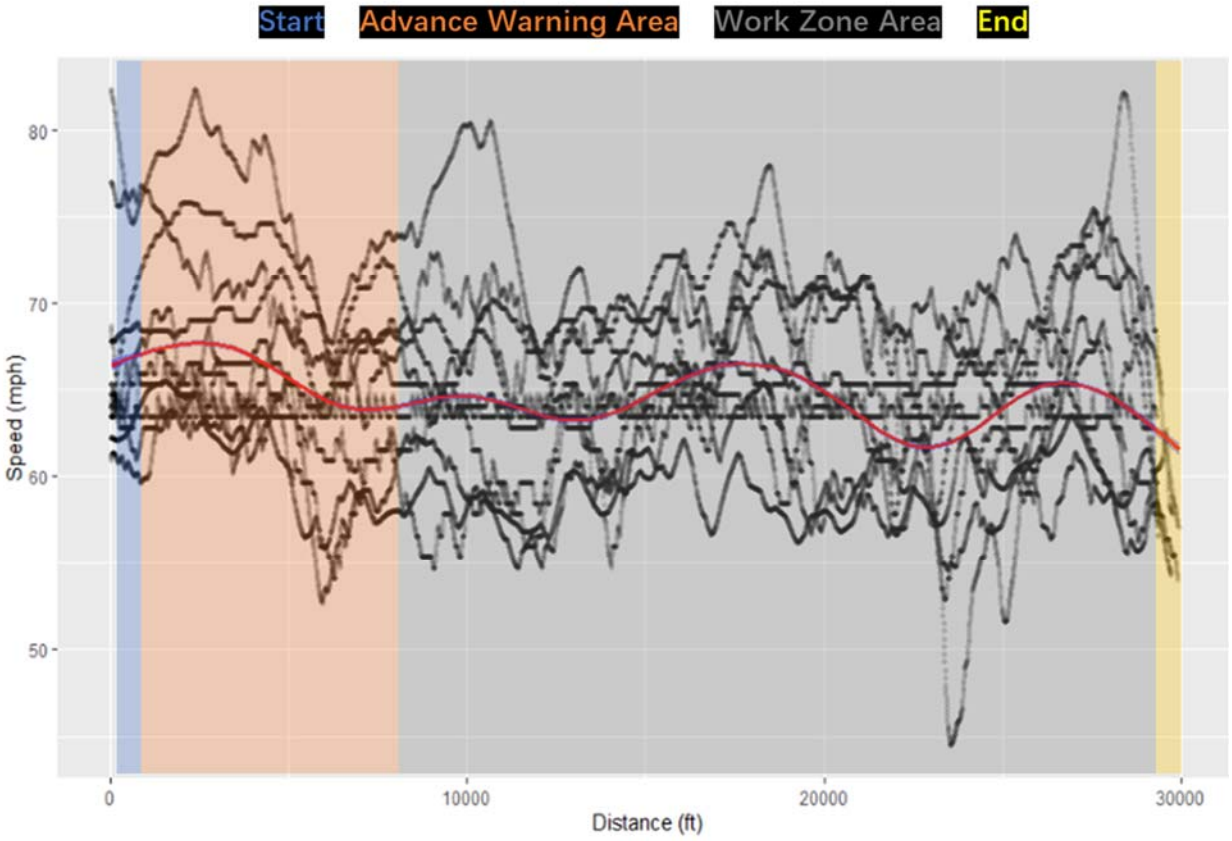
Start
Advance Warning Area
Work Zone Area
End
80
70
60
50
Speed (mph)
0
10000
20000
30000
Distance (ft)

(d)

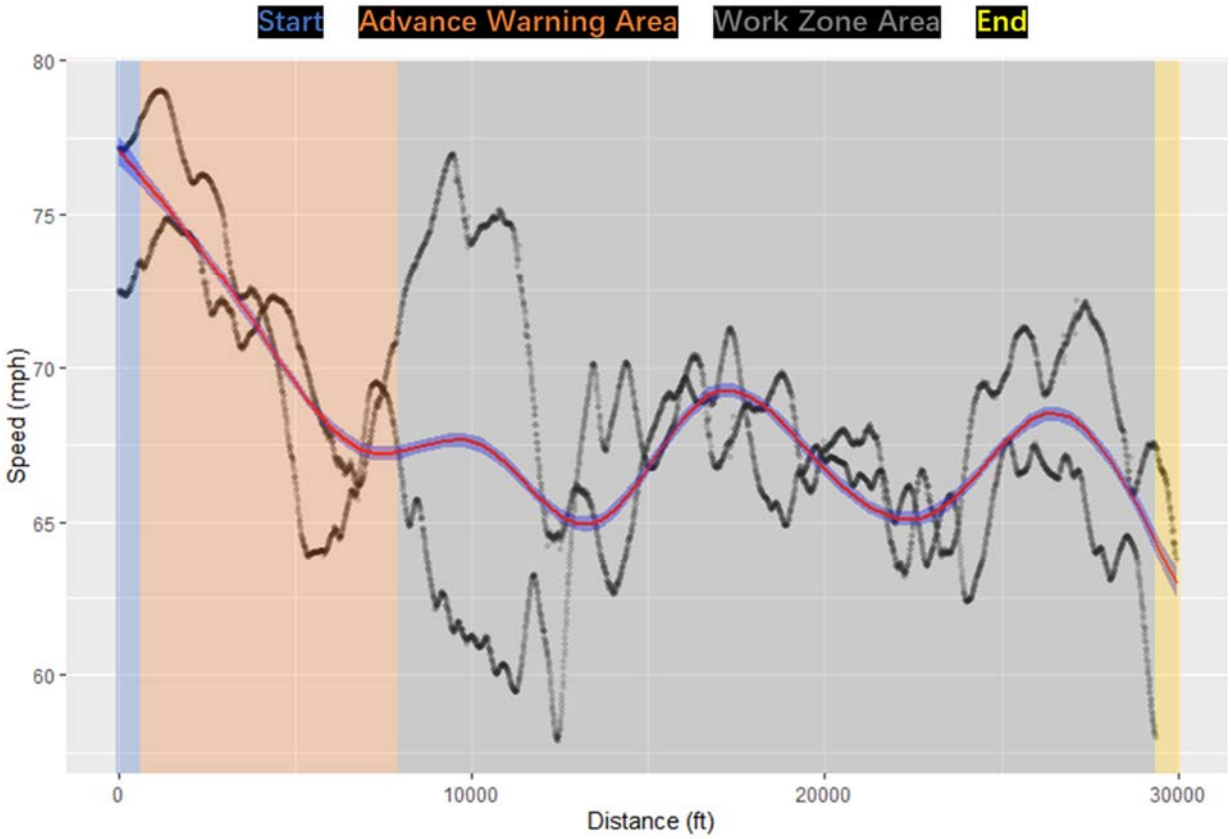
Start
Advance Warning Area
Work Zone Area
End
80
75
70
65
60
Speed (mph)
0
10000
20000
30000
Distance (ft)

(e)

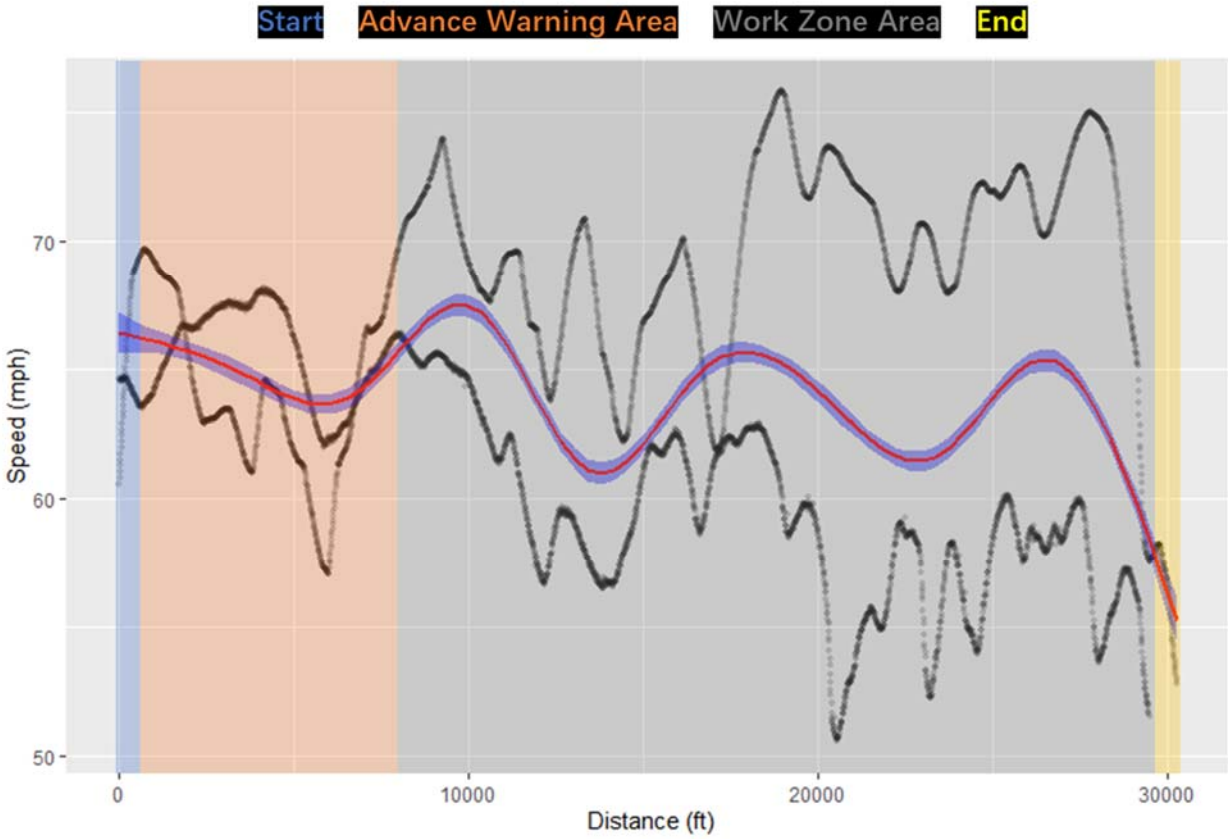
Start
Advance Warning Area
Work Zone Area
End
70
60
50
Speed (mph)
0
10000
20000
30000
Distance (ft)

(*f*)

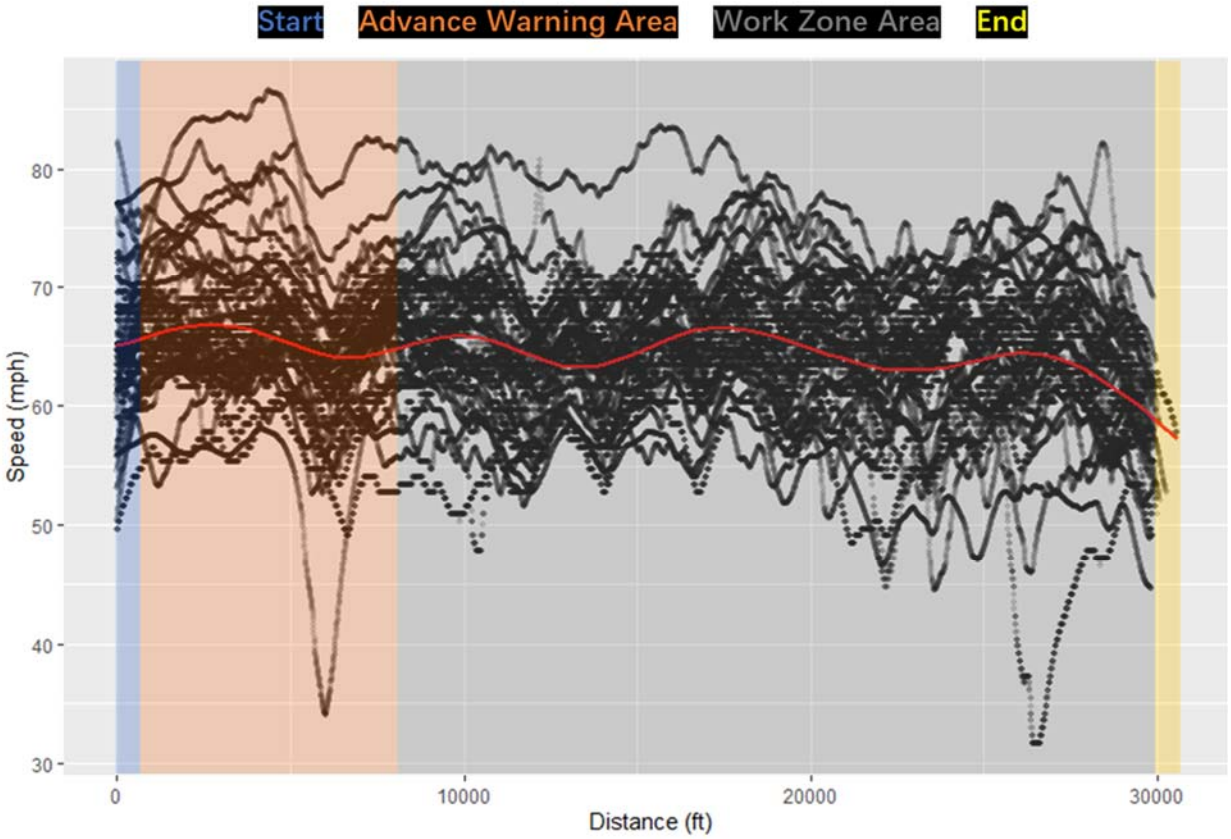

(*g*)

Table F- 1 Speed profile at SC 2-2: (*a*) young female drivers; (*b*) middle-aged female drivers; (*c*) senior female drivers; (*d*) young male drivers; (*e*) middle-aged male drivers; (*f*) senior female drivers; and (*g*) all drivers.